



Surfactant Aggregation in DESs

Thesis submitted for the degree of
Doctor of Philosophy
at the University of Leicester

By

Rokaya Mohammed Mohammed Azaga

Department of Chemistry
University of Leicester
September-2018

Abstract

Surfactant Aggregation in DESs

Rokaya Mohammed Mohammed Azaga

University of Leicester, 2018

Deep eutectic solvents (DESs) have attracted significant attention for a wide range of applications including metal deposition, natural product extraction, metal recycling and catalysis. In general they are good at solubilising polar and charged solutes and hence their properties can be tuned. This study aims to investigate how the properties of DESs can be modified by the addition of surfactants. One aim is to understand how and why surfactants aggregate and how their surface activity differs from aqueous solutions.

Firstly, the physical properties of three DESs are characterised containing different surfactants. The critical micelle concentrations, CMC are analysed together with the extent of aggregation. It was found that CMC values of SDS in Reline and Glyceline are smaller than in aqueous systems while in Ethaline the value are similar to those in water. Dynamic light scattering and viscosity data show that supramolecular aggregates of SDS in Ethaline change from cylindrical to liquid crystalline phases at about 3 times the CMC concentration. Moreover, the thermodynamic parameters of the micellization indicated that SDS aggregation was enthalpy controlled. The pattern of the micelle aggregation was different to that observed in water. Surfactant aggregates are found to form despite the high ionic strength due to that large choline cations having a low charge density.

The interface properties of surfactants were studied and it was found that the aggregation was favoured in media with a higher surface energy as this disfavoured the solubilisation of monomers. The surfactants were found to be less surface active than they were in aqueous solutions. This was proposed to be due to the high ionic strength of the DESs meaning that charge-charge interactions between the interface and the surfactant were less important. The implication of this is demonstrated when surfactants were tested as brighteners in copper electroplating solutions. It was found that surfactants did not affect the deposit morphology as significantly as molecules which specifically adsorbed on the copper surface which indicated the method by which brighteners functioned in DESs was not primarily through charge-charge interactions.

Statement

The work explained in this thesis for the degree of Ph.D. entitled “*Surfactant Aggregation in DESs*” was carried out by the author in the Department of Chemistry at the University of Leicester between November 2014 and September 2018.

In this thesis, the work recorded was original except where acknowledged or referenced.

None of the work has been submitted for another degree at this or any other university.

Signed Date.....

Rokaya Mohammed Mohammed Azaga

University of Leicester,

University of Road,

Leicester,

LE1 7RH.

Acknowledgements

I would like to express my gratitude to several people who helped me all the way through my PhD study. I would like to express my sincere gratitude to all of them.

First and foremost I would like to thank my supervisor, Prof Andrew Abbott, for his continuous support which made completing my PhD possible. I have benefited greatly from his deep knowledge, understanding and his willingness to help with any problem. I would like to thank him for always keeping his door open for me even when he is busy. I feel myself really lucky and blessed to have him as my supervisor.

I would like to thank all the Materials Centre group members whom I have had a pleasure to work with him; Prof Robert Hillman, Prof Karl Ryder, Dr Robert Harris, Dr Christopher Zaleski, Dr Andrew Ballantyne, and Dr Kamalesh Prasad. I would also like to thank all my colleagues and my friends, past and present who were always there to help me at any stage of my studies where I found any difficulty (you know who you are!). I also give acknowledgement to Prof Rachel O'Reilly and Maria Inam at Warwick University for help with measuring zeta potentials. I am also thankful to Graham Clark from the Engineering Department and Miss Natalie Allcock from Centre for Core Biotechnology Services for their assistance with SEM and Praful and Carl from workshop.

My thesis would not have been possible without the support, love and help of my dear husband, Salem Alkashkari, who has always been a constant source of strength and encouragement during all these years. You are always my best motivator.

I am deeply grateful to my parents, who made me what I am today and all my family members who have helped me out not just throughout the PhD, but also through all my life. A special thanks goes to my beloved and precious children, Fatima, Mohamed, Zeneb and Sabreen thank you for your unconditional love. All of you have been the source of my strength and motivation for success especially in periods of uncertainties and difficulties.

Lastly, I must also acknowledge and thank the Libyan Government and University of Sebha for the financial support provided to me during my PhD studies.

Contents

Abstract.....	i
Statement.....	ii
Acknowledgements.....	iii
Contents.....	iv

Chapter 1

Introduction

1.1	Surfactant.....	2
1.1.1	Classification of Surfactants.....	2
1.2	Phase Behaviour of Surfactant Solutions.....	3
1.2.1	Aggregation Behaviour.....	3
1.2.2	Adsorption Behaviour of Surfactant.....	8
1.3	Applications of Surfactants.....	10
1.4	Ionic Liquids (ILs)	11
1.5	Deep Eutectic Solvents (DESs)	13
1.5.1	Classification of DESs.....	16
1.5.2	Physical Properties of DESs.....	17
1.5.3	Applications of DESs.....	20
1.6	Self-assembly of Surfactants in Non-aqueous System.....	22
1.7	Project Aims.....	27
1.8	References.....	29

Chapter 2

Experimental Section

2.1	Materials.....	39
2.2	Preparation of Solutions.....	39
2.2.1	Preparation of DESs.....	39
2.2.2	Preparation of Surfactant Solutions in DESs.....	40
2.2.3	Preparation of Surfactant Solutions with Probe in DESs.....	40
2.2.4	Preparation of Emulsions.....	40
2.3	Physical Properties of Surfactant Solutions in DESs.....	40
2.3.1	Determination of Critical Micelle Concentration.....	40
2.3.2	Viscosity.....	44

2.3.3	Contact Angle.....	45
2.3.4	Conductivity.....	45
2.3.5	Zeta Potential.....	45
2.3.6	Aggregation Analysis.....	45
2.4	Electrochemical Study.....	47
2.4.1	Cyclic Voltammetry.....	48
2.4.2	Chronoamperometry.....	48
2.4.3	Bulk Electrodeposition of Copper.....	48
2.5	Surface Analysis.....	49
2.5.1	Scanning Electron Microscopy.....	49
2.5.2	X-Ray Diffraction.....	49
2.5.3	3D Optical Microscopy.....	49
2.6	References.....	50

Chapter 3

Physical Properties of Surfactants Solutions in DESs

3.1	Introduction.....	52
3.1.1	Stability of Micelles.....	53
3.1.2	The Critical Micelle Concentration.....	56
3.1.3	Self-assembly Structures.....	58
3.1.4	Thermodynamics of Micelles.....	59
3.2	Results and Discussion.....	61
3.2.1	Surfactant Solubilisation in DESs.....	61
3.2.2	Aggregation in DESs.....	63
3.2.3	Critical Micelle Concentration (CMC) in DESs.....	66
3.2.4	Micelles Size Analysis.....	78
3.2.5	Thermodynamics of SDS Micellization in Ethaline.....	83
3.3	Conclusions.....	88
3.4	References.....	89

Chapter 4

Surfactant Aggregation at DES Interfaces

4.1	Introduction.....	95
4.1.1	Surfactant as Wetting Agents.....	97
4.1.2	The Structure of Surfactants at the Charged Surface.....	98
4.1.3	The Structure of DESs at the Electrode Interface.....	100

4.2	Results and Discussion.....	104
4.2.1	Adsorption of SDS at Air-DES Interface.....	104
4.2.2	The Wettability of Solid Surfaces by Surfactants in DESs.....	109
4.2.3	Adsorption of SDS at Electrode-DES Interface.....	113
4.2.4	Adsorption of SDS at Oil-DES Interface.....	133
4.3	Conclusion.....	138
4.4	References.....	140

Chapter 5

Effect of Surfactants on Electrodeposition of Copper from DESs

5.1	Introduction.....	146
5.1.1	Surfactant as Additives in Metal Electroplating.....	146
5.1.2	Electrodeposition of Metals from DESs in Presence of Additives.....	148
5.2	Results and Discussion.....	150
5.2.1	Cyclic Voltammetry Study.....	150
5.2.2	Diffusion Coefficients Study.....	153
5.2.3	Chronoamperometry Study of the Nucleation Mechanisms.....	157
5.2.4	Characterization of Surface Morphology.....	161
5.2.5	Effect of Temperature on Cu Morphology.....	167
5.3	Conclusion.....	175
5.4	References.....	177

Chapter 6

Summary and Future Work

6.1	Conclusions.....	181
6.2	Suggestions for Further Work.....	184

Chapter 7

An appendix

7.1	Surface Tension Raw Data.....	187
7.2	Conductivity Raw Data.....	192

1 Introduction

1	Introduction.....	1
1.1	Surfactant	2
1.1.1	Classification of Surfactants	2
1.2	Phase Behaviour of Surfactant Solutions.....	3
1.2.1	Aggregation Behaviour.....	3
1.2.2	Adsorption Behaviour of Surfactant	8
1.3	Applications of Surfactants	10
1.4	Ionic Liquids (ILs)	11
1.5	Deep Eutectic Solvents (DESs).....	13
1.5.1	Classification of DESs	16
1.5.2	Physical Properties of DESs	17
1.5.3	Applications of DESs.....	20
1.6	Self-assembly of Surfactants in Non-aqueous System.....	22
1.7	Project Aims.....	27
1.8	References	29

1.1 Surfactant

The term surfactant is a blend of Surface Active Agent and was coined by Antara Products in 1950.¹ Surfactants are amphipathic organic molecules composed of at least one solvent-loving group 'lyophilic' and one solvent-fearing group 'lyophobic'. Since they are usually used in water, these groups are usually referred to as 'hydrophilic' and 'hydrophobic'. In the simplest terms, a surfactant is composed of at least one hydrophobic tail and a hydrophilic head portion^{2,3,4} and this is shown schematically in Figure 1-1. The hydrophobic part is a straight or branched hydrocarbon or fluorocarbon chain containing 8–18 carbon atoms, while the hydrophilic part can be ionic, or non-ionic, or zwitterionic. The hydrocarbon chain interacts weakly with the polar molecules whereas the ionic head group interacts strongly with the polar molecules via dipole or ion–dipole interactions.^{5,6}

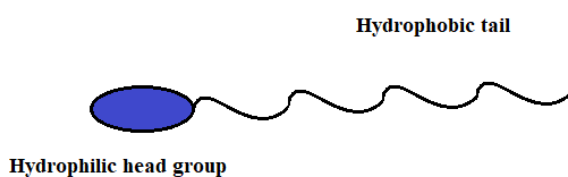


Figure 1-1: Structure of typical surfactant molecule.

1.1.1 Classification of Surfactants

Surfactants can be classified into four types depending on the formal charge present in their hydrophilic head: non-ionic, cationic, anionic and amphoteric (zwitterionic).^{4, 7, 8} Each of these have physical and chemical properties that are characteristic of that class of compound.^{4,9}

Anionic surfactants: a surfactant in which the hydrophilic part carries a negative charge. They are the most commonly used surfactant class. Most of them are easy and cheap to manufacture and they are known as emulsifiers and used in detergent formulations. Most commonly used anionic surfactants are based on carboxylate, sulphate, sulfonate and phosphate ions.

Cationic surfactants: a surfactant in which the hydrophilic part carries a positive charge. They are the second most common surfactant class. They are used in herbicides, fabric softeners and as anti-corrosion agents as most natural surfaces are negatively charged. The most common of the cationic surfactants is cetyltrimethylammonium bromide (CTAB). Other commonly used cationic surfactants are benzalkonium chloride, and cetylpyridinium chloride.

Non-ionic surfactants: a surfactant in which the hydrophilic part is uncharged. Non-ionic surfactants are less common than anionic and cationic surfactants. They can be classified as polyol esters, polyoxyethylene esters and poloxamers. The most commonly used of non-ionic surfactants is as co-surfactants in detergency formulations and as emulsifying agents.

Amphoteric (zwitterionic) surfactants: they are the least commonly used class of surfactant and they are important in personal care products as they do not irritate skin and eyes. Amphoteric surfactants are a surfactant in which the hydrophilic part contains both negative and positive charges. The charge can be negative, positive or without a charge in a solution depending on the pH of that solution. In general, the negatively charged amphoteric surfactants are based on carboxylate, sulphate or sulphonate, whereas the positively charged ones are almost always based on ammonium cations.

1.2 Phase Behaviour of Surfactant Solutions

Surfactant solutions have unusual properties which can be ascribed to the presence of a hydrophilic head group and a hydrophobic chain in the molecule.² Surfactant solutions act as normal electrolytes at low concentrations, but are less ideal at higher concentrations. The change in properties arise from the formation of self-aggregates of large numbers of molecules, called micelles^{2,10} and adsorption at phase interfaces.¹¹

1.2.1 Aggregation Behaviour

The most important phenomenon related to surfactants is their aggregation behaviour. When surfactant molecules are added to water, they tend to distribute themselves between the bulk solution and the solid-liquid and gas-liquid interfaces.

Increasing the amount of surfactant in solution leads to the surface becoming saturated with surfactant molecules. When this occurs, the surfactant molecules find it more thermodynamically efficient to aggregate in the bulk phase with the hydrophobic tails of the surfactant interacting with each other leaving the hydrophilic head groups to interact with water. When the concentration of the surfactant increases, two opposing forces arise; the hydrocarbon-water interactions, the hydrophobic interactions that support the aggregation and the electrostatic repulsions between the head groups for ionic surfactants. These two forces result in the hydrocarbon tails interacting in the centre of the micelle to minimise the repulsion from of the hydrophilic group.¹² This leads to the creation of a micelle as shown in Figure 1-2.

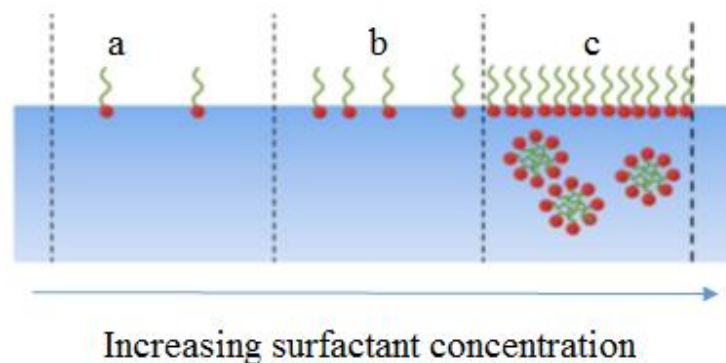


Figure 1-2: Schematic diagram of the behaviour of a surfactant solution.

There are many forces responsible for surfactant aggregation including hydrogen bonding, hydrophobic effect, electrostatic interaction, and van der Waal's forces. However, both hydrogen bonding and hydrophobic effects are the main driving forces for surfactants to aggregate into supramolecular structures. It is well known that the nonpolar molecules disrupt the network of water molecules in solution to organise the hydrophobic moieties as the methylene groups can neither hydrogen bond nor form dipole bonds with water. Water molecules surrounding the tail of surfactants therefore order, hence increase the number of bonds to other neighbouring solvent molecules. As results this increase the local order in another word decrease the entropy and then increase the free energy of surrounding solvent molecules compare to these in bulk solution. The hydrophobic effect drives the hydrophobic part of the surfactant to self-aggregate.¹³

The critical micelle concentration (CMC) is the minimum surfactant concentration required for aggregation to occur.^{14,15} As shown in Figure 1-3, the structure of the micelles formed by ionic surfactants consists of a the hydrophobic part of the aggregate forms the core of the micelle and a Stern layer surrounding the core, which is a concentric shell of hydrophilic head groups with counter ions, where the polar head groups are organised at the micelle-solvent interface in contact with, and hydrated by, a number of solvent molecules.^{2, 10,5}

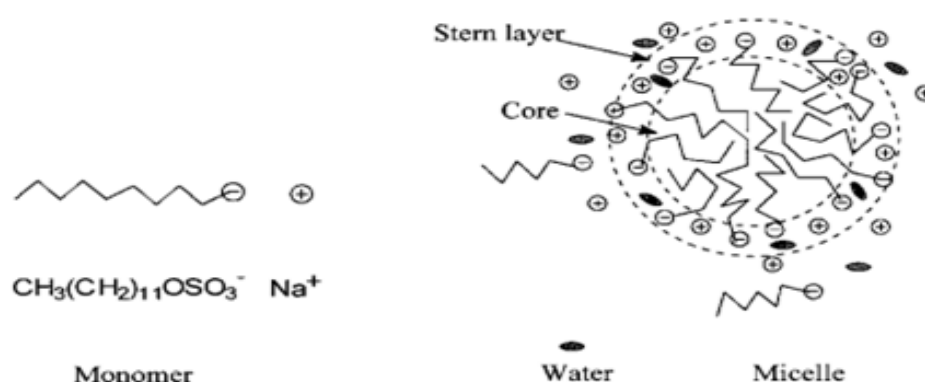


Figure 1-3: An idealized model for a spherical micelle of sodium dodecyl sulphate showing the core and the Stern layer, taken from Ref.¹⁶

The ability of surfactants to form micelles depends on many factors such as the structure, concentration and type of solvent.^{14, 15} The physicochemical properties of surfactant solutions vary considerably depending on whether the concentration of surfactants is above or below the CMC value. This means that the CMC can be determined by observing discontinuity changes in physical properties such as surface tension, viscosity, electrical conductivity, and solute solubility compared to the measured concentration of surfactant.^{5, 14, 17} These properties are shown as a function of concentration in Figure 1-4. The CMC value is actually an arbitrary concentration within a narrow range of concentration depend on the technique that used for the determination of CMC because the change in slope happen over a more or less narrow range of concentrations, whose magnitude depends on the physical property that used to measure CMC and sometimes on the nature of the data and on the way they are plotted.

In aqueous solutions, the CMC of most surfactants is in the range 10^{-4} to 10^{-2} mol dm⁻³. It should, however be noted that the CMC decreases when salt is added to the solution

which is important to the topic of this study.¹⁸ The CMC value may also be affected by factors such as temperature, buffer pH and the addition of organic modifiers.⁵

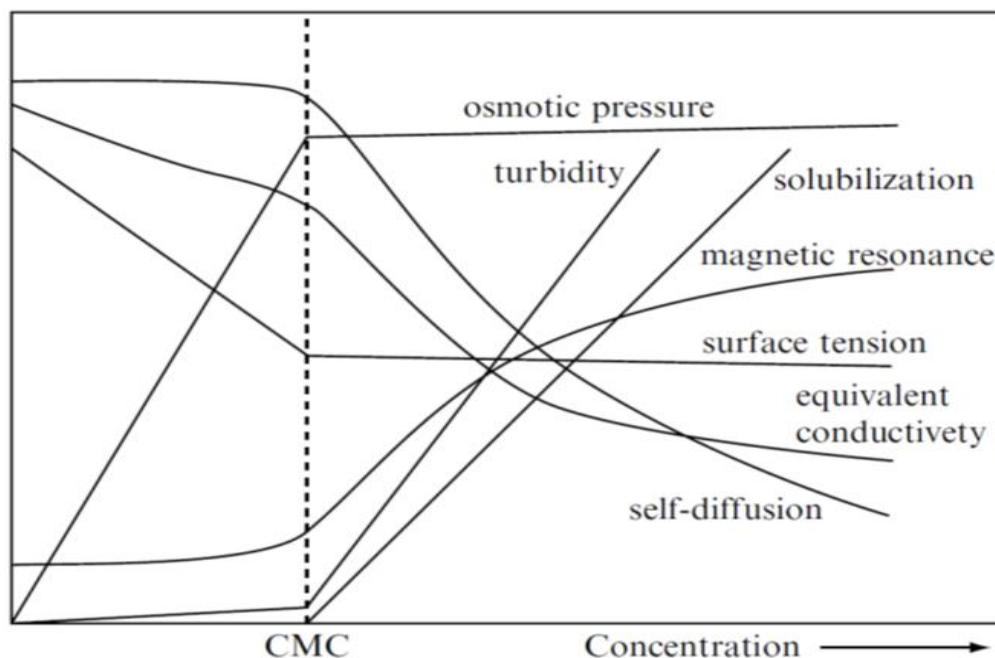


Figure 1-4: Physical properties of surfactants as a function of concentration, taken from Ref.¹⁹

Depending on the chemical structure of the surfactant, the micelle can also be anionic, cationic, non-ionic or amphoteric.¹⁶ Usually micelles are spherical, but depending on physicochemical conditions, such as temperature and the presence of electrolytes, micelles can also form cylindrical, worm-like, double layers or disk-like.⁷ Although the exact structure of micelles is still somewhat controversial, a simple schematic in Figure 1-5 represent the main structures that micelles can form. This unique ability of surfactants to form micellar structures means that surfactant solutions can be viewed as micro-heterogeneous media: i.e. while they appear homogenous on a macroscopic scale, they are in fact heterogeneous when viewed microscopically.¹⁶

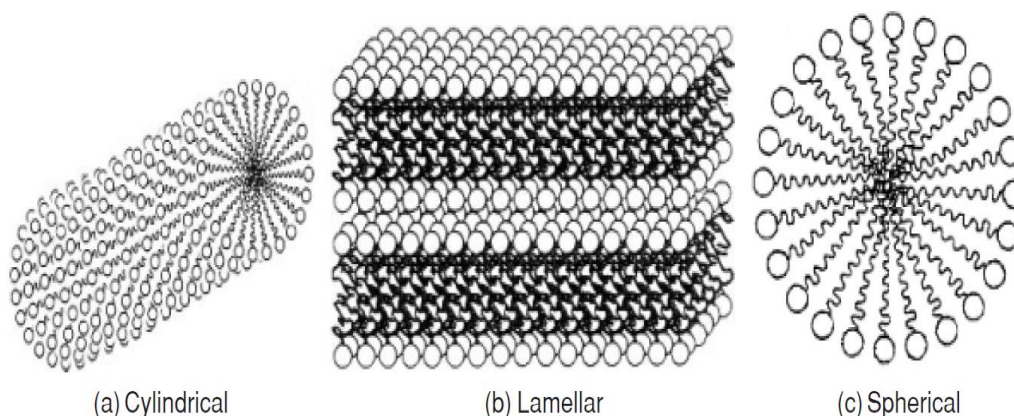


Figure 1-5: Typical micelle configurations, taken from Ref.²⁰

The formation of micellar aggregates results in present two solutions having regions with differing polarity; polar in the bulk aqueous phase and non-polar in the centre of the micelle. This enables the solubilisation of molecules which would normally be insoluble in water. This property is of use in variety of chemical applications. For example, the micelles of anionic surfactants can be used to remove pollutants such as metallic ions and organic material from water. The metallic ions bind to the negatively charged surface of the micelles, while and organic material is solubilized in the interior of the micelles. The water is then cleaned by forcing the micellar solution through an ultrafiltration membrane with pores small enough to block the passage of the micelles with their associated metallic ions and organic material.²¹ Another use of micelles is to separate and remove some metal ions from dilute solutions using micellar-enhanced ultrafiltration.²² This use of surfactant solutions is utilised in many industrial processes such as oil recovery, detergency, emulsification and polymerization.^{23, 24}

Micellar solutions are also used in electrochemical applications such as brighteners in electroplating industry and to stabilize the ion radicals produced at electrodes by Coulombic and hydrophobic interactions with micelles.²⁵

Reverse micelles are aggregates of surfactant molecules in an organic solvent where the core is a polar phase made by the surfactant hydrophilic head groups where the hydrophobic tails are in the organic solvent. The core is a nano-meter-sized droplet of water which is stabilized in an organic solvent with the help of a surfactant.²⁶ Generally they are known as water-in-oil microemulsions and their structure is shown

schematically in Figure 1-6. Another important application of micellar systems is for liquid-liquid extraction.

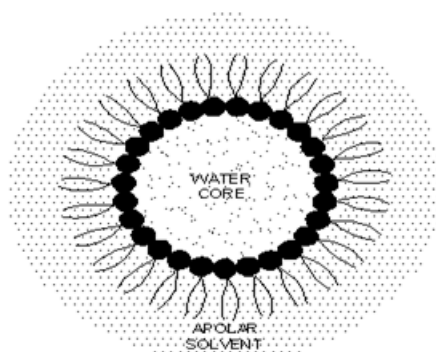


Figure 1-6: Structure of a reverse micelle, taken from Ref.²⁷

This form of liquid-liquid extraction is often applied to the extraction of complex biomolecules and involves extraction of the bioactive molecules from an aqueous phase into reverse micelles in the organic phase. The biomolecules are then transferred and concentrated back into the aqueous phase.^{26,27} Using reverse micelles for liquid-liquid extraction is an ideal tool for purifying antibiotics²⁶ and amoxicillin.²⁸

1.2.2 Adsorption Behaviour of Surfactant

Surfactant adsorption is the process by which surfactant molecules are transferred from the bulk solution phase to the surface-interface.¹¹ Surfactant molecules tend to accumulate at the interface to lower the Gibbs free energy of that phase boundary. There are five different interfaces: solid-gas, solid-liquid, solid-solid, liquid-gas and liquid-liquid, and surfactant can be absorbed at all of these interfaces.⁸

Adsorption of surfactant at the air-liquid interface is the simplest interface to describe. At the interface, the surfactant molecules will be arranged with hydrophilic 'heads' pointing towards the polar solvent, and the hydrophobic 'tails' (the hydrocarbon chain part of the surfactant) pointing towards the gas.⁶ This results in a reduction in the surface tension of the solution, even at low surfactant concentrations.²⁹ At air-liquid interfaces, therefore, the interfacial energy is typically reduced to about 30-35 mJ m⁻², meaning that the surface appears more like that of a hydrocarbon. The surfactant molecules are in a lower energy state when immersed in the bulk solvent, then when absorbed at the surface.³⁰

The surfactant molecules can also be adsorbed at the solid-liquid interface. The adsorption will be affected by the properties of the surface and adsorption will change the properties of the surface e.g. the wettability. In an analogous manner to the factors affecting aggregation of the surfactants in solution, surfactants adsorption at the solid surface is controlled by hydrogen bonding, electrostatic attraction, covalent bonding and van der Waal's forces. The amount of surfactants at the surface (the surface coverage) is an important parameter as it controls many processes such as oil recovery, mineral flotation, detergency, dispersion of solids and corrosion inhibition.³¹

The stabilization of emulsions and microemulsions is controlled by the adsorption of surfactants at liquid-liquid interfaces. Emulsions and microemulsions are defined as dispersions of two immiscible liquids by surfactants or surfactants and co-surfactants that form a thermodynamically stable system.^{32,33} The surfactant molecules adsorb at the liquid-liquid interface and result low interfacial energies, with some important consequences.^{6,30} If surfactants are added to an immiscible mixture of oil and water as shown in Figure 1-7, the hydrophilic head groups are attracted to the aqueous phase while the hydrocarbon chain faces the oil phase. The surfactant molecules will therefore tend to occupy the interfacial region.

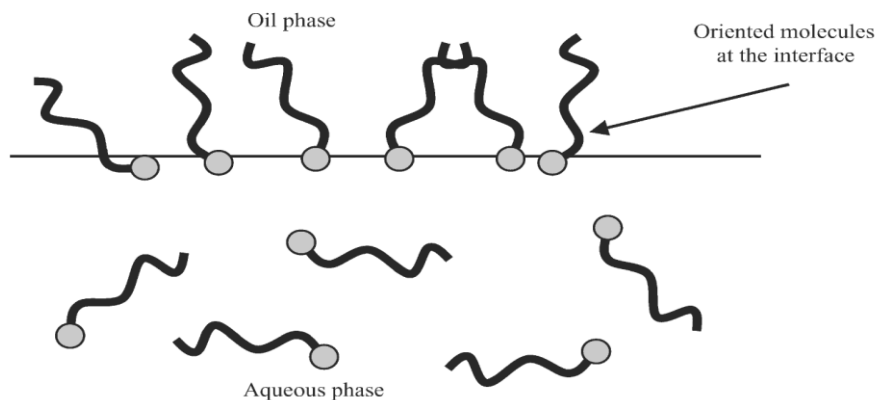


Figure 1-7: The preferential orientation of surfactant molecules at an immiscible mixture, taken from Ref.⁹

Emulsions are inherently thermodynamically, unstable systems^{34, 35} but the time scale over which they break down can vary significantly. In certain cases, provided that there is sufficient repulsion between the droplets to prevent their coalescence, and that the solubility of the dispersed phase is sufficiently small to prevent significant Ostwald ripening, the coarsening period can be very long (up to several years).³⁵

During emulsification, external shear energy is used to rupture large droplets into smaller ones.³⁴ The presence of many small droplets in the system means that the system as a whole has a larger interfacial area, implying that energy has to be added to emulsion to keep it stable (i.e. to counteract the tendency of the dispersed phase droplets to coalesce).³⁶ The reduced surface tension in a surfactant solution, helps to prevent the dispersed droplets from coalescing.^{37,38, 39} The stability of the droplets is determined mainly by the type and concentration of the surfactant in the system.⁴⁰

Emulsions are important materials with a wide variety of applications arising their ability to solubilize hydrophobic substances in an aqueous phase.³⁸ Hence the study of emulsions system is important in many industrial applications such as cosmetics, paints, agrochemicals, pharmaceuticals, bitumen emulsions, inks and paper coatings, adhesives and many household products.⁴¹

1.3 Applications of Surfactants

Surfactant systems are used in many areas such as drug delivery, cleaners, material fabrication, catalysis and biochemistry. The applications of surfactants are specified by the desired properties. Table 1-1 shows some examples of specific properties required by surfactants for different applications.

Table 1-1: Properties of surfactant required for specific applications, taken from Ref.⁹

Application	properties
Detergency	Low CMC, good salt and pH stability, biodegradability, desirable foaming properties
Emulsification	Proper HLB, environmental and biological (safety) for application
Lubrication	Chemical stability, adsorption at surfaces
Mineral flotation	Proper adsorption characteristics on the ore(s) of interest, low cost
Petroleum recovery	Proper wetting of oil-bearing formations, microemulsions formation and solubilisation properties, ease of emulsion breaking after oil recovery
Pharmaceuticals	Biocompatibility, low toxicity, proper emulsifying properties

Multiple properties of surfactant extend their application area as noted in Figure 1-8. For that reason, it seems to be more important to understand the physio-chemical properties of surfactants especially when introduced in to a new system e.g. a novel solvent.

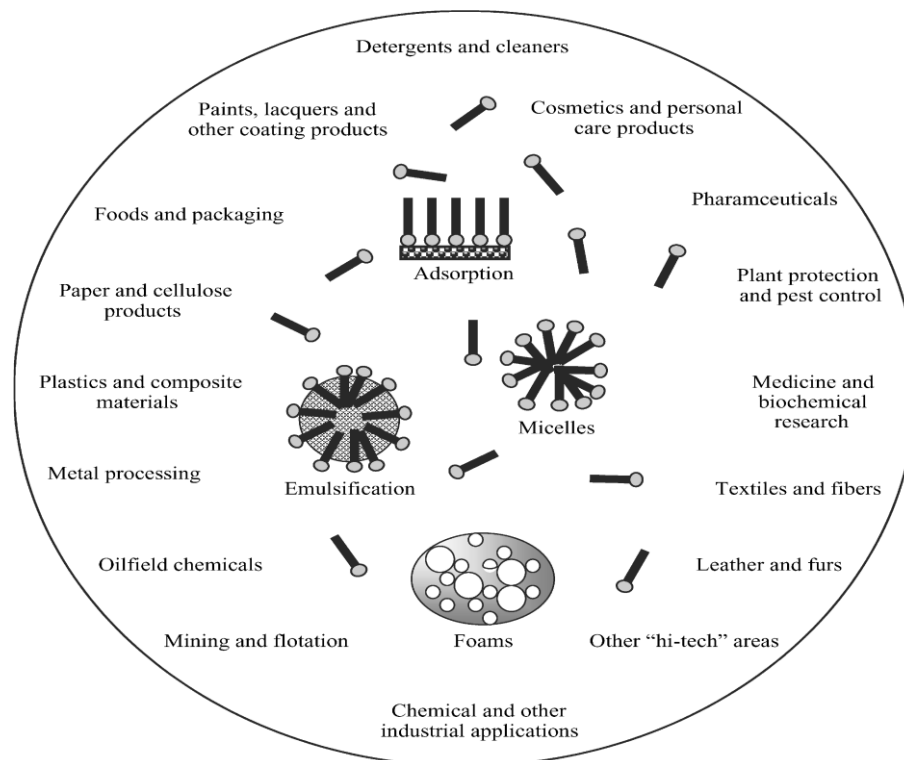


Figure 1-8: Some important, high-impact areas of surfactant applications, taken from Ref.⁹

1.4 Ionic Liquids (ILs)

This study will focus on the properties of surfactants in ionic media and will focus specifically on a type of ionic liquid known as a deep eutectic solvent (DES). It is important to describe ionic liquids (ILs) in general and focus in more detail on DESs. Salts usually have a very high melting point due to their large lattice energies. Despite melting points which can be in excess of 500 °C, molten salts are commonly used for metal processing. The lattice energy of salts decreases as the cation or anion radius increases and in the extreme where large non-symmetric organic cations and anions are used the melting point of the salts can be in the region of room temperature and often below. Walden in 1914 is often credited with the synthesis of the first ionic liquid, ethylammonium nitrate [EtNH₃]-[NO₃], which has a melting point of 12°C.⁴² The

development of ionic liquids has been recently reviewed.⁴³ Ionic liquids are organic salts, composed solely of ions, with melting points below the boiling point of water.⁴⁴ This is an arbitrary classification and one which over time has been expanded to include systems which are primarily ionic i.e. they can contain molecular components but electrostatic interactions should be important in controlling the properties of the liquids.

The properties of an ionic liquid can be tuned by variation of the ionic components. This means the property of the solvent can be regulated according to the requirement of specific application. Therefore, ionic liquids have been described as designer solvents.⁴⁵ Figure 1-9 shows the different classes of IL.

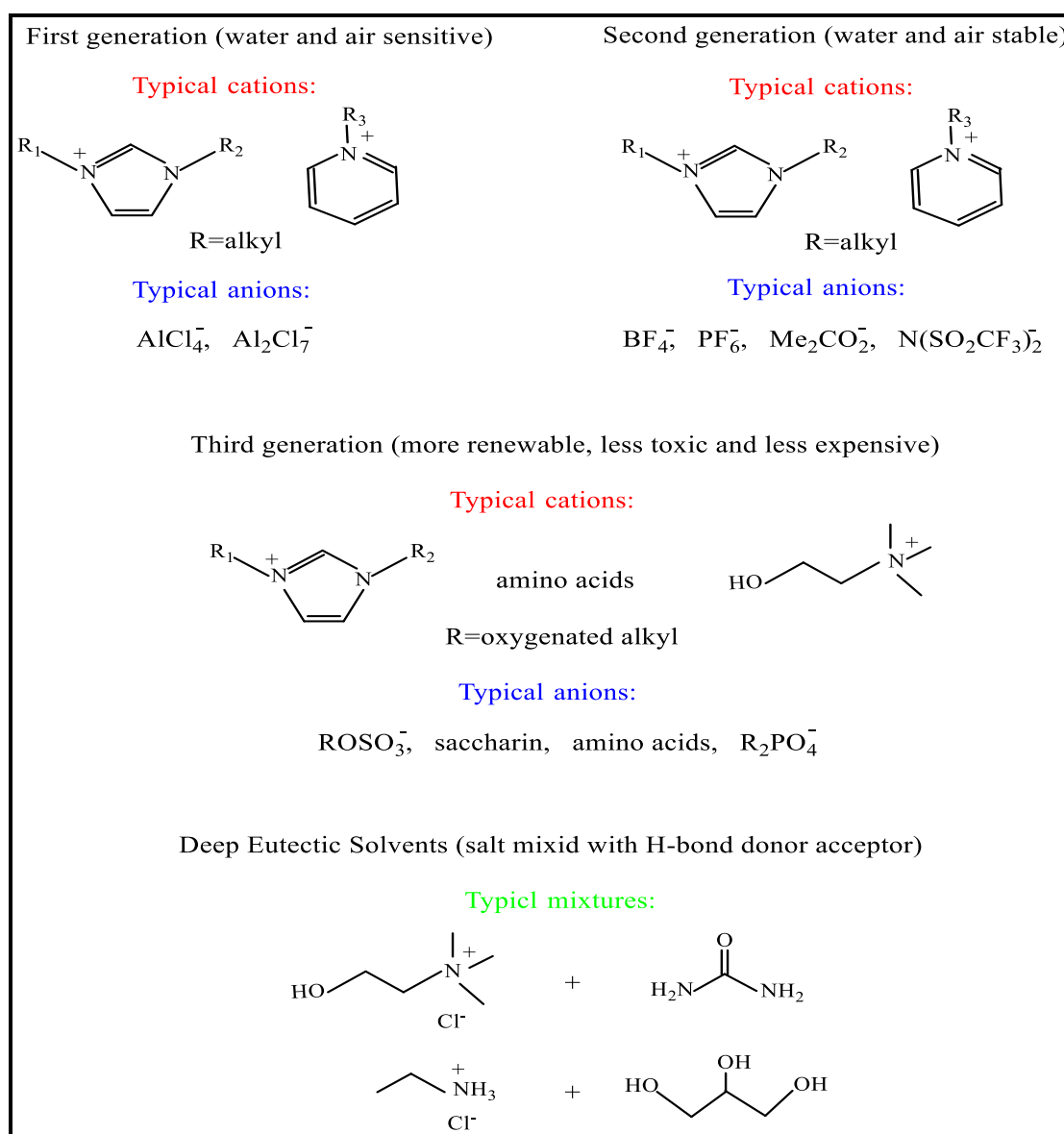


Figure 1-9: The different classes of IL by changing the start components, taken from Ref.⁴⁶

Ionic liquids generally have lower volatility and higher thermal stability compared with molecular solvents. In general, they are non-flammable and show good solubility for both organic and inorganic compounds. They tend to have wide electrochemical windows, higher conductivity and higher viscosities compared with common molecular solvents.⁴⁷ The interest in ILs was sparked by the impression that they were green solvents due to their low vapour pressure and they could largely replace organic solvents. This has however largely been discredited due to the toxicity of many ILs. These solvents have been studied in a wide range of fields such as organic and inorganic synthesis, separations, drug delivery, catalysis, electrochemistry and process chemistry.⁴⁸ A few of these areas have led to commercial processes an issue which still restricts the use of ionic liquids is the complexity of their synthesis and the associated cost of their manufacture. To this end the only processes which have so far been adopted are those where only a small volume of liquid are used and/or where significant process intensification has been achieved e.g. in the case of the BASIL process.⁴⁹

Less expensive and less toxic analogues exist although it should be understood that these tend to be less thermally stable and these tend to have a higher vapour pressure, albeit less than most molecular solvents. There is no class of solvent which is perfect for all applications and ionic liquids are gaining a reputation for designing individual solvents for specific applications. One such alternative class of liquids is known as Deep Eutectic Solvents.⁵⁰

1.5 Deep Eutectic Solvents (DESS)

The term "Deep Eutectic Solvents" was coined to describe a liquid formed from eutectic mixtures of quaternary ammonium salts and hydrogen bond donors such as amides, alcohols and carboxylic acids. One of the first of these and one of the most commonly found in the literature is, Reline, a mixture of choline chloride and urea with melting point of 12°C when mixed in a 1:2 molar ratio.^{51,52} Although, DESs have similar properties to ionic liquids, they are easy and economical to prepare and biodegradable.⁵³ They can be prepared from non-toxic components and can even be made from food grade materials such as glycerol and glucose.^{49, 54} The toxicity and biodegradability of DESs was studied by Radosevic *et al.*⁵⁵ who reported that "DESs have a green profile and a good prospect for a wide use in the field of green technologies".

While DESs have a significant (and often dominant) molecular component, these are highly associated with the anions in the mixture and tend to behave like co-crystals would in the solid state. They have similar physiochemical properties to ionic liquids and they are often considered as a sub-set of ionic liquids in the same way that protonic ionic liquids ($R_3NH^+ An^-$) would be as tri-alkylamine, R_3N can be considered as a molecular component which is largely associated with the acid $H^+ An^-$.

DESs are usually prepared by the interaction of a quaternary ammonium or phosphonium halide salt with a metal halide salt or hydrogen bond donor (HBD) such as an amide, carboxylic acid or alcohol moiety.⁵⁶ One of the main characteristics of these novel solvents is the large number of eutectic mixtures that can be created by changing either component. It has been estimated that more than 10^6 binary mixtures can be made from widely available components. Figure 1-10 show examples for components that have been used to prepare DESs.

The eutectic mixture forms a liquid due to strong interactions between the two components. In the case of type 1 eutectics the metal halide complexes with the chloride anion from the quaternary ammonium salt forming an ionic bond. The depression of freezing point compared with that of an ideal mixture of the same composition can be in the region of 250 °C.⁵⁷ For the Type 3 DESs the hydrogen bond donor forms a hydrogen bond with the halide anion and the depression of freezing point can be up to 200 °C. Recent work by Abbott *et al.*⁵⁸ determined the enthalpy of hydrogen bond formation using differential scanning calorimetry and they showed that the depression of freezing point correlated well with the enthalpy of hydrogen bond formation. It was shown using Heteronuclear Overhauser Effect Spectroscopy (HOESY), which can be used to assess the spatial proximity between two heteronuclei, for Reline that hydrogen bond formed between the hydrogens on urea and the halide anion (in this case they substituted Cl^- for F^- so that it was NMR active).⁵⁹

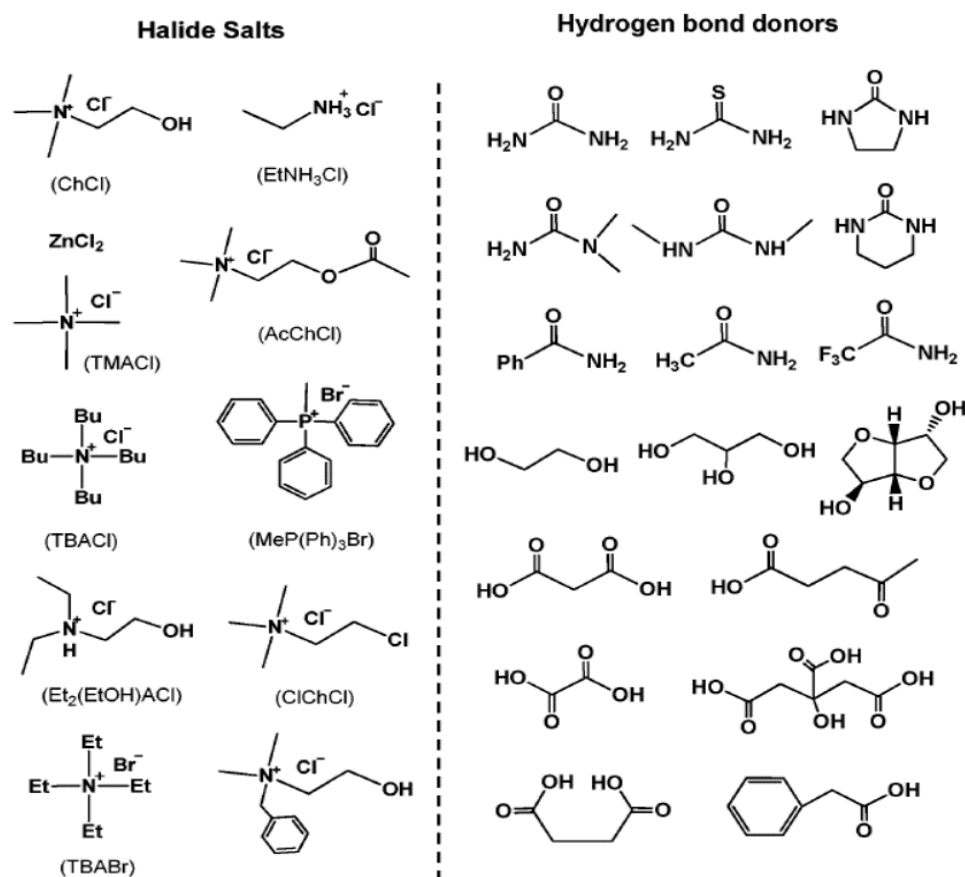


Figure 1-10: The chemicals structures of common halide salts and hydrogen bond donors used to prepare DESs, taken from Ref.⁶⁰

A recent study by Stefanovic *et al.*⁶¹ reported using quantum mechanical molecular dynamics (QM/MD) simulations to probe Ethaline, Glyceline and Reline and they found that the different in the bulk hydrogen bond donors resulted in different hydrogen bond strengths. Reline forms stronger hydrogen bond network and results in a larger melting point depression while Ethaline and Glyceline exhibit largely preserved for hydrogen bond donors based on hydroxyl. Moreover, Glyceline show over-saturation of hydrogen bond donor groups compare with Ethaline which leads to more extensive hydrogen bond donor self-interaction and hence higher cohesive forces within the bulk liquid.

Ashworth *et al.*⁶² examined Reline by density functional theory (DFT) and they reported that “In contrast to many traditional solvents, an “alphabet soup” of many different types of H-bond (OH...O=C, NH...O=C, OH...Cl, NH...Cl, OH...NH, CH...Cl, CH...O=C, NH...OH and NH...NH) can form. These H-bonds exhibit substantial flexibility in terms of number and strength”. Moreover, the variety of H-bonds formed

in DESs contrasts with traditional molecular solvents where H-bonding character tends to be more homogeneous. The DES H-bonds are strong and produce significant ordering in the liquid as confirmed by Hammond *et al.*⁶³ using neutron diffraction. This group also simulated the structure of Reline and they concluded that the hydrogen bonds formed in Reline were between all elements in the DES, not just between urea and the chloride anion. Another simulation study by Perkins *et al.* for Reline and Ethaline⁶⁴, Glyceline and Maline⁶⁵ reported that the high relative present of hydrogen bonding observe for is the interactions between the chloride anion of ChCl and the HBD. The two studies using molecular simulations and experimental IR spectroscopy concluded that this was the main interaction responsible for the decrease in freezing point.

1.5.1 Classification of DESs

DESs can be characterized by the general formula and the complex anionic species are formed between X^- and either a Lewis or Bronsted acid Y.⁶⁶



Where

Cat⁺ Cation (ammonium, phosphonium, or sulphonium)

X⁻ Lewis base (halide anion)

Y Lewis or Bronsted acid

z Number of Y molecules that interact with the anion

The classification of DESs depends on the nature of the complexing agent used.⁶⁶ Abbott *et al.*⁶⁷ (2007) defined DESs into four types, as listed in Table1-2.

Table 1-2: General formula for the types of DESs, taken from Ref.⁶⁶

Type	General formula and Terms	Example
I	$\text{Cat}^+\text{X}^- + z\text{MCl}_x$ where M = Zn, Sn, Fe, Al, Ga	Organic salt + Metal salt Choline chloride + ZnCl_2
II	$\text{Cat}^+\text{X}^- + z\text{MCl}_x \cdot y\text{H}_2\text{O}$ where M = Cr, Co, Cu, Ni, Fe	Organic salt + Metal salt (hydrate) Choline chloride + $\text{CoCl}_2 \cdot 6\text{H}_2\text{O}$
III	$\text{Cat}^+\text{X}^- + z\text{RZ}$ where Z = CONH_2 , COOH , OH	Organic salt + Hydrogen bond donor Choline chloride + Urea
IV	$\text{MCl}_x + \text{RZ}$ where M = Al, Zn Z = CONH_2 , OH	Metal salt (hydrate) + Hydrogen bond donor Zinc chloride + Urea

Type (I) DESs are an extension of some of the first ionic liquids which studied mixtures of quaternary ammonium salts and aluminium chloride. This idea was extended by a number of groups who studied other low melting point metal halides most notably zinc, iron and tin. These liquids are much more viscous than the corresponding chloroaluminate analogues. A variety of chlorometallate anions are formed in the liquids e.g. ZnCl_3^- and Zn_2Cl_5^- . They have been used for metal deposition and a range of catalytic reactions but their high viscosity significantly decreases mass transport.

This idea was extended to include metal hydrate salts, Type (II) such as $\text{CoCl}_2 \cdot 6\text{H}_2\text{O}$ and $\text{CrCl}_3 \cdot 6\text{H}_2\text{O}$. These are much less viscous and a range of metal containing complex anions is formed in solution. These liquids have been used for metal deposition, most notably chromium electroplating. The most commonly studied DESs are the type (III) solvent which are formed from a quaternary ammonium salt and a hydrogen bond donor. So far, different kinds of hydrogen bond donors have been studied including amides, carboxylic acids, and alcohols.

1.5.2 Physical Properties of DESs

In order to use DESs for an application it is important to know their physical properties such as polarity, surface tension, viscosity, conductivity and density.⁶⁸ Reference 68 highlights the common properties of various DESs described in the literature. The physical properties are significantly affected by the structure of HBD as can be seen in

Table1-3 and that is mean that their properties can be readily adjusted by changing the HBD or the salt or the ratio of the two in the mixture. The following is a brief description of some physical properties of DESs.

Table 1-3: Physical properties of common type (III) DESs at 25 °C, taken from Ref. ⁶⁶

DES	Surface Tension (mN m ⁻¹)	Viscosity (cP)	Conductivity (mS cm ⁻¹)	Density (g cm ⁻³)
Ethaline	49	36	7.61	1.12
Glyceline	56	376	1.05	1.18
Reline	52	632	0.75	1.24

Polarity: solvent polarity is very useful in characterizing solvents because it can significantly influence the course of the reaction. Although there are few papers related to the polarity of DESs those that exist report DESs to have high polarities.^{66, 67} Polarity is most commonly determined in terms of semi-empirical parameters such as the Kamlet Taft scale. This produce a normalised scale with a non-polar solvent like cyclohexane having a value of 0.00 and polar dimethyl sulfoxide having a value of 1.00. Solvatochromic indicators are used to see how a solvent stabilised an indicator molecule when it is excited with visible light. Linear solvation energy relationship (LSER) has the general form.^{69, 70}

$$XYZ = XYZ_0 + s\pi^* + bB + a\alpha \quad \text{Equation 1-1}$$

Where XYZ and XYZ_0 are solvent-dependent properties for a given solvent and a standard reference solvent respectively. XYZ could represent reaction rates, equilibrium constants or a position/intensity of spectral absorption. The α term is a measure of the hydrogen bond donor properties β is the hydrogen bond acceptor property and π^* is the polarisability/ dipolarity parameter. The terms s , a and b are constants obtained from experiment.

Table1-4 shows π^* , α and β values for the DESs used in this study. All of the polarity parameters are high and not dissimilar to those for polar solvents such as methanol and water showing that they are all polarisable and capable of donating and accepting hydrogen bonds.

Table 1-4: Kamlet and Taft solubility parameters for the DESs used in this study, taken from Ref.⁷¹

DES	π^*	α	B
Ethaline	0.96 ± 0.001	1.02 ± 0.02	0.33 ± 0.007
Glyceline	0.96 ± 0.04	1.04 ± 0.06	0.32 ± 0.01
Reline	0.98 ± 0.02	1.05 ± 0.02	0.30 ± 0.04

Surface Tension: surface tension is defined as the energy required to increase the fluid surface per unit area. This energy is caused by the effect of intermolecular forces at the interface. It is one of the essential physical properties for characterizing DESs since it provides an important information about the molecular influences on the intensity of interactions in the mixture.⁷² Surface tension plays a key role in mass transfer processes such as distillation, absorption, separation and extraction.⁷² Studies of DESs show high surface tension when compared with the surface tensions of most organic solvents, ionic liquids and high temperature molten salts.^{50, 68}

The Abbott group showed a linear decrease in surface tension of DESs with increasing temperature.⁷³ They also showed the importance of surface tension in controlling the fluidity and conductivity in ionic liquids. It was also recently shown that the surface tension controls the ability of forming a cavity in a DES and this is the over-riding factor controlling the extraction of species from an immiscible liquid into a DES.⁷⁴

Viscosity: viscosity is the measurement of the internal friction of a moving fluid or, in other words, the resistance of a substance to flow. For DESs, the viscosity is very important for the selection of suitable applications.^{68, 75-77} The viscosity of DESs is generally very high compared with conventional molecular solvents⁷⁷ and hence it limits mobility of species in solution.⁷⁸ This high viscosity can be explained by the extensive hydrogen bond network between each component in DESs, which serve to reduce the mobility of free species in the material. The large ion size and very small void volume of most DESs contribute to the high viscosity of DESs.⁶⁷ The solvent ions, have relatively large radii (about 3 to 4 Å) compared to the average radius of the voids which is about 2 Å. It has recently been shown that the viscosity of a fluid is related to the free volume and the probability of finding holes of suitable dimensions for the solvent molecules-ions to move into.⁷⁹

Conductivity: conductivity is the ability of a substance to allow the flow of an electric current. The conductivity of a solvent is an important for electrochemical applications.^{68, 80} DESs are therefore a highly investigated medium for that field.⁸⁰ The conductivity of DESs is low compared with aqueous ionic solutions with most DESs exhibiting ionic conductivities less than 2 mS cm^{-1} at room temperature.⁶⁶ This is 10 to 50 times lower than aqueous solutions. This is understandable given the relative viscosities of the two liquids. Ionic mobility is also slower in DESs as the ions are larger compared to inorganic salts typically used in aqueous electrolytes.^{66, 80}

Density: density is an important characteristic for understanding the liquid's behaviour and for determining solvent diffusion and miscibility with other liquids.⁸¹ Overall, it is notable that the density of DESs is high when compared to the density of water and most organic solvents.⁷⁸ The large extent of Coulombic interactions as well as hydrogen bonding means that the free-volume of DESs is less than that on most molecular liquids leading to the differences in the density of DESs.^{78, 82} DESs also contain high concentrations of heavy atoms such as metals and chloride which increase the mass per unit volume.⁷⁸ Increasing the proportion of salt in the DES will accordingly increase the density of the liquid. Understanding the impact of temperature on free volume and density is very important from the perspective of solvent design.^{75, 83} Increase in temperature causes a decrease in the density of DESs as the free volume increases.^{78, 84, 71.}

It is clear from the discussion above that the properties of DESs can be tuned so it would be expected that this fine tuning of structure through composition could have a significant effect on surfactants aggregation. Undoubtedly a solvent which is able to form hydrogen bonds, A high cohesive energy and high polarity will affect surfactant aggregation and micellization.^{85,86} The high ionic strength will also significantly affect the zeta potential around the micelle which could change the aggregation of the head groups.

1.5.3 Applications of DESs

DESs have been widely studied in many research areas. They have been scaled up to pilot-scale processes although few of these have resulted in commercial success to date.^{68, 83} There have been several reviews of the properties and applications of DESs.⁸⁷⁻

⁹¹ Continuing the research in DESs show more and more advantages. Although DESs

can be simply produced by mixing the two starting components and heated results in a clear liquid DES more detail about preparation process of DESs described by Abbott *et al.*⁵⁰ A study by Gutierrez *et al.*⁹² shows a new method to prepare DESs in the pure state. They used a freeze-drying of aqueous solutions of the individual starting component of DES. This well open the window for further application of DESs that require high purity of DESs. It was also recently shown that DESs could be prepared using mechano-synthetic techniques such as ball milling or extrusion. It was shown that purer DESs could be prepared by this method as it stopped decomposition of the HBD especially where it was relatively unstable at elevated temperatures e.g. sugars.⁹³

Most DESs are miscible with water and in general they have hydrophilic properties. New hydrophobic DESs were successfully prepared by Van Osch *et al.*⁹⁴ which may widen the field of applications especially for extraction. Here the hydrophobic DESs were prepared from a quaternary ammonium salt mixed with a fatty acid, decanoic acid, as hydrogen bond donor. Some groups have proposed that natural deep eutectic solvents (NADESs) can be prepared from naturally occurring compounds.⁹⁵ The issue with this description is that the term *natural* is very arbitrary. Many of the compounds described in the original papers are naturally occurring compounds such as urea, glycerol, glucose, oxalic acid and citric acid. The authors seek to create an image that natural ingredients are safe whereas some of those listed here clearly have some toxicity.

Since their discovery in 2003, DESs have attracted significant attention of various industrial and academic research groups and they have already been reported for a wide range of applications. The first interest of DESs has been in metal processing.⁹⁶⁻⁹⁹ in addition synthesis of many of organic compounds was carried out in DESs that were used as reaction media as well as catalysts.¹⁰⁰⁻¹⁰² DESs have been successfully applied as solvents or polymer synthesis.¹⁰³ Moreover, DESs uses in extraction,¹⁰⁴⁻¹⁰⁶ drug solubilisation,¹⁰⁷ lubricants¹⁰⁸ and Leather tanning.¹⁰⁹

As mentioned above surfactant could use to improve solvent propriety through their aggregation and adsorption process. It is believed that some of DESs application can be developed or improved by adding surfactants.

1.6 Self-assembly of Surfactants in Non-aqueous System

The self-aggregation and behaviour of surfactants in polar solvents, other than water, has been increasingly studied over the last two decades. Although, micelles are formed in both aqueous media and non-polar aqueous solvents, studies in water far outnumber those in other solvent.¹¹⁰ Studies have been carried out in an attempt to explain the parameters that control the formation of micelles or similar structures.¹¹¹ It is known that surfactants can aggregate in non-polar organic solvents and form inverted micelles. To differentiate micelles that formed in polar organic solvents, researchers coined the term "solvophobic interactions" instead of "hydrophobic interactions" to explain micellization in non-aqueous solution.¹¹⁰

The interest with non-aqueous media started with a study by Evans and co-workers who showed that surfactants self-aggregate to form micelles in different types of solvents.¹¹² Accordingly, several interesting studies have been published about surfactants in traditional organic solvent and mixtures of these with water.^{113, 114} Some of the solvents studied include ethyleneglycol,^{111, 115-117} formamide,^{58, 111, 118} formic acid,¹¹¹ hydrazine,¹¹² glycerol,⁵⁸ and other organic solvent.^{119, 120}

With the advent of ionic liquids some studies have been carried out into the ability of surfactants to form amphiphilic associated structures such as micelles, vesicles and liquid crystalline phases in ionic liquids. A more detailed summary of the literature in this area is contained in four reviews on the topic.¹²¹⁻¹²⁴ Based on the understanding of the self-aggregation of surfactant in ILs, the driving force to aggregate in ILs is the solvophobic interaction between the tails of the surfactant and ILs which is depend on the anionic species of the ILs.¹²⁵

In this context, Anderson's group¹²⁶ reported that various surfactants including polyoxyethylene-23-lauryl ether (Brij35), Polyoxyethylene (100) stearyl ether (Brij700), dioctyl sulfosuccinate (docSS), sodium dodecylsulfate (SDS) and caprylyl sulfobetaine (SB3-10) can form micelles in 1-butyl-3-methyl imidazolium chloride (BMIM-Cl) and hexafluorophosphate (BMIM-PF₆) and they showed that the decrease in surface tension as well as formation self-assembly in the bulk solution was due to the solvatophobic interactions between the hydrocarbon portion of surfactants and ILs. Likewise, a study by Fletcher *et al.*¹⁴ investigated the aggregation behaviour of different common

surfactants in 1-ethyl-3-methylimidazolium bis (trifluoromethylsulfonyl) imide (EMIM Tf₂N) and they reported that all non-ionic surfactants polyoxyethylene-23-lauryl ether (Brij35), Polyoxyethylene (100) stearyl ether (Brij700), Polyethylene glycol sorbitan monolaurate (Tween 20), and 4-(1,1,3,3-Tetramethylbutyl)phenyl-polyethylene glycol (Triton X100) form micelles, while the cationic surfactant Cetyltrimethylammonium bromide (CTAB) cannot form any aggregations and the anionic surfactant sodium dodecylsulfate (SDS) was not soluble. They used the change of solvatochromic probe response as a method to confirm presence of aggregation in the bulk solution. The non-ionic surfactants, polyoxyethylene alkyl self-assembly in ionic liquid, ethylammonium nitrate was reported by Araos and Warr¹²⁷ and in this study they concluded that the behaviour of aggregation is similar to that in aqueous solution however longer alkyl chains of ionic liquid are necessary to drive the aggregation process. Patrascu group¹²⁸ shows that the non-ionic surfactants, alkyl poly-(oxyethyleneglycol) ethers in ionic liquids 1-butyl-3-methyl-imidazolium with various counter ions, form aggregates that look like micelles and the nature of the IL affects the aggregation number and the size of the micelles.

Inoue's group studied the aggregation of non-ionic surfactants, polyoxyethylene (POE) in a typical room temperature ionic liquid, 1-butyl-3-methylimidazolium tetrafluoroborate. They noted that the cloud point increased with the elongation of the POE chain, but decreased with the increase in the hydrocarbon chain length which can be explained in terms of the solvophilicity/solvophobicity of the surfactants in IL.¹²⁹ The same group used differential scanning calorimetry to study the Kraft point which was in contrast with aqueous systems.¹³⁰ López-Barrón *et al.*¹³¹ showed the a thermos-reversible transition from a first-order sponge to lamellar occurred at high surfactant concentration for di-dodecyl ammonium bromide (DDAB) in the ionic liquid, ethylammonium nitrate which is in contrast to the behaviour of DDAB in aqueous solutions. The same group reported¹³² that vesicles of DDAB form spontaneously in ethylammonium nitrate, using small and ultra-small angle neutron scattering. The interfacial behaviour of charged cationic surfactants was studied by the Chen group¹³³ and they found that the interfacial energy depends on the IL structure and this was the main factor affecting the surfactant aggregation process.

Recently Chen's group¹³⁴ explored the behaviour of SDS in 1-ethyl-3-methyl imidazolium ionic liquids. They combined the results of tensiometry and NMR

techniques to conclude that the behaviour of SDS in ionic liquid is complicated by the incorporation of ionic liquid ions into the SDS micelles.

Unlike all previous studies, Atkin and Warr¹³⁵ studied the adsorption of surfactant, hexaethylene glycol monohexadecyl ether (C₁₆E₆) aggregates on graphite in presence of the ionic liquid, ethylammonium nitrate (EAN). They used atomic force microscopy in contact mode, and found that surface aggregation and the adsorption of surfactants in EAN occurs when surfactants interact strongly via their tail with the surface. This was in contrast to aqueous systems where long tails and high surfactant concentration was required to produce surface aggregates.

Fluorinated surfactants have also been studied in ionic liquid. Zhang *et al.*¹³⁶ studied the surface properties of fluorinated surfactant (FC-4) in both [BMIM][BF₄] and [BMIM][PF₆]. They concluded that the surface activity of fluorinated surfactant was greater than for traditional surfactants and thermodynamic data showed that FC-4 formed traditional micelle in [BMIM][BF₄] but it formed nano droplets in [BMIM][PF₆].

Deep eutectic solvent as medium for surfactant aggregation have had much less attention however, the last four years have attracted initial studies. The first study by Pal *et al.*¹³⁷ using fluorescence probes, electrical conductivity, and surface tension experiments identified that SDS assemblies were present in Reline containing a different amounts of water but this was not the case in pure Reline. Moreover, it was reported that SDS was able to solubilise hydrophobic cyclohexane and form microemulsions. This microstructure was confirmed using different techniques such as surface tension, dynamic light scattering and small-angle X-ray scattering. The same group¹³⁸ reported that cationic surfactants of the n-alkyltrimethylammonium family self-aggregate in Glyceline using fluorescence probe, electrical conductivity, surface tension, small-angle X-ray, dynamic light scattering, and transmission electron microscopy experiments.

Arnold *et al.*¹³⁹ used X-ray reflectivity (XRR) and small angle neutron scattering (SANS) to support the idea that SDS self-aggregate in pure DESs, Reline and this behaviour of SDS aggregate in Reline is significantly different from that in water. The same group by Sanchez-Fernandez *et al.*¹⁴⁰ reported the shape of SDS aggregates in Reline using small angle neutron scattering and again they confirmed that the SDS form

a cylindrical aggregate in that medium. In their next study, Sanchez-Fernandez *et al.*¹⁴¹ investigated the behaviour of cationic alkyltrimethylammonium bromide surfactants in Glyceline. Using surface tension, X-ray, neutron reflectivity and small angle neutron scattering, they reported that these surfactants aggregate into globular micelles with ellipsoidal shapes. Moreover, the CMC values were comparable to these published in water. The study for these cationic surfactants expanded to DES mixtures of choline chloride and malonic acid with water.¹⁴² Their result using surface tension showed that adding water affected the behaviour of the surfactants. Small-angle neutron scattering show that micelle shape was varied as a function of surfactant chain length and water content. Moreover, the effect of different counter ions on micellization of dodecylsulfate surfactants within DESs, Reline and Glyceline was reported by Sanchez-Fernandez *et al.*¹⁴³ As in aqueous solutions, the CMC and shape of micelles was found to depend on the counter ion. The type of HBD in the DES affected the morphology of micelles: more elongated aggregates formed in Reline than in Glyceline.

Li *et al.*¹⁴⁴ investigated the phase behaviour of a cationic surfactant, cetylpyridinium bromide (CPBr), in Glyceline and Ethaline using small angle X-ray scattering, polarized optical microscopy and rheological measurements. As the surfactant concentration increased, micelles changed from hexagonal phases to bicontinuous cubic phases and lamellar phases.

Deep eutectic solvents have been investigated as media for the self-assembly of other amphiphilic solutes including lipids,¹⁴⁵ proteins¹⁴⁶ and polymers.¹⁴⁷ It reported that the ability of Reline to promote phospholipid self-assembly into vesicles.¹⁴⁵ Another studies showed that lysozyme and bovine serum albumin can be structured in DES and their mixtures with water.¹⁴⁶ The conformation of poly (ethylene oxide) (PEO) was studied in DESs based on ethyl or butyl ammonium bromide with a molecular HBD, glycerol or ethylene glycol.¹⁴⁷

As some of long-chain ionic liquids behave like surface active agents Tan *et al.*¹⁴⁸ studied the aggregation of IL, $C_n\text{mimCl}$ in Glyceline. Different techniques were used to conclude that the intermolecular hydrogen-bond interactions promote aggregation processes and as in aqueous systems the solvophobic effect controls micellization. Banjare *et al.*¹⁴⁹ reported the aggregation behaviour of a short-chain IL, 1-butyl-3-methylimidazolium octylsulphate [Bmim][OS] in media of aqueous DESs, Reline and

Glyceline. The aggregation size of [Bmim][OS] measured by Dynamic Light Scattering (DLS) was larger in aqueous Reline mixtures compared with aqueous Glyceline and the CMC decreased when water was added to DESs showing that water promotes aggregation.

All above studies using ILs or DESs focus first and foremost of whether aggregation occurs and what the size and shape of the aggregates are. However, the driving force for surfactants to aggregate in a liquid of high ionic strength is still unclear.

1.7 Project Aims

Surfactants have previously been studied in the Abbott group as additives for electrodeposition. Very little was known about these systems other than a few cursory studies of the surface tension. The aim of the current study is to investigate the physical and chemical properties of surfactants in DESs. Self-aggregation will be studied in solution and at interfaces to see how it differs from aqueous solutions. A variety of surfactants will be used in three DESs; Ethaline, Glyceline, and Reline. These are chosen as they have significantly different properties. Hydrogen bonding is significantly different in the three liquids. To that direction, its objectives have been organized as follows:

In chapter 3, the bulk aggregation of surfactants in DES solutions has been studied. The physical properties of surfactants in DESs will be determined and the properties compared to its behaviour in aqueous system. Different types of surfactants with different hydrocarbon chain length have been investigated. The aim of this part is to examine the aggregates formed and the parameters such as the critical micelle concentration. Physical properties such as surface tension, viscosity, conductivity will be used to probe the solutions. Dynamic light scattering (DLS) and nanoparticle tracking analysis (NTA) will be used to give information about size and concentration of micelles in DESs. Moreover, thermodynamic of surfactants in DESs will study by electrical conductivity.

Chapter 4, will focus on the aggregation of surfactants at the interfaces. The study will start with adsorption of surfactant at air-DESs interface by mean of measurement of surface tension followed by an investigation of the wettability of metal surfaces by measuring the contact angle. While surfactants have been found to modify the nucleation metals in some DESs they do not appear to be surface active when the hydrogen bond donor is changed. The reason behind this has been probed using electrochemical measurements. Herein the study will focus on analysis the cyclic voltammetry of different probes in micellar solution to determine the diffusion coefficient and the adsorption of surfactant at the electrode surface in DESs. Finally, adsorption of surfactant at oil-DESs interface will be examined.

In Chapter 5, the study has been investigated the effect of surfactants as additive on the morphology of copper in electrodeposition experiments. The behaviour of the surfactants will be compared with that of polar molecules known to interact specifically with metal surfaces. This should provide evidence of whether charge-charge interactions or physisorption interactions control the way in which metals grow on the electrode surface.

1.8 References

1. L. L. Schramm, *Surfactants: Fundamentals and Applications in the Petroleum Industry*, Cambridge University Press, 2000.
2. L. L. Schramm, E. N. Stasiuk and D. G. Marangoni, *Annual Reports Section "C" (Physical Chemistry)*, 2003, **99**, 3-48.
3. A. Zapf, R. Beck, G. Platz and H. Hoffmann, *Advances in Colloid and Interface Science*, 2003, **100**, 349-380.
4. G. Kume, M. Gallotti and G. Nunes, *Journal of Surfactants and Detergents*, 2007, **11**, 1-11.
5. E. A. El-Hefian and A. H. Yahaya, *Australian Journal of Basic and Applied Sciences*, 2011, **5**, 1221-1227.
6. T. F. Tadros, *Applied Surfactants: Principles and Applications*, John Wiley and Sons, 2006.
7. T. Chakraborty, I. Chakraborty and S. Ghosh, *Arabian Journal of Chemistry*, 2011, **4**, 265-270.
8. K. Holmberg, B. Jönsson, B. Kronberg and B. Lindman, *Journal of Synthetic Lubrication*, 2004, **20**, 367-370.
9. D. Myers, *Surfactant Science and Technology*, John Wiley and Sons, 2005.
10. Y. Bayrak, *Turkish Journal of Chemistry*, 2003, **27**, 487-492.
11. S. Paria and K. C. Khilar, *Advances Colloid and Interface Science*, 2004, **110**, 75-95.
12. Z. Mingzheng, X. Guodong, L. Jian, C. Lei and Z. Lijun, *Experimental Thermal and Fluid Science*, 2012, **36**, 22-29.
13. D. Lombardo, M. A. Kiselev, S. Magazù and P. Calandra, *Advances in Condensed Matter Physics*, 2015, **2015**, 1-22.
14. K. A. Fletcher and S. Pandey, *Langmuir*, 2004, **20**, 33-36.
15. A. Modaressi, H. Sifaoui, B. Grzesiak, R. Solimando, U. Domanska and M. Rogalski, *Colloids and Surfaces A: Physicochemical and Engineering Aspects*, 2007, **296**, 104-108.
16. A. Dominguez, A. Fernandez, N. Gonzalez, E. Iglesias and L. Montenegro, *Journal of Chemical Education*, 1997, **74**, 1227-1231.
17. H. Ritacco, J. Kovensky, A. Fernández-Cirelli and M. J. Castro, *Journal of Chemical Education*, 2001, **78**, 347-348.

18. T. Cosgrove, *Colloid science: principles, methods and applications*, John Wiley and Sons, 2010.
19. B. Kronberg and B. Lindman, *Surfactants and Polymers in Aqueous Solution*, John Wiley and Sons, 2003.
20. R. J. Farn, *Chemistry and Technology of Surfactants*, John Wiley and Sons, 2008.
21. M. J. Rosen and J. T. Kunjappu, *Surfactants and Interfacial Phenomena*, John Wiley and Sons, 2012.
22. R.-S. Juang, Y.-Y. Xu and C.-L. Chen, *Journal of Membrane Science*, 2003, **218**, 257-267.
23. S. Shah, K. Naeem, S. W. Shah and G. M. Laghari, *Colloids and Surfaces A: Physicochemical and Engineering Aspects*, 2000, **168**, 77-85.
24. R. Hosseinzadeh, R. Maleki, A. A. Matin and Y. Nikkhahi, *Spectrochimica Acta Part A: Molecular and Biomolecular Spectroscopy*, 2008, **69**, 1183-1187.
25. J. F. Rusling, *Accounts of chemical research*, 1991, **24**, 75-81.
26. M. Setapar, S. Hamidah, W. Shiew, E. Toorisaka, M. Goto, S. Furusaki and H. Mat, *Jurnal Teknologi F*, 2008, **49**, 69-79.
27. B. Kilikian, M. Bastazin, N. Minami, E. Gonçalves and A. Junior, *Brazilian Journal of Chemical Engineering*, 2000, **17**, 29-38.
28. S. C. Chuo, S. H. Mohd-Setapar, S. N. Mohamad-Aziz and V. M. Starov, *Colloids and Surfaces A: Physicochemical and Engineering Aspects*, 2014, **460**, 137-144.
29. F. Hernáinz-Bermúdez de Castro, A. Galvez-Borrego and M. Calero-de Hoces, *Journal of Chemical & Engineering Data*, 1998, **43**, 717-718.
30. R. Pashley and M. Karaman, *Applied Colloid and Surface Chemistry*, John Wiley and Sons, 2005.
31. S. Paria and K. C. Khilar, *Advances in Colloid and Interface Science*, 2004, **110**, 75-95.
32. C. Mo, M. Zhong and Q. Zhong, *Journal of Electroanalytical Chemistry*, 2000, **493**, 100-107.
33. T. G. Mason, J. N. Wilking, K. Meleson, C. B. Chang and S. M. Graves, *Journal of Physics: Condensed Matter*, 2006, **18**, 635-666.
34. T. Mason, *Current Opinion in Colloid and Interface Science*, 1999, **4**, 231-238.
35. J. Bibette, *Journal of Magnetism and Magnetic Materials*, 1993, **122**, 37-41.

36. T. D. Dimitrova, S. Cauvin, J. P. Lecomte and A. Colson, *The Canadian Journal of Chemical Engineering*, 2014, **92**, 330-336.
37. R. K. Shah, H. C. Shum, A. C. Rowat, D. Lee, J. J. Agresti, A. S. Utada, L.-Y. Chu, J.-W. Kim, A. Fernandez-Nieves, C. J. Martinez and D. A. Weitz, *Materials Today*, 2008, **11**, 18-27.
38. J. Bibette and F. Leal-Calderon, *Current Opinion in Colloid and Interface Science*, 1996, **1**, 746-751.
39. M. V. Tzoumaki, T. Moschakis, V. Kiosseoglou and C. G. Biliaderis, *Food Hydrocolloids*, 2011, **25**, 1521-1529.
40. S. R. Derkach, *Advances Colloid and Interface Science*, 2009, **151**, 1-23.
41. T. F. Tadros, *Colloids and Surfaces A: Physicochemical and Engineering Aspects*, 1994, **91**, 39-55.
42. T. Welton, *Chemical Reviews*, 1999, **99**, 2071-2084.
43. K. Marsh, J. Boxall and R. Lichtenthaler, *Fluid Phase Equilibria*, 2004, **219**, 93-98.
44. A. P. Abbott, G. Frisch, J. Hartley and K. S. Ryder, *Green Chemistry*, 2011, **13**, 471-481.
45. R. Dixit, *Quest*, 2013, **1**, 12-15.
46. J. Gorke, F. Srienc and R. Kazlauskas, *Biotechnology and Bioprocess Engineering*, 2010, **15**, 40-53.
47. J. F. Wishart and E. W. Castner, *The Journal of Physical Chemistry B*, 2007, **111**, 4639-4640.
48. M. C. Buzzeo, R. G. Evans and R. G. Compton, *ChemPhysChem*, 2004, **5**, 1106-1120.
49. M. A. Kareem, F. S. Mjalli, M. A. Hashim and I. M. AlNashef, *Journal of Chemical and Engineering Data*, 2010, **55**, 4632-4637.
50. A. P. Abbott, D. Boothby, G. Capper, D. L. Davies and R. K. Rasheed, *Journal of the American Chemical Society*, 2004, **126**, 9142-9147.
51. A. P. Abbott, G. Capper, D. L. Davies, R. K. Rasheed and V. Tambyrajah, *Chemical Communications*, 2003, 70-71.
52. D. V. Wagle, H. Zhao and G. A. Baker, *Accounts of Chemical Research*, 2014, **47**, 2299-2308.
53. K. R. Siongco, R. B. Leron, A. R. Caparanga and M.-H. Li, *Thermochimica Acta*, 2013, **566**, 50-56.

54. Z. Maugeri and P. D. de María, *Royal Society of Chemistry Advances*, 2012, **2**, 421-425.
55. K. Radošević, M. C. Bubalo, V. G. Srček, D. Grgas, T. L. Dragičević and I. R. Redovniković, *Ecotoxicology and Environmental Safety*, 2015, **112**, 46-53.
56. A. Popescu, C. Donath and V. Constantin, *Bulgarian Chemical Communications*, 2014, **46**, 452-457.
57. R. B. Leron, A. N. Soriano and M.-H. Li, *Journal of the Taiwan Institute of Chemical Engineers*, 2012, **43**, 551-557.
58. X. Auvray, C. Petipas, R. Anthore, I. Rico and A. Lattes, *The Journal of Physical Chemistry*, 1989, **93**, 7458-7464.
59. A. P. Abbott, G. Capper, D. L. Davies, R. K. Rasheed and V. Tambyrajah, *Chemical Communications*, 2003, 70-71.
60. Q. Zhang, K. D. O. Vigier, S. Royer and F. Jérôme, *Chemical Society Reviews*, 2012, **41**, 7108-7146.
61. R. Stefanovic, M. Ludwig, G. B. Webber, R. Atkin and A. J. Page, *Physical Chemistry Chemical Physics*, 2017, **19**, 3297-3306.
62. C. R. Ashworth, R. P. Matthews, T. Welton and P. A. Hunt, *Physical Chemistry Chemical Physics*, 2016, **18**, 18145-18160.
63. O. S. Hammond, D. T. Bowron and K. J. Edler, *Green Chemistry*, 2016, **18**, 2736-2744.
64. S. L. Perkins, P. Painter and C. M. Colina, *The Journal of Physical Chemistry B*, 2013, **117**, 10250-10260.
65. S. L. Perkins, P. Painter and C. M. Colina, *Journal of Chemical and Engineering Data*, 2014, **59**, 3652-3662.
66. E. L. Smith, A. P. Abbott and K. S. Ryder, *Chemical Reviews*, 2014, **114**, 11060-11082.
67. Q. Zhang, K. De Oliveira Vigier, S. Royer and F. Jerome, *Chemical Society Reviews*, 2012, **41**, 7108-7146.
68. B. Tang and K. H. Row, *Monatshefte für Chemie - Chemical Monthly*, 2013, **144**, 1427-1454.
69. M. J. Kamlet and R. Taft, *Journal of the American chemical Society*, 1976, **98**, 377-383.
70. M. J. Kamlet, J. L. M. Abboud, M. H. Abraham and R. Taft, *The Journal of Organic Chemistry*, 1983, **48**, 2877-2887.

71. R. C. Harris, PhD Thesis, University of Leicester, 2009.
72. K. Shahbaz, F. S. Mjalli, M. A. Hashim and I. M. AlNashef, *Fluid Phase Equilibria*, 2012, **319**, 48-54.
73. A. P. Abbott, R. C. Harris, K. S. Ryder, C. D'Agostino, L. F. Gladden and M. D. Mantle, *Green Chemistry*, 2011, **13**, 82-90.
74. A. P. Abbott, A. Y. Al-Murshedi, O. A. Alshammari, R. C. Harris, J. H. Kareem, I. B. Qader and K. Ryder, *Fluid Phase Equilibria*, 2017, **448**, 99-104.
75. A. Hayyan, F. S. Mjalli, I. M. AlNashef, T. Al-Wahaibi, Y. M. Al-Wahaibi and M. A. Hashim, *Thermochimica Acta*, 2012, **541**, 70-75.
76. Z. Maugeri and P. Domínguez de María, *Royal Society of Chemistry Advances*, 2012, **2**, 421-425.
77. F. S. Mjalli and J. Naser, *Asia-Pacific Journal of Chemical Engineering*, 2015, **10**, 273-281.
78. R. Yusof, E. Abdulmalek, K. Sirat and M. B. Rahman, *Molecules*, 2014, **19**, 8011-8026.
79. A. P. Abbott, G. Capper and S. Gray, *Chemphyschem: A European Journal of Chemical physical and Physical Chemistry*, 2006, **7**, 803-806.
80. C. Ruß and B. König, *Green Chemistry*, 2012, **14**, 2969.
81. B. Jibril, F. Mjalli, J. Naser and Z. Gano, *Journal of Molecular Liquids*, 2014, **199**, 462-469.
82. A. P. Abbott, J. C. Barron, K. S. Ryder and D. Wilson, *Chemistry-A European Journal*, 2007, **13**, 6495-6501.
83. K. Shahbaz, F. S. Mjalli, M. A. Hashim and I. M. AlNashef, *Thermochimica Acta*, 2011, **515**, 67-72.
84. A. Popescu, C. Donath and V. Constantin, *Bulgarian Chemical Communications*, 2014, **46**, 452-457.
85. K. Gracie, D. Turner and R. Palepu, *Canadian Journal of Chemistry*, 1996, **74**, 1616-1625.
86. C. C. Ruiz, L. Díaz-López and J. Aguiar, *Journal of Dispersion Science and Technology*, 2008, **29**, 266-273.
87. Q. Zhang, K. D. O. Vigier, S. Royer and F. Jerome, *Chemical Society Reviews*, 2012, **41**, 7108-7146.
88. E. Durand, J. Lecomte and P. Villeneuve, *European Journal of Lipid Science and Technology*, 2013, **115**, 379-385.

89. A. Paiva, R. Craveiro, I. Aroso, M. Martins, R. L. Reis and A. R. C. Duarte, *ACS Sustainable Chemistry and Engineering*, 2014, **2**, 1063-1071.
90. D. Carriazo, M. C. Serrano, M. C. Gutiérrez, M. L. Ferrer and F. del Monte, *Chemical Society Reviews*, 2012, **41**, 4996-5014.
91. X. Ge, C. Gu, X. Wang and J. Tu, *Journal of Materials Chemistry A*, 2017, **5**, 8209-8229.
92. M. C. Gutiérrez, M. L. Ferrer, C. R. Mateo and F. del Monte, *Langmuir*, 2009, **25**, 5509-5515.
93. D. Crawford, L. Wright, S. James and A. Abbott, *Chemical Communications*, 2016, **52**, 4215-4218.
94. D. J. van Osch, L. F. Zubeir, A. van den Bruinhorst, M. A. Rocha and M. C. Kroon, *Green Chemistry*, 2015, **17**, 4518-4521.
95. Y. Dai, J. van Spronsen, G.-J. Witkamp, R. Verpoorte and Y. H. Choi, *Analytica Chimica Acta*, 2013, **766**, 61-68.
96. M. Starykevich, A. N. Salak, D. K. Ivanou, A. D. Lisenkov, M. L. Zheludkevich and M. G. S. Ferreira, *Electrochimica Acta*, 2015, **170**, 284-291.
97. C. A. Nkuku and R. J. LeSuer, *The Journal of Physical Chemistry B*, 2007, **111**, 13271-13277.
98. Q. Xu, T. S. Zhao, L. Wei, C. Zhang and X. L. Zhou, *Electrochimica Acta*, 2015, **154**, 462-467.
99. A. P. Abbott, R. C. Harris, F. Holyoak, G. Frisch, J. Hartley and G. R. Jenkin, *Green Chemistry*, 2015, **17**, 2172-2179.
100. Y. A. Sonawane, S. B. Phadtare, B. N. Borse, A. R. Jagtap and G. S. Shankarling, *Organic Letters*, 2010, **12**, 1456-1459.
101. B. S. Singh, H. R. Lobo and G. S. Shankarling, *Catalysis Communications*, 2012, **24**, 70-74.
102. S. Handy and K. Lavender, *Tetrahedron Letters*, 2013, **54**, 4377-4379.
103. J.-H. Liao, P.-C. Wu and Y.-H. Bai, *Inorganic Chemistry Communications*, 2005, **8**, 390-392.
104. F. S. Oliveira, A. B. Pereiro, L. P. Rebelo and I. M. Marrucho, *Green Chemistry*, 2013, **15**, 1326-1330.
105. K. M. Jeong, M. S. Lee, M. W. Nam, J. Zhao, Y. Jin, D.-K. Lee, S. W. Kwon, J. H. Jeong and J. Lee, *Journal of Chromatography A*, 2015, **1424**, 10-17.
106. E. Yilmaz and M. Soylak, *Talanta*, 2015, **136**, 170-173.

107. H. G. Morrison, C. C. Sun and S. Neervannan, *International Journal of Pharmaceutics*, 2009, **378**, 136-139.
108. A. P. Abbott, E. I. Ahmed, R. C. Harris and K. S. Ryder, *Green Chemistry*, 2014, **16**, 4156-4161.
109. A. P. Abbott, O. Alaysuy, A. P. M. Antunes, A. C. Douglas, J. Guthrie-Strachan and W. R. Wise, *ACS Sustainable Chemistry and Engineering*, 2015, **3**, 1241-1247.
110. M. S. Akhter, *Colloids and Surfaces A: Physicochemical and Engineering Aspects*, 1997, **121**, 103-109.
111. W. Binana-Limbele and R. Zana, *Colloid and Polymer Science*, 1989, **267**, 440-447.
112. M. S. Ramadan, D. F. Evans and R. Lumry, *The Journal of Physical Chemistry*, 1983, **87**, 4538-4543.
113. J.-B. Huang, M. Mao and B.-Y. Zhu, *Colloids and Surfaces A: Physicochemical and Engineering Aspects*, 1999, **155**, 339-348.
114. Y. Li, G. Fei, Z. Honglin, L. Zhen, Z. Liqiang and L. Ganzuo, *Journal of Thermal Analysis and Calorimetry*, 2009, **96**, 859-864.
115. A. Ray, *Journal of the American Chemical Society*, 1969, **91**, 6511-6512.
116. L. G. Ionescu and D. S. Fung, *Journal of the Chemical Society, Faraday Transactions 1: Physical Chemistry in Condensed Phases*, 1981, **77**, 2907-2912.
117. H. Gharibi, R. Palepu, D. Bloor, D. Hall and E. Wyn-Jones, *Langmuir*, 1992, **8**, 782-787.
118. M. Thomason, D. Bloor and E. Wyn-Jones, *Langmuir*, 1992, **8**, 2107-2109.
119. H. Singh, S. M. Saleem, R. Singh and K. Birdi, *The Journal of Physical Chemistry*, 1980, **84**, 2191-2194.
120. T. L. Greaves, A. Weerawardena and C. J. Drummond, *Physical Chemistry Chemical Physics*, 2011, **13**, 9180-9186.
121. M. M. Hoffmann, M. P. Heitz, J. B. Carr and J. D. Tubbs, *Journal of Dispersion Science and Technology*, 2003, **24**, 155-171.
122. J. Hao, A. Song, J. Wang, X. Chen, W. Zhuang, F. Shi, F. Zhou and W. Liu, *Chemistry-a European Journal*, 2005, **11**, 3936-3940.
123. T. L. Greaves and C. J. Drummond, *Chemical Society Reviews*, 2008, **37**, 1709-1726.

124. T. L. Greaves and C. J. Drummond, *Chemical Society Reviews*, 2013, **42**, 1096-1120.
125. T. Inoue, K. Kawashima and Y. Miyagawa, *Journal of Colloid and Interface Science*, 2011, **363**, 295-300.
126. J. L. Anderson, V. n. Pino, E. C. Hagberg, V. V. Sheares and D. W. Armstrong, *Chemical Communications*, 2003, DOI: 10.1039/b307516h, 2444.
127. M. U. Araos and G. G. Warr, *The Journal of Physical Chemistry B*, 2005, **109**, 14275-14277.
128. C. Patrascu, F. Gauffre, F. Nallet, R. Bordes, J. Oberdisse, N. de Lauth-Viguerie and C. Mingotaud, *ChemPhysChem: A European Journal of Chemical physical and Physical Chemistry*, 2006, **7**, 99-101.
129. T. Inoue and T. Misono, *Journal of Colloid and Interface Science*, 2008, **326**, 483-489.
130. T. Inoue, Y. Higuchi and T. Misono, *Journal of Colloid and Interface Science*, 2009, **338**, 308-311.
131. C. R. López-Barrón, M. G. Basavaraj, L. DeRita and N. J. Wagner, *The Journal of Physical Chemistry B*, 2011, **116**, 813-822.
132. C. R. López-Barrón, D. Li, L. DeRita, M. G. Basavaraj and N. J. Wagner, *Journal of the American Chemical Society*, 2012, **134**, 20728-20732.
133. L. G. Chen and H. Bermudez, *Langmuir*, 2012, **28**, 1157-1162.
134. L. G. Chen, S. H. Strassburg and H. Bermudez, *Journal of Colloid and Interface Science*, 2016, **477**, 40-45.
135. R. Atkin and G. G. Warr, *Journal of the American Chemical Society*, 2005, **127**, 11940-11941.
136. N. Li, S. Zhang, L. Zheng, J. Wu, X. Li and L. Yu, *The Journal of Physical Chemistry B*, 2008, **112**, 12453-12460.
137. M. Pal, R. Rai, A. Yadav, R. Khanna, G. A. Baker and S. Pandey, *Langmuir*, 2014, **30**, 13191-13198.
138. M. Pal, R. K. Singh and S. Pandey, *ChemPhysChem: A European Journal of Chemical physical and Physical Chemistry*, 2015, **16**, 2538-2542.
139. T. Arnold, A. J. Jackson, A. Sanchez-Fernandez, D. Magnone, A. Terry and K. Edler, *Langmuir*, 2015, **31**, 12894-12902.

140. A. Sanchez-Fernandez, K. J. Edler, T. Arnold, R. K. Heenan, L. Porcar, N. J. Terrill, A. Terry and A. J. Jackson, *Physical Chemistry Chemical Physics*, 2016, **18**, 14063-14073.
141. A. Sanchez-Fernandez, T. Arnold, A. J. Jackson, S. L. Fussell, R. K. Heenan, R. A. Campbell and K. J. Edler, *Physical Chemistry Chemical Physics*, 2016, **18**, 33240-33249.
142. A. Sanchez-Fernandez, O. S. Hammond, A. J. Jackson, T. Arnold, J. Douth and K. J. Edler, *Langmuir*, 2017, **33**, 14304-14314.
143. A. Sanchez-Fernandez, O. Hammond, K. Edler, T. Arnold, J. Douth, R. Dalglish, P. Li, K. Ma and A. Jackson, *Physical Chemistry Chemical Physics*, 2018, **20**, 13952-13961.
144. Q. Li, J. Wang, N. Lei, M. Yan, X. Chen and X. Yue, *Physical Chemistry Chemical Physics*, 2018, **20**, 12175-12181.
145. S. J. Bryant, R. Atkin and G. G. Warr, *Soft Matter*, 2016, **12**, 1645-1648.
146. A. Sanchez-Fernandez, K. Edler, T. Arnold, D. A. Venero and A. Jackson, *Physical Chemistry Chemical Physics*, 2017, **19**, 8667-8670.
147. Z. Chen, S. McDonald, P. FitzGerald, G. G. Warr and R. Atkin, *Journal of Colloid and Interface Science*, 2017, **506**, 486-492.
148. X. Tan, J. Zhang, T. Luo, X. Sang, C. Liu, B. Zhang, L. Peng, W. Li and B. Han, *Soft matter*, 2016, **12**, 5297-5303.
149. M. K. Banjare, K. Behera, M. L. Satnami, S. Pandey and K. K. Ghosh, *Royal Society of Chemistry Advances*, 2018, **8**, 7969-7979.

2 Experimental Section

2	Experimental Section.....	38
2.1	Materials.....	39
2.2	Preparation of Solutions.....	39
2.2.1	Preparation of DESs.....	39
2.2.2	Preparation of Surfactant Solutions in DESs.....	40
2.2.3	Preparation of Surfactant Solutions with Probe in DESs.....	40
2.2.4	Preparation of Emulsions.....	40
2.3	Physical Properties of Surfactant Solutions in DESs.....	40
2.3.1	Determination of Critical Micelle Concentration.....	40
2.3.2	Viscosity.....	44
2.3.3	Contact Angle.....	45
2.3.4	Conductivity.....	45
2.3.5	Zeta Potential.....	45
2.3.6	Aggregation Analysis.....	45
2.4	Electrochemical Study.....	47
2.4.1	Cyclic Voltammetry.....	48
2.4.2	Chronoamperometry.....	48
2.4.3	Bulk Electrodeposition of Copper.....	48
2.5	Surface Analysis.....	49
2.5.1	Scanning Electron Microscopy.....	49
2.5.2	X-Ray Diffraction.....	49
2.5.3	3D Optical Microscopy.....	49
2.6	References.....	50

2.1 Materials

Table 2-1 lists the chemicals used in this work. All chemicals were used as received without further purification.

Table 2-1: List of chemicals and their specifications.

Chemicals	Source	Purity %
Choline chloride	Sigma-Aldrich	≥98.0
Ethylene glycol	Sigma-Aldrich	≥99.0
Glycerol	Fischer	98.0
Urea	Sigma-Aldrich	99.9
Lithium chloride (LiCl)	Sigma-Aldrich	≥99.0
Sodium dodecyl sulfate (SDS)	Sigma-Aldrich	99.0
Cetyltrimethylammonium bromide (CTAB)	Sigma-Aldrich	≥99.0
Polyethylene glycol hexadecyl ether (Brij-58)	Sigma-Aldrich	-
Bis (2-ethylhexyl) sulfosuccinate sodium salt (AOT)	Sigma-Aldrich	98.0
7,7,8,8-Tetracyanoquinodimethane (TCNQ)	Sigma-Aldrich	98.0
Pyrene	Sigma-Aldrich	99.0
Iron (II) chloride (FeCl ₂)	Alfa Aesar	99.5
Tetrathiafulvalene (TTF)	Sigma-Aldrich	97.0
Copper chloride dehydrate CuCl ₂ .2H ₂ O	Sigma-Aldrich	99.9%
Hexane (C ₆ H ₁₄)	Fisher	99

2.2 Preparation of Solutions

2.2.1 Preparation of DESs

Ethaline and Glyceline were prepared by mixing choline chloride with ethylene glycol and glycerol respectively in a 1:2 molar ratio. The mixtures were then stirred and heated on a hotplate at 50 °C until homogeneous liquids were obtained. Reline was made by mixing choline chloride with urea in a 1:2 molar ratio. The mixture was stirred and kept in an oven at 50°C. Once a slurry was formed in the oven, a homogenous liquid was formed by further stirring and heating at 50°C on a stirrer hotplate. DESs based between lithium chloride and ethylene glycol were prepared for some experiments by mixing

lithium chloride with ethylene glycol in 1:4 molar ratio. The mixtures stirred and heated on a hotplate at 50°C until a homogeneous liquid were obtained.

2.2.2 Preparation of Surfactant Solutions in DESs

Stock solutions of surfactants, SDS and AOT were prepared in DESs. These stock solutions were diluted in order to obtain solutions at different concentrations. All solutions were left for at least 72 h in the oven at 50°C to reach equilibration before any measurement was taken.

2.2.3 Preparation of Surfactant Solutions with Probe in DESs

Pyrene and 7,7,8,8-tetracyanoquinodimethane (TCNQ) were used as probe to determine the (CMC) by fluorescence spectrophotometer and UV-Vis spectroscopy respectively. Moreover, iron (II) chloride (FeCl_2), tetrathiafulvalene (TTF) were used as probe for the determination of the diffusion coefficient of micelles in DESs by electrochemical techniques, cyclic voltammetry. In all cases a known amount of probe was dissolved in DES either Ethaline, Glyceline or Reline in a volumetric flask with well-known probe concentration. This solution was used to prepare different concentration of surfactants in order to have only same concentration of the probe in surfactant solutions in DESs. Again all solutions were left in the oven at 50°C for about 72 h to reach equilibration before any measurements were taken. It is well know that the temperature effected CMC values and the diffusion coefficient therefore, all measurements were done under constant temperature.

2.2.4 Preparation of Emulsions

The surfactant, SDS was used to prepare oil-in-DESs (O/DES) emulsions. A 10 ml of 25 mM SDS in either DESs or water were mixed with 1 ml of hexane. The mixture was then stirred and heated on hotplate at about 50°C for approximately 2 h.

2.3 Physical Properties of Surfactant Solutions in DESs

2.3.1 Determination of Critical Micelle Concentration

To determine the critical micelle concentration (CMC) values of surfactants, in DESs three common techniques in this work were used. The change in physical and chemical properties of SDS solutions when micelles are formed are observe by direct method,

tensiometric technique and indirect methods, the UV-visible spectrum of TCNQ and the fluorescence emission spectrum of pyrene monomers. The change in the surface tension of surfactants solutions is because of adsorption of surfactant at the liquid-air interface whereas UV-visible spectroscopy and fluorescence spectroscopy indicate changes in the medium of the probe solubilize in surfactants solutions. Experimentally, CMC can be determined by detect the discontinuity change of a suitable physical property as a function of surfactant concentration. The point of intersection at the abrupt change marks the critical micelle concentration CMC.

2.3.1.1 Surface Tension

The surface tension is perhaps the most important technique to measure the CMC value. In this work a Wilhelmy plate method was employed and will be described here.

The principle under-pinning the Wilhelmy plate method is quite simple. A thin platinum plate, which is cleaned by insertion into a hot Bunsen flame, is attached to a balance and dipped into the vessel containing the liquid as shown in Figure 2-1. The liquid level is raised until it just touches the hanging plate and the force, F on the plate is recorded. The surface tension, γ , can be calculated using the Wilhelmy Equation 2-1.

$$\gamma = \frac{F}{l \cos \theta} \quad \text{Equation 2-1}$$

Where l is the wetted perimeter of the plate and θ is the contact angle. When the plate is just wetted by the solution the contact angle will be zero between the plate and the liquid. Therefore, the Wilhelmy equation simplifies to Equation 2-2.

$$\gamma = \frac{F}{l} \quad \text{Equation 2-2}$$

The Wilhelmy plate technique measures equilibrium surface tension and does not require correction for the liquid meniscus. When the surface tension is measured, the plate was dipped right at the surface of the liquid. Therefore, the surfactant has sufficient time to reach equilibrium.

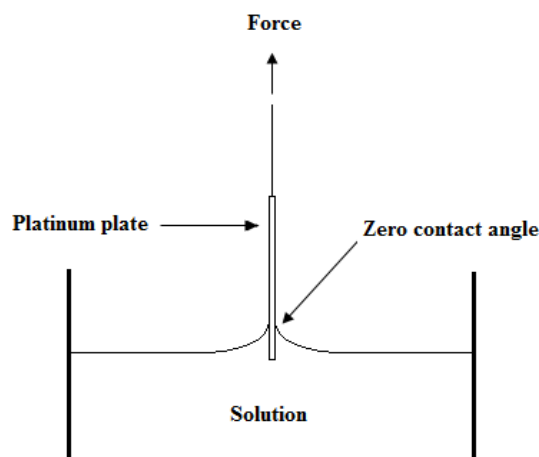


Figure 2-1: *The Wilhelmy plate method.*

The surface tension of surfactants, SDS and AOT in DESs was measured using A KRÜSS tensiometer K9 model K9MK1. Measurements were taken using a Pt-Ir alloy plate (KRUSS, part number PL01). A surfactant solution in DESs was placed in a glass dish surrounded by thermostat flask at the required temperature, 25°C. The procedure was repeated at least three times for each sample. The plate used in the measurement was cleaned using a Bunsen flame.

2.3.1.2 UV- Vis Spectroscopy

Dye solubilisation is one of the simplest methods used to determine the CMC of surfactants where the dye absorbance is changed as a function of the surfactant concentration hence the break in the spectrum can be used to determine the CMC. All 7,7,8,8-tetracyanoquinodimethane (TCNQ) solubilised in SDS in DESs samples were prepared as mentioned in ref.¹ The absorption spectra were measured using a Shimadzu UV- Visible spectrophotometer 1601. The path length for the quartz cell was 10 mm and the spectra were measured in the range 200-950 nm.

2.3.1.3 Fluorescence Spectroscopy

This method is often used to determine the CMC of surfactant solutions. In this method, the vibrational band intensities of pyrene are changed based on pyrene monomer environment. Where the intensities of the vibrational bands of pyrene presented a strong dependence on solvent environment. The typical fluorescence emission spectrum of pyrene clearly shows significant vibration structure consisting five distinct peaks (see

Figure 2-2). Intensities located at 373 nm, first vibronic bands (I_i) and 384 nm, third vibronic bands (I_{iii}) were used to determine the ratio I_i/I_{iii} , a well-known solvent polarity scale “hydrophobic index”.^{2, 3} The vibronic band (I_i) is promoted in the polar environment, whereas the vibronic band (I_{iii}) is noted to be insensitive to the changes in the medium.⁴ This ratio I_i/I_{iii} is a useful method to determined CMC. The decrease in the I_i/I_{iii} ratio with increasing surfactant concentration results from solubilisation of pyrene, a hydrophobic compound, in the micellar core. So its spectrum alters depend on surfactant concentration below or above the CMC.³

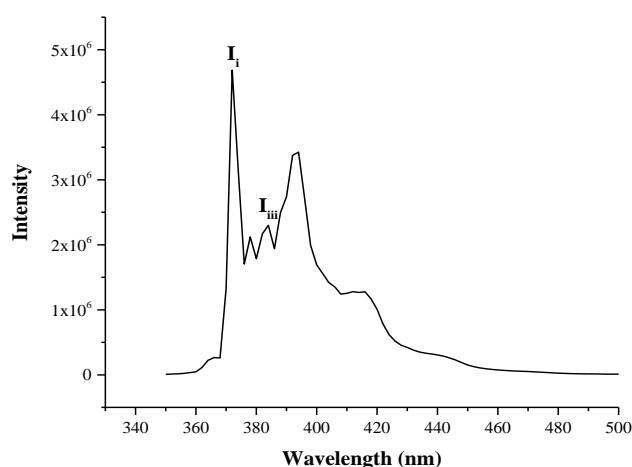


Figure 2-2: Typical fluorescence emission spectrum of pyrene 1µM in DESs, Ethaline.

The spectrum change of pyrene has been employed for determination CMC of SDS in DESs. All fluorescence measurements using pyrene as the fluorescent probe were carried out in a Jobin Yvon Horiba FluoroMax-P spectrometer using a 10 mm path length quartz cuvette. Excitation was set to a wavelengths at 265, 310 and 320 nm and the emissions were recorded in the wavelength range 275-500, 320-500 and 230-500 nm for SDS solutions in Ethaline, Glyceline and Reline respectively. The slit widths fixed at 5 and 1 nm for the excitation and emission, respectively.

For the determination of CMC, a 1µM pyrene solution was prepared in the DESs. This solution was used to prepared different solutions of surfactants in the DESs. The final solutions were stirred for 7 day in the oven at 50°C to solubilize the pyrene into the SDS micelles.

2.3.2 Viscosity

The viscosity of surfactants in DESs was measured using both rotational viscometers and quartz crystal microbalance (QCM). The viscosity of SDS in DESs were measured using a Brookfield DV-E Viscometer fitted with a thermostat jacket to detect the temperature. Moreover, the viscosity has also been measured using the QCM Agilent Technologies E5061A300 KHz ENA Series Network Analyzer at 25°C. The thin wafer (~ 0.2 mm of thickness) of the 10 MHz quartz crystals has the surface finish of 2 μm for the smooth crystals. The advantage of using this technique is that a minimal sample volume is required of about 1 ml.

The principal of QCM as viscometer depends on the change of the fundamental frequency, f_0 of a flat quartz surface operating in a vacuum compared to the frequency upon its immersion in a liquid, f_l , of given viscosity, η_l and density, ρ_l . This change in frequency, Δf is proportional to $-(\eta_l \rho_l)^{1/2}$ as follows:⁵

$$\Delta f = f_0 - f_l = -f_0^{\frac{3}{2}} \sqrt{\frac{\eta_l \rho_l}{\pi \rho_q \mu_q}} \quad \text{Equation 2-3}$$

Where ρ_q and μ_q represent the crystal density and crystal shear modulus respectively. Figure 2-3 shows a schematic diagram of the QCM cell used to make viscosity measurements.

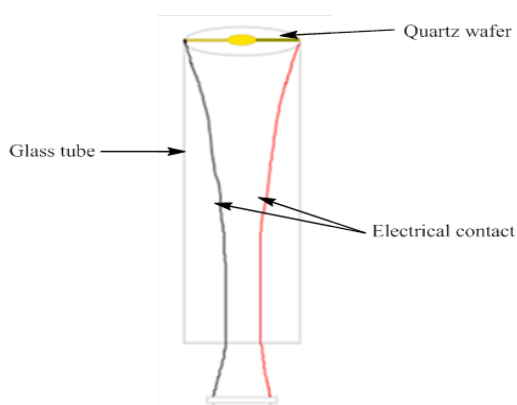


Figure 2-3: A schematic diagram of the QCM cell used to measure viscosity.

2.3.3 Contact Angle

The contact angle of surfactant solutions in DESs were carried out using Theta Lite optical tensiometer produced by Biolin Scientific. Drops of solutions of approximately 5 μl were applied to a flat horizontal stainless steel surface. The measurements were repeated 3 times using different drops on the same plate. The average contact angle of both sides of the drop was taken into consideration.

2.3.4 Conductivity

An electrical conductivity meter (Jenway 4510) was used to measure the conductivity of SDS solutions of different concentrations in Ethaline at different temperatures in the range 30 to 60°C to calculate the thermodynamic of micellization. The temperature of the measuring solutions was controlled by using water bath to $\pm 1^\circ\text{C}$. The conductivity was recorded three times for each concentration and an average and standard deviation were calculated.

2.3.5 Zeta Potential

The zeta potential was determined using a technique based on the electrophoretic mobility of charged colloidal particles under the impact of an external electric field. To measure the zeta potential the micelle or colloidal particle must have a charge.⁶ Zeta potential of SDS and AOT solutions in either Ethaline or ethylene glycol were carried out using a Malvern instrument, Zetasizer Nano dynamic light scattering instrument. Each solution was measured three times and an average value was calculated.

2.3.6 Aggregation Analysis

2.3.6.1 Dynamic Light Scattering

Many techniques that can be used to measure the size of particle such as scanning electron microscopy (SEM), and size exclusion chromatography (SEC), however, these techniques are difficult or impossible to apply to surfactant based systems because they significantly change the solvent environment of the micellar aggregates. Therefore, dynamic light scattering (DLS) has been used extensively to study micellar size and shape as in this technique there is not disturb the monomer-micelle equilibrium.⁷

The main principle of DLS depends on the Brownian motion of particles, micelles, or molecules in suspension in a medium which produces random motion by collision with solvent molecules that are also randomly moving. The sample is illuminated by a laser beam that causes the scattered light intensity to fluctuate strongly. The fluctuations of the scattered light from random motion of particles are detected by a photon detector at a particular angle θ (scattering angle) as shown in Figure 2-4. Analysis of these intensity fluctuations of scattered light allows determination of the diffusion coefficients, which simply used to calculate the particle size through the Stokes-Einstein equation.⁸

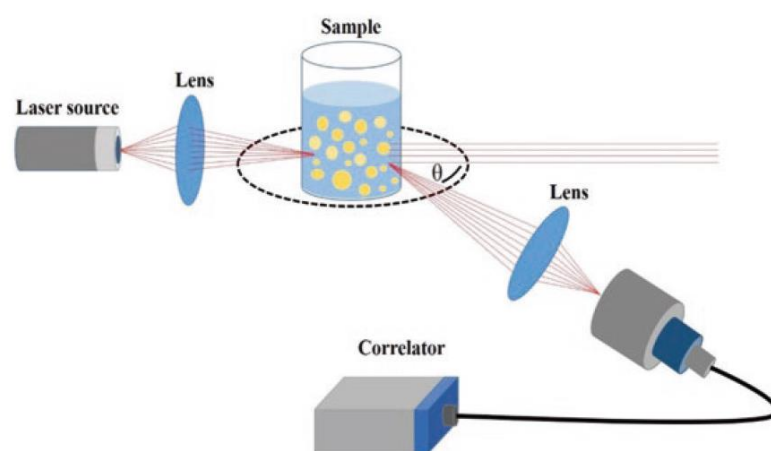


Figure 2-4: Scheme present the principle of the dynamic light scattering, taken from Ref.⁸

The diameters of the surfactant aggregates in DESs were carried out using a Nano-S Zetasizer (Malvern Instruments, UK) at 25°C. The samples were prepared at concentration below and above the critical micelle concentration suggested by the surface tension measurements. The samples were filtered through nylon membrane syringe filters, with a pore size of 0.2 μm to avoid interference from dust. The samples were then equilibrated for at least two days before measurement to ensure they were at equilibrium. The data were recorded using the solvent parameters for Ethaline, dielectric constant, 15, viscosity, 36 cP and refractive index, 1.46 as measured using an automatic digital Refractometer, RFM 732. The measurement was repeated three times for each sample, and an average value was calculated.

2.3.6.2 Nanoparticle Tracking Analysis

Nanoparticle tracking analysis (NTA) by NanoSight, is a characterization technique that complements DLS,⁹ and is used for sizing particles from about 30 to 1000 nm. It can count the particles and measure their concentration. In this technique, the nanoparticles are directly visualised in nanoscale in suspension liquids using only a conventional optical microscope fitted with a low cost camera and a dedicated analytical software package see Figure 2-5.¹⁰ NTA merges laser light scattering microscopy with a charge-coupled device (CCD) camera, which enables the visualization and recording of nanoparticles in a liquid environment. The NTA software is then able to identify and track individual nanoparticles moving under Brownian motion and relate them to the movement and particle size according to the Stokes-Einstein equation.¹¹

In this work, SDS micelles in Ethaline at concentrations above the CMC were visualized by light scattering using a light microscope by NanoSight LM10, UK. A video was recorded and the software of NTA tracks the Brownian motion of individual micelles and calculates their total concentration.

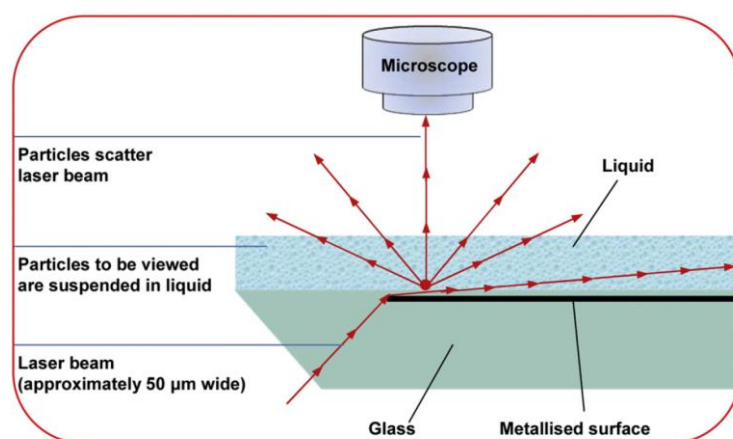


Figure 2-5: NanoSight instrument configuration, taken from Ref.¹²

2.4 Electrochemical Study

The electrochemical experiments, cyclic voltammetry (CV) and chronoamperometry (CA) used in this work were carried out using an Autolab PGSTAT20 potentiostat

(Ecochemie, Holland) controlled by GPES software (version 4.9). The electrochemical cell consisted of a three-electrode system with a 0.5 mm diameter platinum disc working electrode, a 1cm² platinum flag counter electrode and a silver wire as a pseudo-reference electrode. The working electrode was polished with 0.3 μm alumina paste to get a smooth surface followed by rinsing with deionised water and dried before each measurement. The temperature of the measuring solutions was controlled by using water bath whose temperature was maintained at required temperature $\pm 1^\circ\text{C}$.

2.4.1 Cyclic Voltammetry

Diffusion coefficients for two probes were determined in micellar DESs using iron (II) chloride (FeCl₂) 20 mM and tetrathiafulvalene (TTF) 5 mM using cyclic voltammetry as a function of potential sweep rate. All sample solutions were prepared as described above. All measurements were made at 25°C. The electrodeposition of copper was also studied using cyclic voltammetry using copper chloride (II) dehydrate (CuCl₂.2H₂O) as the solute. These experiments were carried out at 50°C.

2.4.2 Chronoamperometry

Chronoamperometry experiments were undertaken to study the nucleation mechanism of Cu deposition. Potential-step chronoamperometry was undertaken using a sample time of 0.01 s. The cathodic step potential was chosen as the reduction peak potential in all experiments. In Ethaline this was -0.39 V while in Glyceline it was -0.36 V. The conditions and electrodes were the same as in the cyclic voltammetry experiments.

2.4.3 Bulk Electrodeposition of Copper

Electrodeposition of Cu from DESs was carried out in Ethaline and Glyceline containing 100 mM CuCl₂.2H₂O in the absence and presence of surfactants, SDS and AOT and was performed on a nickel substrate. The electrodeposition of copper was achieved in a two electrode cell; the anode was copper plate and the cathode nickel substrate. The nickel substrates were first manually polished with progressively finer grades of silicon carbide polishing paper and washed with water then etched in acidic solution of ammonium persulfate and finally washed again with water. Copper films were electrodeposited at a constant current density of 1.25 mA cm⁻² and 50 and 80°C

for 2 h. After the deposition the substrates were removed from solution and washed with water and acetone.

2.5 Surface Analysis

2.5.1 Scanning Electron Microscopy

Scanning Electron Microscopy (SEM) was carried out to analysis the surface morphology of Cu deposits in absence and present of surfactants from DESs using a Phillips XL30 ESEM instrument with an accelerator voltage of 20 keV, giving an average beam current of *c.a.* 120 μ A. Energy Dispersive X-ray Analysis (EDX) was also carried out to determine the elemental composition of the coatings.

2.5.2 X-Ray Diffraction

X-ray diffraction (XRD) was used to characterise the crystallinity of the copper deposits obtained using electrodeposition in the absence and presence of surfactants from DESs. XRD was carried out using a Phillips model PW 1730 X-ray generator, with a PW 1716 diffractometer and PW 1050/25 detector. The X-ray tube was a long fine-focus Cu anode with Ni K α -filtered radiation of wave. It was typically operated at 40 kV, 30 mA, and scanned between 15 and 110° 2 θ with a step size of 0.02° 2 θ . Angle calibration was carried out using a synthetic Si sintered standard.

2.5.3 3D Optical Microscopy

3D Optical Microscopy (3DM) was used to measure the surface roughness, *Sa* of Cu coated in DESs in absence and present of surfactants. A Zeta instruments Zeta-20 optical profiler using Zeta3D software version 1.8.5 was used to create a 3-D colour image of the surface. This technique involves imaging the surfaces with very low reflectivity and very high roughness. Surface roughness measurements start at the manually set maximum height and stops at the lowest height set. Then the software can collect the measurements taken at each step and create a 3D coloured micrograph with an accurate representation of the surfaces roughness.

2.6 References

1. S. Muto, K. Deguchi, Y. Shimazaki, Y. Aono and K. Meguro, *Bulletin of the Chemical Society of Japan*, 1971, **44**, 2087-2090.
2. B. R. Masters, *Journal of Biomedical Optics*, 2008, **13**, 029901.
3. M. Pisárčik, F. Devínsky and M. Pupák, *Open Chemistry*, 2015, **13**.
4. N. Kundu, D. Banik, A. Roy, J. Kuchlyan and N. Sarkar, *Physical Chemistry Chemical Physics*, 2015, **17**, 25216-25227.
5. K. K. Kanazawa and J. G. Gordon II, *Analytica Chimica Acta*, 1985, **175**, 99-105.
6. E. Olson, *Journal of GXP Compliance*, 2012, **16**, 81.
7. R. Dorshow, J. Briggs, C. Bunton and D. Nicoli, *Journal of Physical Chemistry*, 1982, **86**, 2388-2395.
8. R. C. Choudhary, R. Kumaraswamy, S. Kumari, A. Pal, R. Raliya, P. Biswas and V. Saharan, *Nanotechnology*, 2017, 227-247.
9. P. Harrison, C. Gardiner and I. L. Sargent, *Extracellular Vesicles in Health and Disease*, Pan Stanford, 2014.
10. A. Malloy and B. Carr, *Particle and Particle Systems Characterization*, 2006, **23**, 197-204.
11. V. Filipe, A. Hawe and W. Jiskoot, *Pharmaceutical Research*, 2010, **27**, 796-810.
12. R. A. Dragovic, C. Gardiner, A. S. Brooks, D. S. Tannetta, D. J. Ferguson, P. Hole, B. Carr, C. W. Redman, A. L. Harris and P. J. Dobson, *Nanomedicine: Nanotechnology, Biology and Medicine*, 2011, **7**, 780-788.

3 Physical Properties of Surfactants Solutions in DESs

3	Physical Properties of Surfactants Solutions in DESs	51
3.1	Introduction	52
3.1.1	Stability of Micelles	53
3.1.2	The Critical Micelle Concentration	56
3.1.3	Self-assembly Structures	58
3.1.4	Thermodynamics of Micelles	59
3.2	Results and Discussion.....	61
3.2.1	Surfactant Solubilisation in DESs	61
3.2.2	Aggregation in DESs.....	63
3.2.3	Critical Micelle Concentration (CMC) in DESs	66
3.2.4	Micelles Size Analysis	78
3.2.5	Thermodynamics of SDS Micellization in Ethaline.....	83
3.3	Conclusions	88
3.4	References	89

3.1 Introduction

It is well known that surfactant undergo self-assembly in solution to form a liquid colloidal structure in general called micelles. These systems are of significant interest in several applications as described above in chapter 1. The main properties of surfactants, their aggregation and interfacial behaviour, are dependent on the solvent environment.¹ It is known that surfactant molecules can form micelles in different types of solvents. To that end it is important to understand surfactants self-aggregation in new solvents such as DESs which might lead these novel aggregation systems to be tuned for particular applications.

On one hand, because of the polarity of DESs, amphiphilic compounds, such as surfactants, are expected to dissolve and form self-assemblies as a result of solvophobic interactions with the hydrophobic amphiphilic tail groups. In addition, the potential of DESs to form a wide range of intermolecular bonds such as hydrogen-bond networks should promote amphiphilic compounds to aggregate. On the other hand, DESs contain both ionic and organic groups and so can be thought of as solutions with high ionic strength.² As example, the commonly studied DESs, Ethaline is formed by complexation of choline chloride and ethylene glycol as 1:2 molar ratio. The concentration of ionic species, Ch^+ and Cl^- is about 4.8 M.³ It is well-established that the addition of simple inorganic electrolytes to aqueous ionic surfactant solutions (where the concentration is in the range of 0.001 to 0.1 M) affects micellization because of the interaction between the counter ion and charged micelles. It generally results in a decreases of the CMC together with an increase in the aggregation size, lowering the surface tension and an increasing the viscosity of the solution.⁴ As the ionic strength increases, the CMC of ionic surfactants decreases as a result of screening of the electrostatic repulsion between charged head groups, meaning that the presence of salt facilitates the aggregation between surfactants. Moreover, some studies show that co-ions can also affect the micellization phenomenon and their influence depends on the nature of the co-ions and the structure of surfactants.⁵

Fundamentally, surfactants tend not to aggregate in solutions of high ionic strength and so it could be expected that self-assembly of surfactants would not occur in DESs due to coagulation, according to DLVO theory. Therefore, for the system with high ionic

strength such as DESs, the aggregation behaviour will be more complex than in an aqueous system.

In this chapter the self-assembly of surfactants will be examined in type (III) DESs and compared with aqueous solutions. Three key questions will be addressed;

- 1) How does self-assembly of surfactants occur in media of high ionic strength?
- 2) What is the difference in surfactant properties between DESs and aqueous solutions in terms of CMC and the structure of self-assembled aggregates?
- 3) What forces drive aggregation in DESs? This will be answered through characterization of thermodynamics quantities of the micellization.

Before answering these questions it is necessary to review some important points related to them.

3.1.1 Stability of Micelles

A model for the stability of lyophobic colloids was developed by Derjaguin, Landau, Verwey and Overbeek under the so-called DLVO theory. In brief, the stability of any colloid particle depends on the balance between two opposite potential energies, the attractive Van der Waals force and the repulsive double-layer forces.⁶

3.1.1.1 Van der Waals Forces in Micelles Solutions

Van der Waals forces arise from atomic and molecular level interactions due to induced and permanent dipoles in the system. Van der Waals forces are weak attractive forces and always negative in sign. There are many interactions under the title van der Waals forces such as Keesom interactions that form from permanent dipole-permanent dipole interactions, Debye interactions which originated from permanent dipole-induced dipole interactions and London interactions that form from induced dipole-induced dipole interactions.

3.1.1.2 The Double Layer in Micellar Solutions

It is well known that ionic surfactants aggregate in aqueous solutions and form charged micelles. Each micelle carries an electrical charge depend on the type of surfactant that formed the micelle. An anionic surfactant forms negatively charged micelles and the

positive, counter-ions form a layer around the surface of the micelles which is known as the Stern layer. The rest of the counter-ions form a more diffuse layer of charge around the micelle as shown in Figure 3-1. All of the ions in the Stern and diffuse layer are in dynamic equilibrium. The reverse is the case for cationic surfactants. Both the Stern layer and the diffuse layer together are called the double layer and the thickness of this layer is called the Debye length. The electrostatic repulsive forces between micelles in general are Coulombic in origin and they are positive in sign and strong.

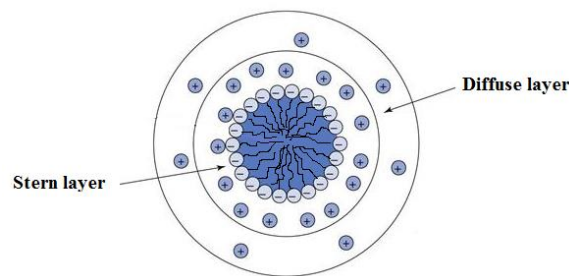


Figure 3-1: Schematic diagram of the electrical double layer of charged micelles.

The balance between attractive Van der Waals forces and repulsive double-layer forces can be described theoretically by assuming that the total potential energy of the interaction, V_t can be expressed as:

$$V_t = V_a + V_r \quad \text{Equation 3-1}$$

Where V_a is the attractive force and V_r is repulsive force. The DLVO curve in Figure 3-2 describes the energy changes (the combination) as two charged particles approach each other as a function of the inter particle distance. The DLVO curves show that in colloidal systems the repulsive double-layer forces must be overcome to get beyond the flocculation minimum such that attractive forces which cause the particles to coagulate can occur at the primary minimum. In another words, the van der Waals attraction always dominates at both small and large separations. In between, however, the behaviour depends critically upon the repulsive double-layer forces. The DVLO repulsive maximum is what keeps the micelle stable and prevents them coagulating. A high ionic strength of inorganic electrolytes in aqueous solutions collapses the diffuse layer such that the repulsive maximum is decreased and colloidal aggregates can coagulate and ultimately precipitate.

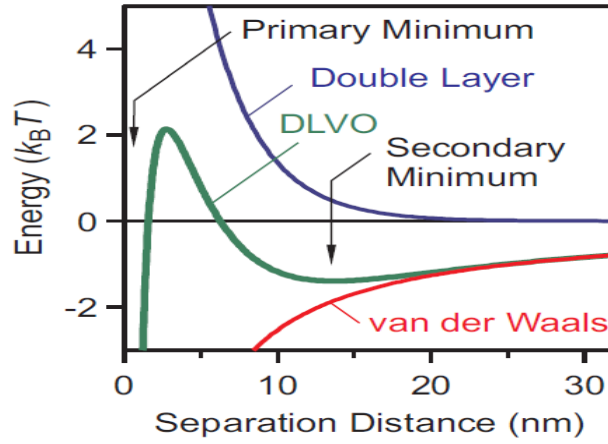


Figure 3-2: Schematic of the interaction energy–distance curve according to DLVO theory.

The repulsive interaction V_r is given by the following expression:

$$V_r = 2\pi R \epsilon_r \epsilon_0 \psi_0^2 \ln[1 + \exp - (Kh)] \quad \text{Equation 3-2}$$

Where ϵ_r is the relative permittivity, ϵ_0 the permittivity of free space, ψ is the surface potential and k is the Debye–Hückel parameter. The extension of the double layer, double layer thickness (known as Debye length) is linked to K through the following relationship:

$$\text{Debye length} = \left(\frac{1}{K}\right) = \left(\frac{\epsilon_r \epsilon_0 k_B T}{2n_0 Z_i^2 e^2}\right) \quad \text{Equation 3-3}$$

Where n_0 is the number of ions per unit volume of each type present in the bulk solution, Z_i is the valence of the ions and e is the electronic charge.

The Equation 3-3 shows that the Debye length relies on the electrolyte concentration and valency where the Debye length increases with lowering the electrolyte concentration and the valency. In fact, the electrolyte concentration plays a role in the entropy of ions at a charged colloid surface that affected the stability of colloid system as shown in Figure 3-3. At low electrolyte concentrations, there is a big entropy to confining the ions to the surface and this gives a greater Debye length resulting in greater repulsive force between neighbouring micelles. However, at high electrolyte

concentration the entropic loss of confining ions to the surface is less, leading to a shorter Debye length and reduction in repulsion forces which favours coagulation of colloidal particles.

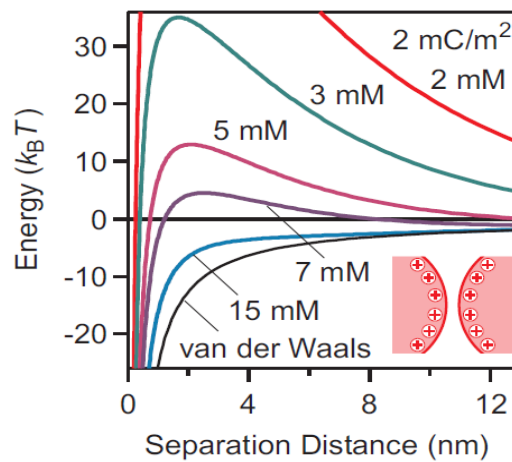


Figure 3-3: Effect of the electrolyte concentration on the stability of colloid system according to DLVO theory.

3.1.2 The Critical Micelle Concentration

The critical micelle concentration (CMC) is an important characteristic for surfactant solutions as it describes the concentration required to form the first micelles in solution and it controls their uses in application such as emulsion stabilization, drug-delivery and detergency.⁷ By way of illustration, surfactants with low CMC exhibit can irritate the skin more compared with those with a high CMC.⁸ Furthermore, CMC reflects both the ability of the surfactant to form micelles and its surface properties through its value where low CMC mean more ability to aggregate and have a better surface activity.^{9, 10} The CMC also reflects the balance between the hydrophobic interaction of the hydrocarbon tail of surfactant molecules and electrostatic repulsive effects of the hydrophilic head groups.¹¹

The CMC is defined as the concentration of a surfactant in the bulk solution above which micelles start to form and the solution property shows an abrupt change. The sudden change in physical properties as the concentration of the surfactant increases indicates that the micelles form and hence the point of that change is used to determine the value of the CMC which is characteristic for each surfactant and is dependent on

temperature, type of solvent and ionic strength. Where adding salt to ionic surfactant solutions a decrease in CMC results due to electrostatic screening caused by the salt ions which causes decrease the repulsion between the ionic head groups of surfactant. It is worth noting that the concentration of surfactant monomers is nearly constant above the CMC and micelles do not show surface activity. Hence increasing of the surfactant concentration will affect the structure of micelles but not the number of monomers in the solution.⁸ Certain factors such as surfactant structure, ionic strength, temperature and presence of a second liquid have an effect on CMC value of surfactant in their solution. Some factors contribute to decrease CMC such as:⁸

- An increase in the number of carbon atoms in the hydrophobic tails.
- A fluorocarbon structure.
- An increased degree of binding of the counter ions.
- The addition of electrolyte to ionic surfactants.
- The existence of polar organic compounds such as alcohols and amides.

And other factors contribute to an increase in the CMC such as:

- A branched hydrophobic structure
- Double bonds between carbon atoms
- Polar groups (O or OH) in the hydrophobic tail
- Strongly ionised polar groups (sulphates and quaternaries)
- An increase in the effective size of hydrophilic head
- Addition of polar molecules such as urea, formamide, dioxane, ethylene glycol and water soluble esters

Several techniques used to measure the CMC although only a few are cited here. These include; surface tension, fluorescence, conductivity, osmotic pressure, self-diffusion measurements and NMR chemical shifts.¹² The surface tension method is amongst the most commonly used technique. A plot of surface tension as a function of concentration results in a break at the CMC.⁸

Other direct methods include conductivity and light scattering. Indirect methods including fluorescence emission of pyrene monomers and solubilisation of dyes involve the addition of organic compounds to measure the CMC value. As presented in the

chapter 1, Figure 1-4, the physical properties change with surfactant concentration and these plots can be used to determine the CMC.

3.1.3 Self-assembly Structures

The size of micelles can be described by the radius of the micelle or by the micelle aggregation number; the number of monomers in a micelle. Different techniques have been used to estimate the radius of the micelle such as scattering methods, quasielastic light scattering and neutron scattering as well as NMR pulsed-gradient spin-echo method by the determination of the micellar diffusion coefficient.¹³ Whereas scattering methods and fluorescence quenching are more common techniques to measure the aggregation number.^{14, 15} Studies have shown that the structure and particularly systematic trends in morphology of micelles can be explained using the molecular packing parameter:

$$\text{Packing parameter} = \frac{V_o}{al_o} \quad \text{Equation 3-4}$$

where V_o is the volume of a surfactant hydrocarbon tail, l_o is the length of the surfactant tail and a is the effective area per head group.¹⁶ The shape and size of aggregation depend on packing parameter value, where spherical micelles tend to form if the packing parameter ≤ 1 , rod-like micelles are preferred if the packing parameter between $\frac{1}{3}$ and $\frac{1}{2}$ and bilayers form if the packing parameter between $\frac{1}{2}$ and 1.¹⁷ However, in the aqueous solution micelles structures of the same surfactant change depend upon three main factors, surfactant concentration, ionic strength of the solution and temperature.¹⁸

At surfactant concentrations slightly above the CMC, spherical self-aggregated structures formed and it is known as micelles with aggregation numbers in the region of 50–100 and the solution in general is isotropic. Different self-aggregated structures may also exist in aqueous surfactant solutions such as cylindrical, disk-like, worm-like and vesicles that are anisotropic depending on the physicochemical parameters.⁷ However, The micelles tend to grow at concentrations much higher than the CMC forming diverse liquid-crystalline phases such as bilayer stacks (lamellar phase) and hexagonal phases.⁹ The repulsive forces between head groups, for ionic surfactants are responsible for increasing the micelles size and forming larger aggregation as the concentration

increased. Generally, as surfactants concentration increased three types of behaviour can be noted:¹²

- 1- For surfactants with high solubility in water the physicochemical properties such as viscosity and light scattering change smoothly as the concentration is increased up to saturation. In this case, the micelles remain small and generally they are spherical.
- 2- For surfactants with high solubility in water the physicochemical properties such as flow birefringence vary dramatically as the concentration increases. In this case, there are significant changes in the aggregation structures forming a liquid with crystalline structures.
- 3- Phase separation of solid hydrated phase at low concentrations are shown by surfactants with low solubility in water.

On one hand, the thermodynamic mixing of surfactants with solvents favours a low number of monomers in each micelle in terms of the entropy. Subsequently the micelles formed are small meaning the interfaces are curved at low surfactant concentrations in the absence of added salt.¹⁹ The addition of electrolyte on the other hand, can strongly influence the growth of micelles. Theoretically, the repulsive force should be reduced by adding salt to the solution resulting in less self-assembly. However, the size of the micelle should initially increase as the ionic strength increases as result of screening of inter-molecular repulsion.¹² It is therefore difficult to decide which effects will be dominant in the end. As a general rule, studies show that the counter ion have a stronger effect where less hydrated ions produces higher counter ion binding to micelles.²⁰

When an electrolyte is added to a micellar solution they affect the structure of the diffuse layer reducing the magnitude of the electrostatic contribution to the free energy. Moreover, because of geometrical packing constraints the micelles must become increasingly non-spherical as they grow in size.¹⁹ Studies show that by increasing the concentration of the added electrolyte, micelles grow from small spherical structures to large elongated aggregates.^{13, 21, 22}

3.1.4 Thermodynamics of Micelles

The thermodynamic properties of surfactant solutions can provide information about the interactions between surfactant molecules themselves and surfactant molecules with the

solvent as well as offers information about the driving force of micellization. The standard Gibbs energy of micellization is a useful way to measure the tendency of surfactant towards micelle formation in any solvent. Surfactants stabilize in solution through forming self-assembly and the stability depends on the solvation of the head group and the insertion of the tail with the solvent. When they have a negative Gibbs energy the enthalpic gain from solvation should be exothermic since the entropic gain will probably be small.¹⁸

In water it is well known that the total change in free energy of micellization ΔG_{mic}^0 is negative and it balanced by two expression as follows:

$$\Delta G_{mic}^0 = \Delta G_{HI}^0 + \Delta G_R^0 \quad \text{Equation 3-5}$$

Where ΔG_{HI}^0 is a negative part due to hydrophobic interactions and ΔG_R^0 a positive part as results of electrostatic charge repulsion between the ionic head groups and hydration of the polar groups at the micelle-solvent interface.²³ Furthermore, the stabilising of micelles by the effect of counter ions bind to micelles via surfactant monomer head groups will screen the electrostatic repulsions between micelles.⁹

Surfactant aggregation at the CMC is energetically favourable. The new interface between the micelle and the solvent requires an energy which is minimised by decreasing the surface area of the aggregate. It is well known the negative values of free energy of micellization ΔG_{mic}^0 indicate that the spontaneous process of micellization whereas the negative values of enthalpy of micellization ΔH_{mic}^0 indicated that the major attractive force for micellization is London-dispersion interactions.²⁴ The large negative entropy ΔS_{mic}^0 may be related with confining surfactant to the small volume of the micelle.²⁵

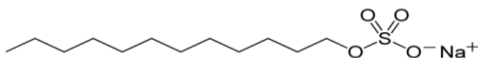
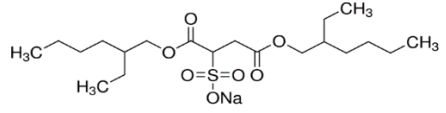
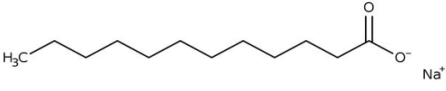
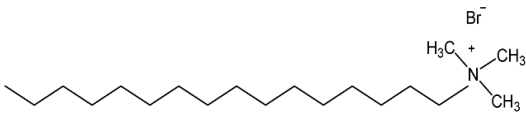
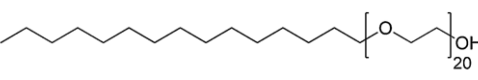
3.2 Results and Discussion

The experiments in the section below, initially investigate which types of surfactants are soluble in different DESs. They go on to probe the CMC of the soluble surfactants using a variety of techniques and investigate differences between the behaviour in DESs and that in water. The thermodynamics of aggregation are also investigated along with the dimensions of the surfactant aggregates using DLS.

3.2.1 Surfactant Solubilisation in DESs

Initially a screen was carried out to determine the solubility of different surfactants (anionic, cationic and neutral) in different DESs. The solubilisation of 5 surfactants; SDS, AOT, sodium dodecanoate, CTAB and Brij-58, presented in Table 3-1, were examined in 3 DESs; Ethaline, Glyceline and Reline. Brij-58 was found to be insoluble in all types of DESs that were studied. However, the cationic surfactants CTAB was soluble just in Glyceline and in Ethaline at temperatures higher than room temperature. CTAB was insoluble in Reline. The low solubility of these surfactant stems, in part, from the long alkyl chain 56 carbon atom of Brij-58 and 16 of CTAB. In contrast the anionic surfactants, SDS and AOT (≤ 12 carbon atom), showed solubility in Ethaline, Reline and Glyceline. At this point it should be noted that AOT, while soluble in DESs shows poorly solubility in water due to hydrophilic-hydrophobic imbalance.²⁶ Similar behaviour has been observed by the Mahi group when they examined the solubility of some surfactants in Reline.²⁷

Table 3-1: The chemical structure of used surfactants.

Surfactant	Chemical structure
Sodium dodecyl sulfate (SDS)	
Bis (2-ethylhexyl) sulfosuccinate sodium salt (AOT)	
sodium dodecanoate	
Cetyltrimethylammonium bromide (CTAB)	
Polyethylene glycol hexadecyl ether (Brij-58)	

As discussed above, it could be questioned why micellar solutions exist at all in media of high ionic strength when comparable ionic strengths in aqueous solutions would not enable micelle formation. The hypothesis is that the large Ch^+ cations pack poorly around the micelle and their large size (*c.a.* 6 Å in diameter) makes a thick Stern layer which screen micelles from each other. To test this hypothesis, it is possible to create an analogous eutectic using ethylene glycol and lithium chloride. If the screening is due solely to size of the cation then SDS should not form a micelle in a mixture of 1 LiCl: 4 ethylene glycol. This was tested and it was found that SDS appears to be insoluble in this liquid suggesting that the unique property that enables micelle formation in DESs (and ionic liquids) is the large size of the cationic group.

It is often thought that the solubilisation process of anionic surfactant in polar solvent is controlled with the head group, sulphate in case of SDS. In Ethaline, Reline and Glyceline the hydrophilic sulphate group will associate with the cationic choline ion. However, with lithium chloride and ethylene glycol, the charge on the sulfate will be more effectively neutralised by the small lithium ion meaning that the micelles carry less of a negative charge and so they will aggregate and become insoluble in solution.

The nature of the headgroup was also tested by investigating the properties of sodium dodecanoate, (replacing the sulfate headgroup in SDS by a carboxylate group) in Ethaline, Reline and Glyceline and it was found to have low solubility. The ability of a surfactant to dissolve will be dependent on the lattice energy of the surfactant and the enthalpy of solvation of the dissolved ion and the thermodynamics of the aggregation.²⁸
²⁹ It is more likely that a carboxylate will have a higher lattice energy and a lower solvation enthalpy than the corresponding sulfate.

3.2.2 Aggregation in DESs

The stability of micelles dispersions in a solvent depends on the surface chemistry of the micelles. When surfactants aggregate, an electrical double layer is created around the micelle as results of adsorption of counter ions. According to Stern's model, two regions of an electrical double layer can be distinguished; the Stern layer where the counter ions are more strongly held onto the micellar surface and the diffused layer of counter ions which are more weakly coordinated. The electrical potential decreases linearly across the Stern layer and more gradually across the diffuse layer, as shown in Figure 3-4.

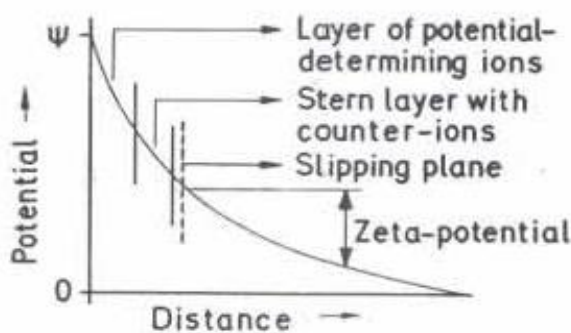


Figure 3-4: Schematic represent the drop of the potential versus distance, taken from Ref.³⁰

For micellization in DESs, ionic species of the solvent will play an important role in the Stern layer. When 25 mM SDS is dissolved in Ethaline there will be 25×10^{-3} M of Na^+ and 4.8 M of Ch^+ so the Stern layer will be mostly composed of Ch^+ . According to Equation 3-3 the Debye length decreases as the ionic concentration increases this approach assumes that the ions are point charges. From a practical perspective, however the 6.6 Å diameter of Ch^+ means that the micelles can never come close enough for the

micelles to coagulate ensuring their long-term stability. In the case of DESs based on lithium chloride and ethylene glycol the size of Li^+ is small and hence SDS cannot be soluble or the Debye length is too small and agglomeration occurs. So here the size of counter ion dominates the stability of the micelles. This finding is consistent with the study of fluorinated quaternary ammonium salts where the authors reported that the repulsive force between the head-groups decreases as result of the presence of big counter-ions like I^- near to the polar head groups of the surfactant molecules. This decrease in repulsion leads to larger aggregates.³¹ This result suggest that the aggregation of surfactants in DESs will result in larger aggregates than those observed in aqueous solutions as will be proved later with DLS.

The zeta-potential is an important parameter used in colloid chemistry to observe the behaviour of micelles dispersions in their system. In this study, the zeta-potential, was measured for SDS and AOT micellization in Ethaline and ethaline glycol to investigate the effect of ionic strength. Table 3-2 shows the zeta-potential for SDS and AOT in DESs is much more negative than in pure ethaline glycol. It is proposed that this is due to the large size of the cation. This effectively increases the shielding effect of the double layer, thus decreasing the measured zeta potential.³²

Table 3-2: Zeta potentials for 15 mM SDS and AOT micelles in Ethaline and ethaline glycol at 25°C.

Surfactant	Zeta potentials of micelles in Ethaline (mV)	Zeta potentials of micelles in Ethylene glycol (mV)
SDS	-165.67 ± 20.5	-36.73 ± 2.0
AOT	-163.33 ± 13.9	-44.13 ± 2.4

It is also worth noting that the values of the zeta potential for both surfactants, SDS and AOT are very similar and this could explain why their CMC are very similar and the question is why the CMCs for either SDS or AOT in different DESs are very different even though the ion type and ionic strengths are identical in all the DESs (see section 3.2.3). These results together with those of other groups^{27, 33, 34} clearly show that surfactants can form aggregates in DESs.

It is well known that 70-90% of the counter ions are bound in the Stern layer in an aqueous solution in the absence of an external electrolyte. Table 3-2 shows a zeta potential of approximately -160 mV which shows that the Ch^+ is relatively poor at neutralising the charge on the micelle as would be expected from such a large cation. This can have the effect of increasing the micelle size or changing the shape from spherical to rods or disks.³⁵

There are no studies about the behaviour of SDS in pure ethylene glycol although Gracie *et al.*²⁸ showed the micellization of SDS in mixed water- ethylene glycol solutions. They reported that no micelles form in solvent mixtures containing more than 60% ethylene glycol. The experiments carried out with DLS show no larger aggregates although a signal was noted for 0.44 nm which could be due to monomers. As discussed later, the Ch^+ is found to enable the formation of large aggregates which are not possible in pure ethylene glycol. Figure 3-5 (a) shows a schematic diagram of how surfactants self-aggregate in aqueous solution and how they grow by adding salt or increase surfactant concentration. In contrast Figure 3-5 (b) shows the likely case for aggregation in DESs.

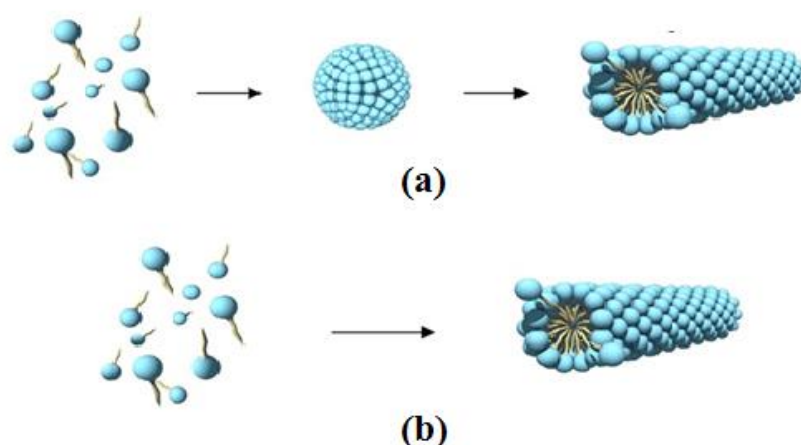


Figure 3-5: Schematic diagram of how surfactants self-aggregate in (a) aqueous solution and how they grow by adding salt (b) probable representation of behaviour in DESs.

Interestingly, in the case of forming micelles in ILs it might be a different situation. A study by Chen *et al.*¹ showed that SDS forms micelles in the IL, 1-ethyl-3-methyl

imidazolium ethylsulfate and the IL ions were incorporated along with surfactants into micelles which is completely different to aqueous solutions.

3.2.3 Critical Micelle Concentration (CMC) in DESs

The surface tension of surfactant solutions was measured in DESs to investigate the CMC of two types of surfactants, SDS and AOT (the main difference between these two surfactants is the structure of their tails: one chain of 12 carbon atoms for SDS and two chains of 6 carbon atoms with C₂H₅ group in the second C in each chain for AOT (see Figure 3-6)

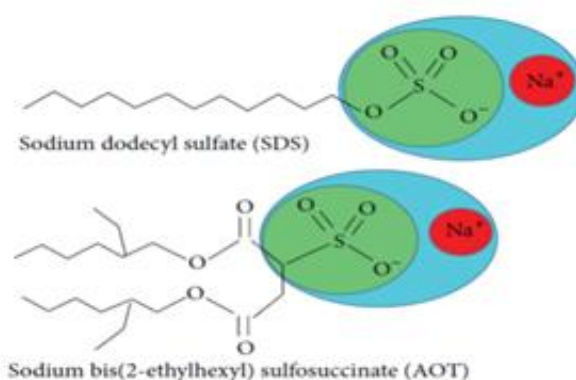


Figure 3-6: The chemical structure of SDS and AOT.

Figures 3-7 and 3-8 show plots of the variation in surface tension as a function of concentration of SDS and AOT in different DESs; Ethaline, Glyceline and Reline. The surface tension isotherm shows two straight line regions; at low concentration, a steep linear decrease and at higher concentrations a slower decrease. The first line corresponds to the concentration range below the CMC where monomers exist at the air-solution interface.

The trend in surface tension is similar to those observed for the same surfactants in aqueous solutions but the rate of change for both surfactants in Ethaline is less marked than in water.³⁶ This suggests that the surfactants are both less surface active and more stable existing as monomers in the DES than they are in water.

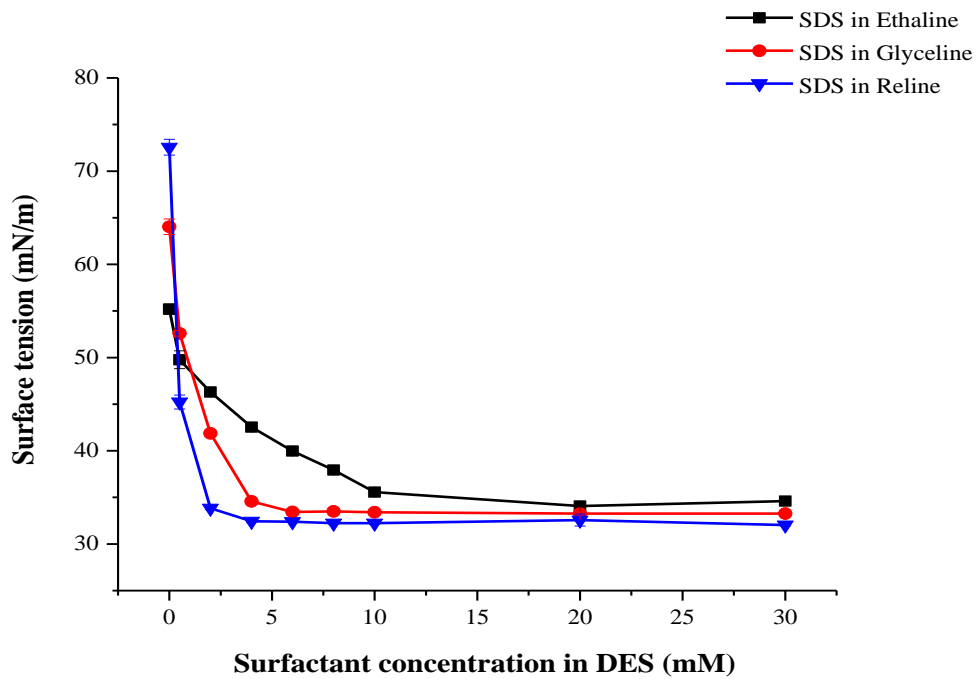


Figure 3-7: Surface tension versus SDS concentration in DESs.

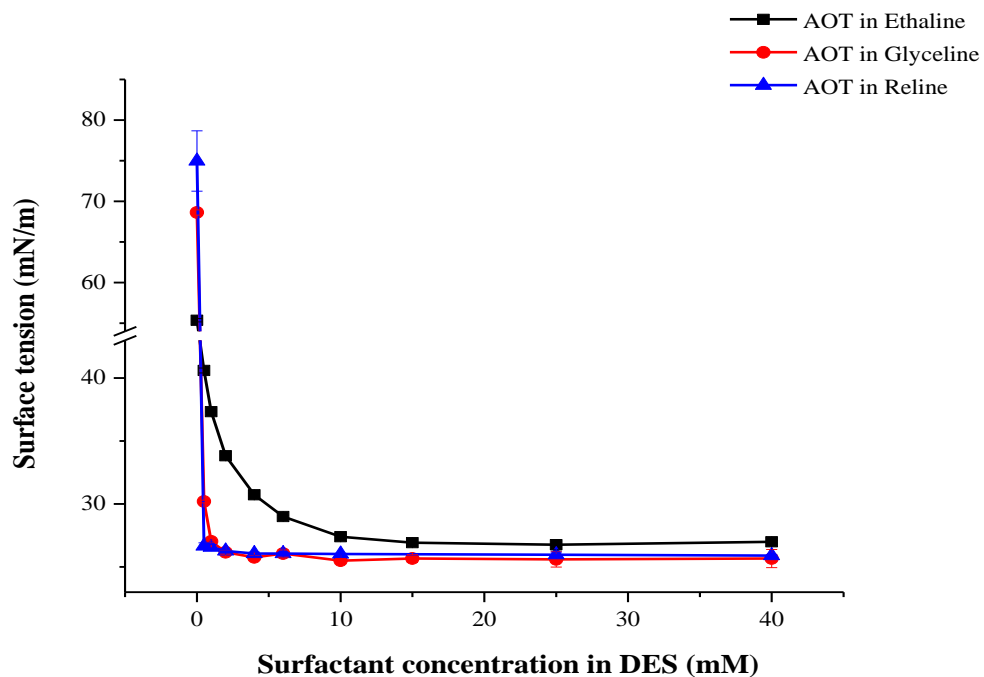


Figure 3-8: Surface tension versus AOT concentration in DESs.

Table 3-3 shows the CMC values of SDS and AOT in DESs which were determined as the intersection between the linear decline and the baseline of minimal surface tension

as shown in appendix. These result agree well with those by Arnold *et al.*³⁴ when they determined the CMC of SDS in Reline which was reported to be 2 ± 1 mM. Surprisingly, there is negligible difference between the CMC value of SDS and AOT in each of the DESs which is in contrast with the results in aqueous systems where the CMC is different for SDS and AOT even when changing the ionic strength. A study by Chatterjee *et al.*³⁷ showed that adding NaCl to aqueous solutions significantly decreased the CMC of SDS but for AOT the effect on the CMC was only minor. Another study by Umlong and Ismail showed that there was no effect on CMC for AOT in aqueous system by adding sodium chloride, sodium acetate, sodium propionate, or sodium butyrate.³⁸

Table 3-3: CMC values (mM) for SDS and AOT in DESs and water at 25°C measured by surface tension.

Surfactant	Ethaline	Glyceline	Reline	Water
SDS	9.00 ± 0.31	3.76 ± 0.08	1.91 ± 0.04	8.2^{39}
AOT	8.56 ± 0.07	3.40 ± 0.09	2.58 ± 0.21	2.2^{40}

It is observed from Table 3-3 that CMC values of SDS in Reline and Glyceline are smaller than in aqueous systems while in Ethaline is similar to the value in water. The CMC values for AOT are similar in Reline and Glyceline but the value in Ethaline is much higher. What is interesting about these results is that all three DESs contain the same salt (ChCl) in the same concentration but the CMCs are quite different. This shows that the HBD must have a significant effect on the CMC which is opposite to what might be expected.

The cause for this difference in the behaviour of DESs could result from differences in the anion and cation activity i.e. which could affect the ionic strength and accordingly the zeta potential. It could also result from the hydrophobicity of the HBD where urea is more polar than glycerol so it is easier to solvate the monomer in the less polar HBD.

The ability of DES to form hydrogen bond via OH group in the case of Ethaline and Glyceline,⁴¹ and via the NH₂ group in the case of Reline may have an important role in dissolving the hydrophobic group. This can lead to an increase in the entropy on micelles formation, and decrease the CMC values. A study by Stefanovic *et al.* reported that the hydrogen bond density was in the order Reline > Glyceline > Ethaline with

13.8, 10.8 and 9.4 bonds nm^{-3} respectively.⁴² This can be seen from the slightly higher density of Reline compared to the other two DESs. Based on this, Reline is more structure than Glyceline and Ethaline so micelles will break down the structure of the solvent which will be easier in case of Ethaline and then more surfactant is required to form micelles and the opposite is the case of Reline. In other words, the decrease in CMC could be due in part to an increase in the cohesive energy as result of increase hydrogen bond density.

Another probable cause for this in all DESs studied here, the hydrogen bond formed between $\text{Cl}\dots\text{HO}$ in case of Ethaline and Glyceline while $\text{Cl}\dots\text{HN}$ in Reline. The strong hydrogen bond networks formed ($\text{H}\dots\text{Cl}$) reflect their higher viscosity.⁴³ Moreover, an increase in the repulsion between the ionic head groups of both surfactant and Cl^- in Ethaline which is less viscous than Reline and Glyceline would result to increase the CMC value.

In respect to the same hydrogen bond network formed in Ethaline and Glyceline Abbott *et al.*⁴⁴ found that the role of the chloride was different in the two liquids. Glycerol is a three dimensionally hydrogen bonded liquid with a high degree of order and hence a high viscosity. When chloride is added it breaks up the hydrogen bonding structure and the viscosity decreases. With ethylene glycol there is less order in the pure liquid and the addition of chloride creates order and increases the viscosity (albeit significantly less than that in Ethaline).

The other question that must be answered is why there is no difference of the CMC values of SDS and AOT in DESs? To answer this question, it would be beneficial to know the CMC of SDS and AOT in different solvents. Table 3-4 summarises the CMC of SDS and AOT reported in the literature in different solvents. Direct comparison of the two systems is not really possible because SDS tends to be soluble in polar solvents whereas AOT is more soluble in non-polar solvents. It is, however clear that the CMC for AOT is generally lower than that for SDS. It is interesting to note that SDS and AOT are not only both soluble in Ethaline but actually have very similar CMC values to those in water. This probably suggests that the structuring in Ethaline is more like that in water than an organic molecular solvent.

Table 3-4: CMC values (mM) of SDS and AOT in different solvents.

Solvent	SDS	AOT
Water	8.2 ⁽³⁹⁾	2.2 ⁴⁰
Formamide	220 at 60 °C ⁽⁴⁵⁾	1.6 ⁽⁴⁶⁾
Formic acid	46 ⁽⁴⁷⁾	-
Hydrazine	22 ⁽⁴⁸⁾	-
Dimethylacetamide	15 ⁽⁴⁹⁾	-
Dimethyl sulfoxide	39.5 ⁽⁴⁹⁾	-
N,N'-dimethylformamide	14.62 ⁽⁵⁰⁾	-
Ethylene glycol	-	0.9 ⁽⁴⁶⁾
Dioxane	-	1.6 ⁽⁴⁶⁾
Chloroform	-	0.4 ⁽⁵¹⁾
Benzene	-	2 ⁽⁵¹⁾

It is interesting to compare the CMC in DESs with those in ionic liquids which share many properties and applications with DESs. Critical micellar concentrations of SDS have been studied in aqueous solutions of a variety of room temperature ionic liquids⁵²⁻⁵⁶ Beyaz *et al.*⁵² found that the CMC of SDS in aqueous solutions with added ionic liquids depends on the nature of the alkyl groups of ILs. The CMC was found to be 170 and 70 mM for 1,3-dimethylimidazolium iodide and 1-butyl-3-methylimidazolium chloride, respectively, when its concentration was 30 mM. Whereas, under the same condition the CMC was 2.8, 1.9 and 1.9 mM for other ILs 1-hexyl-3-methylimidazolium chloride, 1-methyl-3-octylimidazolium chloride and 1-methyl-3-octylimidazolium tetrafluoroborate respectively. Moreover, the nature of ILs ions, Cl⁻ or BF₄⁻, has no noticeable effect on the observed CMC values. The same group in another study⁵³ reported the CMC of SDS in 30 mM aqueous solutions of two ILs. Their results show that the CMC of SDS is significantly lower in the presence of 1-methyl-3-(pentafluorophenyl)imidazolium chloride as compared to that of 1-benzyl-3-methylimidazolium chloride where the CMC values were 0.04 and 18 mM respectively as results of increased hydrophobicity due to the fluorinated side chain.

Pal and Chaudhary, in different studies,⁵⁴⁻⁵⁶ reported the changes in the micellization behaviour of SDS in aqueous solutions upon addition of ILs in different polarity,

hydrophobic and hydrophilic. The effect of hydrophobic ILs, 3-methyl-1-pentylimidazolium hexafluorophosphate was recorded at different IL concentration to maximum 0.1 wt%. These results were qualitatively interpreted in terms of hydrophobic and hydrophilic effects. The authors did not discuss the probability that the water and IL were heterogeneous or that the IL ions have surfactant properties themselves.

Very few papers have reported the CMC of SDS in pure ILs. Jared *et al.*⁵⁷ examined the formation of micelles in pure 1-butyl-3-methyl imidazolium chloride (BMIM-Cl) and hexafluorophosphate (BMIM-PF₆). Their results using surface tension show that the CMC of SDS was 48 ± 4.4 mM in 1-butyl-3-methyl imidazolium chloride (BMIM-Cl). Another study by Fletcher *et al.*⁵⁸ showed that SDS was not soluble in 1-ethyl-3-methylimidazolium bis-(trifluoromethylsulfonyl) imide. However, in 1-ethyl-3-methyl imidazolium ethylsulfate the CMC of SDS was 167 mM at 90 °C.¹ They interpreted the high CMC value as being due to the presence of alkyl groups of IL cation.

It is well known that the solubility of non-polar compounds is generally higher in ILs than in water, hence the solvophobic interactions are decreased which leads to an increase in the CMC. Moreover, the larger quasi-lattice energy between the ions in the liquid state will make it more difficult to break up the structure and open a void in which to place the micelle. It was recently shown that partition coefficient of molecules into a DES was controlled by the enthalpic term required to make a void in the liquid.⁵⁹ The same idea was also discussed in terms of the solubility of hydrophobic tails by amphiphilic nanostructure in ILs.⁶⁰ Taking this into account and comparing the CMCs of SDS in DESs with those in ILs it is clear that there is a significantly high tendency for SDS to aggregate in DESs rather than in IL. However, this is not the case when compare the CMC of AOT in ILs with DESs, where in IL, ethylammonium nitrate the CMC was 0.97 mM⁶¹ which is lower than in DESs.

In addition to determining the CMC using surface tension there are several other methods which can be used. To ensure that the above results are not an artefact of the measuring technique the CMC was also investigated using a spectroscopic probe. It is well known that 7,7,8,8-tetracyanoquinodimethane (TCNQ) is an oil-soluble dye (insoluble in water) which has an absorption peak for the neutral molecule at 405 nm in benzene solution.⁶² However, many authors noted the extra absorption bands at 680, 750 and 850 nm appear when TCNQ was solubilized in aqueous surfactant solutions

above the CMC and they confirmed that these peaks are due to the anion radical of TCNQ as result of its interaction with surfactant aggregates. The absorbance peak at 480 nm has been generally interpreted as resulting from a charge transfer interaction.⁵¹ Several studies^{51, 62, 63} have focused on the use of this spectroscopic shift to determine the CMC values of ionic and non-ionic surfactants in both aqueous and non-aqueous systems. Herein, the CMC values of SDS in DESs have been achieved by looking at how TCNQ influence these systems as the charge transfer interaction reflects the internal structure of micelles.

In our work, as presented in Figure 3-9 TCNQ was soluble in all DESs under this study but its absorption spectra are different than that reported in organic solvents⁵¹ i.e. the interaction was between TCNQ and Ethaline shows peaks at 850, 750, 478, 408 and 344 nm while with Glyceline they show peaks at 850, 750 and 362 nm and that may cause by the interaction between TCNQ and the oxygen atom of hydroxyl group in ethylene glycol and glycerol for Ethaline and Glyceline respectively.⁶² In Reline peaks appear at 317 and 246 nm. Although the TCNQ interacts with DESs, a change in the peak intensity was observed when SDS was added to the solution and this indicated that TCNQ interacted with SDS as well. The absorption spectra of TCNQ solubilized in SDS solutions in Ethaline, Glyceline and Reline are shown in Figures 3-10, 3-11 and 3-12 respectively. The change could be interpreted as the TCNQ anion radicals produce from interaction of TCNQ with either DESs or SDS resulting in a competition in solvation media. The CMC values listed in Table 3-6 were obtained from these spectral changes based on the charge-transfer solubilisation of TCNQ.

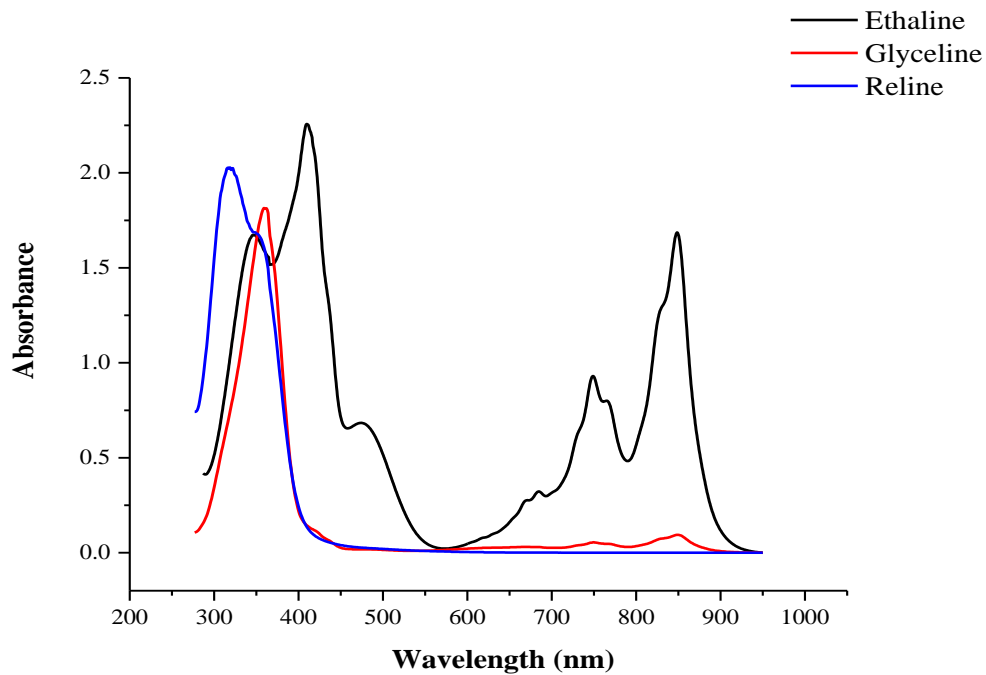


Figure 3-9: Absorption spectra of TCNQ solubilized in DESs.

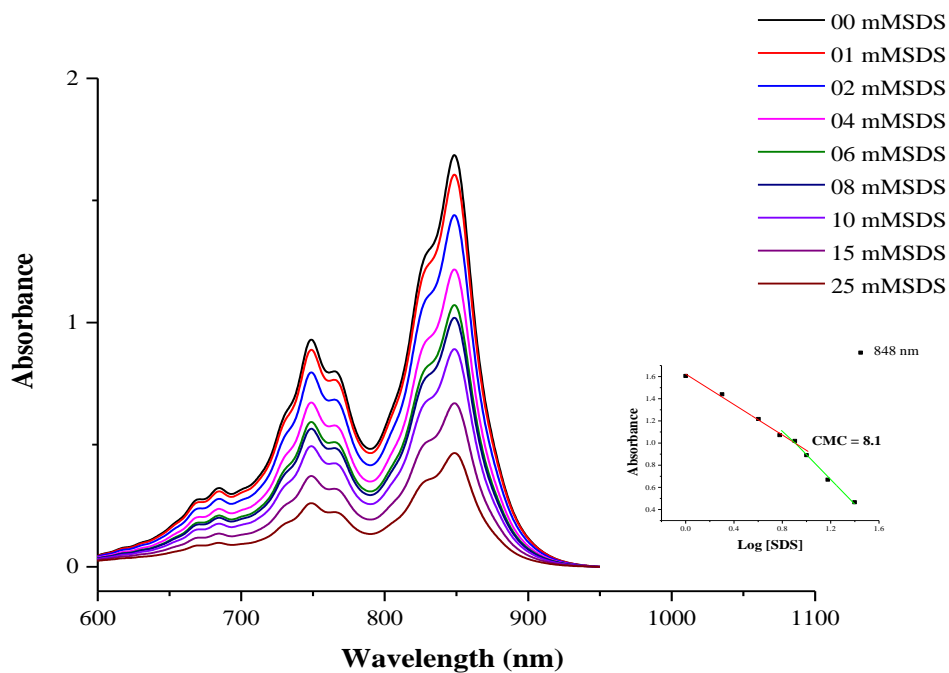


Figure 3-10: Absorption spectra of TCNQ (0.3mM) solubilized in SDS in Ethaline.

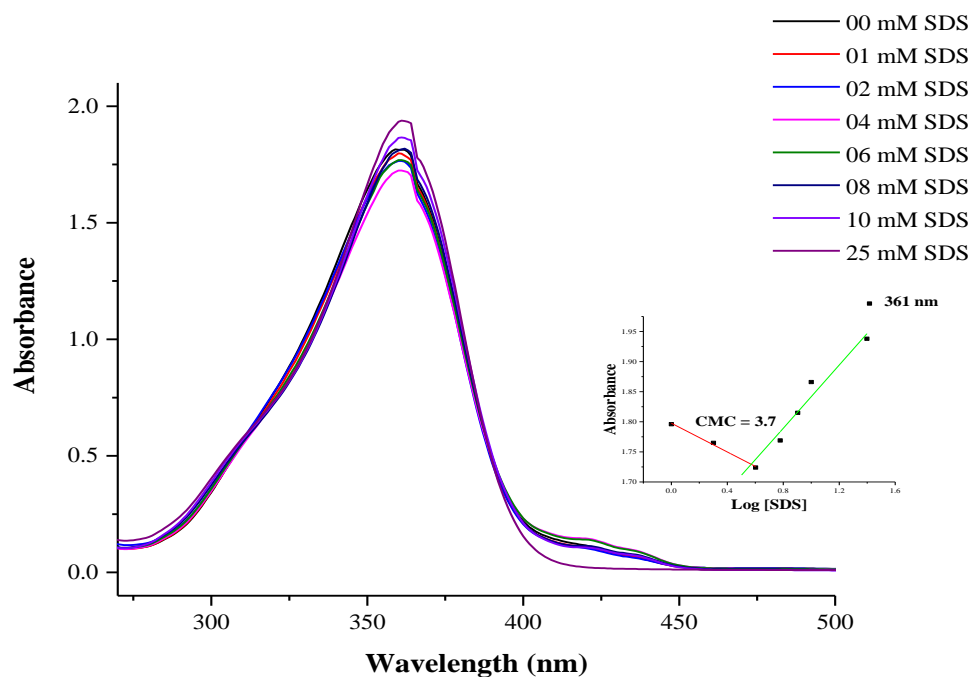


Figure 3-11: Absorption spectra of TCNQ (0.15mM) solubilized in SDS in Glyceline.

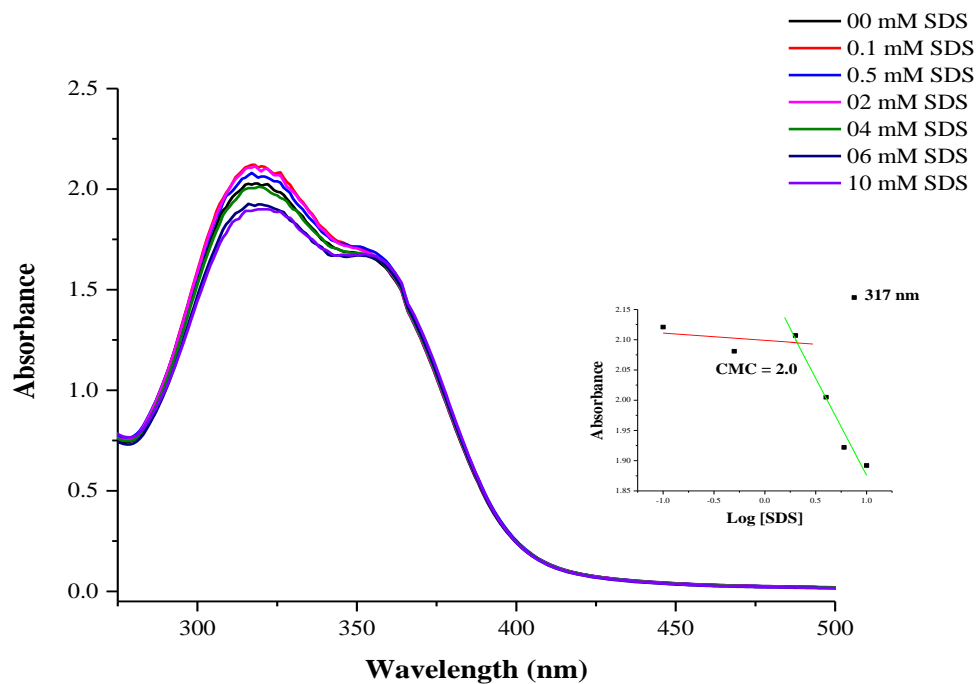


Figure 3-12: Absorption spectra of TCNQ (0.2mM) solubilized in SDS in Reline.

A third method was also used to determine the CMC based on the fluorescence spectra of an indicator molecule, pyrene. The method uses the vibrational band intensities of pyrene which shows a strong dependence on the solvent environment.⁶⁴ The method uses the intensities located at 373 nm, (the first vibronic bands (I_i)) and 384 nm, (the third vibronic bands (I_{iii})). The ratio I_i/I_{iii} , is a well-known solvent polarity scale known as the “hydrophobic index”.^{65, 66} This ratio I_i/I_{iii} proved to be a useful method to determine the CMC. One of the advantages of this method is that the small amount of pyrene used does not affect the CMC value.⁶⁷ The spectrum change of pyrene has been employed for determination CMC of SDS solutions in DESs. Plots of monomer fluorescence spectra and the dependence of I_i/I_{iii} ratio on SDS concentration of pyrene in Ethaline, Glyceline and Reline are shown in Figures 3-13, 3-14 and 3-15 respectively.

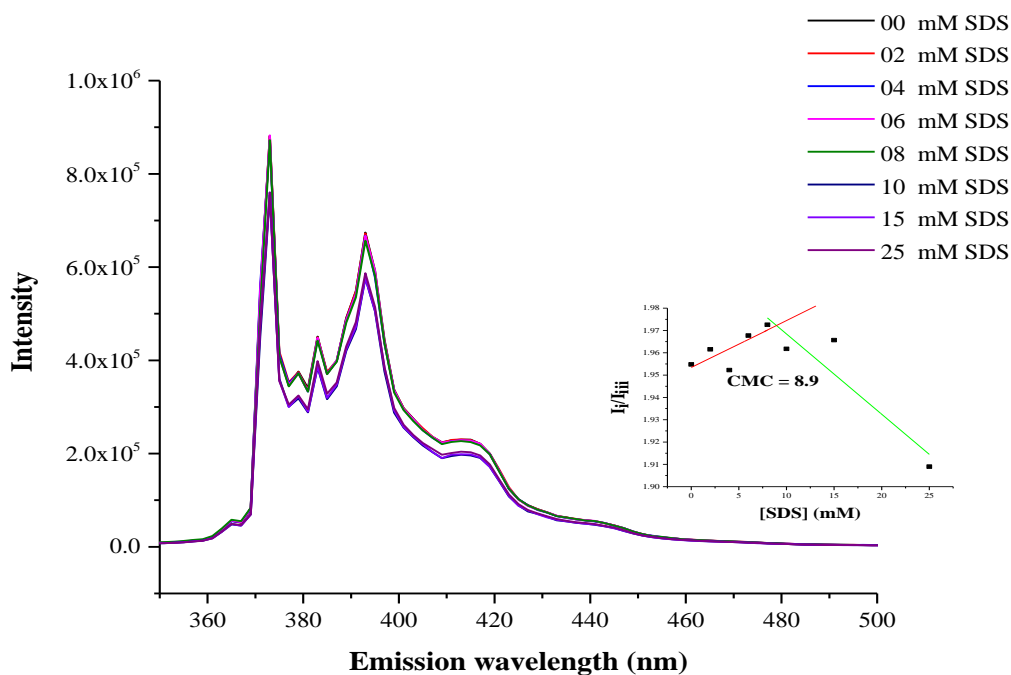


Figure 3-13: Fluorescence emission spectrum of pyrene ($1\mu\text{M}$) at the excitation wavelength (265 nm) in SDS in Ethaline.

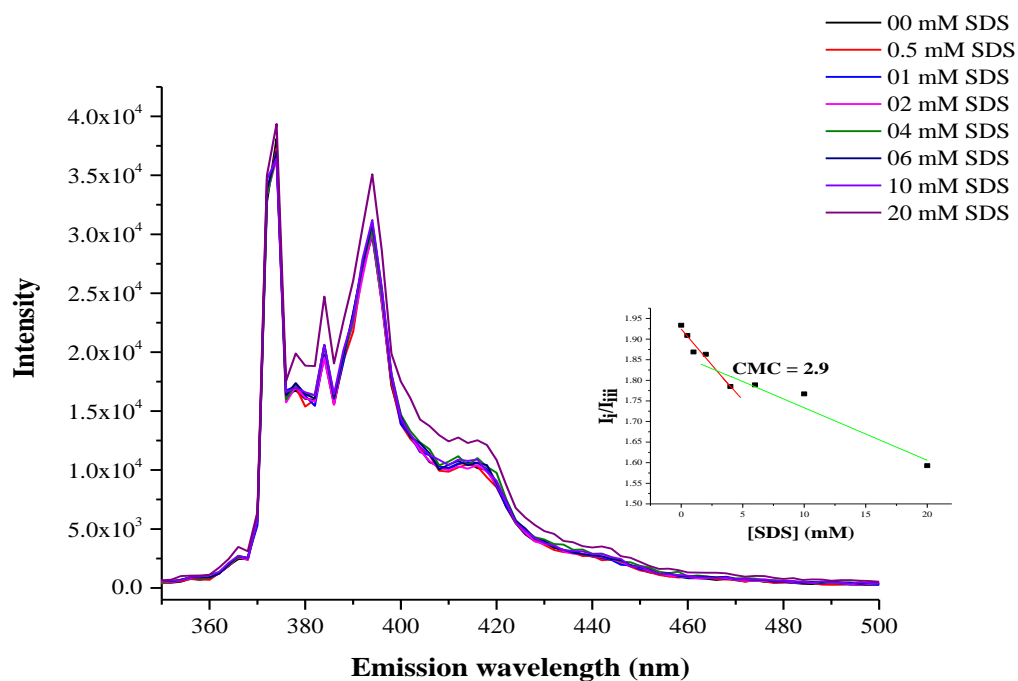


Figure 3-14: Fluorescence emission spectrum of pyrene ($1\mu\text{M}$) at the excitation wavelength (310nm) in SDS in Glyceline.

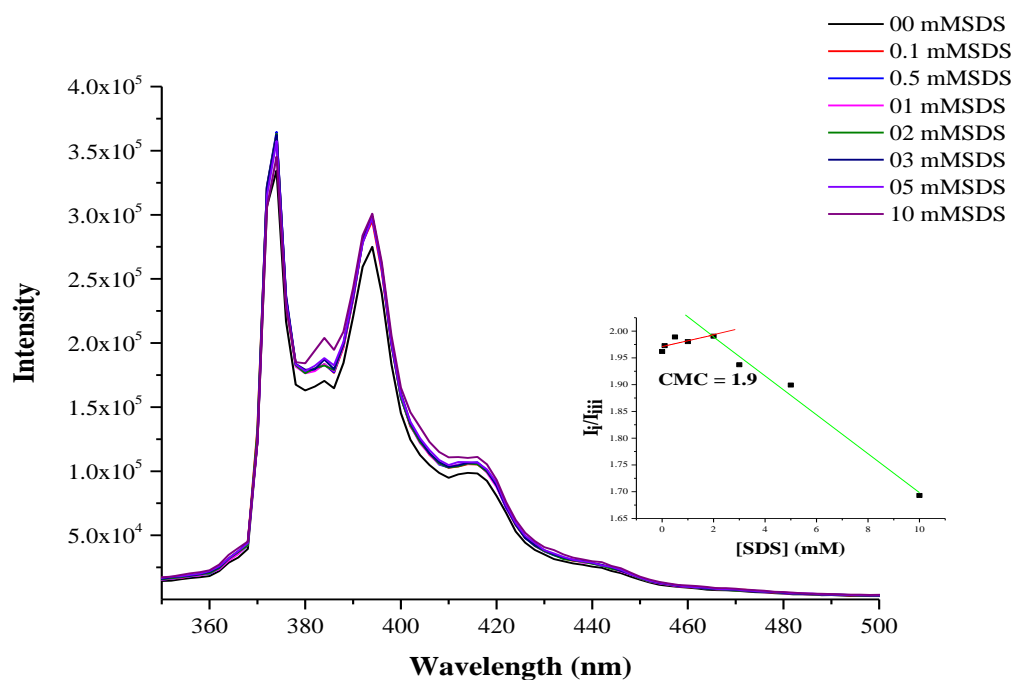


Figure 3-15: Fluorescence emission spectrum of pyrene ($1\mu\text{M}$) at the excitation wavelength (320nm) in SDS in Reline.

It is clear that the intensity ratio I_i/I_{iii} decreases as the SDS concentration is increased above CMC. This results can be explained by a decrease in medium polarity, when the pyrene monomer goes into the micelle.^{68, 69} The CMC can be determined from the intersection point on the sigmoidal curve and the data obtained are summarized in Table 3-6.

The ratio I_i/I_{iii} is a measure of solvent polarity; the higher the value, the more polar the fluid. Table 3-5 shows values of Kamlet and Taft solubility parameters for the DESs that found by Harris⁷⁰ compared to those for water together with the I_i/I_{iii} ratio determined by this study. It can be seen that all the liquids have similar polarity parameters as would be expected. These parameters are well known to measure different effects and the solvent parameters required to support micelle formation are naturally complex. These parameters probe the ability of the fluid to donate and accept hydrogen bonds and to be electronically polarised. They do not, however, contain a measure of the cohesive energy which is important in this case as it explains how easy it is to form a cavity in the liquid for the surfactant and more importantly the micelle to fit into.

Table 3-5: π^* , α , β and I_i/I_{iii} value for DESs and water.

Solvent	π^*	α	β	I_i/I_{iii}
Water	1.09	1.17	0.18	1.45
Ethaline	0.955 ± 0.001	1.022 ± 0.02	0.33 ± 0.007	2.04
Glyceline	0.964 ± 0.04	1.042 ± 0.06	0.32 ± 0.01	1.97
Reline	0.975 ± 0.02	1.050 ± 0.02	0.30 ± 0.01	1.65

π^* , α and β for DESs taken from Ref.⁷⁰

π^* , α and β for water taken from Ref.⁷¹

I_i/I_{iii} for water taken from Ref.⁷²

I_i/I_{iii} for DESs this work.

Summarising all of the CMC data determined above in Table 3-6, it is clear that the CMC values of SDS in DESs are in good agreement with each other. This confirms the validity of the above discussion and shows that the high CMC values for Ethaline are a real effect.

Table 3-6: CMC values (mM) for SDS in DESs at 25°C by three techniques.

Solvent	Surface tension	UV-spectroscopy	Fluorescence spectroscopy
Ethaline	9.00	8.1	8.9
Glyceline	3.76	3.7	2.9
Reline	1.91	2.0	1.9
Water	8.2 ⁽³⁹⁾	6.1 ⁽⁶³⁾	7.05 ⁽⁷³⁾

3.2.4 Micelles Size Analysis

Dynamic light scattering, DLS is one technique that can be used to analyse the aggregation of surfactants as well as a qualitative test to show that aggregation occurs in DESs. In this part, the experiments were carried out at different concentrations of SDS in Ethaline below and above the CMC value. The light scattering experiments were carried out in duplicate on solutions 24h after filtration and after two weeks. The reason for that is to investigate the life time and stability of aggregation. Before discussing the DLS results it is important to note that the replicate measurements for one sample show a change in the average size of the aggregate and it seem to be random with the time and number of measurements. That is might indicate that the formation of micelles is a dynamic process whereby they continually get grow and divide changing the size distribution. Figure 3-16 shows the scattering intensity as a function of particle size distribution obtained for SDS solution in Ethaline. The results show there is no detectable aggregation below the CMC and the intensity of scattered light measured at concentration above CMC suggested the existence of molecular aggregates for SDS in Ethaline. As the surfactant concentration increases a significant increase in the hydrodynamic diameter of the aggregate was observed as shown in Figure 3-16. Moreover, SDS micelles in Ethaline show stability for more than two weeks with a slow increase of the size.

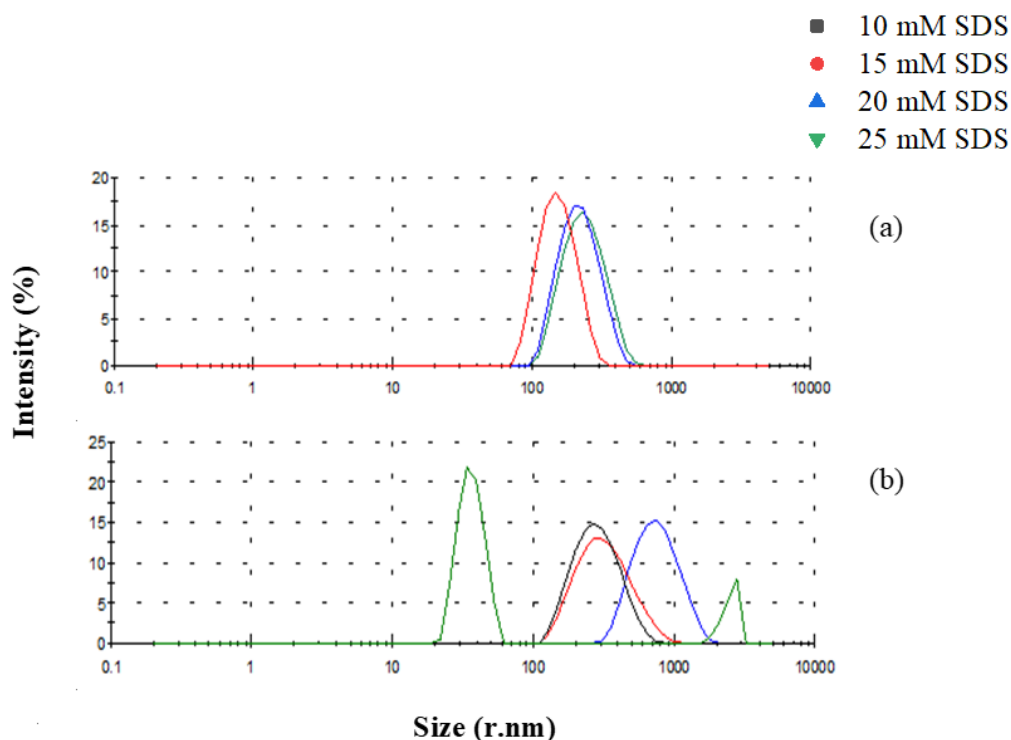


Figure 3-16: The size distribution for SDS aggregates in Ethaline at 25°C after (a) 24 h (b) two weeks.

At a concentration close to the CMC, (10 mM SDS) there was initially no indication of micelles but after 2 weeks there are clear aggregates observed which shows that the equilibrium between monomers and aggregates is relatively slow. For the sample at 15, 20 and 25 mM SDS the fact is that the micelles are disrupted during filtration producing similar size distributions but over 2 weeks these reach true equilibrium. Moreover, at 25 mM SDS concentration the aggregation behaviour is seen to change significantly after two weeks. The DLS result is not mono-modal where the two distinct peaks at 26.3 ± 2.76 nm and 2535 ± 55 nm indicate a bimodal distribution and this may be due to transition from rod like (cylindrical) to 3D networks (liquid crystals) resulting in change of average micelles size³¹ that is confirmed by the viscosity data.

The apparent hydrodynamic radius for SDS estimated to be 187 ± 24.1 nm at concentration 15 mM. The larger aggregate size is consistent with a rod like or cylindrical morphology but not a simple spherical as this would be approximately twice the length of the SDS molecule i.e. approximately 2-3 nm.⁷⁴ As mentioned above, the hydrodynamic radius of SDS aggregates increase with increasing surfactant

concentration. The DLS data suggest that the system grow from small cylindrical to elongated wormlike micelles. This aggregation in Ethaline is significantly different compared with SDS spherical micelles formed in water with diameter 3.5 - 4 nm.

A study of dodecylsulfate surfactants with different counter ions (Li^+ , Cs^+ , Mg^{2+} , Bmim^+ , Emim^+ , cholinium^+) in Reline and Glyceline showed that the shape of the aggregate formed is a function of the DES. More elongated aggregates formed in Reline compared with Glyceline.⁷⁵ This result also contrast with the aggregation in organic solvent where Rico-Lattes and Lattes showed that SDS forms small spherical micelles in formamide even at high concentrations which is different to the behaviour in water.⁷⁶ Moreover, the Anderson group⁵⁷ studied micelle formation in ILs, 1-butyl-3-methyl imidazolium chloride and hexafluorophosphate and they showed the aggregation of SDS produced significant scattering.

The relationship between the viscosity and the concentration of SDS in Ethaline has been investigated and the results are present in Figure 3-17. The data show there is slight change in viscosity at concentration below 15 mM SDS. However, there is a more significant increase in viscosity at 25 mM SDS. These results are agreed with the data for SDS in aqueous solutions as it is reported that there is a suddenly increase in the viscosity above the CMC due to micellization.⁷⁷ Some studies of viscosity of surfactants in aqueous solution show that the increase of the viscosity is related to the growth of micelles.⁷⁸⁻⁸⁰ In the case of SDS in Ethaline the change of the viscosity strongly suggested that there is growth of aggregation or more accurate change in the shape by increase the concentration of surfactant as clear from DLS results. Equation 3-6 shows the relationship between the zero shear viscosity, η and the size, in terms of aggregation number N_{agg} . It is clear that the viscosity increases strongly with both increasing aggregation number and volume fraction, ϕ .¹²

$$\eta = \text{constant } N_{agg}^3 \phi^{3.75}$$

Equation 3-6

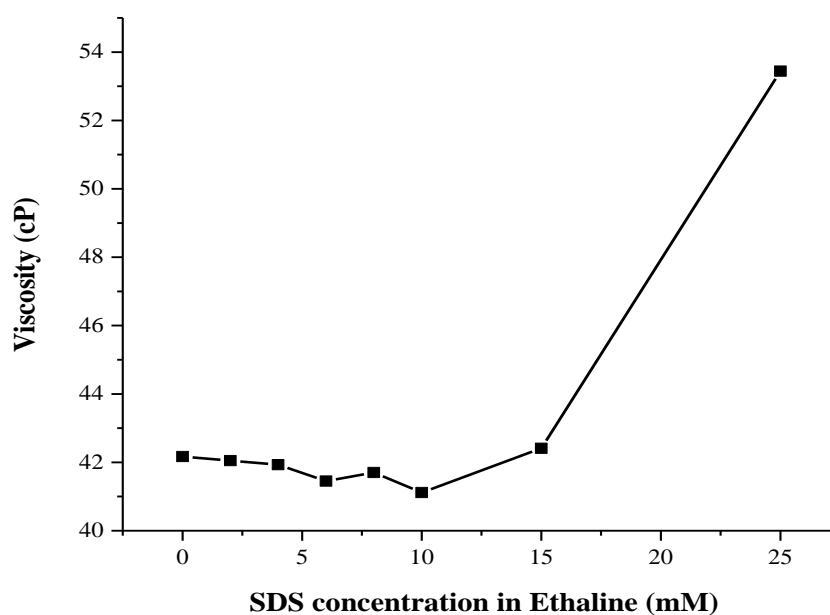


Figure 3-17: The viscosity of SDS solutions in Ethaline at 25°C as a function of concentration.

It well known that the shape and growth of any aggregation is affected by the nature of the environment. In order to explain that, it was decided to examine the effect of addition of water as a co-solvent on the size of SDS micelles in Ethaline. Figure 3-18 shows a comparison of micelle sizes in pure Ethaline and Ethaline with different water content see, it clear that there is a change of micelle size. When water was added to Ethaline the SDS micelle size initially decreased and then increased above 20% W/W water in Ethaline. This illustrates the interactions between H₂O and Ethaline which affect the micelle structure. This results agree with a study of alkyltrimethylammonium bromide surfactants in DESs based on choline chloride with malonic acid and mixtures of that with water. The authors noted that the shape of aggregates was less elongated in hydrated DES and they interpreted this as being due to an increase in the charge density at the micelle interface by presence of water.⁸¹

Studies show that the size of the micelles decreases as a result of adding polar organic solvents in aqueous media and eventually leads to a breakdown of the micellar structure. Moreover, in aqueous media it is noted that the aggregation of SDS is changed to cylindrical and bilayer micelles by adding alcohols.⁸²

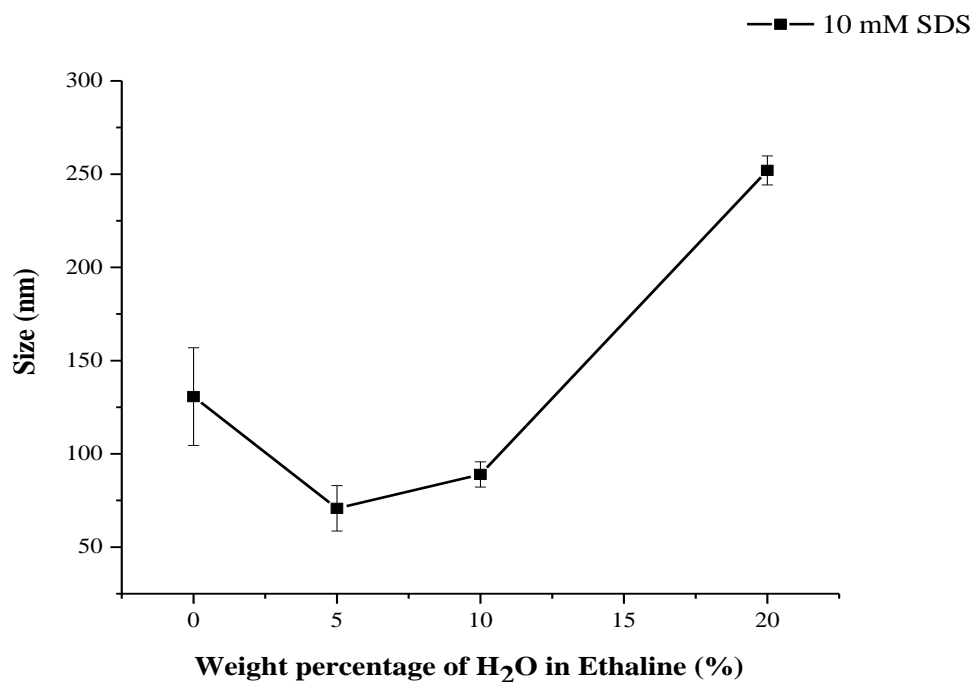


Figure 3-18: The effect of water on micelle size of SDS in Ethaline as determined using DLS.

Nanoparticle tracking analysis, NTA is a technique that complements DLS. It can be used to size particles from about 30 to 1000 nm. It can also count particles and measure particles concentrations. This technique was used by Filipe *et al.* to analyse the size of particles and protein.⁸³ In this work, NTA was used to support the DLS results and measure the concentration of SDS aggregates in Ethaline to obtain the aggregation number, N_{agg} . The NTA results confirmed the existence of micelles at 10 mM SDS as can be seen in Figure 3-19. However, this aggregation is highly asymmetric as the images flash on and off due to their rotation which indicates that SDS aggregates are non-spherical. The NTA technique also confirmed that there is no aggregation at 10 mM SDS immediately after filtration which is consistent with the DLS results and shows that filtration disrupts micellization and it is relatively slow to reform after filtration. For other concentration and again because of the big aggregation the data not reliable for the analysis but after filtration as the size become smaller, the technique was able to measuring the concentration of micelles which was 0.28×10^8 and 1.3×10^8 particles ml^{-1} for samples 15 and 20 mM SDS respectively. The repeated measurement after two weeks for the same samples show an increase in the size as noted with the DLS results.

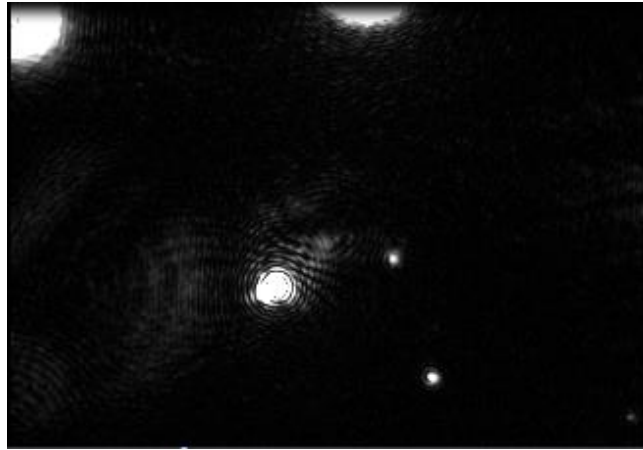


Figure 3-19: Nano Sight image for 10 mM SDS in Ethaline without filtration.

From the micelles concentration rough estimates have been made to calculate the aggregation number, N_{agg} from Equation 3-7.⁸⁴

$$[Mic] = \frac{[S] - CMC}{N_{agg}} \quad \text{Equation 3-7}$$

Where $[Mic]$ is the micelle concentration and $[S]$ is the surfactant concentration. Table 3-7 shows the aggregation number of SDS in Ethaline which is several orders of magnitude larger than that found in water.⁸⁵ However, this is not surprising given the DLS results.

Table 3-7: The aggregating number for SDS in Ethaline at 25°C.

[SDS] (mM)	$[Mic]$ (particles/ml)	Aggregation number
15	0.28×10^8	12.9×10^{10}
20	1.3×10^8	5.1×10^{10}

3.2.5 Thermodynamics of SDS Micellization in Ethaline

It is well known that the electrical conductivity of solution depends on the size and charge of the ions and the number of ions species in the solution. Thus in ionic surfactant solution there is a change in the slope of the conductivity-concentration curve at the concentration where micelles form, CMC. That is because below CMC an ionic surfactant monomers behave as normal electrolytes and they are completely dissociated and as the concentration increase the conductivity increase in linear relationship.

However, above CMC the concentration of monomer surfactants decreases as micelles form. Hence the electrical conductivity decrease as micelles behave like weak electrolyte. In aqueous solutions the solvent does not conduct and so the changes observed are due solely to the behaviour of the surfactant. In DESs or ILs, the medium itself conducts but the addition of a surfactant disrupts the ionic mobility, principally due to changes in viscosity (see above).

The results in Figure 3-20 shows a decrease of electrical conductivity after reaching CMC (primarily due to an increase in viscosity) in sharp contrast to that of aqueous solution where there is slight increase in conductivity as concentration increases.⁸⁶ Such decrease in the conductance of micellar solutions suggests that the size of micelles increases, presence of bigger aggregates and their shape is also varied.¹² In addition, taken the conductivity results, Figure 3-20 together with viscosity data, Figure 3-20, it show that there is a correlation at high SDS concentration where the dramatically increase in the viscosity causes the decrease in the conductivity as it well known that the conductivity of ions depends on their mobility rather than ionic activity.

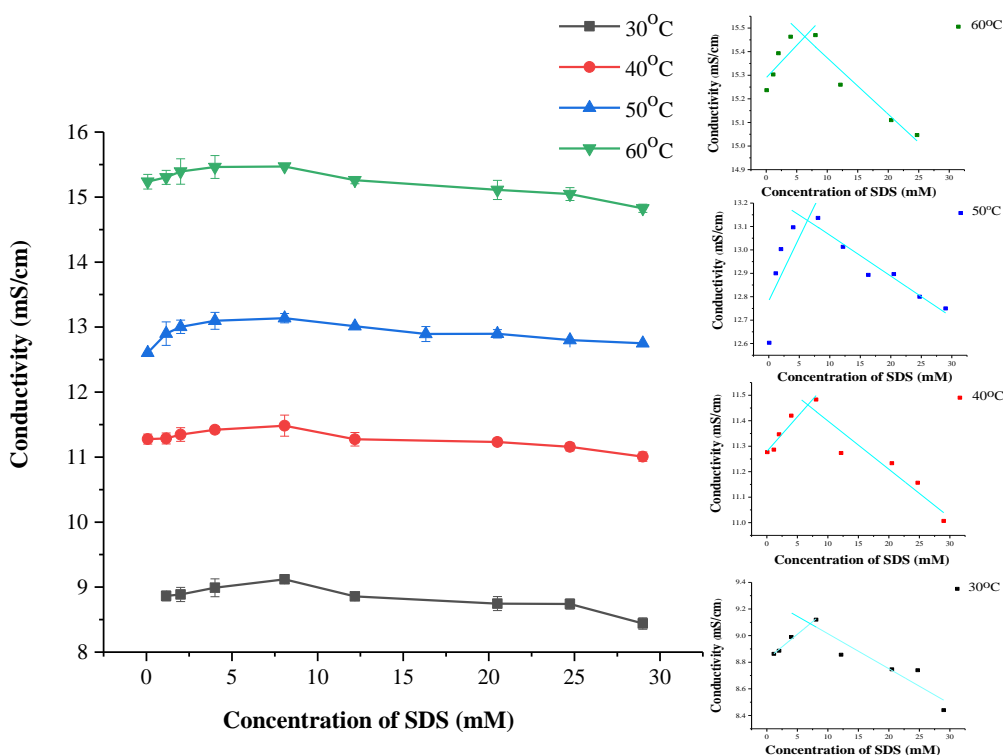


Figure 3-20: Plots of electrical conductivity versus concentration of SDS at different temperatures.

Calculation of Thermodynamic Parameters.

The electrical conductivity data can be used to calculate thermodynamic parameters for ionic surfactant. The standard Gibbs' energy of micellization ΔG^0 was calculated using the following Equation;⁸⁷

$$\Delta G_{mic}^0 = (2 - \alpha)RT \ln X_{CMC} \quad \text{Equation 3-8}$$

Where R is the gas constant, T is the absolute temperature, X_{CMC} is CMC in terms of mole fraction and α is the effective degree of dissociation of the counter-ion of surfactant which can be calculated from the ratio of straight line slopes of post-micellar, S_2 and pre-micellar, S_1 of conductivity-concentration plots that can be rewritten as:

$$\alpha = \frac{S_2}{S_1} \quad \text{Equation 3-9}$$

The value of enthalpy of micellization, ΔH^0 can be determined from the dependence of the CMC on temperature according to the following Equation:

$$\Delta H_{mic}^0 = -(2 - \alpha)RT^2 \left[\frac{d(\ln X_{CMC})}{dT} \right] \quad \text{Equation 3-10}$$

In this expression, the factor $d(\ln X_{CMC})/dT$ was calculated from the slope of straight line plotted between $d(\ln X_{CMC})$ and T .

The entropy of micellization, ΔS^0 can be obtained from:

$$\Delta S_{mic}^0 = \frac{\Delta H_{mic}^0 - \Delta G_{mic}^0}{T} \quad \text{Equation 3-11}$$

The thermodynamic parameters of micellization were obtained and reported in Table 3-8 in terms of the degree of dissociation α , Gibbs energy of micellization ΔG_{mic}^0 , entropy of micellization ΔS_{mic}^0 , and enthalpy of micellization ΔH_{mic}^0 at different temperatures. The same parameters in aqueous media are presented in Table 3-9 for comparison.

Table 3-8: The data of critical micelle concentrations (CMC), degree of dissociation (α), free energy of micellization (ΔG_{mic}^0), enthalpy of micellization (ΔH_{mic}^0), entropy of micellization (ΔS_{mic}^0) for SDS in Ethaline solutions.

T (K)	CMC (mM)	α	ΔG_{mic}^0 (kJmol ⁻¹)	ΔH_{mic}^0 (kJmol ⁻¹)	ΔS_{mic}^0 (Jmol ⁻¹ K ⁻¹)
303	7.06	0.70	-20.95	3.38	80.2
313	6.64	0.70	-21.84	3.60	81.3
323	6.66	0.58	-24.61	4.19	89.1
333	6.29	0.87	-20.37	3.55	71.8

Table 3-9: The data of critical micelle concentrations (CMC), degree of dissociation (α), free energy of micellization (ΔG_{mic}^0), enthalpy of micellization (ΔH_{mic}^0), entropy of micellization (ΔS_{mic}^0) for SDS in aqueous solutions, taken from Ref.⁸⁸

T (K)	CMC (mM)	α	ΔG_{mic}^0 (kJmol ⁻¹)	ΔH_{mic}^0 (kJmol ⁻¹)	ΔS_{mic}^0 (Jmol ⁻¹ K ⁻¹)
303	8.2	0.22	-21.6	-8.3	44
313	8.7	0.24	-21.8	-12.5	30
323	9.2	0.25	-22.1	-16.7	17
333	9.2	0.26	-22.3	-21.0	4

It is clear that the CMC value slightly decreased with increase temperature in the range investigated which is the opposite of what happens in water. The Gibbs energies of aggregation are negative in both water and Ethaline showing that both processes are spontaneous. The significant difference between the thermodynamics of micelle formation in Ethaline and water is that in the former the enthalpy of aggregation is positive while in the latter it is negative. The negative Gibbs energy in DESs is driven by the larger entropy change on micelle formation.⁸⁹ A similar observation was made by Kareem⁹⁰ who studied the transfer of molecules from decane into DESs. It was found that the enthalpy of transfer was positive and the larger the molecule, the more positive the enthalpy of transfer. It was concluded that this arose due to the endothermic

enthalpy required to form a hole in the DES in which to put the solute. The partition coefficient of molecules into DESs was found to be inversely proportional to the surface tension as surface tension is a measure of the cohesive energy density. The higher the surface tension, the harder it is to make a hole for the molecule to fit into. This fits with the data seen above, as Ethaline has the lowest surface tension of the DESs tested which means that monomers are more stable in solution and accordingly the CMC will be higher (higher concentrations are required to get the monomers to aggregate). This may also explain why the CMC in the pure ionic liquids were so high as they have relatively low surface tensions, particularly those with fluorinated anions.

The effective degree of micellar dissociation, α increases with increasing temperature, resulting in more free Na^+ ions to carry the current. For ionic surfactants, the degree of dissociation, α in range between 0.2 and 0.3 which means about 70–80% of the counter ions may be considered to be bound to the micelles.⁹¹ However, our result show high degree of dissociation 0.7 indicating that fewer Na^+ ions remain associated with the anions. This is due to the high concentration of Ch^+ compared to Na^+ ions as discussed early in section 3.2.2.

These results show that micelle formation is driven by entropic factors. This could be interpreted as resulting from the highly ordered DESs which are replaced by the more disordered micelles decreasing the order per unit volume. The thermodynamics of micelle formation are endothermic which probably arises from the need to break up the ordered DES and create a cavity for the aggregate to fit into. Creating a larger aggregate probably means that the cavity created per surfactant molecule is proportionately smaller. A rod-shaped micelle would pack monomers together more efficiently than a spherical micelle.

3.3 Conclusions

The aggregation of surfactants was studied in three DESs. It was shown that surfactants are able to self-assemble in DESs which was surprising due to the high ionic strength. This is counter to what occurs in aqueous solutions with inorganic salts, although the addition of ionic liquids to aqueous solutions is known to enable micelle formation. This observation can be explained when considering the size of the cation which has a low charge density and enables the micelle to retain a negative zeta potential which stops micelle coalescence.

The aggregation properties of SDS was investigated in three DESs and the properties were compared to aqueous solutions. It was found that surface tension, fluorescence and UV-Visible techniques all provided CMC values which were very similar, however, the values for the CMC of SDS were different in Reline and Glyceline from those in water which were similar to those in Ethaline. Replacing the ChCl with LiCl or omitting a salt at all did not result in any micelle formation confirming the importance of the large organic cation in controlling the zeta potential around the micelle.

The size of the SDS aggregates in Ethaline was found to increase with increasing SDS concentration. DLS and viscosity showed that the supramolecular aggregates of SDS in Ethaline changed from cylinders to liquid crystalline phases at about $3 \times \text{CMC}$ of SDS in Ethaline.

Finally, the aggregation behaviour of SDS was investigated in Ethaline at different temperatures to understand the thermodynamics of micellization. It was found that micelles form as spontaneously as they do in aqueous solutions but the driving force for micelle formation was entropic changes. The micelle formation was endothermic due to the large energy required to form a cavity in which to form the aggregate. This explains why it is easier to form micelles in DESs with lower surface tensions, however, this means that the CMC is slightly higher than more polar DESs such as Reline.

This chapter has shown the importance of the cation in stabilising aggregates in solution. In the next chapter the aim is to understand how the high ionic strength governs the aggregation of surfactants at air-DES and solid-DES interfaces.

3.4 References

1. L. G. Chen, S. H. Strassburg and H. Bermudez, *Journal of Colloid and Interface Science*, 2016, **477**, 40-45.
2. E. L. Smith, A. P. Abbott and K. S. Ryder, *Chemical Reviews*, 2014, **114**, 11060-11082.
3. A. Abbott, G. Frisch, S. Gurman, A. Hillman, J. Hartley, F. Holyoak and K. Ryder, *Chemical Communications*, 2011, **47**, 10031-10033.
4. H. Hooshyar and R. Sadeghi, *Journal of Chemical and Engineering Data*, 2015, **60**, 983-992.
5. I. Umlong and K. Ismail, *Journal of Surface Science and Technology*, 2006, **22**, 101.
6. M. J. Rosen and J. T. Kunjappu, *Surfactants and Interfacial Phenomena*, John Wiley and Sons, 2012.
7. T. Chakraborty, I. Chakraborty and S. Ghosh, *Arabian Journal of Chemistry*, 2011, **4**, 265-270.
8. R. J. Farn, *Chemistry and Technology of Surfactants*, John Wiley and Sons, 2008.
9. A. Tyowua, S. Yiase and R. Wuanna, *Chemical Sciences Journal*, 2012, **79**, 1-9.
10. C. Dai, M. Du, Y. Liu, S. Wang, J. Zhao, A. Chen, D. Peng and M. Zhao, *Molecules*, 2014, **19**, 20157-20169.
11. V. Mosquera, J. M. del Rio, D. Attwood, M. Garcia, M. N. Jones, G. Prieto, M. J. Suarez and F. Sarmiento, *Journal of Colloid and Interface Science*, 1998, **206**, 66-76.
12. T. F. Tadros, *Applied Surfactants: Principles and Applications*, John Wiley and Sons, 2006.
13. O. Söderman, M. Jonströmer and J. van Stam, *Journal of the Chemical Society, Faraday Transactions*, 1993, **89**, 1759-1764.
14. N. J. Turro and A. Yekta, *Journal of the American Chemical Society*, 1978, **100**, 5951-5952.
15. P. Hansson, B. Jönsson, C. Ström and O. Söderman, *The Journal of Physical Chemistry B*, 2000, **104**, 3496-3506.
16. R. Nagarajan, *Langmuir*, 2002, **18**, 31-38.
17. M. U. Araos and G. G. Warr, *Langmuir*, 2008, **24**, 9354-9360.

18. D. Lombardo, M. A. Kiselev, S. Magazù and P. Calandra, *Advances in Condensed Matter Physics*, 2015, **2015**, 1-22.
19. M. Bergström and J. S. Pedersen, *Physical Chemistry Chemical Physics*, 1999, **1**, 4437-4446.
20. S. Kumar, S. L. David, V. Aswal, P. Goyal and Kabir-ud-Din*, *Langmuir*, 1997, **13**, 6461-6464.
21. N. A. Mazer, G. B. Benedek and M. C. Carey, *The Journal of Physical Chemistry*, 1976, **80**, 1075-1085.
22. M. Toernblom, U. Henriksson and M. Ginley, *The Journal of Physical Chemistry*, 1994, **98**, 7041-7051.
23. N. J. Chang and E. W. Kaler, *The Journal of Physical Chemistry*, 1985, **89**, 2996-3000.
24. J. J. H. Nusselder and J. B. Engberts, *Journal of Colloid and Interface Science*, 1992, **148**, 353-361.
25. D. F. Evans, A. Yamauchi, R. Roman and E. Z. Casassa, *Journal of Colloid and Interface Science*, 1982, **88**, 89-96.
26. E. Y. Sheu, S. H. Chen and J. S. Huang, *The Journal of Physical Chemistry*, 1987, **91**, 3306-3310.
27. M. Pal, R. Rai, A. Yadav, R. Khanna, G. A. Baker and S. Pandey, *Langmuir*, 2014, **30**, 13191-13198.
28. K. Gracie, D. Turner and R. Palepu, *Canadian Journal of Chemistry*, 1996, **74**, 1616-1625.
29. C. C. Ruiz, J. A. Molina-Bolívar, J. M. Hierrezuelo and E. Liger, *International Journal of Molecular Sciences*, 2013, **14**, 3228-3253.
30. B. Salopek, D. Krasic and S. Filipovic, *Rudarsko-Geolosko-Naftni Zbornik*, 1992, **4**, 147-151.
31. G. Padoan, E. T. de Givenchy, A. Zaggia, S. Amigoni, T. Darmanin, L. Conte and F. Guittard, *Soft Matter*, 2013, **9**, 8992-8999.
32. E. Olson, *Journal of GXP Compliance*, 2012, **16**, 81-105.
33. M. Pal, R. K. Singh and S. Pandey, *Chemphyschem : a European Journal of Chemical Physics and Physical Chemistry*, 2015, **16**, 2538-2542.
34. T. Arnold, A. J. Jackson, A. Sanchez-Fernandez, D. Magnone, A. Terry and K. Edler, *Langmuir*, 2015, **31**, 12894-12902.

35. R. A. Mackay, *Colloids and Surfaces A: Physicochemical and Engineering Aspects*, 1994, **82**, 1-28.
36. B. Kronberg and B. Lindman, John Wiley and Sons Ltd., Chichester, Editon edn., 2003.
37. A. Chatterjee, S. Moulik, S. Sanyal, B. Mishra and P. Puri, *The Journal of Physical Chemistry B*, 2001, **105**, 12823-12831.
38. I. Umlong and K. Ismail, *Journal of Colloid and Interface Science*, 2005, **291**, 529-536.
39. P. Griffiths, N. Hirst, A. Paul, S. King, R. Heenan and R. Farley, *Langmuir*, 2004, **20**, 6904-6913.
40. K. Mukherjee, S. Moulik and D. Mukherjee, *Langmuir*, 1993, **9**, 1727-1730.
41. R. Stefanovic, M. Ludwig, G. B. Webber, R. Atkin and A. J. Page, *Physical Chemistry Chemical Physics*, 2017.
42. R. Stefanovic, M. Ludwig, G. B. Webber, R. Atkin and A. J. Page, *Physical Chemistry Chemical Physics*, 2017, **19**, 3297-3306.
43. H. Ghaedi, M. Ayoub, S. Sufian, A. M. Shariff and B. Lal, *Journal of Molecular Liquids*, 2017.
44. A. P. Abbott, R. C. Harris and K. S. Ryder, *The Journal of Physical Chemistry B*, 2007, **111**, 4910-4913.
45. I. Rico and A. Lattes, *The Journal of Physical Chemistry*, 1986, **90**, 5870-5872.
46. K. Mukherjee, D. C. Mukherjee and S. P. Moulik, *The Journal of Physical Chemistry*, 1994, **98**, 4713-4718.
47. W. Binana-Limbele and R. Zana, *Colloid and Polymer Science*, 1989, **267**, 440-447.
48. M. S. Ramadan, D. F. Evans and R. Lumry, *The Journal of Physical Chemistry*, 1983, **87**, 4538-4543.
49. M. Almgren, S. Swarup and J. Löfroth, *The Journal of Physical Chemistry*, 1985, **89**, 4621-4626.
50. H. Singh, S. M. Saleem, R. Singh and K. Birdi, *The Journal of Physical Chemistry*, 1980, **84**, 2191-2194.
51. S. Muto and K. Meguro, *Bulletin of the Chemical Society of Japan*, 1973, **46**, 1316-1320.
52. A. Beyaz, W. S. Oh and V. P. Reddy, *Colloids and Surfaces B: Biointerfaces*, 2004, **35**, 119-124.

53. A. Beyaz, W. S. Oh and V. P. Reddy, *Colloids and Surfaces B: Biointerfaces*, 2004, **36**, 71-74.
54. A. Pal and S. Chaudhary, *Colloids and Surfaces A: Physicochemical and Engineering Aspects*, 2013, **430**, 58-64.
55. A. Pal and S. Chaudhary, *Fluid Phase Equilibria*, 2013, **352**, 42-46.
56. A. Pal and S. Chaudhary, *Fluid Phase Equilibria*, 2014, **372**, 100-104.
57. J. L. Anderson, V. Pino, E. C. Hagberg, V. V. Sheares and D. W. Armstrong, *Chemical Communications*, 2003, 2444-2445.
58. K. A. Fletcher and S. Pandey, *Langmuir*, 2004, **20**, 33-36.
59. A. P. Abbott, A. Y. Al-Murshedi, O. A. Alshammari, R. C. Harris, J. H. Kareem, I. B. Qader and K. Ryder, *Fluid Phase Equilibria*, 2017, **448**, 99-104.
60. R. Hayes, G. G. Warr and R. Atkin, *Chemical Reviews*, 2015, **115**, 6357-6426.
61. L.-L. Xie, *Journal of Dispersion Science and Technology*, 2009, **30**, 100-103.
62. K. Deguchi and K. Meguro, *Journal of Colloid and Interface Science*, 1972, **38**, 596-600.
63. S. Muto, K. Deguchi, Y. Shimazaki, Y. Aono and K. Meguro, *Journal of Colloid and Interface Science*, 1971, **37**, 109-114.
64. K. Kalyanasundaram and J. Thomas, *Journal of the American Chemical Society*, 1977, **99**, 2039-2044.
65. J. R. Lackowicz, *Plenum Press, (New York, 1983) Chapter*, 1983, **5**, 111-150.
66. M. Pisárčik, F. Devínsky and M. Pupák, *Open Chemistry*, 2015, **13**, 922-931.
67. A. M. Khan and S. S. Shah, *Journal Chemical Society of Pakistan*, 2008, **30**, 186.
68. W. Li, Y.-C. Han, J.-L. Zhang and B.-G. Wang, *Colloid Journal*, 2005, **67**, 159-163.
69. N. Kundu, D. Banik, A. Roy, J. Kuchlyan and N. Sarkar, *Physical Chemistry Chemical Physics*, 2015, **17**, 25216-25227.
70. R. C. Harris, University of Leicester, 2009.
71. D. C. Dong and M. A. Winnik, *Canadian Journal of Chemistry*, 1984, **62**, 2560-2565.
72. P. Sansanwal, *Journal of Scientific and Industrial Research*, 2006, **65**, 57-64.
73. G. B. Ray, I. Chakraborty and S. P. Moulik, *Journal of Colloid and Interface Science*, 2006, **294**, 248-254.

74. X. Auvray, C. Petipas, R. Anthore, I. Rico and A. Lattes, *The Journal of Physical Chemistry*, 1989, **93**, 7458-7464.
75. A. Sanchez-Fernandez, O. Hammond, K. Edler, T. Arnold, J. Douth, R. Dalglish, P. Li, K. Ma and A. Jackson, *Physical Chemistry Chemical Physics*, 2018, **20**, 13952-13961.
76. T. Perche, X. Auvray, C. Petipas, R. Anthore, I. Rico-Lattes and A. Lattes, *Langmuir*, 1997, **13**, 1475-1480.
77. H. Akbas and T. Sidim, *Colloid Journal*, 2005, **67**, 525-530.
78. G. C. Kalur and S. R. Raghavan, *The Journal of Physical Chemistry B*, 2005, **109**, 8599-8604.
79. S. Kumar and Z. A. Khan, *Journal of Surfactants and Detergents*, 2002, **5**, 55-59.
80. G. C. Kalur, B. D. Frounfelker, B. H. Cipriano, A. I. Norman and S. R. Raghavan, *Langmuir*, 2005, **21**, 10998-11004.
81. A. Sanchez-Fernandez, O. S. Hammond, A. J. Jackson, T. Arnold, J. Douth and K. J. Edler, *Langmuir*, 2017, **33**, 14304-14314.
82. J. G. Méndez-Bermúdez and H. Dominguez, *Journal of Molecular Modeling*, 2016, **22**, 33.
83. V. Filipe, A. Hawe and W. Jiskoot, *Pharmaceutical Research*, 2010, **27**, 796-810.
84. M. H. Gehlen and F. C. De Schryver, *Chemical Reviews*, 1993, **93**, 199-221.
85. S. S. Berr and R. R. Jones, *Langmuir*, 1988, **4**, 1247-1251.
86. E. Goddard and G. Benson, *Canadian Journal of Chemistry*, 1957, **35**, 986-991.
87. C. C. Ruiz, *Colloid and Polymer Science*, 1999, **277**, 701-707.
88. J. P. Marcolongo and M. Mirenda, *Journal of Chemical Education*, 2011, **88**, 629-633.
89. C. C. Ruiz, L. Díaz-López and J. Aguiar, *Journal of Dispersion Science and Technology*, 2008, **29**, 266-273.
90. J. H. Kareem, PhD Thesis, University of Leicester, 2017.
91. D. Attwood and A. T. Florence, *FAST track Physical Pharmacy*, Pharmaceutical Press, 2012.

4 Surfactant Aggregation at DES Interfaces

4	Surfactant Aggregation at DES Interfaces.....	94
4.1	Introduction.....	95
4.1.1	Surfactant as Wetting Agents.....	97
4.1.2	The Structure of Surfactants at the Charged Surface.....	98
4.1.3	The Structure of DESs at the Electrode Interface.....	100
4.2	Results and Discussion.....	104
4.2.1	Adsorption of SDS at Air-DES Interface.....	104
4.2.2	The Wettability of Solid Surfaces by Surfactants in DESs.....	109
4.2.3	Adsorption of SDS at Electrode-DES Interface.....	113
4.2.4	Adsorption of SDS at Oil-DES Interface.....	133
4.3	Conclusion.....	138
4.4	References.....	140

4.1 Introduction

Surfactants are a surface active agent and that means the surfactant molecules accumulate at an interface by an adsorption process. In general this process consists of at least three steps first bulk diffusion then adsorption-desorption between the sub-surface, and finally surface re-arrangement. The surfactant molecules transfer from the bulk solution phase to the interface, where the hydrophilic part of the surfactant orients itself towards the polar phase (either the polar liquid or the hydrophilic solid surface) while hydrocarbon chains point towards the non-polar phase which may be air, a non-polar liquid or hydrophobic solid surface. The reason for this phenomenon is to minimise the contact between hydrophobic groups of the surfactant and the solvent which leads to changes in the interface properties.

Many studies have focused on the mechanism of surfactant adsorption at the interface as this is an important property for several applications such as foaming (liquid-gas interfaces), emulsification (liquid-liquid interfaces) and dispersion, coating, detergency (liquid-solid interfaces). The liquid-solid interface in particular has an important role in many technological and industrial applications such as oil recovery, colloidal stabilization, templating and detergency and so on.¹ Of special interest in this regard, is the behaviour of surfactant molecules at charged interfaces e.g. for modifying the behaviour at the electrode-solution interface this has many applications including controlling plating morphology and limiting corrosion.²

In chapter 3 the aggregation behaviour of surfactants in bulk DESs, Ethaline, Glyceline and Reline was investigated. Clear differences were observed in the CMC of the same surfactant in three DESs. The difference was attributed to the difference in solvent polarity where the aggregation behaviour of surfactants was strongly dependent on the polarity of DESs. This issue is shown schematically in Figure 4-1. But it is unclear which factors affect their partitioning from bulk solution to the DES-air, DES-oil and DES-solid interface. It is also unclear how charged interfaces affect the aggregation of surfactants at the electrode-DES interface in media with high ionic strength.

The surface tension experiments show that the energy required to break the surface which is also a measure of the energy required to create a cavity in the liquid, decreases in the order Reline > Glyceline > Ethaline. This order was the same as that obtained for

the surface activity at the DES-air interface of surfactants determined by measuring the surface tension as a function of the surfactant concentration.

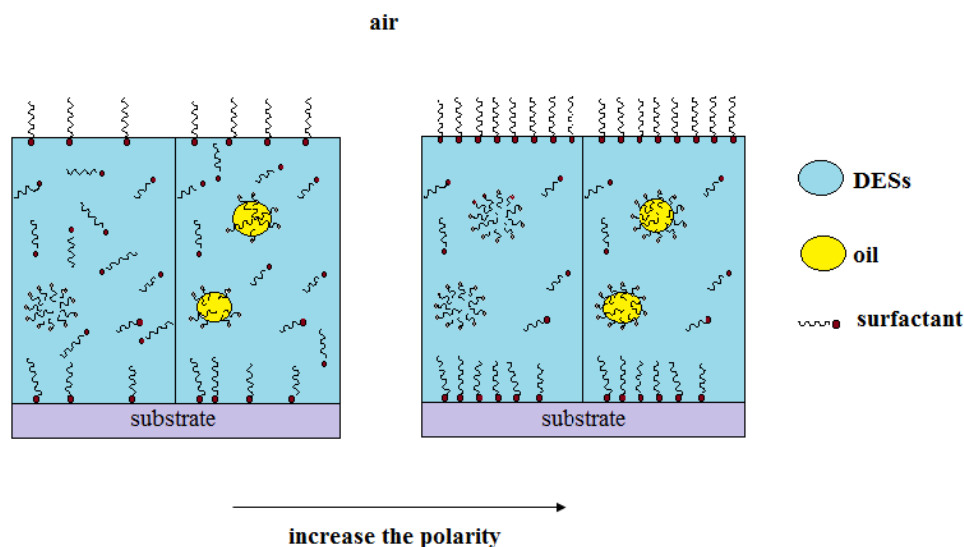


Figure 4-1: The effect of polarity of DESs in surfactants aggregation and adsorption at interfaces.

In this chapter the way in which surfactants, SDS accumulates at the interface will be studied in DESs, Ethaline and Glyceline. Experimental data could not be reliably collected for Reline due to the high viscosity. First, the adsorption of SDS at the air-DES interface will be analysed using surface tension data. Secondly, the adsorption on a metal surface and charged surface will be investigated using contact angle, CV and QCM. Finally, the adsorption of SDS between two immiscible liquids one of them DES will be invested to validate the above hypothesis. Within this chapter two key questions will be addressed;

- 1- Is the polarity of DESs important in adsorption of surfactants at DESs interfaces? (Is Figure 4-1 valid)
- 2- Is the ionic strength, especially the activity of Cl ions, competing with the adsorption of anionic surfactants at the charged interface?

A simple overview of the adsorption of surfactants at interfaces is a good starting to answer these questions.

4.1.1 Surfactant as Wetting Agents

Surfactants are often used to modify the wettability of surfaces with water by changing the interfacial tensions which enable the water to wet the solid surface that has surface Gibbs energy less than surface tension of the water, 72.8 mN m^{-1} . This process arises from adsorption of surfactants at the solid-water interface producing a film or layer on the solid surface that affects its surface tension. Theoretically, this can be defined as wettability and practically it can be measured through changes the contact angle between a solid and a liquid drop in air system.^{3,4}

The shape of ad-micelles (the film layer) depends the electrolyte composition and the charge of the substrate. Figure 4-2 shows a schematic representation of the various structures that have been proposed for surfactants at a solid-liquid interface. Either the adsorption of surfactant occurs via its head or its tail. The structure of the aggregate can be monolayers, bilayers, micelles, hemi-spherical micelles and hemi-cylindrical structures.

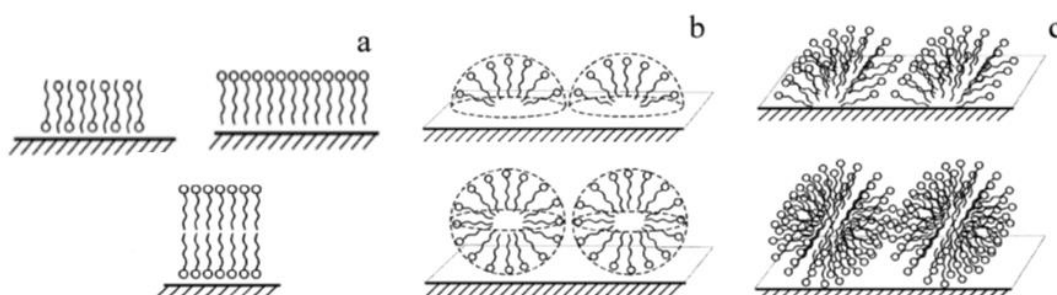


Figure 4-2: Schematic descriptions of the structures of surfactant aggregates at solid surfaces as (a) monolayer and bilayers (b) spherical hemi-micelles and micelles and (c) cylindrical hemi-micelles and micelles, taken from Ref.⁵

Liquid spreading and the wetting behaviour of solid surfaces in the presence of surfactant solution are dependent on the adsorbent, the adsorbate and the environment of the system. The nature of the solid surface is important for its interaction with the contacting liquid and factors such as the presence of highly charged sites or nonpolar functionalities or domains are important. Surfactant adsorption at a solid-liquid interface depends on the nature of surface where the adsorption of surfactants decrease for hydrophobic low energetic surface whereas it does not always reduce in the case of

hydrophilic surfaces.⁶ While for the adsorbate (the surfactants), the adsorption depends on the molecular structure of either being ionic or non-ionic and the structure of the hydrophobic group whether it is long or short, straight chain or branched, aliphatic or aromatic. Moreover, the pH, electrolyte content and temperature affects the environment of the system and hence the adsorption process.^{7, 8} Wetting of surfaces is also affected by the charge on the solid surface. Where the surface is electrically polarisable then electrowetting can occur when an electric field is applied. The contact angle for a surface can be changed as the potential is varied. This works best for a hydrophobic surface. It has found use in adjustable lenses, electronic displays and optical switches.⁹⁻¹¹ Electrowetting can also be important when amphiphilic additives are added to electroplating baths.

A good probe to look at the aggregation of surfactants at charged interfaces is to use electrochemistry. While the electrochemistry of aqueous surfactant solutions has been studied intensely, aggregation from ionic liquids is almost unstudied. In aqueous solutions, Coulombic interactions will dominate the aggregation of surfactants at the electrode-solution interface. In a medium containing 5 M of salt, it could be expected that ionic surfactants would be less active. Previous studies by Barron¹² and Azam¹³ have shown conflicting results on the effect of surfactants at modifying the nucleation of metals.

4.1.2 The Structure of Surfactants at the Charged Surface

It is well known that an electrochemical process involves electron transfer between the electrode and an electroactive species. The presence of surfactants can influence the kinetics of electron transfer or can cause severe perturbation of the measured currents. This influence arises from blocking the electrode surface from the reactants by adsorbed surfactants either totally or just at certain electrode potentials or by electrostatic interactions between the electroactive species and adsorbed surfactants.^{14, 15} The first use of surfactants in electrochemistry was to suppress the polarographic maxima or to stabilize electro-generated intermediates.¹⁶ The presence of surfactants can be used in electrochemistry to; increase the voltage range available for voltammetry and electro synthesis, improve the properties of electrodeposited metals, increase the rate of metals deposition and solubilize organic material in aqueous solutions for electrochemical studies.¹⁷

Modelling the structure of adsorbed surfactants at the electrode surface is more difficult than in bulk solution because of complications due to electrode-surfactant interactions. Generally, in aqueous solutions the adsorption mechanism occurs in two steps as a function of surfactant concentration. At concentrations below the CMC the adsorption process is driven firstly by surfactant-surface interactions, leading to a low surface density of adsorbed surfactant molecules. Then the adsorbate density increases as the concentration increases until it levels off around the CMC and the driving force for the adsorption is governed by interactions between the surfactant molecules themselves until a saturation coverage is reached.¹ At, and above, the CMC, bilayers or hemimicelles form at the electrode surface. As the surfactant concentration increases well above the CMC, multilayers form particularly at extreme potentials of opposite sign of that of the surfactant head group.¹⁸

The structure formed at the electrode surface and the extent of adsorption very much depends upon a number of factors; the nature of the surfactant and electrode, surfactant concentration, the applied potential and presence of supporting electrolyte or electroactive substance.¹⁹ Many of electrochemical studies have been reported in surfactant solutions in order to study the effect of adsorbed surfactants on electron-transfer properties and the surface structure at the electrode interface. Mackay¹⁹ showed that SDS formed a monolayer on a platinum electrode at concentrations of 0.01-0.1 mM when the platinum electrode potential was in the range 0 to 0.4 V vs. Ag/AgCl, and as the potential increase to 0.8 V a bilayer formed. This structure changed as the concentration of SDS increased to 1 mM where a multilayer was formed above 0.4 V. whereas hemi-micelles arranged in a long-range two-dimensional lattice were reported by Burgess at el²⁰ when they studied SDS molecules aggregate at charged Au(111) electrode surfaces. Another study by Marino and Brajter-Toth²¹ using different surfactants of different carbon chain lengths and different charge head groups and different electrodes, rough pyrolytic graphite (RPG) and glassy carbon (GC) reported that the surfactant interacts with the electrode via the head group of the surfactant forming hemi-micelles at the surface. They also showed that the aggregation at the electrode was different for RPG and GC resulting in different electrochemical responses. Increasing the ionic strength promoted the adsorption of surfactants where a study of the effects of < 100 mM NaCl on SDS adsorption to a Quartz Crystal Microbalance (QCM) shows an increase in the adsorption.²²

4.1.3 The Structure of DESs at the Electrode Interface

The presence of excess positive or negative charge on the electrode surface which is in contact with an aqueous electrolyte solution has been intensively investigated resulting in recognised models of the electrical double layer structure. The term, electrical double layer, (EDL), is used to describe the total interfacial region formed in contact between the electrode surface and solution phase. The structure is important, since it affects the electrochemical measurements. the double layer considered as a capacitor in an electrical circuit that used to measure the current at the working electrode.²³ There are three theoretical models of the solid-liquid interface in aqueous electrolyte solution, Helmholtz model, Gouy–Chapman model and Gouy–Chapman–Stern model. Here we will present the modern one, Gouy–Chapman–Stern model which is basically a combination of the Helmholtz and Gouy–Chapman models. Although this model cannot be directly transferred to DESs because the model provides a better approximation to explain dilute electrolyte in aqueous solution where the ions are treated as point charges while DESs have high concentrations of bulky non-centrosymmetrical ions.²⁴ It is a very important concept to understand the differences that arise from these types of ionic fluids.

A modern simplified model of the structure of the electrical double layer is presented in Figure 4-3. When the electrode is immersed in aqueous electrolyte solutions, a layer of water molecules adsorb on the electrode surface. The way of adsorption depend on charge at the electrode surface where the hydrogen atoms of adsorbed water molecules are oriented toward the negative charged electrode while the oxygen atoms will be oriented toward the positive charged electrode surface. Two layers are associated with the double layer, the inner Helmholtz layer, IHP which is more commonly known as the Stern layer which is a thin layer of highly organised region, about 10 Å extends from the electrode surface to approximately the outer Helmholtz plane that made up of solvent molecules, solvated ions of the electrolyte and neutral molecules adsorbed on the electrode surface. The other layer that is a three-dimensional region extends from the centres of the hydrated ions adsorbed to the electrode into the bulk solution is called the outer Helmholtz layer, OHP or more commonly, the diffuse layer and its thickness depends on the electrolyte concentration.^{23, 25} The change in electrical potentials at the electrode surface is linked to the electrical double layers, IHP and OHP and it is illustrated in Figure 4-4. It shows that the drop in the potential is considered to be linear

through the inner layer and an exponential decay through the outer layer to the bulk solution potential. This is because the concentration of counter ions in the outer layer, diffuse layer decreases exponentially as the distance from the electrode surface increases.²⁵ The thickness of the double layer is related to Debye–Hückel length, Equation 3-3. For typical electrolyte systems it is approximately $1.5 \kappa^{-1}$.

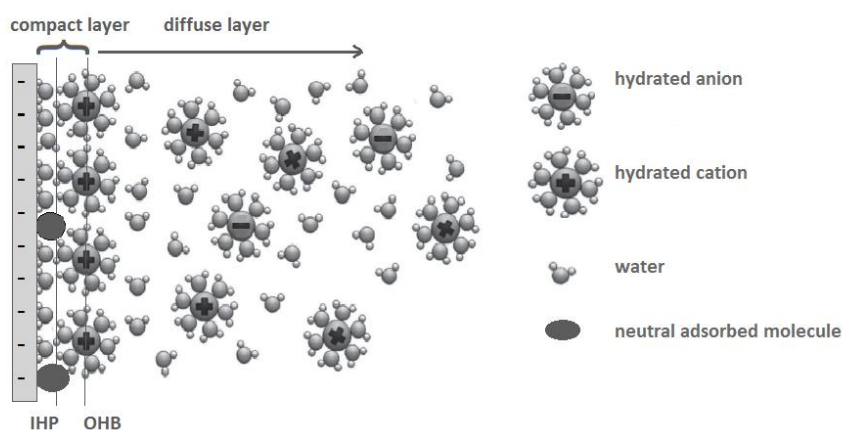


Figure 4-3: Schematic representation of the Gouy–Chapman–Stern model of the electrical double layer formed at the metal–aqueous electrolyte interface.

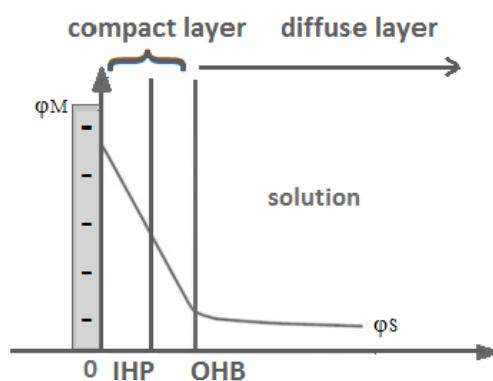


Figure 4-4: Potential profile in the double layer formed at the negatively charged electrode.

It is important to understand the structure of the double layer in concentrated fluids such as ILs or DESs. ILs are not our focus, however, previous findings on the structure of the double layer in ILs are presented as they are similar to DESs and have been studied in slightly more detail. Kornyshev²⁶ proposed a model of IL ions whereby the bulky

cations in combination with more compact anions form structures at the electrode surface as shown in Figure 4-5.

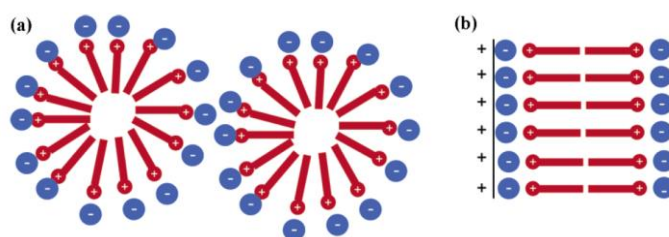


Figure 4-5: Scheme explain the structure of asymmetric ions and their counter ions in (a) the bulk solution of an ionic liquid and (b) near the electrode surface, taken from Ref.²⁶

Despite the extensive use of DESs in electrochemistry,^{27, 28} very little is known about the structure at the electrode-DESs interface where only a few studies are available.²⁹⁻³² Figueiredo *et al.*²⁹ used cyclic voltammetry and electrochemical impedance spectroscopy to study the interface between Glyceline and various electrodes, platinum, gold and glassy carbon. It was reported that the double layer differential capacitance is sensitive to the electrode material and indicated a slight dependence of the potential. The same group³⁰ extend their study using several DESs based on choline chloride using a hanging Hg electrode. They reported that at large negative potentials the cations were surrounded with a layer of HBD molecules followed by and adsorbed layer of Cl^- ions. At less negative or positive polarizations, Cl^- ions are adsorbed at the electrode surface. More recently Chen *et al.*³¹ used atomic force microscopy, density functional theory calculations, and contact angle measurements, and found that at negative potentials Ch^+ ions is attracted to the surface whereas Cl^- is specifically adsorbed at positive potentials at highly ordered pyrolytic graphite electrode interface with Ethaline, Glyceline and Reline which is in consistent to a similar previous study.³⁰ However, the results contrasted with the findings of Costa *et al.*³⁰ who reported that HBD molecules are repelled from the electrode surface at both negative and positive potentials and HBD molecules are located in a surface layer in contact with the Stern layer. This difference may be explained by the change in several factors such as nature and molar ratio of HBD used in DESs as well as the type of electrode used.^{29, 30}

Another study by Vieira *et al.*³² agreed with the observation that Ch^+ and Cl^- adsorb at the electrode surface and they gave more detail about Ch^+ and Cl^- adsorption on glassy carbon electrodes using the spectroelectrochemical study of Ethaline. They indicated that from 0 to -0.6 V mostly of Ch^+ molecules adsorbed to the electrode surface and the reversible scan from -0.6 to +0.4 indicated re-adsorb Ch^+ molecules on the electrode. While at more positive potential from +0.4 V it noted re-arrangement of the interfacial species where Ch^+ is replaced by Cl^- on the electrode.

In this chapter, the experiments will focus on DESs, Ethaline and Glyceline with surfactant, SDS. The difference between the adsorption of Ch^+ and Cl^- is related to the fact that while Ch^+ is a big cation with charge set behind three CH_3 groups and this cation is free from hydrogen bonding that form DESs whereas Cl^- is small and extensively bonded with OH groups to form hydrogen bonds. Moreover, a study by Stefanovic *et al.*³³ reported that the hydrogen bond density in Glyceline was more than in Ethaline hence it would be expected that more non-bonding Cl^- ions are available in Ethaline compared with Glyceline. As SDS is added to Ethaline or Glyceline, therefore, three points should be taken in to account:

- 1- The Ch^+ concentration is higher than Na^+ by about 200 times so the ion neutralizing the negative charge of the micelles or adsorbed on SDS bilayers at the electrode surface will be Ch^+ rather than Na^+
- 2- At positive potentials it is possible for both Cl^- ions and SDS head groups to be adsorbed at the electrode surface. The relative concentrations will depend on the charge density of the ions and the relative amounts of species in solution. It may also depend on entropic facts driving the surfactant to aggregate.
- 3- The DESs used in this study have different Cl^- activities. Ethylene glycol is less strongly bound to the chloride anion than glycerol which means that the double layer should be different in the two DESs.

4.2 Results and Discussion

4.2.1 Adsorption of SDS at Air-DES Interface

The discussion of surface tension in chapter 3 provided information about the bulk aggregation of surfactant and enabled the determination of the CMC. In this chapter, the adsorption layer of surfactants is characterized using the Gibbs equation. The surface tension isotherms can be used to analyse the interfacial behaviour of SDS at the air-DES interface by using the Gibbs adsorption Equation 4-1 which allows the surface excess concentration, Γ_{max} and surface area per molecule A_{min} to be calculated from the relationship between surface tension γ and logarithm of surfactant concentration, C according to:⁷

$$\Gamma_{max} = -\frac{1}{nRT} \left[\frac{d\gamma}{d\ln C} \right] \quad \text{Equation 4-1}$$

Where, Γ_{max} is the surface excess concentration at saturation, n is the total number of chemical species produced in solution per surfactant monomer $n = 1$ for non-ionic surfactants or ionic surfactants in the presence of excess electrolyte, R is the gas constant and T is the temperature in kelvin. As surfactant is added to a solvent its concentration at the surface is higher than that in the bulk solution as a result of the adsorption. The difference of surfactants concentration at the surface and the bulk is called the surface excess concentration, Γ_{max} which is useful to measure the effectiveness of adsorption at the interface.³⁴ From the saturation adsorption, Γ_{max} and Avogadro's number N_0 the minimum area per surfactant molecule, A_{min} can be calculated as follows:

$$A_{min} = \frac{1}{N_0 \Gamma_{max}} \quad \text{Equation 4-2}$$

The surface tension data can also provide the effective surface tension reduction, Π_{CMC} which is given by the following formula:

$$\Pi_{CMC} = \gamma_0 - \gamma_{CMC} \quad \text{Equation 4-3}$$

Where γ_0 is the surface tension of the pure DES and γ_{CMC} is the surface tension of the solution at the CMC. Π_{CMC} is a measure of the effectiveness of the surfactant to reduce the surface tension for a pure solvent.

The standard Gibbs energy of micellization ΔG_{mic}^0 can be calculated using Equation 4-4 and this can be used to calculate the values of standard Gibbs energy of adsorption ΔG_{ad}^0 , using Equation 4-5.³⁵

$$\Delta G_{mic}^0 = RT \ln CMC \quad \text{Equation 4-4}$$

$$\Delta G_{ad}^0 = \Delta G_{mic}^0 - \frac{\pi_{CMC}}{\Gamma_{max}} \quad \text{Equation 4-5}$$

The surface tension versus logarithm of surfactant concentrations obtained for SDS in Ethaline and Glyceline is presented in Figure 4-6. In addition the values of γ_0 , γ_{CMC} , Π_{CMC} , Γ_{max} and A_{min} for SDS in Ethaline and Glyceline are shown in Table 4-1.

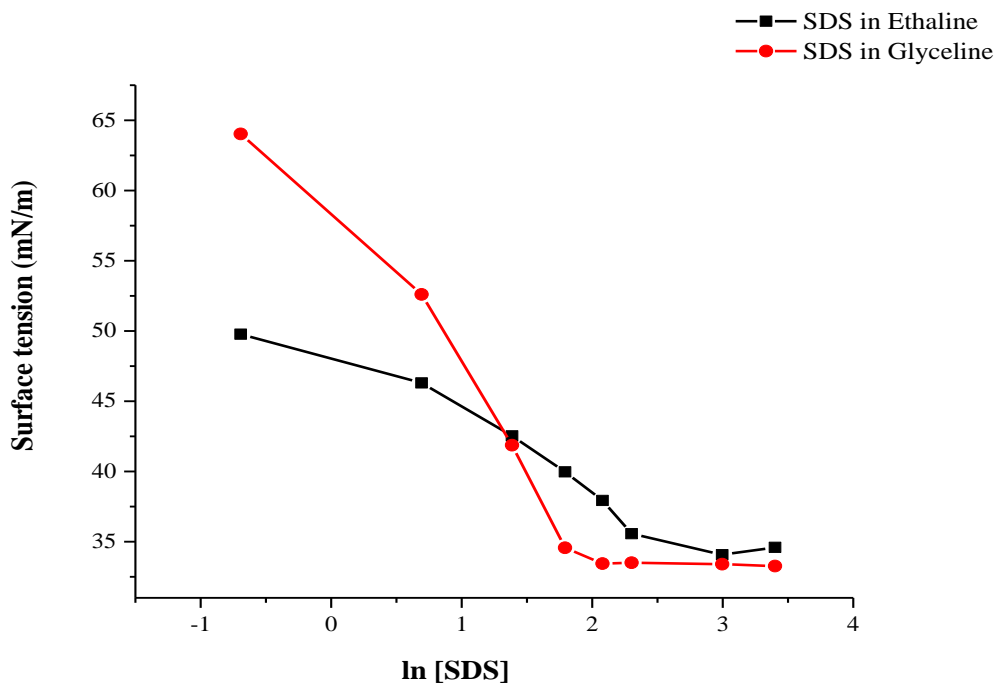


Figure 4-6: Surface tension isotherms for SDS in Ethaline and Glyceline.

Table 4-1: Surface properties of SDS in DESs and water at 25°C.

Solvent	γ_0 (mN m ⁻¹)	γ_{CMC} (mN m ⁻¹)	Π_{CMC} (mN m ⁻¹)	Γ_{max} ($\mu\text{mol m}^{-2}$)	A_{min} (\AA^2)
Ethaline	55.20	35.10	20.10	1.70	97.72
Glyceline	64.03	33.53	30.50	3.45	48.18
water	72 ⁽³⁶⁾	38.6 ⁽³⁷⁾	31.07 ⁽³⁸⁾	2.38 ⁽³⁸⁾	69.78 ⁽³⁸⁾

It is clear that the calculated Π_{CMC} value in Ethaline is smaller than in Glyceline and water because γ_0 value of Ethaline, 55 mN m⁻¹ are lower than for water and Glyceline. However, this is the first sign that the adsorption of SDS at the liquid-air interface is higher in Glyceline compare to Ethaline.³⁴ Moreover, γ_{CMC} values in all cases are somewhat comparable. The surface tension when the surface becomes saturated with surfactant monomers, γ_{CMC} was about 35.1 and 33.53 mN m⁻¹ in case of Ethaline and Glyceline respectively and not far from the value for water. This shows that the liquid surface appears more like that of a hydrocarbon.³⁹ This implies that once the surface is saturated with surfactant it does not really sense the liquid underneath, which is logical. As the monolayer formed at the interface is independent on the chain length of adsorbed surfactant so with the same surfactant it is not surprising that γ_{CMC} does not change.

The value of Γ_{max} and A_{min} obtained from the surface tension isotherms provides information about the molecular arrangement of SDS at the air-DES interface. As can be seen from Table 4-1 the Γ_{max} in Glyceline is higher than in Ethaline. Indicating that the number of SDS molecules accumulate at the interface in Glyceline is greater than in Ethaline. Assuming that the dodecylsulfate group is oriented roughly perpendicular to the interface then the largest part of the cross section would come from the sulfate group. Sulfate has an ionic radius of $2.42 \pm 0.07 \text{ \AA}$.⁴⁰ The square area occupied by SDS in Glyceline is a square of length 7 \AA whereas for Ethaline it is a square of length 10 \AA . This shows that the surfactant molecules are either not close packed, or not perpendicular to the surface.

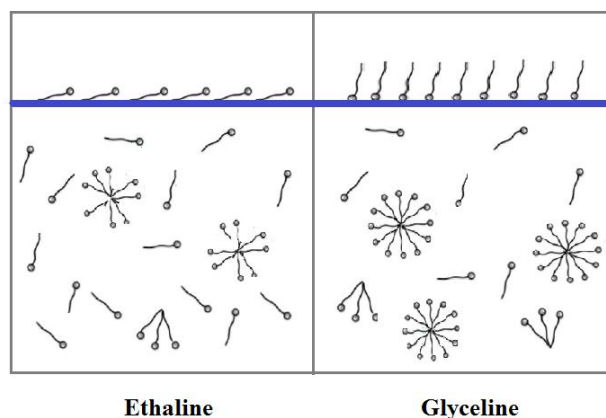


Figure 4-7: Schematic representation of the orientation of SDS at the air-DES interface.

It is well established that the area occupied per surfactant ion or molecule reflects the orientation of the ion or molecule at the interface.⁴¹ Higher A_{min} values for a specific surfactant can indicate weaker solvophobic interactions and vice versa as solvophobic interactions cause the molecules to pack vertically increasing the packing density of the surfactants at the interface.⁴² As can be seen from Table 4-1, the A_{min} values indicate that SDS in Ethaline is less solvophobic than in water or Glyceline. The inference from this is that it is fairly vertical in Glyceline and fairly horizontal for Ethaline. This is the first indication that the adsorption of SDS at air-DES is dependent on the polarity of DESs and corroborates the previous statement about polarity. Figure 4-7 shows potentially the mode of how SDS is expected to orientate at the air-DESs interface.

The values obtained for ΔG_{mic}^0 and ΔG_{ad}^0 are presented in Table 4-2 for both DESs investigated. Both values are negative which indicates that the formation of micelles and the adsorption are spontaneous. However, it may be easily concluded that standard Gibbs energy of adsorption is more negative than that of the standard Gibbs energy of micellization which indicates that the adsorption of SDS molecules at the air-DES interface precedes the micellization in the bulk solution.

Table 4-2: The standard Gibbs energy of micellization ΔG_{mic}^0 and adsorption ΔG_{ad}^0 for SDS in DESs.

DES	ΔG_{mic}^0 (kJ mol ⁻¹)	ΔG_{ad}^0 (kJ mol ⁻¹)
Ethaline	-11.78	-23.61
Glyceline	-13.81	-22.66

A very important feature for a solvent to enable self-assembly of amphiphilic compounds is the high cohesive energy density. The cohesive energy density of a solvent can be described using the Gordon parameter as indicated in Equation 4-6 where γ_{LV} is the air-liquid surface tension and V_m is the molar volume.⁴²

$$G = \frac{\gamma_{LV}}{V_m^{1/3}} \quad \text{Equation 4-6}$$

The data for the Gordon parameters of DES under this study are shown in Table 4-3. Usually solvents which form strongly hydrogen-bonded networks have a high cohesive energy density. It is clear that the cohesive forces in Glyceline are higher than Ethaline from the Gordon parameter in Table 4-3 although the values are not as high as in water. This may suggest that the SDS monomer solubility in Ethaline is higher than in Glyceline therefore; SDS monomers can exist in the bulk phase without forming aggregates. This can be seen in the fact that SDS has a higher CMC in Ethaline (8.6 mM) compared with Glyceline (3.8 mM).

Table 4-3: Surface tensions (γ), Gordon parameter (G), and hole radius (r) for the DESs and water.

Solvent	γ (mN m ⁻¹)	G (J m ⁻³)	r_H (Å)
Ethaline	55.20	1.14 ⁽⁴³⁾	1.44
Glyceline	64.03	1.24 ⁽⁴³⁾	1.34
Water	72 ⁽³⁶⁾	2.74 ⁽⁴³⁾	-

Another parameter related to the surface tension of liquid is the average size of the void, r_H which can be calculated from the surface tension, γ data of the pure liquids, Boltzmann constant, K_B and temperature, T as described in Equation 4-7.⁴⁴

$$4\pi\langle r_H^2 \rangle = 3.5 \frac{k_B T}{\gamma} \quad \text{Equation 4-7}$$

The average size of the holes in Ethaline and Glyceline was calculated and are presented in Table 4-3. It can be seen that the hole in both solvents is too small to fit a SDS monomer, the length of the SDS molecule i.e. approximately 2-3 nm⁴⁵ so a significantly larger hole are required to accept the SDS molecules. To create a large hole it is necessary to overcome the cohesive energy density in a solvent. It is well known that the surface tension is a measure of the cohesive force in a liquid so a high surface tension is found in liquids with a high cohesive force. This means that the force recourse to mead a hole in Glyceline is higher than Ethaline which allow SDS monomer to dissolve in Ethaline and transfer to the interface in Glyceline.

4.2.2 The Wettability of Solid Surfaces by SDS in DESs

The wettability of a surface is a term to describe the affinity of a liquid to form a film and spread on a solid substrate rather than bead upon the surface.⁸ The wetting behaviour of a fluid on a solid surface depends on the physical and chemical properties of the surface, surface tension and contact angle of the liquid.³ It is well known that surfactant solutions alter the wetting process by changing the surface tension of a liquid and solid-liquid interfacial tension as results of adsorption of surfactant molecules at the interfaces. The presence of a film of adsorbed surfactants changes the contact angle in a solid-liquid drop-air system, which is a measure of wettability. Therefore, the most popular method of quantifying wetting is the contact angle measurement.

Measurements of the contact angle for DESs containing SDS on stainless steel were done as a function of SDS concentration and are shown in Figure 4-8. Although DESs are already relatively good at wetting the surface of stainless steel as the contact angel is less than 90°,⁴⁶ the wetting process of SDS on stainless steel surface can be described into two stages. There is a sharp decrease of the contact angle as the surfactant concentration increases until the CMC thereafter the value remains approximately constant. The decreasing contact angle indicates that the surfactant was adsorbed onto to the stainless steel surface.

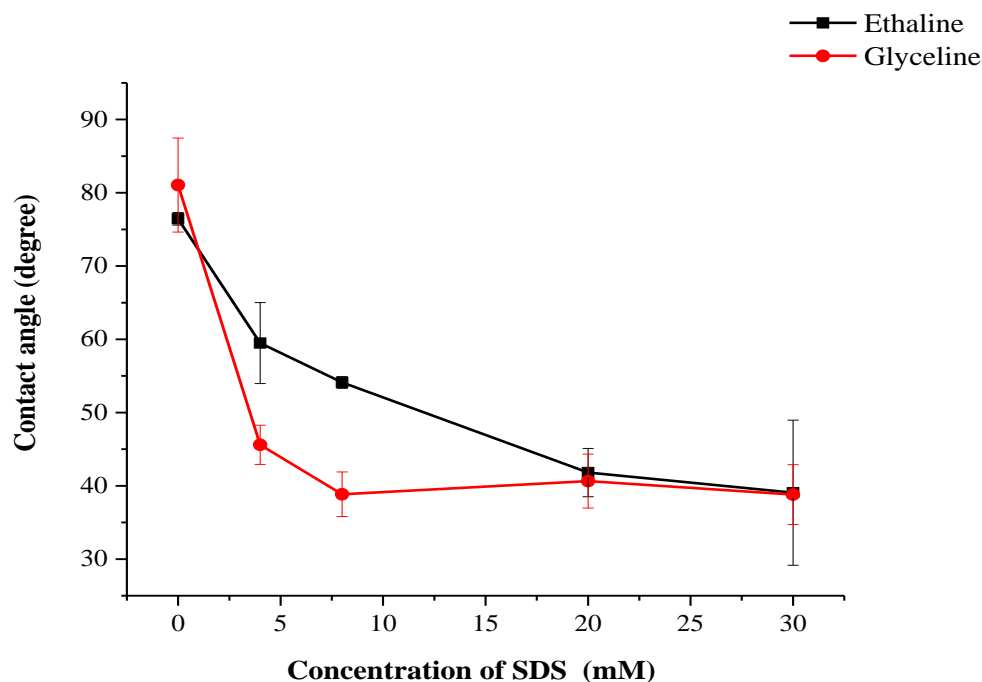


Figure 4-8: Contact angle of SDS solutions in DESs on stainless steel surface versus surfactant concentration.

According to Chaudhuri and Paria³ the decrease in contact angle values in the surfactant solutions was due to the increase in hydrophobicity of the surface, since the expected orientations of the surfactant molecules are similar in nature on hydrophobic surface after the adsorption through tail groups.³ SDS molecules are adsorbed at both air-DESs and stainless steel-DESs interface where the stainless steel surface is a hydrophobic surface⁴⁷ hence the interfacial tension is reduced. That led a decrease in the contact angle for stainless steel-DESs-air systems. A study by Levchenko *et al.*⁵ reported that the affinity of SDS adsorption in aqueous solution towards hydrophobic self-assembled monolayers is greater than the hydrophilic self-assembled monolayers.

The value of contact angle in terms of adsorption and wetting of surfactant solutions have been known to be affected by changes in many factors such as surfactant concentration, ionic strength of solution, pH, and surface roughness.⁴⁸ For the first parameter, the high concentrations of surfactant results in a complete adsorption of surfactants monomer at the solid-liquid interface. For the second, it is well established that the surface tension and CMC decreases by adding electrolytes to the ionic surfactant solutions as well as increases the adsorption density at both air-liquid and

solid-liquid interfaces at low concentration of surfactant.³ The reason behind this is the reduction of the repulsive interaction between the head groups of surfactant molecules at interface as well as in bulk solution as results of presence of electrolyte. Hence as the presence of electrolytes affects the contact angle as well as its wetting properties, Luepakdeesakoon *et al.*⁴⁹ reported that adding NaCl to aqueous SDS solution results in a decrease of the CMC, decreased SDS adsorption onto the solid surface and reduction in the solid-liquid interfacial tension. Chaudhuri and Paria³ observed a significant change in the contact angle by adding salt to an aqueous solution of sodium dodecyl benzene sulfonate and cetyltrimethylammonium bromide surfactant on a hydrophobic solid surface (Teflon) even at very low surfactant concentration. Also the counter ion valency of the electrolyte was very important in decreasing the contact angle.

Herein the high ionic strength of DES would be expected to play an important role in adsorption and wetting of SDS on a stainless steel surface. The wettability of the solid surface should be improved with Ethaline compared to ethylene glycol by adding SDS. The results in Figure 4-9 shows the contact angle of SDS solutions in Ethaline and ethylene glycol on a stainless steel surface at different surfactants concentrations. The results point out that there was only a slight change in contact angle over the range of SDS concentrations in ethylene glycol solutions which indicate that there is unsaturated surfactant layer at the liquid-solid interface in contrast with in Ethaline system. Moreover, it seems that at high SDS concentration the contact angle value are the same in both solvents.

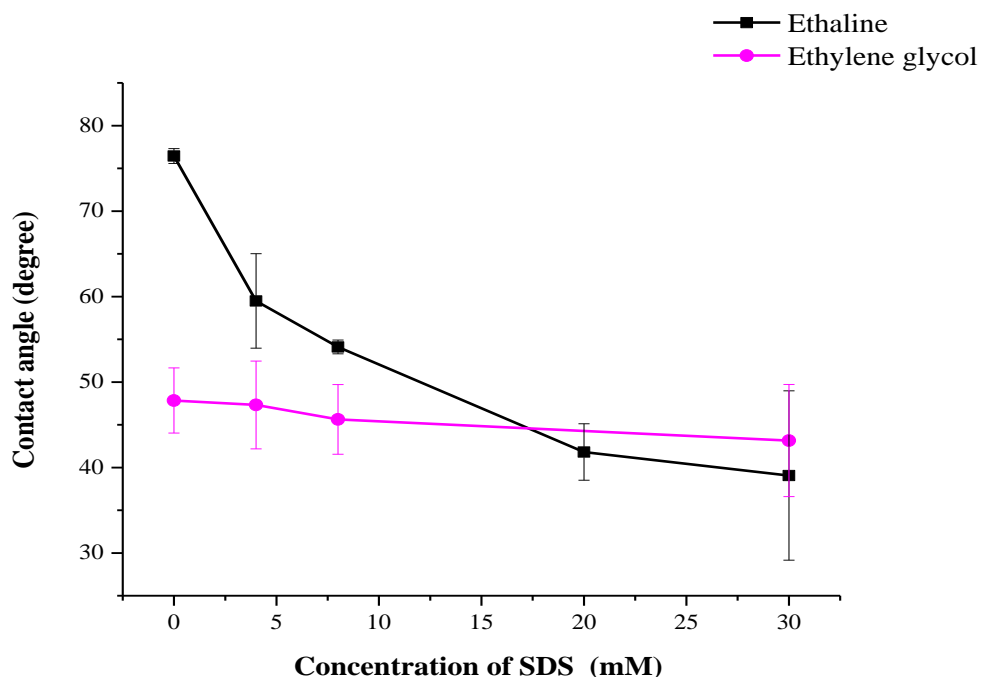


Figure 4-9: Contact angle of SDS solutions in Ethaline and ethylene glycol on stainless steel surface versus surfactant concentration.

Zhang *et al.*⁴⁷ studied SDS adsorption on stainless steel as a function of NaClO₄ in aqueous solutions. They reported that the increase the SDS concentration led to an increase in the mass adsorbed and once a monolayer was filled subsequent adsorption led to hemimicelles. Whereas when NaClO₄ was added the adsorption isotherm shifted to lower SDS concentrations due to a change in electrostatic interactions. This may explain that the difference in ionic strength for Ethaline and Glyceline, the different of Cl⁻ free in the bulk solvent as results of forming hydrogen bond, which leads to a difference in adsorption at the interface. It is already known that the interactions between glycerol and chloride are stronger than those between ethylene glycol and chloride. This means that with a metallic surface there will be a competition between the two anionic species dodecyl sulfate and chloride. A higher chloride activity will lead to a lower surfactant adsorption and cause a smaller decrease in the contact angle. This may then also start to explain why SDS did not function as a surface modifier in the work of Barron¹² or Azam¹³ when studying the electrodeposition of zinc and silver in Ethaline respectively. These previous studies were qualitative in their approach investigating a range of additives and establishing whether they were effective. In this

next section the role of surfactants at blocking electron transfer and diffusion will be established using electrochemical measurements.

4.2.3 Adsorption of SDS at Electrode-DES Interface

4.2.3.1 Cyclic Voltammetric Study in Micellar DES Solutions

In this section FeCl₂ is used as a probe in micellar DES solutions. This was chosen as it is known to have a reversible redox process. The speciation in Ethaline and Glyceline is predominantly [FeCl₄]²⁻ and it is known to partition into the ionic liquid phase of DES-water mixtures.⁵⁰ It is therefore likely that it will not partition into the micelle itself. In the second part of the study tetrathiafulvalene, a more hydrophobic molecule which undergoes two redox processes, will be studied. It may be expected that this would have a stronger interaction with the micelle. If there are significant structures which evolve at the electrode-DES interface then these two probes should have a significantly different behaviour.

The dynamics of micelle formation and solute solubilization play an important role in the electrochemistry results. In aqueous solutions, the lifetime of the surfactant monomer in the micelle is in the range between 10⁻³ and 10⁻⁷ s, while the micelle lifetime is in the range between 10⁻³ and 1 s. The rate of solute enters a micelle k_{in} is diffusion controlled and it related to the solubilisation of solute, S in micelles, M as following:



While the exit rate from the micelle k_{out} is directly proportional to the solubility of the solute in the solvent which is in the order of 10³-10⁶ s. The mechanism of electron transfer between a micelles and the electroactive species are important when these parameters are considered.¹⁹ Moreover, the location of a solute in the micelle should be considered; it could be associated with the surface of the micelle, just below the head-group or buried deep within the core of the micelle.¹⁹ One issue with micelles in DESs could be that the high viscosity of the liquid may make monomer and electroactive species ingress and egress from the micelle slower that would be experienced in aqueous solutions. It should be expected that the presence of interactions between the

substrate surface and the polar head group of the surfactant would alter the spacing between the surfactant head groups and lead to a change in the surface area occupied per surfactant molecule. This change causes a change in the packing parameter. Consequently, the shape of the adsorbed micelle would be different to the bulk solution.

Figure 4-10 shows three common models which are assumed for the adsorption of surfactant at the electrode surface from aqueous solutions. The most common is model (a) where a bilayer is assumed to occur at the charged electrode-solution interface. Model (b) is more likely when the surface is more hydrophobic and model (c) accounts for systems where the surfactant does not specifically adsorb at the metal surface.

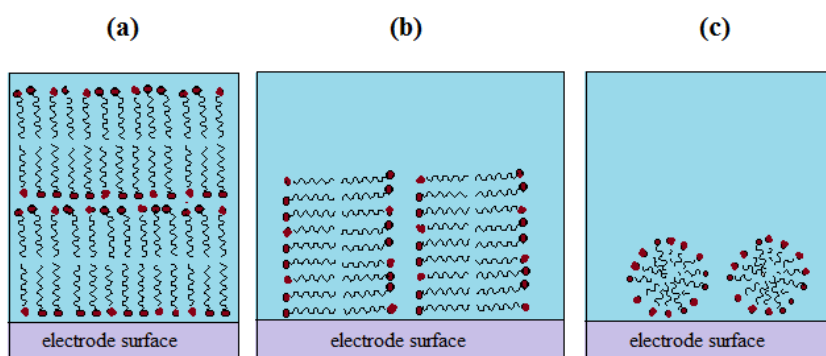


Figure 4-10: Common models for surfactant interactions at an electrode surface.

Wanless and Ducker studied the time dependency of SDS adsorption on graphite and they reported that it took at least 15 min to form a stable layer.⁵¹ The relative stability of the electrochemical signal at different sweep rates suggest that the electrode interface is at equilibrium.

In this study, an anionic surfactant, SDS was used with a platinum electrode which is hydrophilic⁵² so the adsorption of SDS should be via the sulfate head groups. The formation of monolayers or bilayers depends on the electrode potential and the SDS concentration.¹⁹ The other possible suggestions can be seen in Figure 4-10 (b) and (c) the same solvophobic driving force that enables aggregation in bulk DESs helps to organize the surfactants to aggregate on the electrode surface. Herein the surfactants aggregate like tubes extended from the electrode surface to the bulk solution (b) whereas in (c) the aggregation of surfactant will be in the same manner in (b) but the

extent of aggregate surfactants is horizontally. In both of the later cases, there are channels between these tubes either vertically or horizontally which allow electroactive species to reach the electrode surface. Moreover, the position of solubilized solute in micellar solution should be considered when evaluating electrochemical data. Where the electroactive species may be located on or near the surface of the micelle, this can affect the availability of the electroactive species for electron transfer in model (c).^{19, 24}

In voltammetric experiments the half-wave potentials, electron transfer rate constants, charge transfer coefficients, diffusion coefficients, stability of electro generated anion or cation radicals can all be affected by the presence of surfactants.⁵³ Therefore, the electrochemical studies of electroactive compounds is an effective approach to characterise diffusion of redox-active reagents⁵⁴ and estimate interfacial adsorption–desorption processes in micellar solutions.⁵⁵

The cyclic voltammogram is characterized by the peak potentials, cathodic, E_{pc} and anodic, E_{pa} where the average of the peak potentials is the voltammetric half-wave potential, $E_{1/2}$ and the difference between the peak potentials is the peak potential separation, ΔE_p that it is used as a qualitative indication of whether the redox reaction is reversible or not.⁵⁶ For a reversible one electron transfer process at 298 K, $\Delta E_p = 0.059$ V ($2.303RT/nF$).

In this study, iron (II) chloride was used as the electrochemical probe to study the electrochemistry in SDS micellar solution in DESs. It would be expected that $[\text{FeCl}_4]^{2-/-}$ will not bind onto the micellar surfaces as they carry the same charge as the micelle.

Figure 4-11 shows a cyclic voltammogram of FeCl_2 (20 mM) on a Pt electrode in Ethaline and Glyceline at a scan rate 5 mVs^{-1} and 25°C vs a Ag wire reference electrode. The oxidative scan shows one anodic peak at 0.567 and 0.581 V for Ethaline and Glyceline respectively associated with the $[\text{FeCl}_4]^{2-/-}$ couple. The reverse scan shows one cathodic peak at 0.470 and 0.476 V associated with the corresponding reduction. It is clear from the voltammograms that the magnitude of current is much higher in Ethaline than in Glyceline because of the slower mass transport in Glyceline due to its relatively high viscosity 326.0 cP for Glyceline versus 42.2 cP for Ethaline at 25°C .

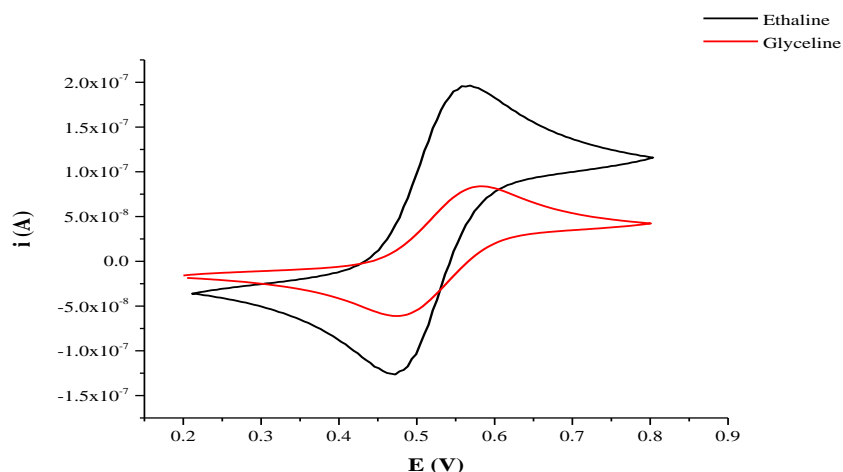


Figure 4-11: Cyclic voltammogram of 20 mM $FeCl_2$ in DESs at scan rate 5 mVs^{-1} and 25°C .

Table 4-4 shows the analysis of the voltammetric parameters as a function of scan rate. For both DESs the anodic and cathodic peak currents increased with increase scan rate and the ratio $-i_{pc}/i_{pa}$ is approximately 1. Moreover, the, ΔE_p values for the $[FeCl_4]^{2/-}$ redox couple are between 0.093 and 0.156 V which is significantly higher than the theoretical 0.059 V. This could be attributed to slow electron transfer or ohmic drop due to resistance of the solution.^{57, 58,59} In addition, $E_{1/2}$ values at all scan rates remained constant.

Table 4-4: Cyclic voltammetric data for oxidation of the $[FeCl_4]^{2/-}$ couple in DESs.

Solvent	Scan rate (mVs^{-1})	i_{pc}/i_{pa}	ΔE_p (V)	$E_{1/2}$ (V)
Ethaline	5	1.07	0.097	0.52
	10	1.07	0.095	0.52
	20	1.03	0.093	0.52
	50	1.05	0.098	0.52
	100	1.02	0.101	0.52
Glyceline	5	0.98	0.105	0.53
	10	1.03	0.116	0.53
	20	0.99	0.126	0.53
	50	0.94	0.139	0.53
	100	1.01	0.156	0.53

The same experiments were repeated in both DESs with different concentrations of SDS added. The results are shown in Figure 4-12 at a scan rate of 5 mV s^{-1} and the parameters of the analysis are listed in Table 4-5.

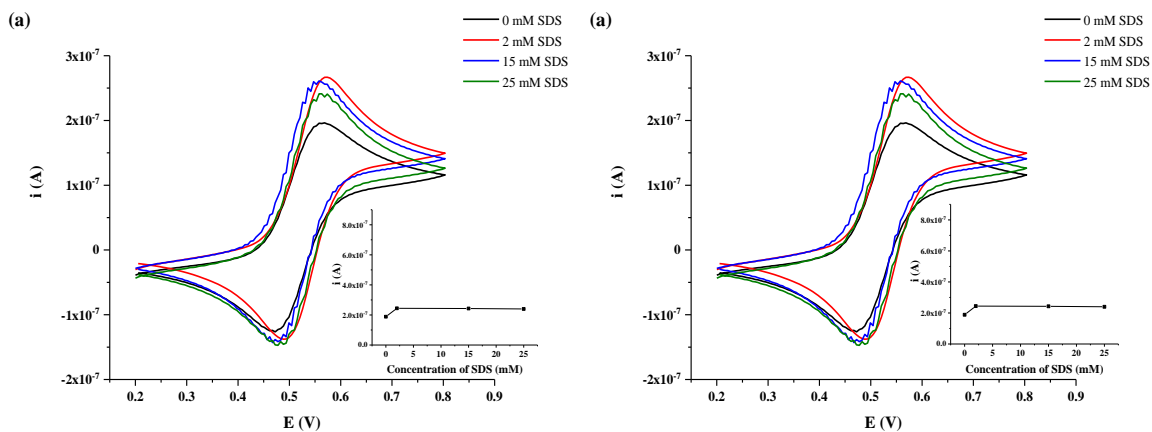


Figure 4-12: Cyclic voltammogram at a scan rate 5 mVs^{-1} for a 20 mM FeCl_2 in (a) Ethaline and (b) Glyceline at 25°C at various concentrations of SDS. Insets show plot of i_{pa} versus SDS concentration.

In Ethaline there is a slight increase in peak current when surfactant is added which remains roughly constant up to an SDS concentration of 25 mM. In Glyceline there is a slight fluctuation in peak current when SDS is added but there is a notable decrease in current at an SDS concentration of 25 mM.

Table 4-5: Cyclic voltammetric data at 5 mVs^{-1} for the $[\text{FeCl}_4]^{2-/-}$ couple in DESs at different SDS concentrations.

Solvent	[SDS] (mM)	i_{pc}/i_{pa}	ΔE_p (V)	$E_{1/2}$ (V)	slope
Ethaline	0	1.07	0.097	0.52	0.43
	2	1.02	0.080	0.53	0.48
	15	1.00	0.084	0.52	0.48
	25	0.98	0.081	0.52	0.48
Glyceline	0	0.98	0.105	0.53	0.43
	2	0.97	0.088	0.52	0.48
	8	0.92	0.099	0.53	0.46
	25	0.94	0.096	0.52	0.52

The data presented in Table 4-5 show that $E_{1/2}$ does not change when surfactant is added i.e. there is no change in the process thermodynamics. In both liquids, there is a small, but significant decrease in i_{pc}/i_{pa} as surfactant is added. Moreover, it is important to note that there is less of a shift in ΔE_p with add SDS than there was in the absence of surfactant. In the absence of surfactant the process became less reversible at increasing sweep rate. The addition of surfactant appears to reverse this trend, which is very unusual. It can clearly be concluded from this study that SDS affects the structure of the double layer at the electrode-DES interface most probably resulting from specific adsorption of surfactant.^{23, 60} It is also evident that the effect is different in both DESs. The role of the surfactant does not appear to be as a blocking layer at the electrode-solution interface.

Mandal and Nair⁶¹ studied the effect of surfactant concentration on the peak current for the reduction of $[\text{Co}(\text{en})_3](\text{ClO}_4)_3$ using aqueous solutions of the cationic surfactants cetyltrimethylammonium bromide, CTAB and cetylpyridinium chloride, CPC. They found that i_p sharply decreased with increasing surfactant concentration, however, above the CMC the i_p value increased again. They claimed that this change in peak current was due to differential partitioning of the electrochemical probe between the bulk solvent and the micelle. They also noted a 35 mV shift in $E_{1/2}$ up to the CMC where after it did not change. The same group⁶² successfully obtained the CMC of SDS, Triton X-100 and Tween-80 using $\text{K}_4\text{Fe}(\text{CN})_6$ as an electrochemical probe and KCl as the supporting electrolyte with Pt as both working electrode and counter electrode and a saturated calomel reference electrode. The same trends were observed and data were explained in the same way.

Zhang and Bard reported that the peak currents increased when surfactants adsorption occurred and they said that this was due to a head-tail-tail-head arrangement. They suggest that there is a short separation between surfactant head groups and the surface in tail-on adsorption that causes this increase in the current.⁵⁹ Moreover, Atta *et al.*⁶³ used terazosin, an antihypertensive drug, as an electroactive species in aqueous SDS solutions and they found that i_{pa} increased and reached a constant value when studied on a glassy carbon electrode. They attributed that to the adsorption of SDS molecules on the electrode surface and the formation of micelle aggregates close to the electrode surface.

The data above do not fit with any of the classical models shown in Figure 4-10. The decrease in ΔE_p and the slight increase in i_p tends to suggest that the surfactant layer is not a complete mono or bi-layer on the surface as has been shown in some aqueous systems (model (a)). If it is assumed that the electrode-DES interface is dominated by a layer of relatively strongly interacting chloride plus HBD as was shown by Atkin group³³ then it could be proposed that the role of the SDS is to compete with chloride for the surface. The partition coefficient of the two species close to the electrode surface would depend on the charge density and their relative concentrations. The chloride concentration in Ethaline is approximately 200 times that of SDS. Assuming the SDS is easier to displace than the chloride this could explain why the current for iron (II) chloride oxidation increases and ΔE_p decreases when the surfactant is added to the DES. This is shown schematically in Figure 4-13.

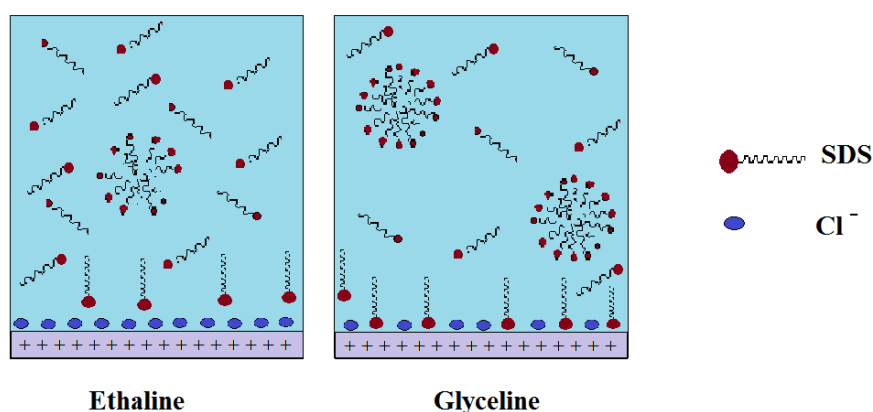


Figure 4-13: Schematic representation of the electrode DES interface with SDS.

The current increase in the Ethaline system may indicate that the change in EDL occurs by replacing the Ch^+ with Na^+ from the SDS. To examine this idea, an experiment was carried out with NaCl instead of SDS. Figure 4-14 shows the peak current for FeCl_2 oxidation decreased only very slightly in the presence of NaCl which shows that it is the dodecyl sulfate which is the active ingredient which changes the current at the electrode surface.

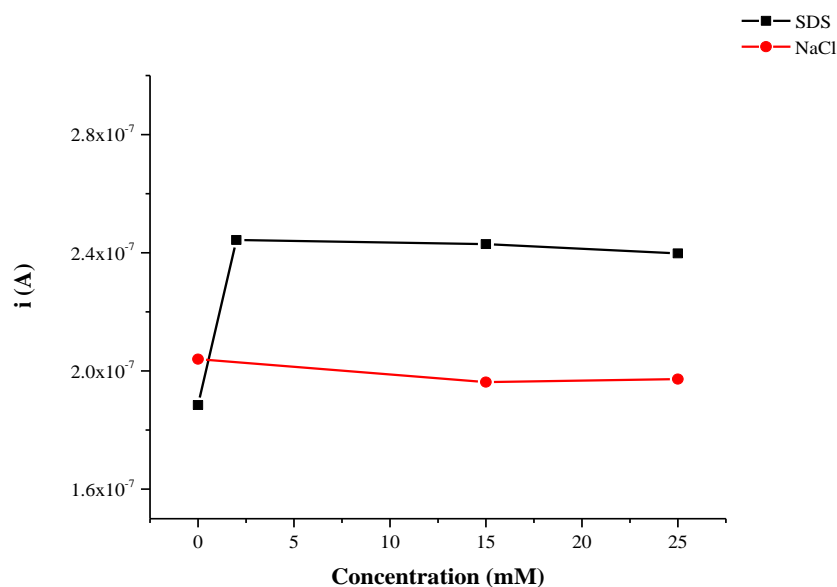


Figure 4-14: The effect of SDS and NaCl on the peak current observed for oxidation of 20 mM FeCl₂ in Ethaline at scan rate 5 mVs⁻¹.

To understand the adsorption process in more detail it is useful to measure the charging of the electrode in the absence of an electroactive species. To do this very slow scan rate voltammetry is carried out and the charging current is determined by integrating the area under the box-shaped curve. Figure 4-15 shows these slow sweep rate voltammogram in Ethaline and Glyceline in the presence and absence of different concentrations of SDS.

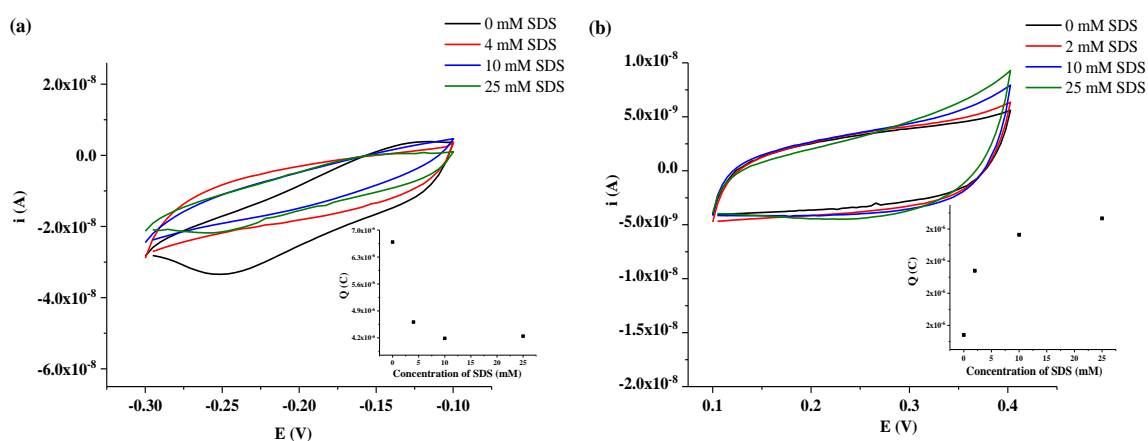


Figure 4-15: Cyclic voltammogram of (a) Ethaline and (b) Glyceline on Pt working electrode, Pt flag counter electrode and Ag wire reference electrode at a scan rate of 1 mVs⁻¹ and at 25 °C as a function of SDS concentration.

Figure 4-15 shows that SDS causes the capacitance of the electrode-DES interface to decrease in the case of Ethaline and to increase in the case of Glyceline. The difference between the capacitance of pure Ethaline and Glyceline can be reconciled when it is considered that the chloride is less strongly bound to ethylene glycol so the surface excess of chloride is larger for Ethaline and so the capacitance will be larger. The addition of SDS displaces some of the chloride and the capacitance decreases. These data support the model shown in Figure 4-10.

Table 4-6 shows the capacitance results obtained from Figure 4-15 and from these values the surface coverage of charged species, Γ_{max} can be determined. From these values the average separation between ions, d can also be determined. When SDS is added to the DESs, these can compete with the chloride anions for spaces in the double layer and this can affect the capacitance of the charging current. Clearly this is an over simplification as it needs to consider the separation of charges from the surface and the charge of the cation, but the trend is clear that adding SDS to Ethaline increases the overall charge separation and doing the same to Glyceline has the opposite effect.

Table 4-6: Charging current, surface coverage and average ionic separation for a Pt electrode in Ethaline and Glyceline as a function of SDS concentration.

DES	SDS (mM)	Q (μC)	Γ_{max} ($\mu\text{mol m}^{-2}$)	d (\AA)
Ethaline	0	6.69	22.1	2.74
	4	4.61	15.2	3.30
	10	4.19	13.8	3.46
	25	4.24	14.0	3.44
Glyceline	0	1.87	6.17	5.19
	2	2.07	6.83	4.93
	10	2.18	7.20	4.80
	25	2.23	7.36	4.75

The capacitance for Ethaline is slightly too large as the ionic radius of chloride is 1.67 \AA which would lead to an average separation greater than 3.3 \AA .

4.2.3.2 Diffusion Coefficients in Micellar DES Solutions

The study of the diffusion coefficient in micelles solution is important as it can provide information such as micellar size, shape, structure of bilayers and the dynamics of liquid crystalline order.⁶⁴ The basic idea of measuring the size and the shape of micelle by this method is that the relationship between the diffusion coefficient and sphere radius provided by Stokes-Einstein Equation 4-13. A variety of techniques can be used to determine the diffusion coefficient of micelles. One of these methods is cyclic voltammetry which can also be used to estimating the adsorption–desorption process for both reactant and product of electroactive compounds in micellar solutions. The amphiphilic behaviour of micelles enables both non-polar and polar electroactive compounds to be solubilized. The solute can be incorporation into a micelle, generally in the hydrophobic regions just below the interface or it can bind at the Stern layer.⁶⁵

The peak currents, i_p for a reversible couple Figure 4-16, (a), is given by the Randles–Sevcik Equation:⁵⁵

$$i_p = (2.69 \times 10^5)n^{3/2}ACD^{1/2}\nu^{1/2} \quad \text{Equation 4-9}$$

Where n is the number of electrons, A (cm^2) the effective electrode area, C (mol cm^{-3}) the concentration of the bulk solution, D ($\text{cm}^2 \text{ s}^{-1}$) the diffusion coefficient of the electrochemical probe, and ν (V s^{-1}) the potential scan rate. If the probe is completely solubilized in the micelles then the diffusion coefficient D in Equation 4-9, would correspond to the micelle diffusion coefficient, D_m where the probe diffuses with the micelle and C would still be the probe concentration.⁶¹ It is clear that the current is directly proportional to the square root of the scan rate. Hence, the diffusion coefficient can be calculated from the slope of linear relationship between plots of i_p vs $\nu^{1/2}$. The Randles–Sevcik equation presumes that the mass transfer takes place mainly by the diffusion. However, for irreversible systems Figure 4-16, (b) the peak current, given by:

$$i_p = (2.99 \times 10^5)n(\alpha n_a)^{1/2}ACD^{1/2}\nu^{1/2} \quad \text{Equation 4-10}$$

Where α is the transfer coefficient and n_a is the number of electrons involved in the charge transfer step. The peak current is still proportional to the square root of the scan rate however the current is smaller, depending on the value of α .

It is important to note that the rate of a redox reaction can be controlled by the rate of mass transport to the electrode surface or by the rate of electron transfer at the interface.⁶⁶ To distinguish between these cases: for a reversible reaction, the electron transfer rate is greater than the rate of mass transport at all applied potentials and the peak potential is independent of the applied voltammetric scan rate. Whereas for irreversible reactions the electron transfer rates are smaller than the rate of mass transport. In between these cases the case of quasi-reversible where the rate of electron transfer becomes comparable to the mass transport rate and the peak potentials increase with the applied scan rate.⁶⁶

By increasing the scan rate, the diffusion layer thickness changes i.e. at low scan rate the diffusion layer is very thick but gets thinner as the scan rate increases. As the scan rate becomes faster the process will become more electrochemically irreversible.⁶⁶ Therefore the changes in the shape of the cyclic voltammogram can be quite helpful for clarifying the redox reaction pathways and for providing reliable chemical information about reactive intermediates.⁵⁵

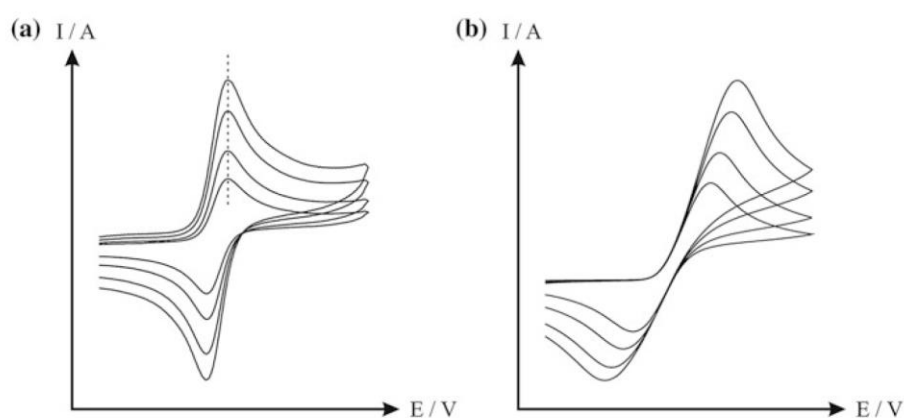


Figure 4-16: Scheme illustrates a typical cyclic voltammogram for (a) reversible and (b) irreversible electron transfer.

Two probes were used for this part of the study Iron (II) chloride (FeCl_2) and Tetrathiafulvalene (TTF). The former is polar and the latter is non-polar. However, TTF becomes ionic upon oxidation and may change its position within the micelle without changing its size. In order to calculate the diffusion coefficient, cyclic voltammograms

were run for a 20 mM of FeCl_2 and 5 mM TTF in DESs at different scan rate in presence of different SDS concentration, below and above its CMC were obtained.

The results are shown in Figures 4-17 and 4-18 for FeCl_2 in presence of different SDS concentrations in Ethaline and Glyceline respectively. These Figures also show the dependence of the peak current versus the square root of scan rates as a test of Equation 4-9. In all cases a good linear correlation is observed. In all cases the redox potential also remains relatively stable suggesting that although a film is clearly forming it is not blocking charge transfer at the electrode surface in the way that has been observed in aqueous solutions. The same trends are also observed in Glyceline although the effect of the surfactant is more marked, particularly at high SDS concentrations. This is clearly due to the viscosity of the DES.

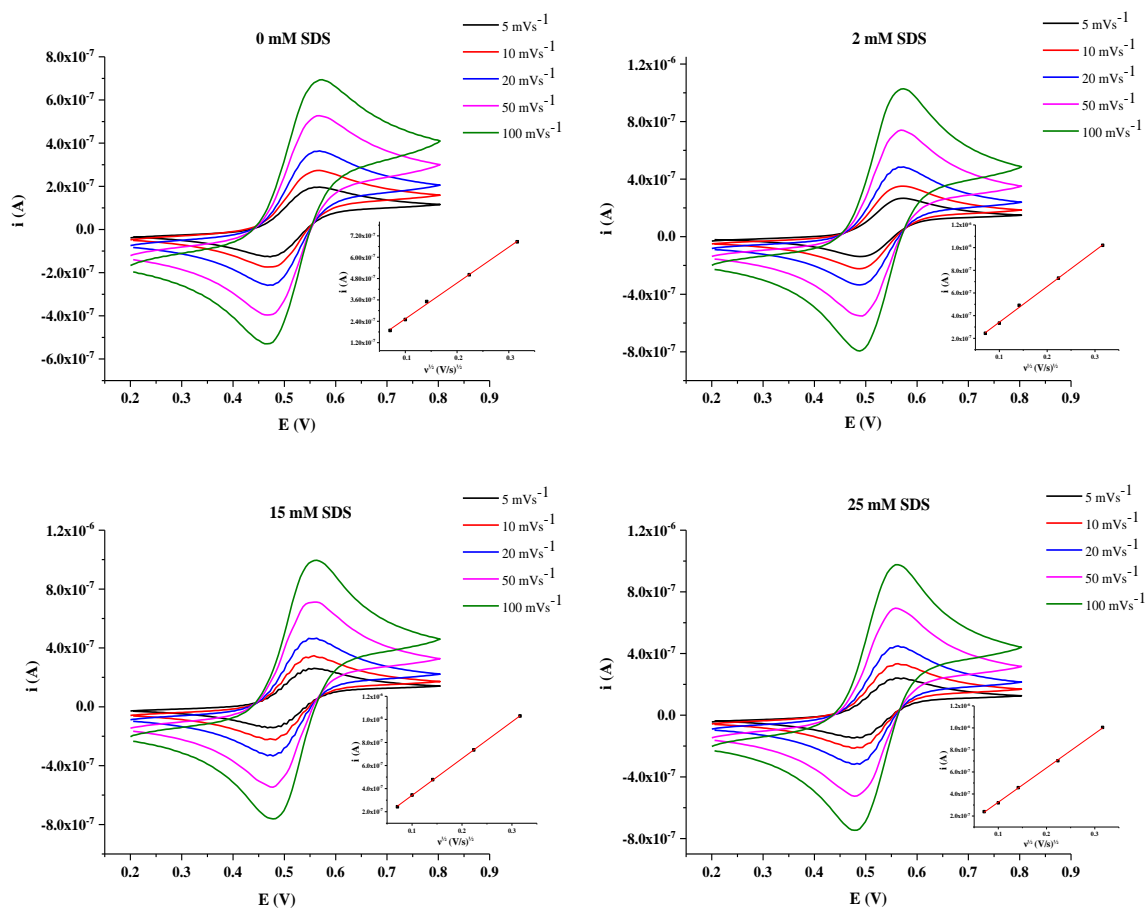


Figure 4-17: Cyclic voltammogram of 20 (mM) FeCl_2 in Ethaline with different SDS concentration and different scan rate at 25°C. Inset is a plot of linear dependence of peak current versus square root of scan rates.

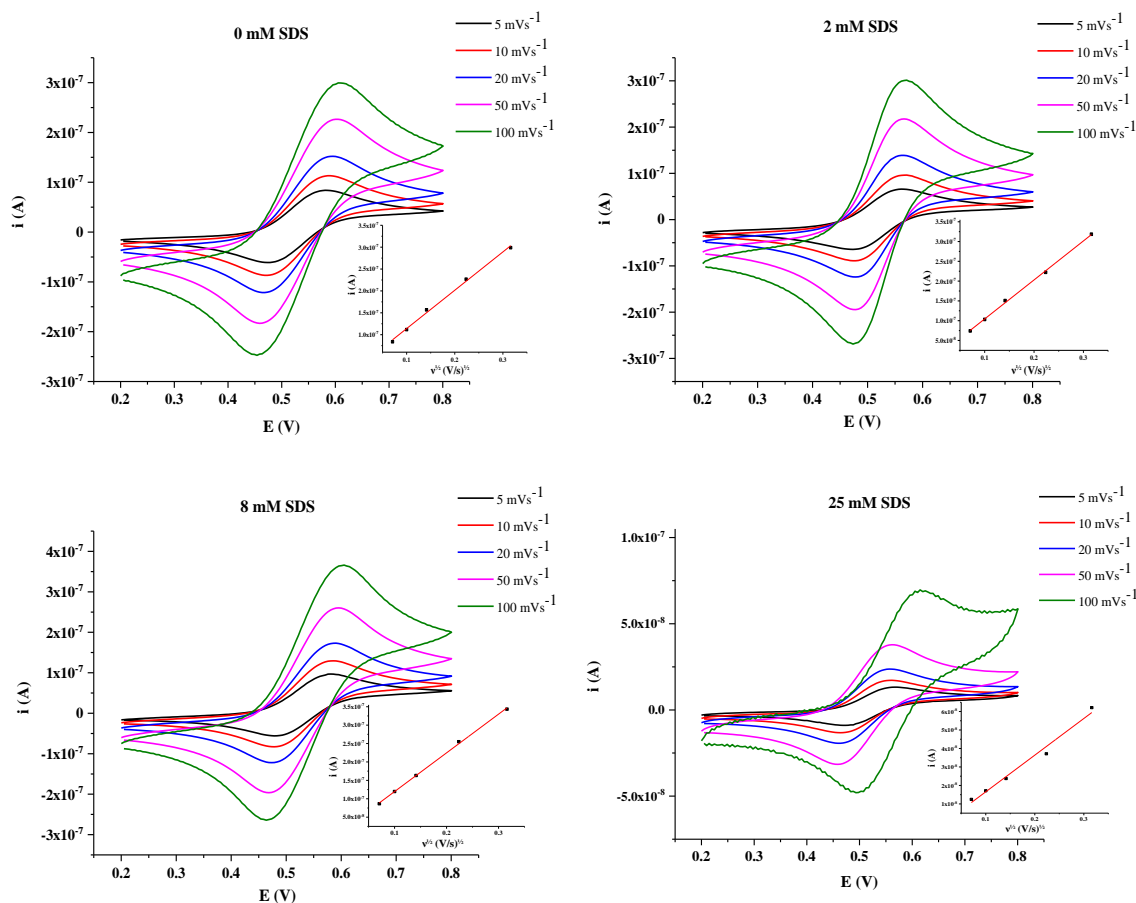
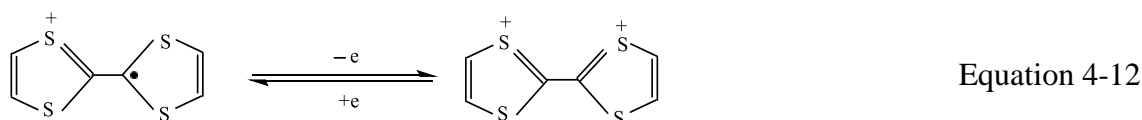
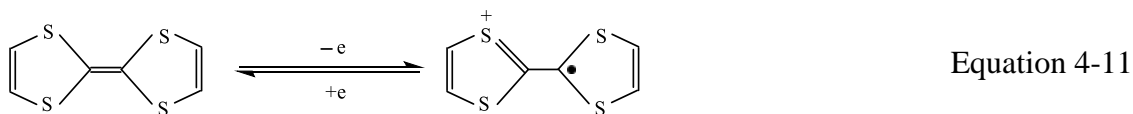


Figure 4-18: Cyclic voltammogram of 20 (mM) $FeCl_2$ in Glyceline with different SDS concentration and different scan rate at 25 °C. Inset is a plot of linear dependence of peak current versus square root of scan rates.

Repeating the experiment for solutions of TTF at the same SDS concentration resulted in two seemingly reversible electron transfer processes.



Tetrathiafulvalene, TTF has 14 p -electron which means it is non-aromatic. It is a well-known reversible redox probe used extensively in non-aqueous solvents.⁶⁷

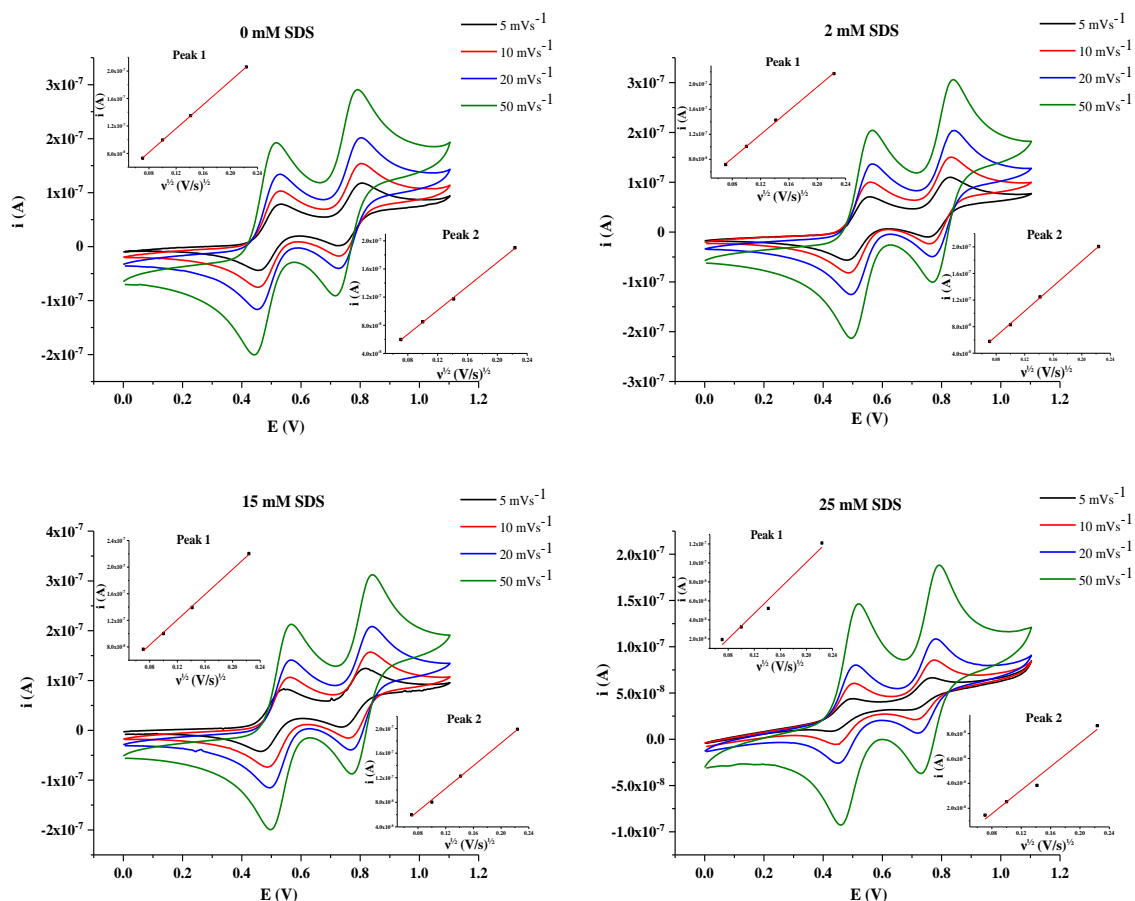


Figure 4-19: Cyclic voltammogram of 5 (mM) TTF in Ethaline with different SDS concentration and different scan rate at 25 °C. Inset is a plots of linear dependence of peak current versus square root of scan rates for both peaks.

In Ethaline, Figure 4-19 the baseline of the voltammogram is relatively flat when the SDS concentration is below the CMC but when the SDS concentration reaches 25 mM there appears to be a resistive artefact causing the baseline to become sloped. The peak current is also markedly reduced. This is not the case with FeCl₂ which suggests a different mechanism for TTF oxidation. Once the micelle forms TTF must partition into the micelle and this apparently affects mass transport. This potentially suggests a model such as shown in Figure 4-10 (c).

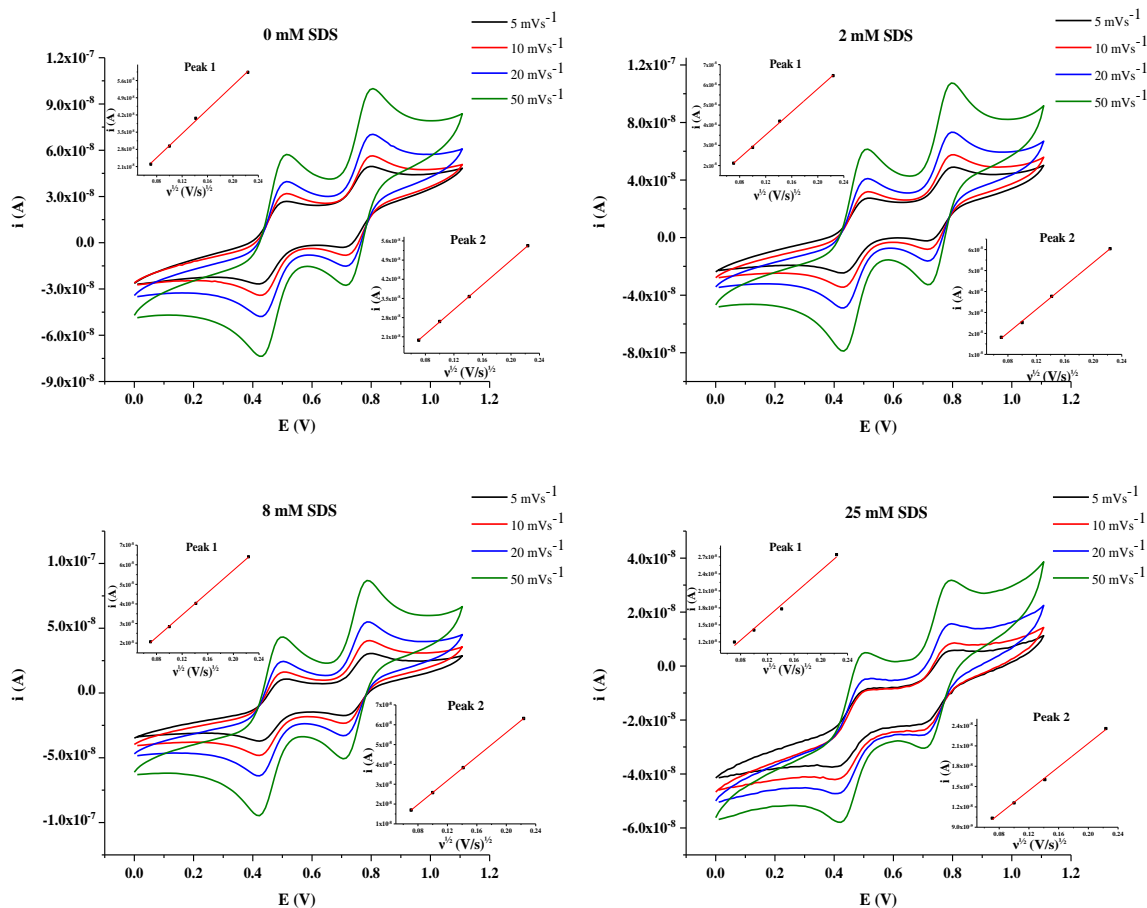


Figure 4-20: Cyclic voltammogram of 5 (mM) TTF in Glyceline with different SDS concentration and different scan rate at 25 °C. Inset is a plots of linear dependence of peak current versus square root of scan rates for both peaks.

Figure 4-20 shows the corresponding results for Glyceline with TTF and again a resistive artefact is observed which is not present with FeCl₂. Figure 4-21 shows the peak potentials for all of the above voltammograms in the two DESs as a function of SDS concentration. It can be seen that for FeCl₂ the oxidation and reduction potentials remain constant whereas for TTF the shift as the SDS concentration is increased. This suggests that FeCl₂ does not partition into the micelle whereas TTF almost certainly does.

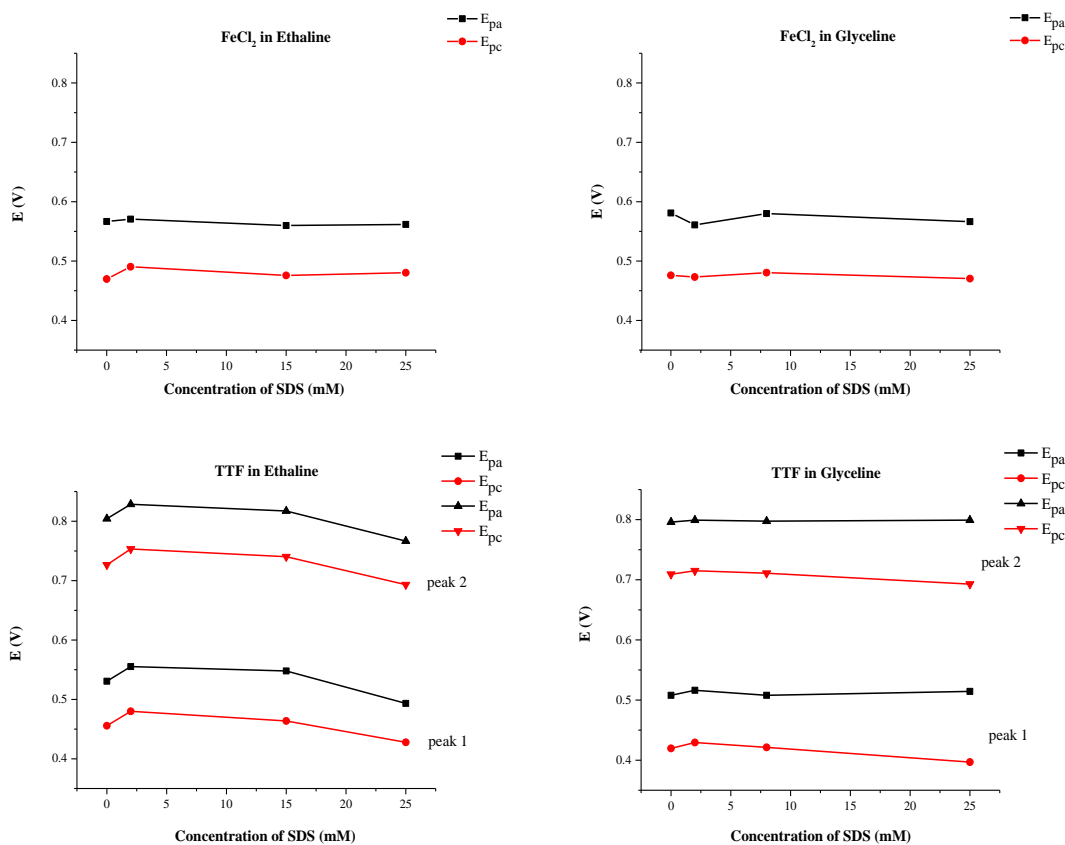


Figure 4-21: Plots of E_{pc} and E_{pa} for the oxidation of $FeCl_2$ and TTF versus surfactant concentration in Ethaline and Glyceline.

TTF is a nonaromatic molecule that is easily oxidized in two steps to form initially the radical cation followed with dication species. Both the oxidation states, the cation radical, $TTF^{\cdot+}$ and dication TTF^{2+} are aromatic in contrast to neutral state of TTF.⁶⁷⁻⁶⁹ This indicates that losing electrons in the oxidation process results in a cation species, creating a positive charge which will be different than probing with $FeCl_2$.

The Randles–Sevcik equation was used to calculate the diffusion coefficient in micellar DES solutions. The diffusion coefficient data of $FeCl_2$ and TTF are presented in Figure 4-22. In all systems there is a slight increase in the diffusion coefficient when surfactant is added below the CMC. This could be accounted for by slight changes in viscosity (see below). Above the CMC there is a more significant decrease in the diffusion coefficient in Glyceline and for TTF in Ethaline, supposedly because the electroactive species partitions into the micelle. The diffusion coefficient is therefore limited by the movement of the micelle rather than the electroactive species.⁷⁰

While micelles form in Ethaline their number and size will be smaller than in Glyceline (Chapter 3) and the partitioning of the electroactive species will still favour it being in the DES rather than in the micelle.

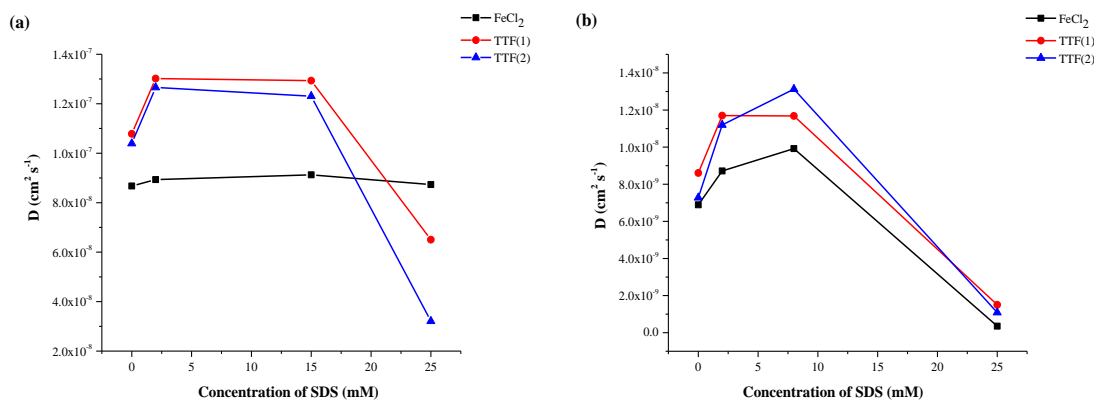


Figure 4-22: The diffusion coefficient of $FeCl_2$ and TTF, the first peak, TTF(1) and the second peak, TTF(2) in (a) Ethaline and (b) Glyceline.

The apparent increase in current when surfactant is added to the DES adds more evidence that SDS does not form a bilayer decreasing the rate of electron transfer and hindrance of diffusing species to the electrode surface.^{14, 60} The apparent activity of chloride in these two liquids could affect the Stern layer which could have a knock-on effect of changing the size of the aggregate as shown in Chapter 3. This will therefore change the diffusion coefficient of the micelles surface where the diffusion coefficients decrease 20 times.¹⁴ Asakawa *et al.* reported that the addition of salt led to a decrease in the measured diffusion coefficient which they inferred resulted from an increase in micelle size and a change of micelle shape.⁷¹

The diffusion coefficient of the redox species is dependent on temperature, viscosity of the solvent and the size and geometry of the diffusing species as defined by the Stokes-Einstein equation as shown in Equation 4-13.

$$D = \frac{k_B T}{6\pi\eta r} \quad \text{Equation 4-13}$$

Where D is the diffusion coefficient, k_B is the Boltzmann constant, T is the temperature, η is the viscosity and r is the hydrodynamic radius. The Stokes-Einstein equation predicts a linear correlation between inverse of the viscosity and the diffusion coefficient

of the species. Strictly speaking this is only valid at infinite dilution. Taylor *et al.*⁷² measured the diffusion coefficient of ferrocene, and derivatives in ionic liquids systems using voltammetric methods. They found that the behaviour was non-Stokesian.

Figure 4-23 shows the correlation of viscosity with the diffusion coefficient of FeCl₂ and TTF in DESs containing different amounts of SDS. It is clear that for Glyceline in both cases and TTF in Ethaline the behaviour is Stokesian whereas in Ethaline for FeCl₂ is not.

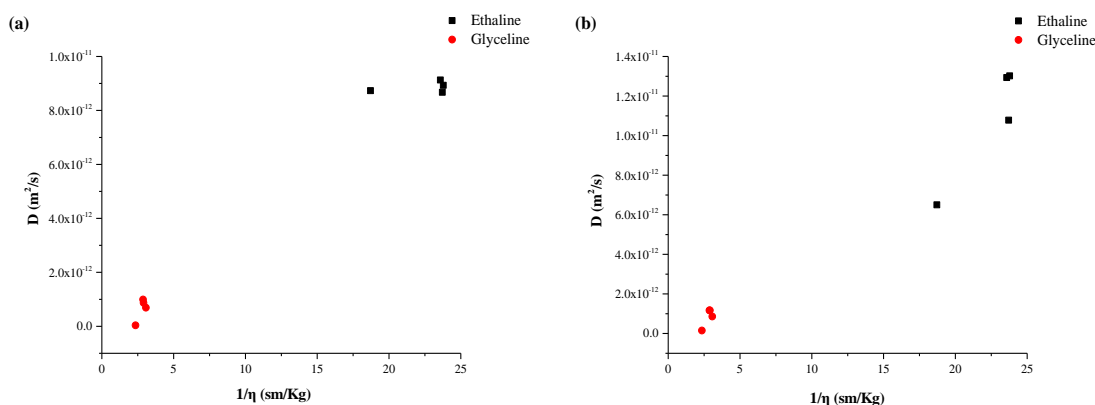


Figure 4-23: Stokes-Einstein plots, D versus η^{-1} (a) FeCl₂ and (b) TTF in DESs.

4.2.3.3 Local versus Bulk Viscosity of Surfactant in DESs

In chapter 3 the viscosity of surfactant DES solutions were measured using a rotating cylinder viscometer (bulk viscosity). This is a technique measures average liquid viscosities over a length-scale of several cm. Al-Murshedi recently showed that a Quartz Crystal Microbalance, QCM, could be used to measure the viscosity of DESs (local viscosity).⁵⁰ The advantage of this technique is that it requires less than 1 cm³ of liquid to make a measurement; it simply has to cover the crystal. The QCM is a technique which is based on an inverse piezoelectric effect. A QCM is formed from a thin quartz crystal, a few hundred μm quartz plate, sandwiched between two metallic electrodes, usually gold, about 0.1 μm thick. These enable an alternating electric field to be applied across the crystal, which leads to vibrational motion of the crystal at its resonant frequency.⁷³ The resonance frequency, f_0 of the QCM determined by the thickness of the quartz plate.⁷⁴ QCM is sensitive to sub-Nano gram.⁷⁵ this changes in the mass of the electrode because of the high resonance frequency that can be with an accuracy of 0.05 Hz or better.

The QCM technique has been used in fundamental and applied sciences to studies of sub-monolayer adsorption, sensor, in situ monitoring of lubricant and petroleum properties and so on.⁷⁶

The Sauerbrey Equation 4-14⁷⁷ relates the change in resonant frequency with the change in mass for rigid masses attached to the crystal via the direct relationship between the change in the frequency, Δf and the mass of a rigidly coupled deposit, Δm on one of the quartz surfaces:

$$\Delta f = -\frac{2f_0^2 \Delta m}{A\sqrt{\mu_q \rho_q}} \quad \text{Equation 4-14}$$

Where f_0 is resonant frequency of the quartz resonator, A is the active vibrating area, μ_q is the shear modulus of the quartz and ρ_q is the density of the quartz.

The QCM can also act as a viscometer. The fundamental resonant frequency, f_0 of a crystal operating in vacuum changes when it is immersed in a liquid to f_i . The basis of this change is the decrease in the fundamental frequency, f_0 by a liquid film due to an effectively rigidly coupled interfacial layer. Where the thickness of this layer is related to the penetration depth, δ which describes the viscous attenuation of the shear wave amplitude by the bulk liquid. Hence, the effective mass of the coupled interfacial layer, Δm and the penetration depth, δ can be identified by Equations 4-15 and 4-16 respectively:⁷⁸

$$\Delta m = \frac{\rho_l A \delta}{2} \quad \text{Equation 4-15}$$

$$\delta = \sqrt{\frac{\eta_l}{\pi f_0 \rho_l}} \quad \text{Equation 4-16}$$

By replacing Δm in Equation 4-14 with Equations 4-15 and 4-16, result the change in the frequency, $\Delta f = f_i - f_0$, Equation 4-17, which is known as Kanazawa and Gordon equation and should be proportional to viscosity of liquid and its density.⁷⁹

$$\Delta f = -f_0^{\frac{3}{2}} \sqrt{\frac{\eta_l \rho_l}{\pi \rho_q \mu_q}} \quad \text{Equation 4-17}$$

Where Δf is the frequency shift occurring on mass loading, f_0 is the crystal frequency under no load, ρ_q is the crystal density, μ_q is the crystal shear modulus, and η_l and ρ_l represent the liquid viscosity and density respectively. Hence the measurement of the frequency shift in liquids allows measuring the viscosity.

Figure 4-24 shows the viscosity of SDS in DESs measured using QCM and a rotating cylinder viscometer. It can be seen that in general the values obtained using both techniques are very similar.

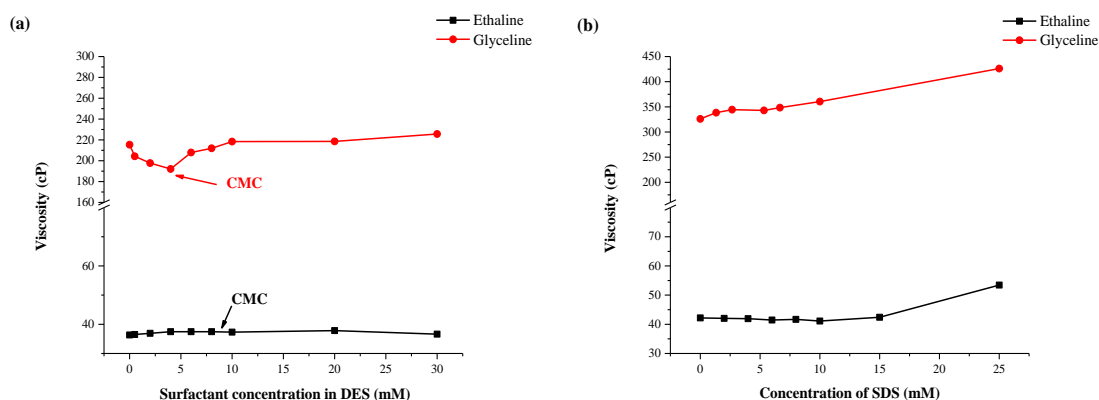


Figure 4-24: Viscosity of SDS solution in DESs measured by (a) QCM and (b) by a rotating cylinder viscometer at 25°C.

In Ethaline, both techniques show little change in the viscosity until the SDS concentration reaches 20 mM i.e. just above the CMC. In Glyceline, the bulk viscosity determined using a rotating cylinder viscometer shows a steady increase as the SDS concentration increases. The results obtained using QCM show there is a small decrease in the local viscosity close to the probe and the minimum occurs at the CMC. This could be due to the presence of SDS molecules which break up the chloride layer at the electrode surface. Above the CMC the viscosity increases as micelles start to form, decreasing the mobility in the DES. Interestingly, the local viscosity does not appear to increase to the same extent as the bulk viscosity.

Using the data of viscosity in Figure 4-25 and diffusion coefficient in Figure 4-22 with Equation 4-13 the hydrodynamic radius of the diffusing species can be determined. The data in Table 4-7 shows that the radius for FeCl_2 is similar in magnitude to that for FeCl_4^-

Table 4-7: Calculated hydrodynamic radius of FeCl₂ and TTF.

DES	[SDS] (mM)	hydrodynamic radius (Å)	
		FeCl ₂	TTF
Ethaline	0	5.96	4.80
	2	5.81	3.99
	15	5.64	3.98
	25	4.67	6.28
Glyceline	0	9.71	7.78
	2	7.27	5.41
	8	6.31	5.36
	25	144.91	34.06

4.2.4 Adsorption of SDS at Oil-DES Interface

In the beginning of this chapter the adsorption of SDS at air-DES and solid-DES interfaces were discussed and the results indicated that in both cases the tendency of SDS to aggregate at interfaces was depend on the polarity of the DES. The higher the surface tension the higher the cohesive energy density and therefore the more likely the surfactant was to aggregate at interfaces and in micelles in solution i.e. the less likely it was to exist as monomers in solution. The same should therefore be valid for adsorption at liquid-liquid interfaces. To test this, emulsions were made in both DESs using hexane as the dispersed phase and SDS as the emulsifier.

Emulsions are colloidal systems that are obtained by the mixing of two normally immiscible liquids typically oil and water. Emulsions are generated by fragmenting one liquid in the form of small drops (the dispersed phase) into another liquid (the continuous phase).^{80, 81} The emulsions are homogenous at macroscopic scale, but heterogeneous at microscopic scale.

The process to prepare emulsions is called emulsification. During emulsification, external shear energy is used to rupture large droplets into smaller ones. The presence of these many small droplets in the system means that the system as a whole has a larger interfacial area, implying that energy has to be added to the emulsion to keep it stable (i.e. to counteract the tendency of the dispersed phase droplets to coalesce). Typically a

surfactant is added to reduce surface tension by its adsorption into interfaces, which, in this scenario, helps to prevent the dispersed droplets from coalescing.^{80, 81} According to the size the droplets two main types of emulsions can be distinguished: emulsion where droplets size fall in the range of 0.1-10 μm , whereas microemulsions the droplets are much smaller, in the 0.01-0.1 μm size range.³⁹

Pal *et al.* demonstrated that DESs could be used as polar phases for the preparation of microemulsions.⁸² It was reported that a microemulsion could be formed from cyclohexane in Reline containing SDS where Reline was the continuous phase. Fischer *et al.*⁸³ used two DESs; Ethaline 400 and Reline/tetrahydrofurfuryl alcohol/diethyl adipate to prepare surfactant-free and water-free microemulsions. Another study by Carranza *et al.*⁸⁴ investigated the use of DESs with non-ionic surfactant to prepare high internal phase emulsions. Their results show improved emulsion stability compared to analogous aqueous systems because of high viscosity of DESs.

In this study the emulsions were prepared using either 11.09 g of Ethaline, 11.95 g of Glyceline or 10.00 g of water as polar phase mixed with 0.079 g of SDS as emulsifier and 0.659 g of hexane as non-polar phase and then stirred for 2 h. The type of emulsion formed was determined by using a dilution experiment. The dilution test is commonly used to determine the dispersed phase and the continuous phase. If DESs were easily dispersed in the continuous phase, the emulsion is termed an oil-in-DES. In contrast if hexane was dispersible in the external phase, the emulsion was termed a DES-in-oil emulsion.⁸⁵ When excess hexane was added to the emulsion a biphasic system was formed as shown in Figure 4-25 (a). But when the emulsion was diluted with used DES a single cloudy liquid was formed. This showed that the emulsion was an oil in DES emulsion (O-DES).

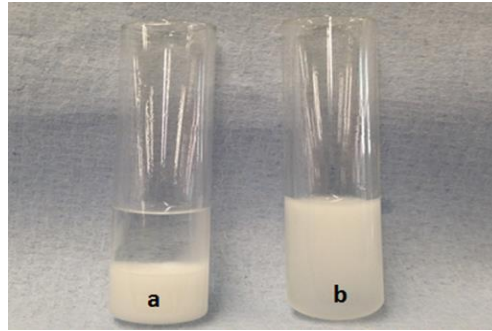


Figure 4-26: Dilution test for an emulsion prepared from SDS in Ethaline with hexane
 (a) diluted by hexane (b) diluted by Ethaline

4.2.4.1 The Effect of Solvent on the Emulsions Stability

The ability of a surfactant to form a stable emulsion depends on the size of the dispersed phase, the density of the dispersed and continuous phase and the viscosity of the fluid. The terminal velocity, v , of a dispersed phase to float or sink (depending on its density) is given by:⁸⁶

$$v = \frac{2r^2(\rho_2 - \rho_1)g_n}{9\eta} \quad \text{Equation 4-18}$$

Where r is the radius of the dispersed phase, ρ_2 is density the continuous phase, ρ_1 is the density of dispersed phase, g_n is the acceleration due to gravity and η is the bulk viscosity. Smaller dispersed phase and a higher viscosity will increase the kinetic stability of the emulsion. Figure 4-26 shows the emulsions prepared by mixing SDS as emulsifier factor and hexane as dispersed phase with DESs or water as continue phase.

Both DESs form an emulsion immediately which does not separate on standing. The water-hexane-SDS mixture forms two cloudy phases almost immediately on standing. The upper (white) phase is a water in oil (W-O) microemulsion whereas the cloudy lower phase is an oil in water (O-W) microemulsion. Clearly the W-O has large droplets of water which rapidly cream to the surface of the liquid. The water droplets are clearly considerably larger than the wavelength of light as they scatter the light making the upper phase appear opaque.

In Ethaline, after 1 day, the emulsion starts to separate into two layers. The upper layer is transparent. After 6 days the separation is complete with two clear layers showing

that an O-DES and DES-O micro-emulsion is not stable. This is presumably because SDS monomers are more easily solvated in Ethaline and the tendency to support large vesicle formation is reduced.

In the case of Glyceline while some separation is observed after 3 days both layers are opaque which is more similar to the response observed in water. There is quite clearly a DES-O phase on the top and an O-DES phase on the bottom. The stability of this emulsion is clearly due to the high viscosity of the DES which decreases the sedimentation velocity. It is clearly the high surface tension of Glyceline which stabilises micelle formation and the stability of emulsions. The same is observed with Reline, however, the very high viscosity of this DES made it inordinately long for the mixtures to reach equilibrium.

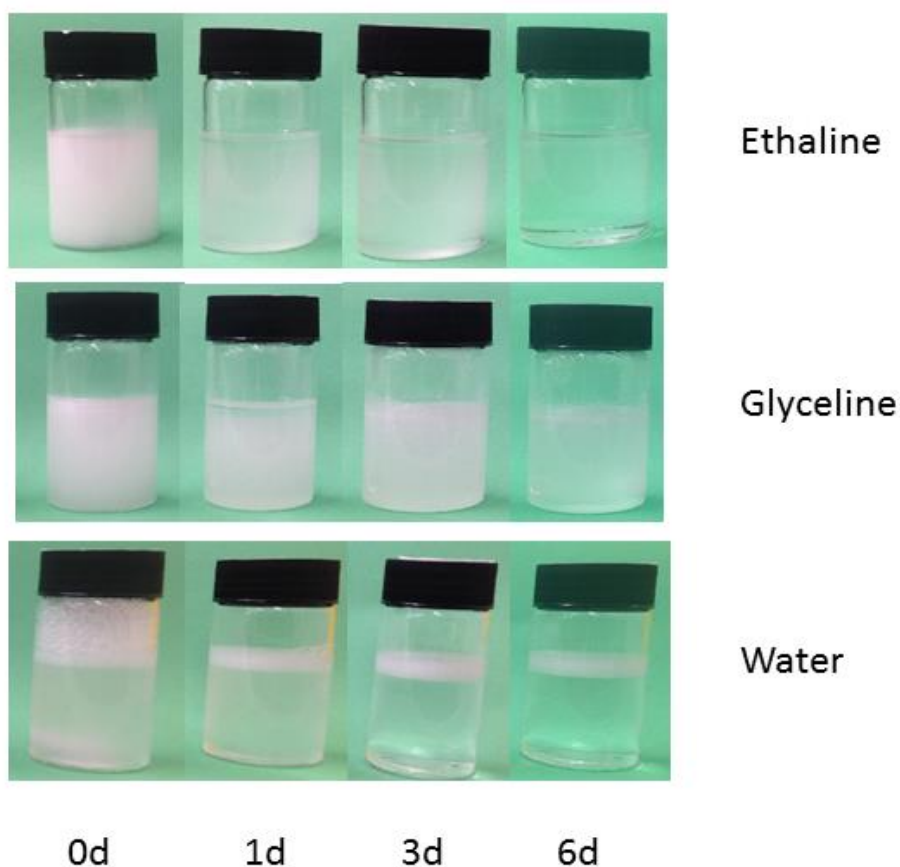


Figure 4-27: Emulsion stability as a function of time; the vials contain SDS, hexane and either DES or water.

Figure 4-27 shows the stability of foams formed by shaking solutions SDS in water and SDS in Ethaline as a function of time. It can be seen that SDS forms a larger foam. After 1h 43 min there is still a foam on Ethaline whereas that on water has been quenched. This may have application in mineral separation with froth floatation of minerals. The high density and extended froth stability could extend the loading of mineral which could be stabilised in a foam. Abbott et al. have shown that metals can be directly be extracted from minerals using DESs.^{87, 88}

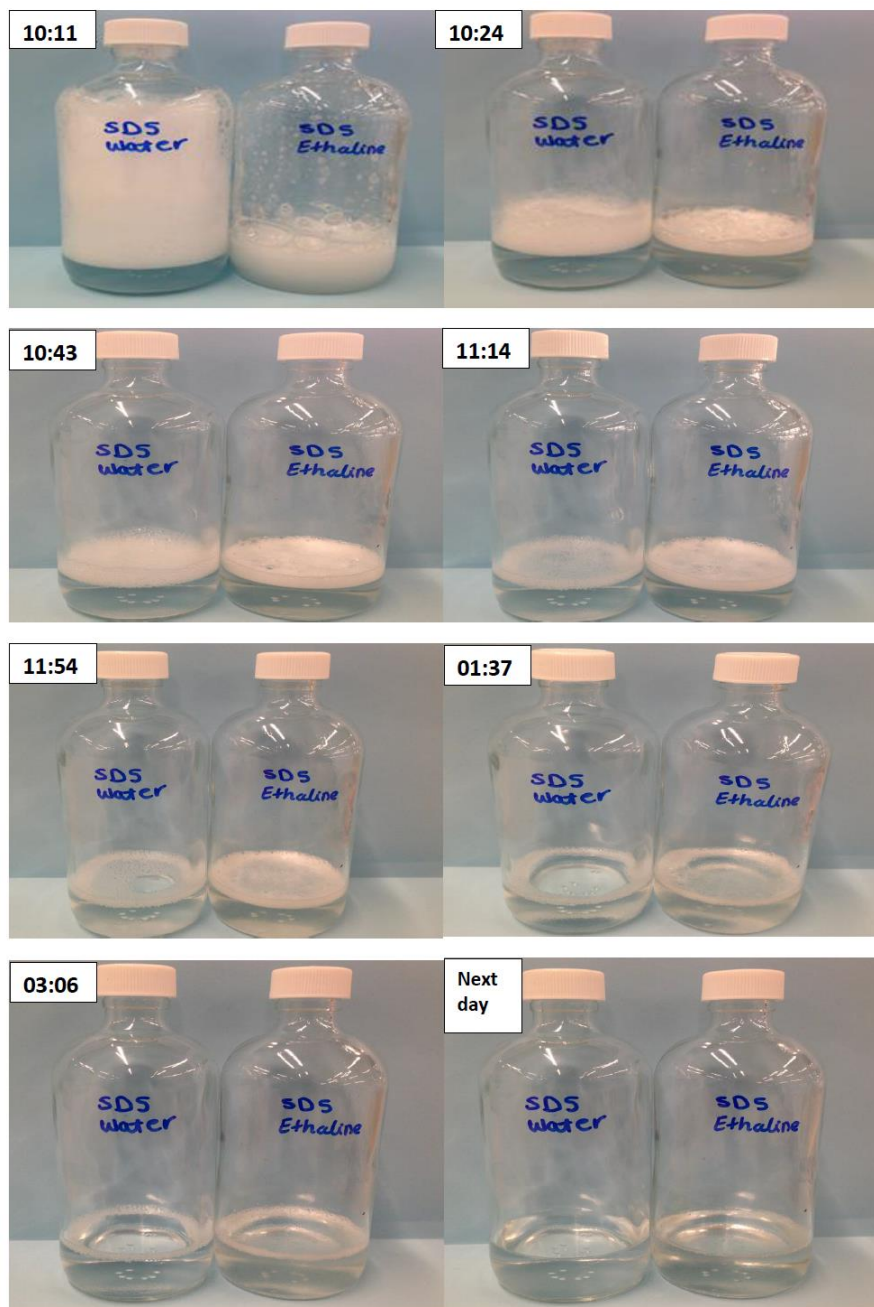


Figure 4-28: Foam stability as a function of time for SDS in water and SDS in Ethaline.

4.3 Conclusion

In the previous chapter the aggregation of surfactants was quantified and it was shown that aggregation was favoured in media with a higher surface energy as this disfavoured the solubilisation of monomers. It was postulated that this would be the same effect at interfaces i.e. in Ethaline surfactants would be less likely to go to interfaces as they were stabilised in solution.

This idea was probed at the gas-DES interface using surface tension, at the solid-DES interface using contact angle and electrochemistry and at the oil-DES interface using emulsion stability tests. Surface tension experiments showed that the area occupied per surfactant molecule at the air-DES interface was considerably larger for Ethaline than for Glyceline. This could either be because the SDS molecule lies inclined to the interface, or more likely that an incomplete monolayer is formed due to the high solubility of SDS monomers in Ethaline.

Contact angle measurements showed that SDS was better at causing Glyceline to wet a stainless steel surface than Ethaline, presumably because it was more active at the interface. Above the CMC both liquids wet the surface equally well but it was clear from the contact angle that neither formed a complete layer on the metal surface as the contact angle was still too high (c.a. 40°).

Electrochemical measurements indicated that far from blocking the electrode as would be expected in an aqueous solution, SDS appeared to promote electron transfer for the oxidation of FeCl₂. It is proposed that this is due to a partial monolayer adsorption of SDS below the CMC breaking up the highly organised chloride layer at the electrode-DES interface and promoting electron transfer. Above the CMC micelles form and there appears to be some evidence that hydrophobic probes such as TTF partition into micelle. Electron transfer is slowed which appears to be due to slower diffusion of the micelle containing the probe to the electrode surface.

Viscosity measurements show that there is a difference in the viscosity close to the electrode compared to the bulk solution. Surfactants appear to cause a larger increase in the bulk liquid than in the local area close to the electrode. This could be because the micelles are larger than the probe depth of the QCM and so the local viscosity sees the

environment observed by the probe rather than the way that the micelles interact in the bulk.

Finally, it was found that O-DES emulsions are more stable in Glyceline than in Ethaline as it is more viscous and the high surface tension of the pure liquid pushes the surfactant to aggregate. It was noted that DES-O emulsions form and are stable with Glyceline. In Ethaline the oil phase separates as the surfactant is less likely to aggregate and stabilise the O-DES phase.

Ethaline	Glyceline
Lower polarity	Higher polarity
Lower viscosity	Higher viscosity
Lower surface tension	Higher surface tension
More monomers	More micelles
More soluble monomers	More adsorbed monomers
Higher chloride activity	Lower chloride activity

4.4 References

1. S. Manne, J. Cleveland, H. Gaub, G. Stucky and P. Hansma, *Langmuir*, 1994, **10**, 4409-4413.
2. M. Jaschke, H.-J. Butt, H. Gaub and S. Manne, *Langmuir*, 1997, **13**, 1381-1384.
3. R. G. Chaudhuri and S. Paria, *Journal of Colloid and Interface Science*, 2009, **337**, 555-562.
4. P. Balasuwatthi, N. Dechabumphen, C. Saiwan and J. F. Scamehorn, *Journal of Surfactants and Detergents*, 2004, **7**, 31-40.
5. A. A. Levchenko, B. P. Argo, R. Vidu, R. V. Talroze and P. Stroeve, *Langmuir*, 2002, **18**, 8464-8471.
6. H. Busscher, A. Van Pelt, H. De Jong and J. Arends, *Journal of Colloid and Interface Science*, 1983, **95**, 23-27.
7. M. J. Rosen and J. T. Kunjappu, *Surfactants and Interfacial Phenomena*, John Wiley & Sons, 2012.
8. D. M. Eckmann, D. P. Cavanagh and A. B. Branger, *Journal of Colloid and Interface Science*, 2001, **242**, 386-394.
9. K. H. Kang, *Langmuir*, 2002, **18**, 10318-10322.
10. X. Wang, A. B. Kharitonov, E. Katz and I. Willner, *Chemical Communications*, 2003, 1542-1543.
11. J. Lahann, S. Mitragotri, T.-N. Tran, H. Kaido, J. Sundaram, I. S. Choi, S. Hoffer, G. A. Somorjai and R. Langer, *Science*, 2003, **299**, 371-374.
12. J. C. Barron, PhD Thesis, University of Leicester, 2010.
13. M. Azam, PhD Thesis, University of Leicester, 2012.
14. J. F. Rusling, *Colloids and Surfaces A: Physicochemical and Engineering Aspects*, 1997, **123**, 81-88.
15. J. Kostela, M. Elmgren, P. Hansson and M. Almgren, *Journal of Electroanalytical Chemistry*, 2002, **536**, 97-107.
16. C. Mousty, P. Pouillen, A.-M. Martre and G. Mousset, *Journal of Colloid and Interface Science*, 1986, **113**, 521-529.
17. T. C. Franklin and S. Mathew, In *Surfactants in Solution*, Springer, Editon edn., 1989, pp. 267-286.
18. R. Vittal, H. Gomathi and K.-J. Kim, *Advances in Colloid and Interface Science*, 2006, **119**, 55-68.

19. R. A. Mackay, *Colloids and Surfaces A: Physicochemical and Engineering Aspects*, 1994, **82**, 1-28.
20. I. Burgess, C. Jeffrey, X. Cai, G. Szymanski, Z. Galus and J. Lipkowski, *Langmuir*, 1999, **15**, 2607-2616.
21. A. Marino and A. Brajter-Toth, *Analytical Chemistry*, 1993, **65**, 370-374.
22. S. Ray, R. Counce and S. Morton III, *Separation Science and Technology*, 2008, **43**, 2489-2502.
23. F. Scholz, *Electroanalytical methods*, Springer, 2010.
24. E. Olson, *Journal of GXP Compliance*, 2012, **16**, 81.
25. H. B. Mark, *Analyst*, 1990, **115**, 667-678.
26. A. A. Kornyshev, ACS Publications, Editon edn., 2007.
27. E. L. Smith, A. P. Abbott and K. S. Ryder, *Chemical Reviews*, 2014, **114**, 11060-11082.
28. Q. Zhang, K. D. O. Vigier, S. Royer and F. Jérôme, *Chemical Society Reviews*, 2012, **41**, 7108-7146.
29. M. Figueiredo, C. Gomes, R. Costa, A. Martins, C. M. Pereira and F. Silva, *Electrochimica Acta*, 2009, **54**, 2630-2634.
30. R. Costa, M. Figueiredo, C. M. Pereira and F. Silva, *Electrochimica Acta*, 2010, **55**, 8916-8920.
31. Z. Chen, B. McLean, M. Ludwig, R. Stefanovic, G. G. Warr, G. B. Webber, A. J. Page and R. Atkin, *The Journal of Physical Chemistry C*, 2016, **120**, 2225-2233.
32. L. Vieira, R. Schennach and B. Gollas, *Physical Chemistry Chemical Physics*, 2015, **17**, 12870-12880.
33. R. Stefanovic, M. Ludwig, G. B. Webber, R. Atkin and A. J. Page, *Physical Chemistry Chemical Physics*, 2017, **19**, 3297-3306.
34. H. Demissie and R. Duraisamy, *Journal of Scientific and Innovative Research*, 2016, **5**, 208-214.
35. H. Hooshyar and R. Sadeghi, *Journal of Chemical and Engineering Data*, 2015, **60**, 983-992.
36. A. Beesley, D. F. Evans and R. Laughlin, *The Journal of Physical Chemistry*, 1988, **92**, 791-793.
37. J.-B. Huang, M. Mao and B.-Y. Zhu, *Colloids and Surfaces A: Physicochemical and Engineering Aspects*, 1999, **155**, 339-348.

38. A. D. Fenta, *International Journal of Physical Sciences*, 2015, **10**, 276-288.
39. R. Pashley and M. Karaman, *Applied Colloid and Surface Chemistry*, John Wiley and Sons, 2005.
40. Y. Marcus, *Chemical Reviews*, 1988, **88**, 1475-1498.
41. T. F. Tadros, *Emulsion Formation and Stability*, John Wiley and Sons, 2013.
42. T. L. Greaves and C. J. Drummond, *Chemical Society Reviews*, 2013, **42**, 1096-1120.
43. Q. Li, J. Wang, N. Lei, M. Yan, X. Chen and X. Yue, *Physical Chemistry Chemical Physics*, 2018, **20**, 12175-12181.
44. A. P. Abbott, A. Y. Al-Murshedi, O. A. Alshammari, R. C. Harris, J. H. Kareem, I. B. Qader and K. Ryder, *Fluid Phase Equilibria*, 2017, **448**, 99-104.
45. X. Auvray, C. Petipas, R. Anthore, I. Rico and A. Lattes, *The Journal of Physical Chemistry*, 1989, **93**, 7458-7464.
46. Y. Yuan and T. R. Lee, in *Surface Science Techniques*, Springer, Editon edn., 2013, pp. 3-34.
47. J. Zhang, Y. Meng, Y. Tian and X. Zhang, *Colloids and Surfaces A: Physicochemical and Engineering Aspects*, 2015, **484**, 408-415.
48. A. Davis, S. Morton III, R. Counce, D. DePaoli and M.-C. Hu, *Colloids and Surfaces A: Physicochemical and Engineering Aspects*, 2003, **221**, 69-80.
49. B. Luepakdeesakoon, C. Saiwan and J. F. Scamehorn, *Journal of Surfactants and Detergents*, 2006, **9**, 125-136.
50. A. Y. M. Al-Murshedi, PhD Thesis, University of Leicester, 2018.
51. E. J. Wanless and W. A. Ducker, *The Journal of Physical Chemistry*, 1996, **100**, 3207-3214.
52. J. Gardner and R. Woods, *Journal of Electroanalytical Chemistry and Interfacial Electrochemistry*, 1977, **81**, 285-290.
53. J. Georges and S. Desmetre, *Electrochimica Acta*, 1984, **29**, 521-525.
54. N. Neghmouche and T. Lanez, *Recent Trends in Physical Chemistry: An International Journal*, 2013, **1**, 1-3.
55. J. Wang, *Analytical Electrochemistry*, John Wiley and Sons, 2006.
56. M. H. Chakrabarti, N. P. Brandon, F. S. Mjalli, L. Bahadori, I. M. Al Nashef, M. A. Hashim, M. Hussain, C. T. J. Low and V. Yufit, *Journal of Solution Chemistry*, 2013, **42**, 2329-2341.

57. M. H. Chakrabarti, N. P. Brandon, M. A. Hashim, F. S. Mjalli, I. M. AlNashef, L. Bahadori, N. Abdul Manan, M. Hussain and V. Yufit, *International Journal of Electrochemical Science*, 2013, **8**, 9652-9676.
58. N. G. Tsierkezos, *Journal of Solution Chemistry*, 2007, **36**, 289-302.
59. X. Zhang and A. J. Bard, *Journal of the American Chemical Society*, 1989, **111**, 8098-8105.
60. D. S. Shishmarev, N. V. Rees and R. G. Compton, *Electroanalysis*, 2010, **22**, 31-34.
61. A. B. Mandal and B. U. Nair, *The Journal of Physical Chemistry*, 1991, **95**, 9008-9013.
62. A. B. Mandal, B. U. Nair and D. Ramaswamy, *Langmuir*, 1988, **4**, 736-739.
63. N. F. Atta, S. A. Darwish, S. E. Khalil and A. Galal, *Talanta*, 2007, **72**, 1438-1445.
64. H. Hakemi, P. Varanasi and N. Tcheurekdjian, *Journal of Physical Chemistry*, 1987, **91**, 120-125.
65. J. F. Rusling, *Accounts of chemical research*, 1991, **24**, 75-81.
66. D. A. Brownson and C. E. Banks, *The handbook of graphene electrochemistry*, Springer, 2014.
67. J. L. Segura and N. Martín, *Angewandte Chemie International Edition*, 2001, **40**, 1372-1409.
68. M. Á. Herranz, L. Sánchez and N. Martín, *Phosphorus, Sulfur, and Silicon and the Related Elements*, 2005, **180**, 1133-1148.
69. M. B. Nielsen, C. Lomholt and J. Becher, *Chemical Society Reviews*, 2000, **29**, 153-164.
70. G. Bell and A. Dunning, *Transactions of the Faraday Society*, 1970, **66**, 500-508.
71. T. Asakawa, H. Sunagawa and S. Miyagishi, *Langmuir*, 1998, **14**, 7091-7094.
72. A. W. Taylor, P. Licence and A. P. Abbott, *Physical Chemistry Chemical Physics*, 2011, **13**, 10147-10154.
73. D. A. Buttry and M. D. Ward, *Chemical Reviews*, 1992, **92**, 1355-1379.
74. V. Tsionsky, *Journal of Chemical Education*, 2007, **84**, 1340-1342.
75. S. K. Vashist and P. Vashist, *Journal of Sensors*, 2011, **2011**, 1-13.
76. M. Rodahl and B. Kasemo, *Sensors and Actuators A: Physical*, 1996, **54**, 448-456.

77. G. Sauerbrey, *Zeitschrift Für Physik*, 1959, **155**, 206-222.
78. D. C. Ash, M. J. Joyce, C. Barnes, C. J. Booth and A. C. Jefferies, *Measurement Science and Technology*, 2003, **14**, 1955.
79. K. K. Kanazawa and J. G. Gordon II, *Analytica Chimica Acta*, 1985, **175**, 99-105.
80. J. Bibette and F. Leal-Calderon, *Current Opinion in Colloid and Interface Science*, 1996, **1**, 746-751.
81. R. K. Shah, H. C. Shum, A. C. Rowat, D. Lee, J. J. Agresti, A. S. Utada, L.-Y. Chu, J.-W. Kim, A. Fernandez-Nieves and C. J. Martinez, *Materials Today*, 2008, **11**, 18-27.
82. M. Pal, R. Rai, A. Yadav, R. Khanna, G. A. Baker and S. Pandey, *Langmuir*, 2014, **30**, 13191-13198.
83. V. Fischer, J. Marcus, D. Touraud, O. Diat and W. Kunz, *Journal of Colloid and Interface Science*, 2015, **453**, 186-193.
84. A. Carranza, K. Song, J. Soltero-Martinez, Q. Wu, J. Pojman and J. Mota-Morales, *RSC Advances*, 2016, **6**, 81694-81702.
85. H. O. Ho, C. C. Hsiao and M. T. Sheu, *Journal of pharmaceutical sciences*, 1996, **85**, 138-143.
86. S. J. Abbott, *Surfactant Science: Principles and Practice*, DEStech Publications, Incorporated, 2017.
87. A. P. Abbott, F. Bevan, M. Baeuerle, R. C. Harris and G. R. Jenkin, *Electrochemistry Communications*, 2017, **76**, 20-23.
88. A. P. Abbott, A. Z. Al-Bassam, A. Goddard, R. C. Harris, G. R. Jenkin, F. J. Nisbet and M. Wieland, *Green Chemistry*, 2017, **19**, 2225-2233.

5 Effect of Surfactants on Electrodeposition of Copper from DESs

5	Effect of Surfactants on Electrodeposition of Copper from DESs	145
5.1	Introduction	146
5.1.1	Surfactant as Additives in Metal Electroplating	146
5.1.2	Electrodeposition of Metals from DESs in Presence of Additives	148
5.2	Results and Discussion.....	150
5.2.1	Cyclic Voltammetry Study	150
5.2.2	Diffusion Coefficients Study	153
5.2.3	Chronoamperometry Study of the Nucleation Mechanisms.....	157
5.2.4	Characterization of Surface Morphology	161
5.2.5	Effect of Temperature on Cu Morphology	167
5.3	Conclusion.....	175
5.4	References	177

5.1 Introduction

There is no doubt that intermolecular interactions of surfactants in the bulk solution leads to spontaneous formation of aggregates. At interfaces, the aggregation process is complicated by competing surfactant-surface and solvent-surface interactions which can produce structures called ad-micelles.^{1, 2} Both self-aggregation into supramolecular structures and the adsorption at interfaces have applications in electrochemistry.³ The former affects the thermodynamics as well as the kinetics of electrochemical reactions where the partitioning of the redox active may be varied.⁴ While adsorption of surfactants at interfaces, can alter the properties of the electrode-solution interface by changing surface characteristics into hydrophobic and hydrophilic regions or block the electrode surface where various redox processes are hindered.⁵ Moreover, a highly charged surface that stabilises by counter ions outside can be created by adsorption of ionic surfactants which the coulombic interactions may then stabilise one of the electroactive forms more than the other.⁴ Surfactants have been used in electrochemistry for a long time in applications such as electroplating, fuel cells, electrocatalysis, corrosion, electrochemical synthesis and catalysis.⁶ In electroplating, surfactants can be used to change the electrode polarization, inhibit hydrogen evolution, helping to produce composite coatings by suspension and incorporation solid particles into a metallic matrix, decrease the roughness of deposits and promote surface brightness by modification of the crystal size of the deposited metal.^{7, 8}

5.1.1 Surfactant as Additives in Metal Electroplating

In metal electroplating an important aspect of the coating metal is its morphology particularly in the evenness of the coating. This is important for aesthetic as well as anti-corrosion and anti-wear properties. A flat coating with low surface roughness is generally achieved by the addition of (typically organic) additives. Additives can include brighteners, surfactants, oxidation inhibitors, and grain refiners.⁷ They are very varied in their chemistries as they fulfil different roles with different substrates, liquids and coating metals.⁹ Additives have been divided into two main groups, levellers and brighteners. As reviewed by Oniciu and Muresan levellers have the ability to produce deposits relatively thicker in small recesses and relatively thinner on small protrusions with an ultimate decrease in the depth or height of the small surface irregularities. Whereas the brighteners are defined as having the ability to produce fine deposits which

consist of crystallites smaller than the wavelengths of visible light and having oriented grain structure.¹⁰

Franklin¹¹ reviewed the mechanisms of additives that have been supposed to affect the rate of metal deposition. It is not the aim to discuss all these mechanisms here, however, generally in aqueous solutions the additives act either as complexing agents or by the adsorption at the electrode surfaces. The former, the complexing agents, i.e. ligands, can change the metal speciation by reacting with the metal ions in the electroplating bath making them more difficult to reduce. Consequently these alter the deposition characteristics of the metal, whereas brighteners adsorb at the electrode surfaces where they act to alter the structure of the electrochemical double layer and consequently block the nucleation sites and hindering the growth of the coating metal.¹²

Considering the proprieties of some surfactants, it is reasonable to assume that they can act as additives in electroplating baths as both brightening and levelling agents. Kardos¹³ explained the theory of levelling where the organic additive can be adsorbed in specific places, the active sites, which are the high points of the electrode surface, and prevent the deposition of metal on these sites. The thickness of the diffusion layer at the active sites is less than that in the recesses therefore organic molecules will be transported faster to these active sites allowing the metals to deposit in the recesses of the electrode surface, as shown in Figure 5-1.

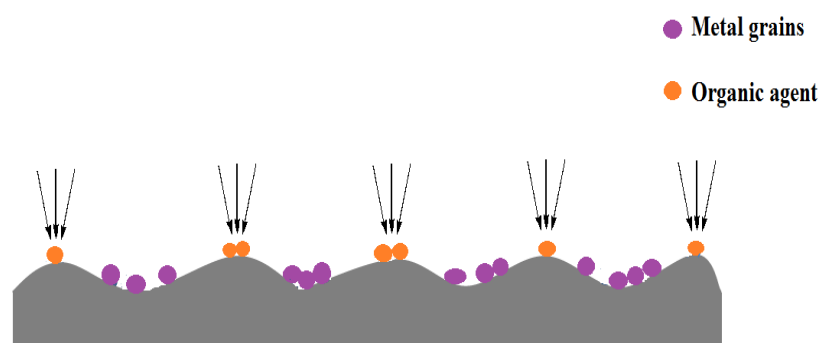


Figure 5-1: Adsorption of levelling molecules on the electrode surface.

5.1.2 Electrodeposition of Metals from DESs in Presence of Additives

Although DESs received significant interest over the past few years in many fields, the most published applications have been in electrochemistry especially in metal electrodeposition. The key advantages of using DESs are their relatively high conductivity and high solubility of metal salts. They are thought to potentially be useful for green solvents as they can avoid the use of hazardous chemicals in some cases e.g. removing Cr(VI) from chromium plating. In addition, some DESs have wide electrochemical windows which permit the electrodeposition of metals that cannot be electroplated from aqueous solutions.¹⁴ Studies of electrodeposition using DESs have focussed on metals such as chromium,¹⁵ aluminium, copper,^{16, 17} nickel,^{18, 19} zinc^{20, 21} and tin²⁰ also for alloys such as zinc/tin²⁰ and zinc/nickel.²² These studies continued to improve the plating layer by varying the composition of the DES as well as adding additives to the electroplating bath such as oxidation inhibitors, grain refiner, brighteners and surfactants.⁷

Surfactants were introduced in both aqueous and ionic liquid electroplating baths to improve the morphology of metal deposits such as thickness, brightness, hardness and roughness. In this respect, while the metals electrodeposition from DESs has been widely studied by many research groups the use of surfactants as additives has not been studied in depth.

Of particular interest to this study was the initial work by Barron²³ who studied the electrodeposition of Zn from Ethaline and Reline. Barron reported that SDS was an effective levelling agent in Ethaline. Another study by Azam²⁴ focused on the nucleation mechanism of silver deposition from Ethaline and Reline. The analysis showed that surfactants, SDS and CTAB had no effect on the nucleation and growth behaviour of silver deposition. The reasons for these two studies focussing on zinc and silver was that it was thought that the differences in reduction potential of the two metals would make them on opposite sides of the potential of zero charge, pzc. It was therefore thought that cationic surfactants, CTAB would adsorb more strongly at negative over-potentials whereas anionic surfactants, SDS would adsorb more strongly at potentials positive of the pzc. Both surfactants are known to function as brighteners for zinc in aqueous solutions which already suggests that it is not only electrostatic interactions which govern their efficacy.²⁵⁻²⁷

Other studies have been carried out in the group investigating classical aqueous additives which are known to specifically adsorb with different metals. Juma²⁸ studied the electrodeposition of Ni from Ethaline in presence of organic and inorganic additives nicotinic acid, methylnicotinate, dimethylhydantion and boric acid. It was found that these did modify the morphology of the Ni deposit but they only functioned at high Ni concentration ($> 0.9 \text{ mol dm}^{-3} \text{ NiCl}_2$) and then only at high temperatures ($< 80 \text{ }^\circ\text{C}$). Under these conditions these additives modify the nucleation and growth mechanism of Ni the adsorption onto the metal surface and occupy most active sites due to specific adsorption at the electrode surface. Another study by Al-Esary²⁹ used ethylenediaminetetraacetic acid disodium salt dihydrate, sodium iodide, boric acid and 5,5-dimethylhydantoin as additives for electrodeposition of Cu from Ethaline. Some of these additives, particularly sodium iodide were shown to increase the rate of Cu deposition and led to bright deposits.

The focus of this chapter is to investigate whether the surfactants adsorb sufficiently on electrode surfaces to cause a difference in the nucleation and growth mechanism of metals. In this study copper deposition will be studied as the in-built diffusion probe with $\text{Cu}^{2+}/\text{Cu}^+$ can be used to determine the reversibility of the process and whether mass transport is a factor in deposition rate. Cu coating, which will be compared and contrasted with previous studies of Zn and Ag, in two DESs Ethaline and Glyceline using different anionic surfactants. The reason behind using Ethaline and Glyceline is the results of chapter 3 and 4 show that surfactant is more surface-active in Glyceline than in Ethaline.

The mode of adsorption of surfactants at aqueous solution-electrode interfaces has been studied in detail. The high polarity of water leads to clear structures, which are relatively well understood. The adsorption mechanism of surfactants at the electrode-DES interface has not been reported and may be less obvious. Further analysis of the adsorption processes and a better understanding of surfactant aggregation on the electrode surface in DESs can inform their potential role in controlling electrochemical processes.

5.2 Results and Discussion

In this chapter, two surfactants were chosen; SDS and AOT. Both SDS and AOT have the same head group but different side chains. SDS has a single chain with 12 carbon atom and AOT has two chains with some branching. In water, SDS can form micelles whereas AOT tends to form reverse micelles. The chosen surfactants have the potential to form very different structures at the electrode-DES interface. The concentration of surfactants was kept constant (25 mM) as was the concentration of copper chloride (100 mM) to be comparable with the previous studies of additives by Barron,²³ Azam²⁴ and Al-Esary.²⁹ The chosen temperatures for this work was 50°C and 80°C for comparison with previous studies.²⁹

5.2.1 Cyclic Voltammetry Study

In this section, the cyclic voltammograms were performed using a polished 0.5 mm Pt disc electrode, a Pt flag counter electrode and a Ag wire as a reference electrode all immersed in 100 mM $\text{CuCl}_2 \cdot 2\text{H}_2\text{O}$ at 50°C either in Ethaline or in Glyceline in the absence and presence of different surfactants. The potential window of the cyclic voltammetry was recorded from +1.0 V toward the negative direction -1.0 V and then reversed to the starting point. The voltammograms in Figure 5-2 were measured in both Ethaline and Glyceline. The speciation of Cu^+ and Cu^{2+} were have been found to be $[\text{CuCl}_3]^{2-}$ and $[\text{CuCl}_4]^{2-}$ complexes respectively giving rise to a yellow coloured solution.^{17, 30} In pure DESs, two separate reduction processes are observed for the $\text{Cu}^{2+}/\text{Cu}^+$ couple at potential onset of +0.40 in both system followed by the reduction from Cu^+ to Cu^0 at -0.39 V in Ethaline and -0.37 V in Glyceline. These voltammograms are consistent with those obtained for copper electrodeposition in both DESs Ethaline and Glyceline.^{16, 29, 31, 32}

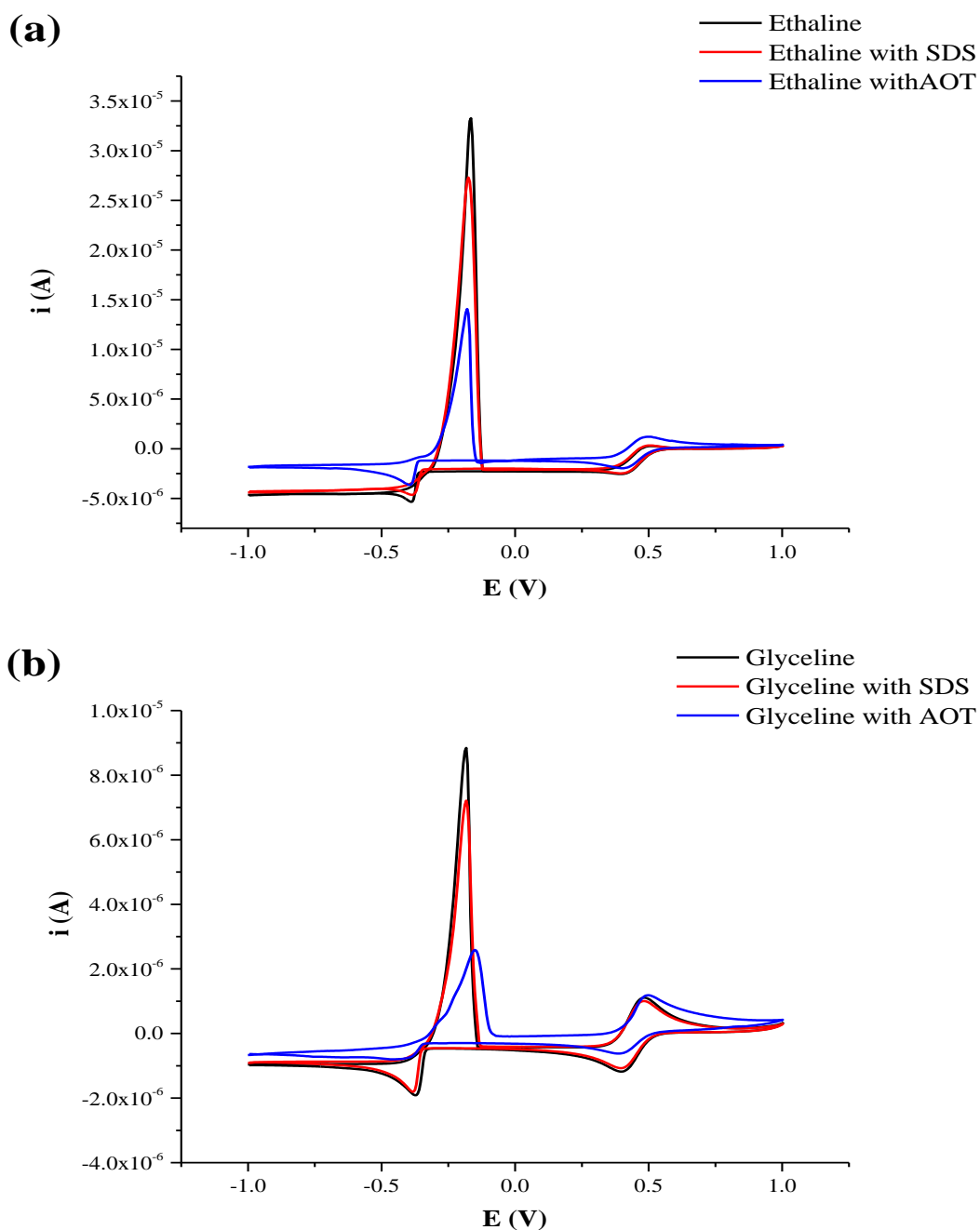


Figure 5-2: Cyclic voltammogram of $100 \text{ mM CuCl}_2 \cdot 2\text{H}_2\text{O}$ at a scan rate 5 mV s^{-1} in (a) Ethaline and (b) Glyceline containing SDS and AOT.

The peak current and peak potential were affected by added surfactants and this was most marked by the addition of AOT which significantly appears to decrease the copper deposition and stripping current. This change can be quantified in terms of the charge (Q) and the shift in peak potential, that can be calculated from the data presented in Figure 5-2.

$$\text{shift in } E_p = E_p^0 - E_p^s$$

Equation 5-1

Where E_p^0 and E_p^s are the peak potential of Cu^+/Cu^0 in the absence and presence of surfactant respectively. Table 5-1 shows the change in charge (Q) of Cu reduction as a function of the type of surfactant and Table 5-2 show the shift in peak potential of Cu^+/Cu^0 . Generally, the data presented in Table 5-1 indicated that there is a decrease in the charge by adding surfactant. The decrease in the charge indicates that the surfactants might have adsorbed onto the electrode surface, leading to a decrease in the active surface area for metal ions to be reduced.⁷ AOT is a more hydrophobic surfactant and the area taken up by the double chain has more potential to block the electrode surface than SDS. Azam observed a slight increase in the peak currents for Ag deposition from Ethaline by adding surfactants SDS and CTAB.²⁴

Table 5-1: The charge of Cu reduction as function of different surfactants in Ethaline and Glyceline.

Surfactant	Q (C) in Ethaline	Q (C) in Glyceline
None	2.27×10^{-3}	6.01×10^{-4}
SDS	2.10×10^{-3}	5.47×10^{-4}
AOT	1.09×10^{-3}	3.76×10^{-4}

The potential at which Cu^+ reduction starts is slightly shifted by adding surfactants (Table 5-2). This was also observed in electrodeposition of Ag in Ethaline by adding SDS and CTAB.²⁴ In aqueous medium, however, the shift to negative potential values was observed in Zn^{2+} reduction by the addition of AOT.³³

Table 5-2: The shift in peak potential of Cu^+/Cu^0 solved in DESs by adding surfactants.

Surfactant	Ethaline		Glyceline	
	Shift in E_{pa} (mV)	Shift in E_{pc} (mV)	Shift in E_{pa} (mV)	Shift in E_{pc} (mV)
SDS	6.89	-0.69	-0.58	9.70
AOT	9.69	8.21	-32.72	75.98

It is well established that the chloride activity in DESs depend on strength of the hydrogen bonding between the HBD and Cl ion and here for Ethaline and Glyceline it is reported that the density of the hydrogen bond is higher in Glyceline than Ethaline.³⁴ Therefore, the Cl ions activity in Ethaline is higher than in Glyceline. An increased chloride activity could shield the electrostatic interactions between the charged electrode and the anionic surfactants.

Figure 5-3 shows the variation of the peak separation (ΔE_p) of Cu^+/Cu^0 with the scan rate. The data show that the peak separation falls in the range of 0.099 – 0.110 V for Ethaline and 0.081-0.144 V for Glyceline. The addition of surfactants has little effect on the peak separation in Ethaline while in Glyceline the separation is slightly shifted to higher values especially by adding AOT indicating that the system become more irreversible. This is not a resistance artefact as the liquids have similar conductivities with and without surfactants. It is therefore likely to arise from electrode blocking. The shift in peak potential for Glyceline with AOT should not be seen as a change in process thermodynamics as the onset potentials for oxidation are similar to those without surfactants.

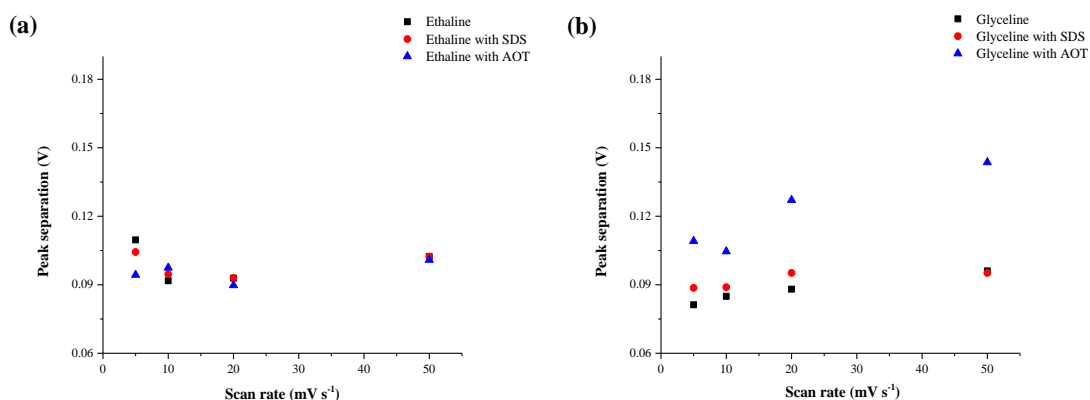


Figure 5-3: Peak separation as function of scan rate of Cu deposition in (a) Ethaline and (b) Glyceline with absence and present of surfactants, SDS and AOT.

5.2.2 Diffusion Coefficients Study

The data presented in Figure 5-2 (a) show that the $\text{Cu}^{2+}/\text{Cu}^+$ couple is relatively reversible at a scan rate 5 mV s^{-1} in Ethaline with the calculated ratio of anodic and cathodic currents was found close to one and the peak potential separation, ΔE_p are 0.110 V, which although higher than the theoretical value of 0.059V at 25°C is typical

of DESs and is due to resistance of the solution.^{35, 36} In Glyceline, (Figure 5-2 (b)) the calculated ratio of anodic and cathodic currents was found to be 0.8 and the peak potential separation, ΔE_p are 0.081V indicated that reduction of the $\text{Cu}^{2+}/\text{Cu}^+$ couple in Glyceline at a scan rate, 5 mV s^{-1} is semi reversible.

The peak current for the reduction of $\text{Cu}^{2+}/\text{Cu}^+$ is proportional to the square root of the potential sweep rate as described by the Randles–Sevcik Equation (5-2). From a plot of i_p vs $v^{1/2}$ the diffusion coefficient can be calculated as:

$$i_p = 0.4463nFCA \sqrt{\frac{nFvD}{RT}} \quad \text{Equation 5-2}$$

Where i_p is the peak current, n is number of electrons, F is the Faraday constant, C is the bulk concentration, A is the area of electrode, v is the scan rate, D is the diffusion coefficient, R is the gas constant and T is the absolute temperature.

Figure 5-4 shows the sweep rate dependency of the cyclic voltammograms of $\text{CuCl}_2 \cdot 2\text{H}_2\text{O}$ in the absence and presence of AOT and SDS. The parameters derived from these voltammograms are listed in Table 5-3. It can be seen that for Ethaline i_{pc}/i_{pa} remains constant at approximately 1 showing that reduction is reversible and the surfactant does not appear block the electrode surface. The addition of AOT decreases the peak current significantly which equates to a reduction in the diffusion coefficient of approximately 50%.

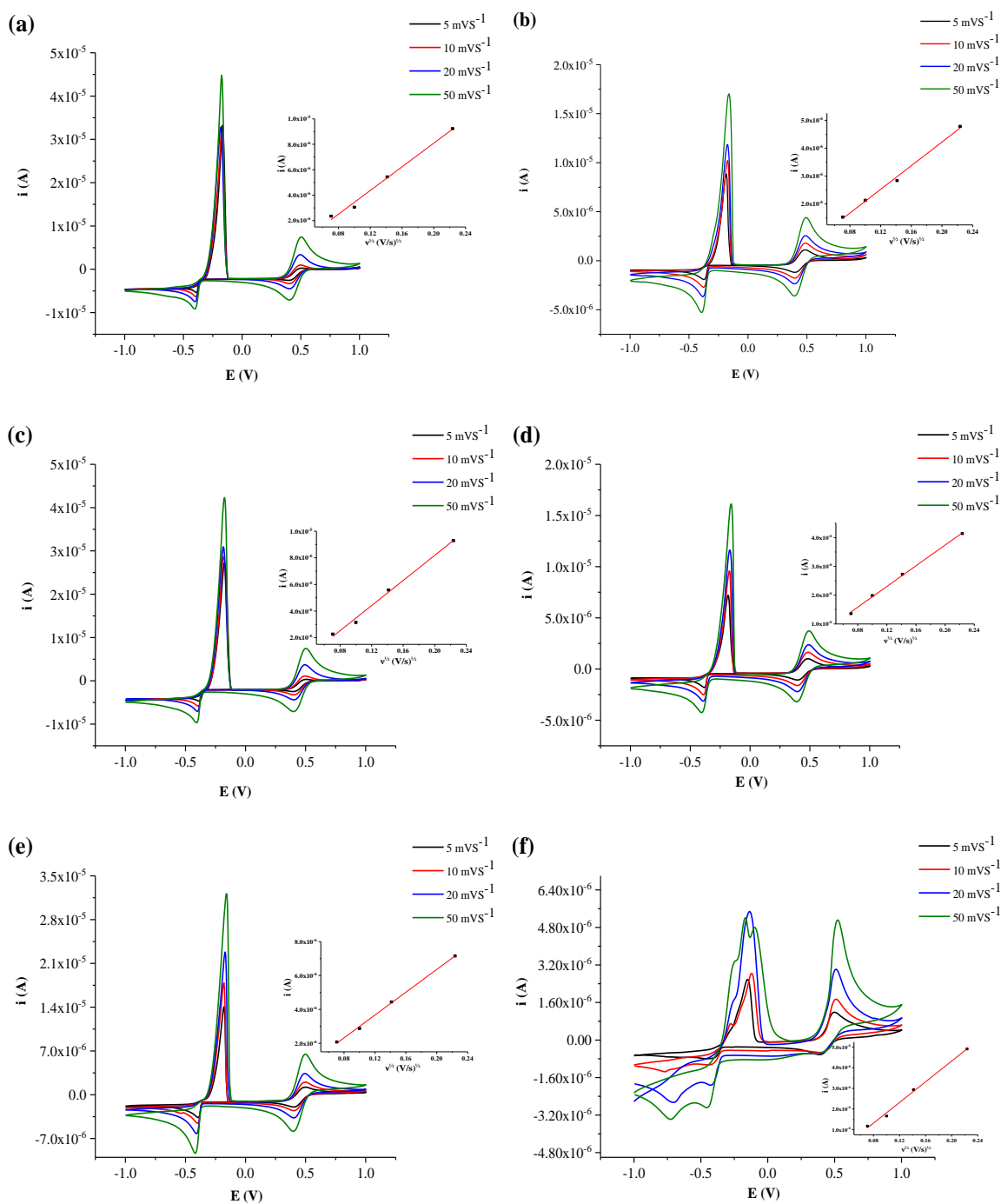


Figure 5-4: Cyclic voltammogram of 100 mM $\text{CuCl}_2 \cdot 2\text{H}_2\text{O}$ in, DESs as a function of the square root of scan rate at 50°C in the absence and presence of different surfactants; (a) pure Ethaline, (b) pure Glyceline, (c) 25 mM SDS in Ethaline, (d) 25 mM SDS in Glyceline (e) 25 mM AOT in Ethaline and 25 mM AOT in Glyceline. Inset is a plot of linear dependence of peak current versus square root of scan rates.

The addition of AOT causes a significant change in the voltammogram shape in Glyceline. The ratio i_{pc}/i_{pa} is strangely < 1 suggesting a smaller cathodic current than the anodic current which is illogical and probably indicates that surfactant adsorption results in an artefact.

Table 5-3: Cyclic voltammetric data at 5 mVs^{-1} for $\text{Cu}^+/\text{Cu}^{+2}$ in DESs with different surfactant.

Solvent	Surfactant	i_{pc}/i_{pa}	ΔE_p (V)	$E_{1/2}$ (V)	D (cm^2s^{-1})
Ethaline	None	1.05	0.110	0.45	8.42×10^{-7}
	25 mM SDS	1.05	0.104	0.45	8.66×10^{-7}
	25 mM AOT	0.96	0.094	0.45	4.41×10^{-7}
Glyceline	None	0.79	0.081	0.44	1.75×10^{-7}
	25 mM SDS	0.80	0.089	0.44	1.26×10^{-7}
	25 mM AOT	0.52	0.109	0.45	2.45×10^{-7}

The diffusion coefficient was calculated and tableted in Table 5-3. The calculated value of D at 50°C are significantly higher compare with the value of D calculated at 25°C of FeCl_2 in chapter 4. This is not surprising that the increase of the temperature leads to a decrease in the viscosity and hence an increase in the mass transport. The diffusion coefficient in Glyceline is significantly lower than in Ethaline although the value calculated for AOT in Glyceline is almost certainly erroneous and due to an artefact.

It is well known that the diffusion coefficient is extremely affected by the viscosity of the solution. At 25°C the viscosity value increased by adding SDS in both DESs (Ethaline from 42.17 to 53.44 cP and Glyceline from 326.00 to 426.11 cP). In case of adding AOT however, the viscosity does not change (45.29 and 319.13 cP for Ethaline and Glyceline respectively). As the temperature increase the viscosity decrease (see Figure 5-5) and this suggest that the bulk viscosity does not increase that much by adding surfactants. Herein the only way can explain the difference in the diffusion coefficient as results of adding surfactants to DESs is present of structure close to the electrode surface which is not caused by specific adsorption.

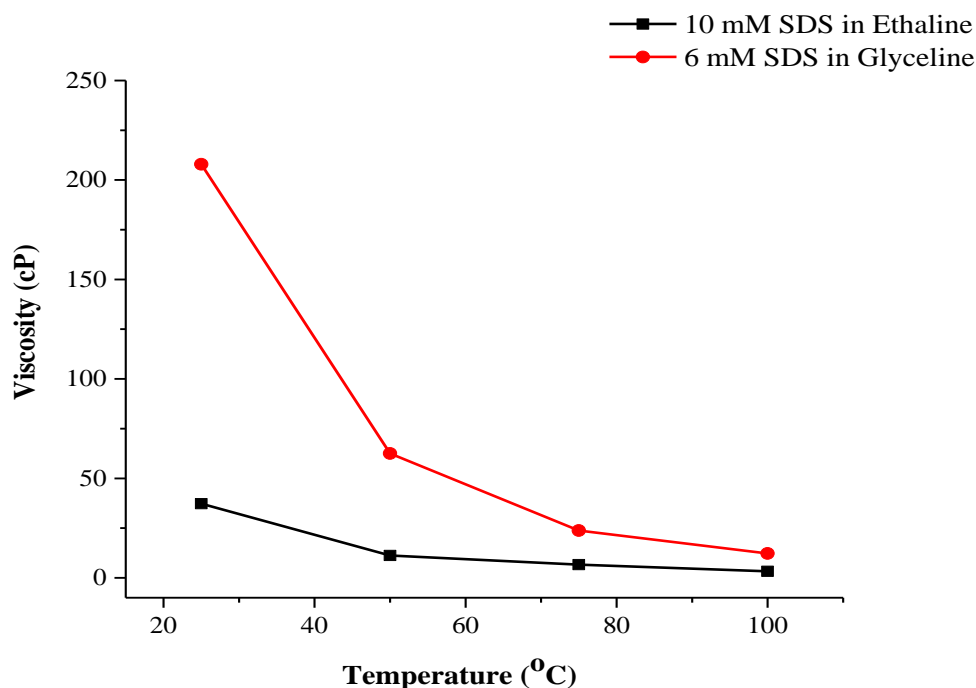


Figure 5-5: Viscosity of SDS solution in DESs versus temperature

5.2.3 Chronoamperometry Study of the Nucleation Mechanisms

The mechanism of metal film nucleation and growth can be detected from the early stages of electrodeposition which can give insights into the properties of bulk deposits such as smoothness and brightness. As mentioned above, the most common effect of surfactants in metal electrodeposition is to alter the nucleation mechanism. When micelles adsorb at active sites they can effect metal nucleation mechanisms.²⁶ Chronoamperometry can be used to understand the mechanism and kinetics of metal nucleation.

In both aqueous and ionic liquid electrolytes the most widely used theoretical model for the nucleation of metals is that proposed by Scharifker and Hills.³⁷ The nucleation in this model assumes to occur at certain specific sites on the surface where two nucleation mechanisms are described; instantaneous and progressive. Instantaneous nucleation describes the rapid rate of nucleation compared with the resultant rate of growth as a result nuclei growing at many sites within a very short time. Progressive nucleation is characteristic of slow nucleation.³⁷

The models of the Scharifker and Hills for instantaneous and progressive nucleation followed by 3D diffusion-limited growth, supposing hemi-spherical nuclei. The normalised current as a function of normalised time are given in Equation (5-3) and (5-4) respectively.^{38, 39}

$$\frac{i}{i_{max}^2} = \frac{1.9542}{\frac{t}{t_{max}}} \left\{ 1 - \exp \left[-1.2654 \left(\frac{t}{t_{max}} \right) \right] \right\}^2 \quad \text{Equation 5-3}$$

$$\frac{i}{i_{max}^2} = \frac{1.2254}{\frac{t}{t_{max}}} \left\{ 1 - \exp \left[-2.3367 \left(\frac{t}{t_{max}} \right) \right]^2 \right\}^2 \quad \text{Equation 5-4}$$

Where i is current density, i_{max} is the maximum current density, t is time and t_{max} is the time at which the maximum current occurs. In order to recognize between an instantaneous or progressive nucleation processes of Cu deposition in DESs, the experimental data are represented in a dimensionless plot of i/i_{max}^2 versus t/t_{max} and compared with theoretical plots derived from Scharifker and Hills equations.

Figure 5-6 shows the chronoamperometric data for Cu electrodeposition in absence and presence of AOT and SDS from 100 mM $\text{CuCl}_2 \cdot 2\text{H}_2\text{O}$ in Ethaline and Glyceline (inset) together with the Scharifker and Hills analysis of the curves according to Equation (5-3) and (5-4). The deposition was achieved at 50°C and on a polished Pt disk with the aim of examining the influence of surfactants under study on the nucleation of Cu from DESs. The applied potential for the nucleation study was -0.39 V in Ethaline and -0.36 V and in Glyceline. The fitting of chronoamperometric data to the theoretical models for 3D instantaneous and progressive nucleation for Cu deposited from DESs, Ethaline and Glyceline are presented in Figure 5-6.

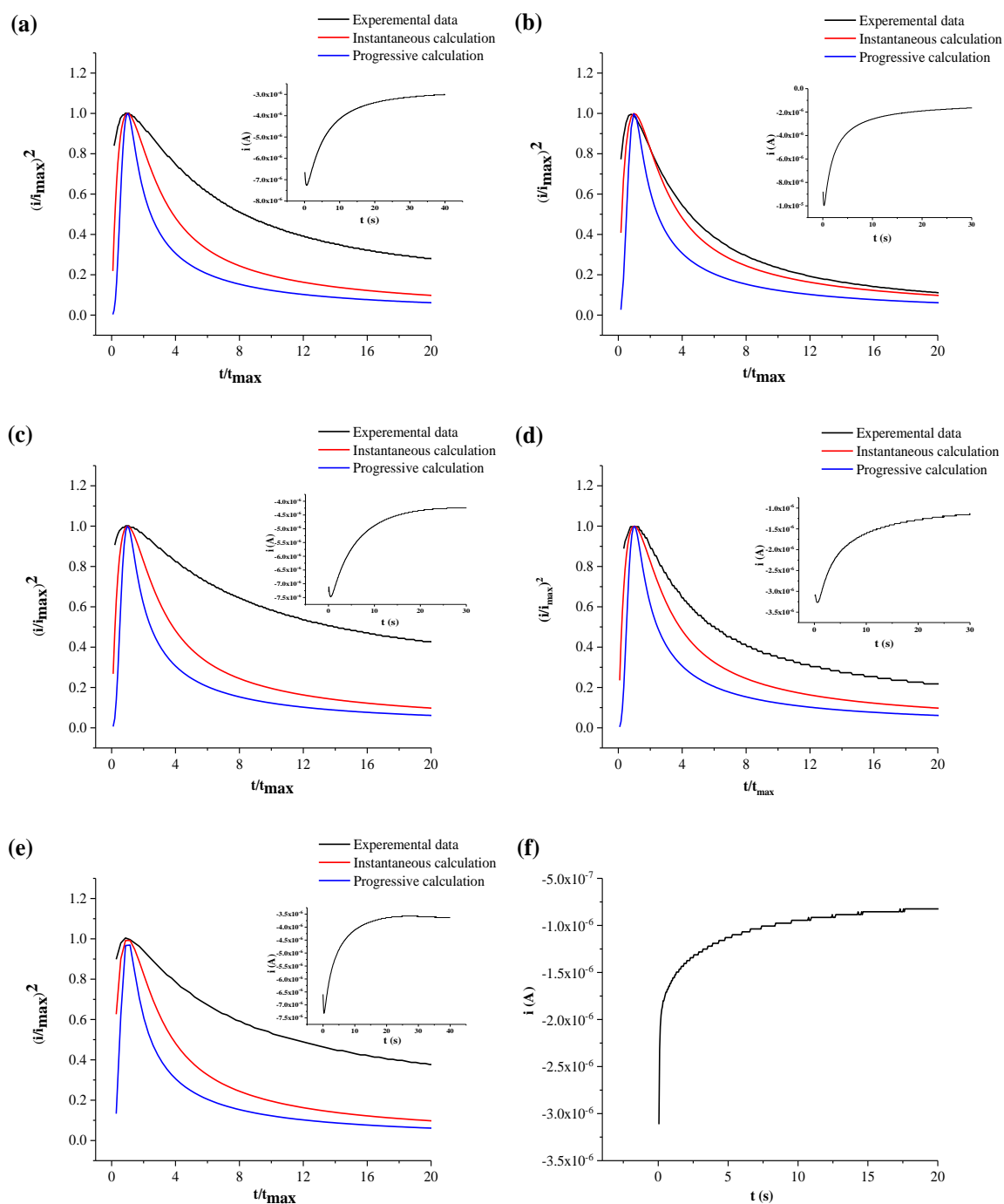


Figure 5-6: Theoretical and experimental dimensionless $(i/i_{max})^2$ versus t/t_{max} for Cu deposition from 100 mM $\text{CuCl}_2 \cdot 2\text{H}_2\text{O}$ in DESs in absence of surfactants; (a) pure Ethaline, (b) pure Glyceline, (c) 25 mM SDS in Ethaline, (d) 25 mM SDS in Glyceline (e) 25 mM AOT in Ethaline and 25 mM AOT in Glyceline. Inset chronoamperograms obtained at 50°C with an applied potential of -0.39 V and -0.36V in Ethaline and Glyceline respectively.

Figure 5-6 (a) shows that the experimental chronoamperometry data for 100 mM $\text{CuCl}_2 \cdot 2\text{H}_2\text{O}$ in Ethaline does not fit well to either a 3D instantaneous or a progressive nucleation mechanism. This result is in agreement with the recent study by Al-Esary.²⁹ The addition of SDS and AOT, Figure 5-6 (c) and Figure 5-6 (e) respectively does not change the nucleation mechanism of Cu significantly compared to pure Ethaline. This would tend to suggest that SDS does not block the electrode. AOT has the same nucleation mechanism but the diffusion coefficient is significantly decreased suggesting that it may function as a viscosity modifier although the change in diffusion coefficient is not an order of magnitude different which would be necessary if the copper was partitioning into the micelle.

In pure Glyceline Figure 5-6 (b) the experimental data for Cu deposition in the surfactant-free solution totally follows the theoretical curve for a 3D instantaneous mechanism relatively well although there is more deviation when SDS is added (Figure 5-6 (d)). In the instantaneous nucleation model, as the nuclei form it is favourable for them to grow in layers rather than the continuous generation of new nuclei. In case of AOT in Glyceline the data does not show a maximum current peak (see Figure 5-6 (f)) so the data could not be fitted.

The data show that the mechanism of nucleation is significantly different in Glyceline than Ethaline. This suggests that films do potentially form at the electrode-DES interface with surfactants. This would tie in with the data from Chapters 3 and 4 suggesting that the chloride activity is lower in Glyceline such that electrode-anionic surfactant electrostatic interactions are less shielded by chloride activity.

Juma carried out a similar nucleation study for additives which are known to specifically interact with nickel through adsorption to the electrode surface. Nucleation of nickel using nicotinic acid and methylnicotinate showed a good fit a progressive nucleation mechanism in Ethaline.²⁸ This is also consistent with the behaviour observed in case of use sodium iodide as an additive for Cu deposition from Ethaline where this additive produce the triiodide, I_3^- ion in solution which may adsorb into the electrode surface.²⁹ Other additives, however, including ethylenediamine tetraacetic acid disodium salt dihydrate, boric acid and 5,5-dimethylhydantoin have shown that the Cu deposition fitted well to the 3D instantaneous nucleation mechanism.²⁹

Specific adsorption using nicotinic acid and methylnicotinate led to very flat surface morphologies with nano-crystalline deposits. These produced harder deposits than those with micro-crystalline deposits obtained from aqueous solutions. Interestingly, similar deposition rates could be obtained in Ethaline and aqueous solutions despite the 10 fold difference in liquid viscosity.

5.2.4 Characterization of Surface Morphology

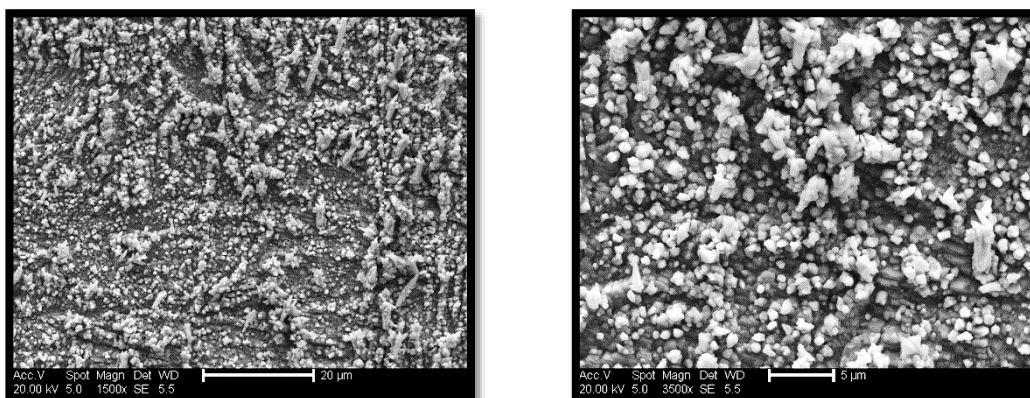
To understand the effect of surfactants on deposition mechanism and surface structures it is important to characterise the morphology of the deposits obtained under comparable conditions. The cyclic voltammograms recorded on platinum electrode of $\text{CuCl}_2 \cdot 2\text{H}_2\text{O}$ have indicated that the addition of surfactants influence the electrodeposition process. In order to determine whether these changes were reflected in the deposit morphology and composition the scanning electron microscopy and X-ray diffraction analysis were performed.

5.2.4.1 Scanning Electron Microscopy

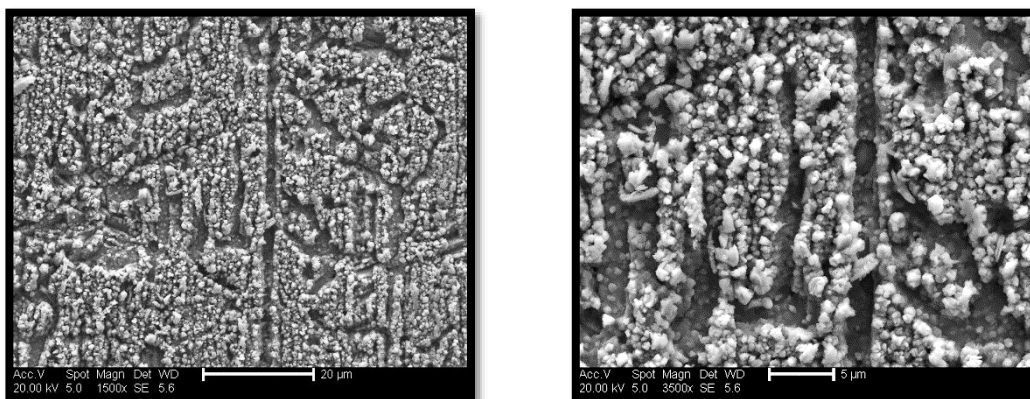
The effect of surfactants on the morphology of Cu deposits obtained using bulk electrolysis has been investigated by the scanning electron microscopy technique, SEM. The Cu was deposited from Ethaline and Glyceline containing 100 mM $\text{CuCl}_2 \cdot 2\text{H}_2\text{O}$ in the absence and presence of SDS and AOT. All bulk electrolysis experiments were carried out on nickel substrates for 2 h with a constant current density of 1.25 mA cm^{-2} at 50°C . The EDX mapping analysis indicates that only Cu is electro-deposited on the nickel substrate. The images show that the surface morphology and the crystal shape and size are affected by the presence of the surfactants.

Figure 5-7 (a) show the electrodeposited film of Cu from Ethaline in the absence of surfactants. A rough surface and large grains in different sizes are observed. However, adding surfactants shows the surface has a significant change in copper morphology, Figures 5-7 (b) and (c). Grooves appear in the microstructures of the deposits obtained with both surfactants. While cracks are common in metal coatings with high internal stress of the coating e.g. chromium they are of very different morphologies and dimensions than those observed here.⁴⁰ The copper around the grooves almost appear to be templated around a liquid crystalline phase. While templated deposits of other metals and ceramic materials have been reported from aqueous solutions, particularly using

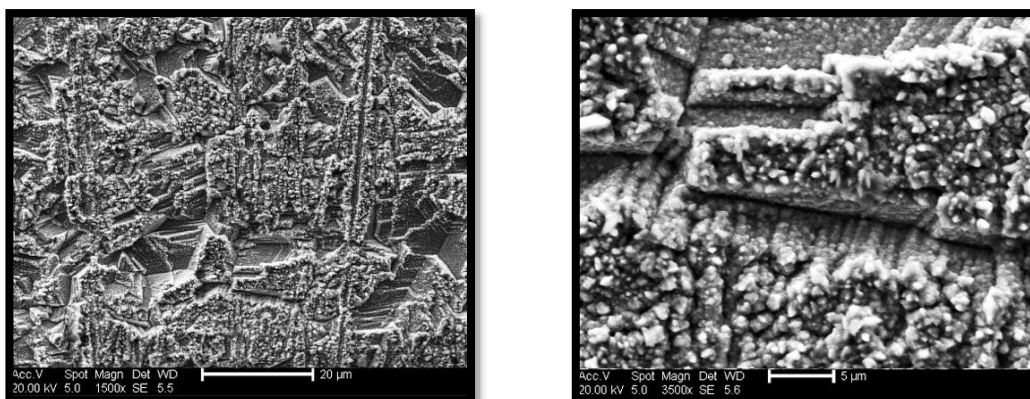
AOT, the dimensions of the templates structures tend to be in the nanometer length-scale.⁴¹



(a)



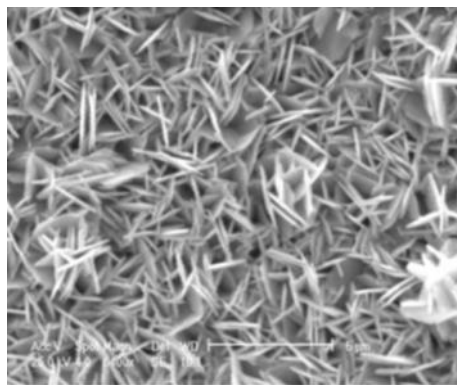
(b)



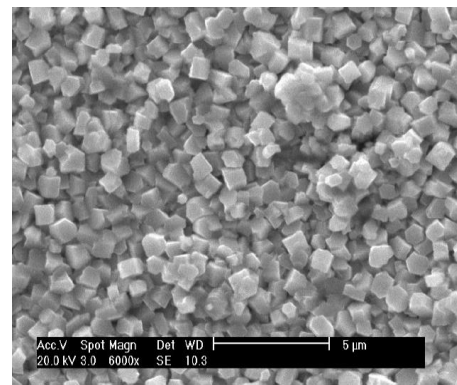
(c)

Figure 5-7: SEM images of Cu coating from 100 mM $\text{CuCl}_2 \cdot 2\text{H}_2\text{O}$ in Ethaline on nickel substrate at 50°C obtained in (a) absence of surfactants, (b) with 25 mM SDS and (c) 25 mM with AOT at two magnifications right scale bar = 20 μm and left 5 μm.

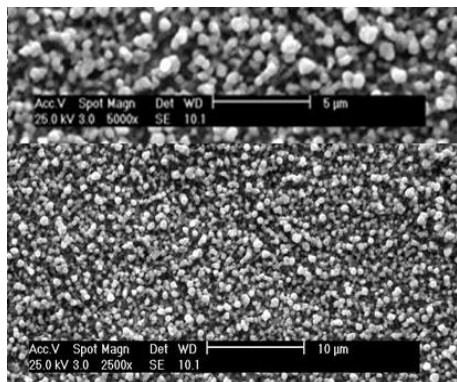
The previous study by Barron to investigate the electrodeposition of Zn from Ethaline showed that SDS altered the Zn morphology. Figure 5-8 (a) and (b) shows the SEM image of a Zn coating in the absence and presence of SDS respectively. It is clear that SDS changes the preferred orientation of the Zn crystallites. Whereas the study of Ag electrodeposition from Ethaline by Azam shows that SDS had a smaller but noticeable effect on the grain size, resulting in small crystallites hence smoother and more dense films as shown in Figure 5-8 (c) and (d).



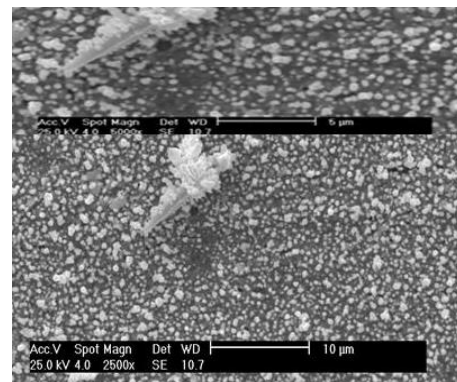
(a)



(b)



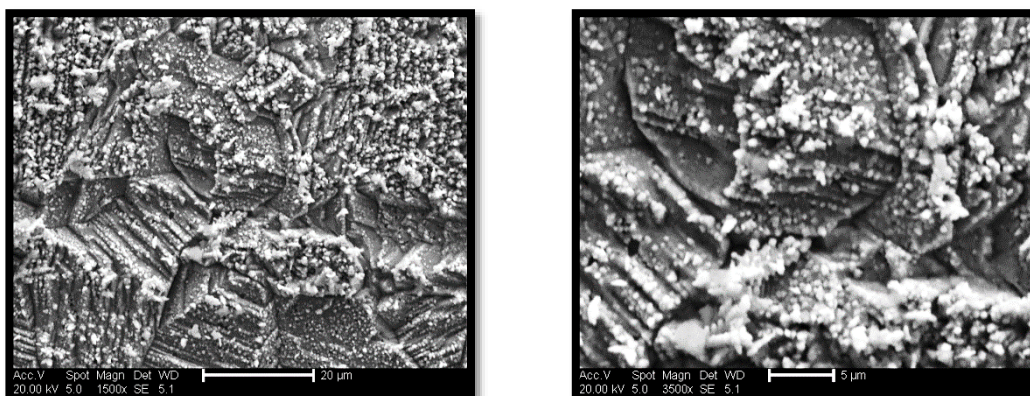
(c)



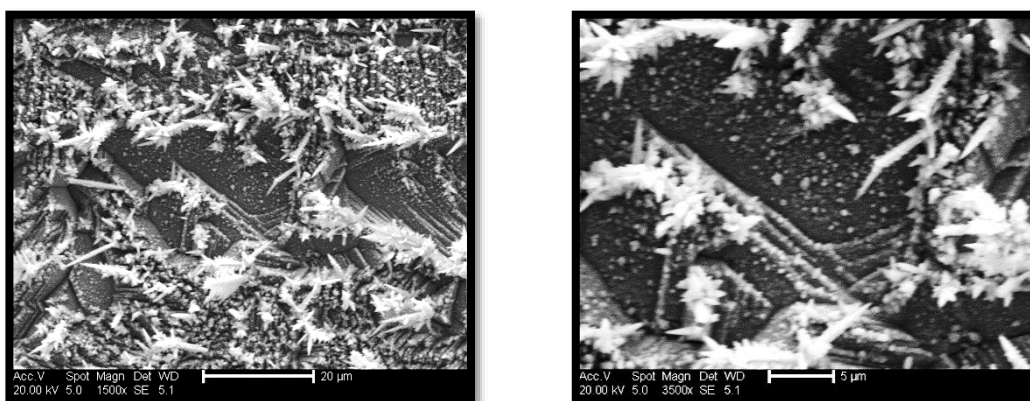
(d)

Figure 5-8: (a) and (b) SEM images of Zn coating from 300 mM ZnCl₂ in Ethaline on mild steel substrate at 50°C obtained in (a) absence of surfactants, (b) with 5 mM SDS. (c) And (d) SEM images of Ag coating from 100 mM AgNO₃ in Ethaline on platinum substrate at 40°C obtained in (c) absence of surfactants, (d) with 10 mM SDS, taken from Ref.²³ and Ref.²⁴ respectively.

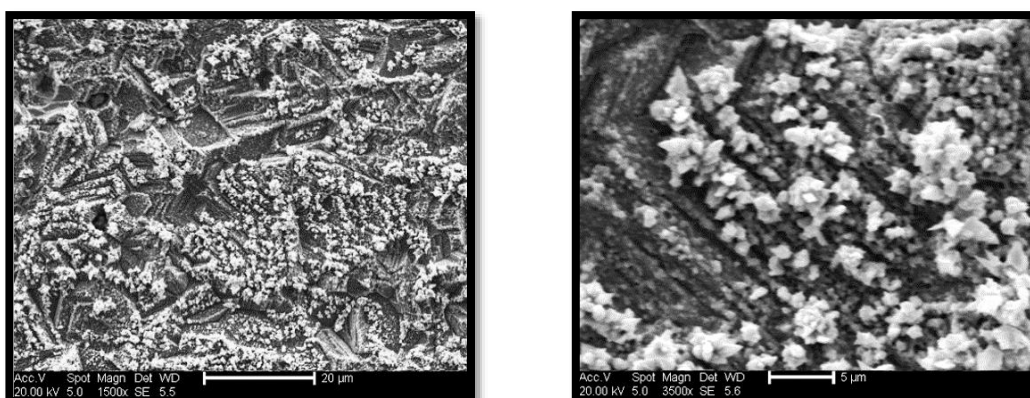
The above experiments were repeated for Glyceline and the SEM images of the deposits are presented in Figure 5-9.



(a)



(b)



(c)

Figure 5-9: SEM images of Cu coating from 100 mM $\text{CuCl}_2 \cdot 2\text{H}_2\text{O}$ in Glyceline on nickel substrate at 50°C obtained in (a) absence of surfactants, (b) with 25 mM SDS and (c) 25 mM with AOT at two magnifications right scale bar = 20 μm and left 5 μm.

It is clear that the morphology in pure Glyceline is different from that in pure Ethaline suggesting that mass transport is important. When SDS and AOT were added large grooves were once again observed in the copper deposit. These were not observed by Barron or Azam because the concentration of SDS was 5 times that used in the earlier experiments and was considerably higher than the CMC. This indicate that the way surfactants adsorb to the electrode surface differ in the two DESs.

In chapter 4, the results indicated that the Cl^- ions adsorb at the electrode surface in Ethaline more than in Glyceline and all surfactants used in this study are anionic hence there will be a competition to be in the double layer. Added to this there is the competition with the copper species which is also anionic, $\text{CuCl}_4^{2-}/\text{ClCl}_2^-$. The surfactant could change the effective concentration of copper in the double layer although the copper is there in a 4 fold excess to the surfactant.

Whatever the exact structure is at the electrode surface, it is clear that the surfactants do not act as levellers as they would in aqueous solutions most probably because they are less well adsorbed at the electrode surface than they are in aqueous solutions. This suggests that brighteners and levellers in DESs are more likely to be active if they have specific interactions with the metal being deposited than if they rely on simple electrostatic interactions. To some extent this is logical given the high ionic strength of the DESs.

5.2.4.2 X-Ray Diffraction Analysis

It is very important to study the crystallographic structure of Cu electrodeposits. Figure 5-10 shows the X-ray diffraction spectra for Cu electrodeposited film obtained in the absence and presence of surfactants from Ethaline and Glyceline containing 100 mM $\text{CuCl}_2 \cdot 2\text{H}_2\text{O}$ at 50°C where all Cu electrodepositions samples were achieved on the nickel substrate for 2 h and applied constant current density of 1.25 mA cm⁻².

The peaks presented in Figure 5-10 assigned to the face-centered cubic (fcc) Cu planes of (111), (200), and (220) at 43.3°, 50.4°, and 74.1° respectively. These peaks agreed well with the standard JCPDS card of Cu.³² All XRD peaks are sharp and distinctive of pure crystalline copper and display that growth of Cu crystallites can occur through a number of different orientations. The other peaks displayed in Figure 5-10 are assigned to the nickel substrate.⁴²

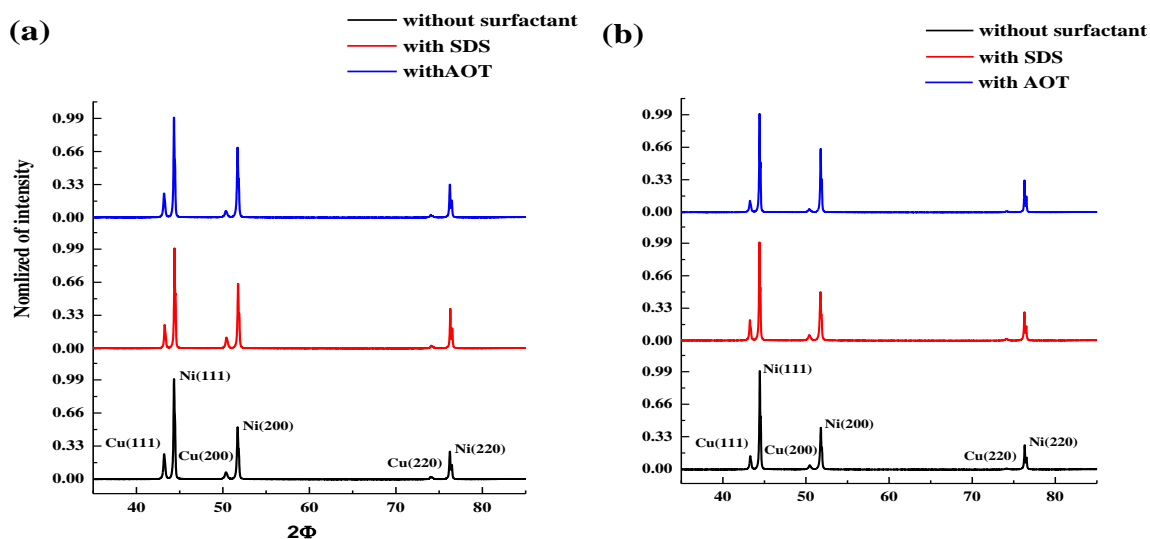


Figure 5-10: XRD patterns for Cu deposit film from DESs, (a) Ethaline and (b) Glyceline in absence and presence of surfactants.

It is clear that Cu(111) is the preferred crystal orientation in all samples both with and without surfactants in both Ethaline or Glyceline see Figure 5-11 (a) and (b) evidence of face-centered cubic (fcc) structures. Figure 5-11 shows the relative intensities of the different signals and it can be seen that there is relatively little difference between the samples. It was previously shown with nicotinic acid and methylnicotinate for both copper and nickel that there was a significant change in the growth of different crystallites which shows that these additives are site specific unlike the surfactants.²⁸

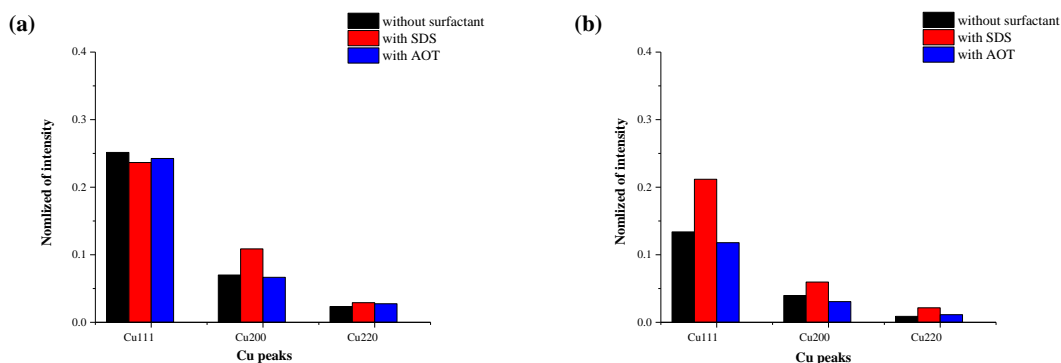


Figure 5-11: Comparison between the intensity of Cu peaks deposited from DESs, (a) in Ethaline and (b) in Glyceline in absence and presence of surfactants.

It is clear that surfactants are not surface active enough to regulate the flow of metal ions to the electrode surface. The presence of aggregate structures close, but not adjacent to the electrode can lead to disruption of flow on a microscopic scale resulting in a rougher surface than would be the case in their absence. It is clear that anionic groups such as nicotinic acid and boric acid act as brighteners and affect the crystallographic faces deposited but sulfate is clearly not able to specifically interact with the copper.

It could also be that the specific adsorption of chloride is stronger than that of the surfactant. Studies by Juma,²⁸ Cihangir⁴³ and Al-Esary²⁹ showed that increasing the temperature significantly improved the surface finish of the nickel, zinc and copper deposits.

5.2.5 Effect of Temperature on Cu Morphology

It is well known that higher temperatures strongly affect the physical properties of the electroplating bath such as viscosity, conductivity, and the mass transport. Herein the experiments were carried out under the same conditions as previously except the temperature was raised to 80°C. Tables 5-4 and 5-7 show images for Cu coated in Ethaline and Glyceline respectively in absent and in presence of surfactants at temperature 50 and 80°C. Also 3D optical microscopy was carried out to characterise the copper deposited film under the optical microscopy with 50x magnification to calculate the surface roughness. The 3D micrographs presented in Tables 5-5 and 5-8 for Cu coated in Ethaline and Glyceline respectively in absent and in presence of surfactants at temperature 50 and 80°C visually show the Cu coated film. All images of Cu deposited film from 100 mM CuCl₂.2H₂O in DESs were carried out on nickel substrate for 2 h and applied current density of 1.25 mA cm⁻². It is clear from the photos and 3D micrographs that the Cu coated films are different when the temperature is increased.

The Cu coating in Ethaline at 50°C (Table 5-4) is darker and more red/orange than the Cu deposit achieved at 80°C. Subsequent addition of SDS and AOT causes the deposit to be darker and in the case of AOT at 80°C the sample is grey rather than orange. The appearance cannot be explained in terms of the surface roughness. Table 5-6 lists the surface roughness values obtained using 3D optical profilometer. It can be seen that the surface roughness values are of a similar magnitude across all experiments. The one

exception is the result in Ethaline at 80°C with AOT added which shows a significantly larger surface roughness than the other samples. This could be the cause of the discolouration of the sample.

Table 5-4: Images for Cu coated in Ethaline in absent and with presence of surfactants at temperature 50 and 80°C.

T (°C)	Ethaline	Ethaline with SDS	Ethaline with AOT
50			
80			

Table 5-5: 3D topographical images of copper deposited film from Ethaline in absent and presence of surfactants at temperature 50 and 80°C.

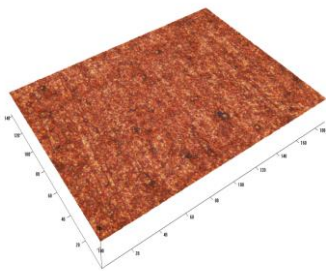
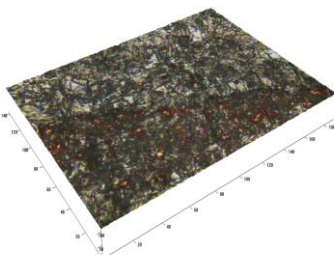
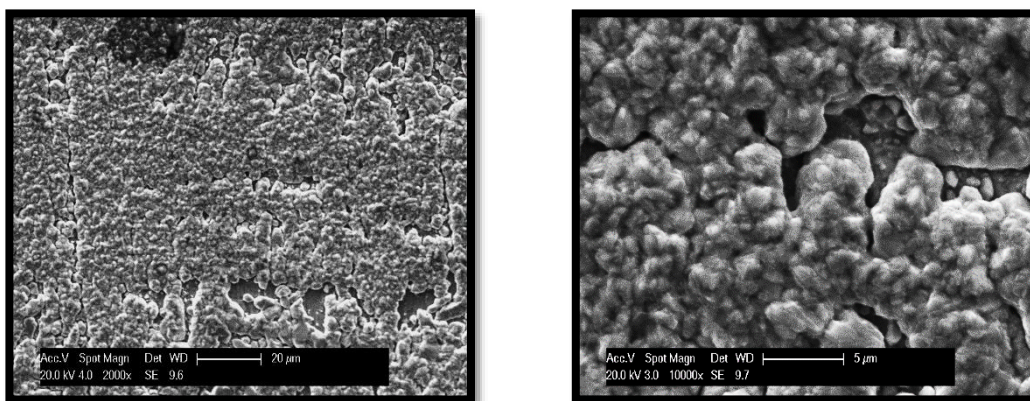
Surfactant	Cu coating at 50 (°C)	Cu coating at 80 (°C)
None		
SDS		
AOT		

Table 5-6: Surface roughness at 50x magnification for Cu deposited from DESs in absence and presence of surfactants at temperature 50 and 80°C.

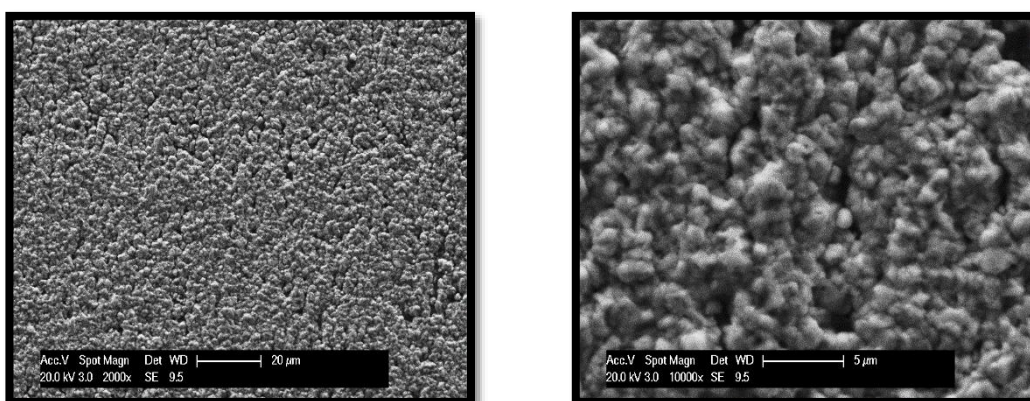
Surfactant	Surface roughness (µm)			
	Ethaline		Glyceline	
	50°C	80°C	50°C	80°C
None	0.390	0.561	0.341	0.420
	±0.030	±0.016	±0.010	±0.032
SDS	0.435	0.482	0.396	0.463
	±0.016	±0.004	±0.011	±0.012
AOT	0.455	0.751	0.408	0.465
	±0.008	±0.064	±0.015	±0.025

Assuming that there is less chloride adsorption at higher temperature must lead to the conclusion that there would also be less surfactant adsorption. The grey coloured deposit in Ethaline when AOT was added suggests that a different type of phase is formed with AOT in Ethaline.

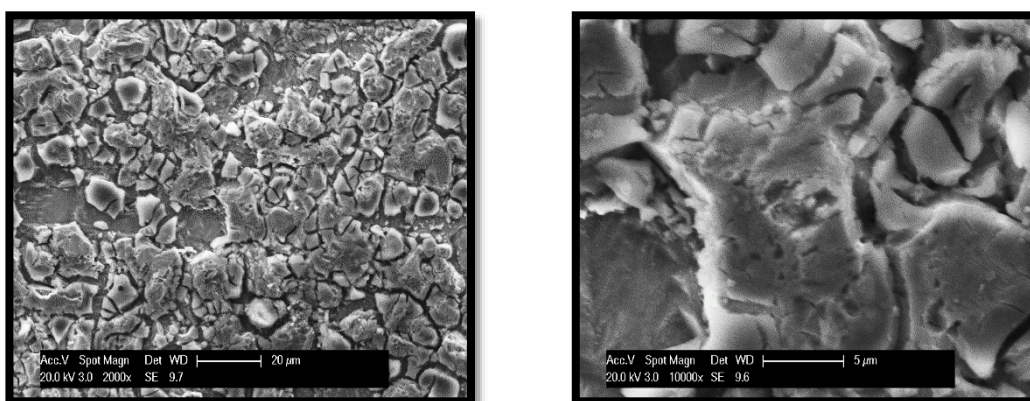
The Cu coatings obtained in Ethaline at 80°C were examined using SEM and are presented in Figure 5-12. It is clear that the morphology of the coating changes as the temperature was increased for both system with and without surfactants. There is not obvious change in the morphology of Cu electrodeposition from Ethaline with and without SDS see Figure 5-12 (a) and (b). Interestingly, there are no grooves observed Figure 5-12 (b) when compared with the analogous coating obtained at 50°C (Figure 5-7 (b)). This indicates that whatever structure caused the grooves at lower temperatures was not present at higher temperatures. Figure 5-12 (c) show the poor Cu coating (Cu coating confirm by Energy Dispersive X-ray Analysis (EDX) as can be seen in Figure 5-13) in the presence of AOT which indicates that the adsorption of AOT, inhibiting Cu deposition.



(a)



(b)



(c)

Figure 5-12: SEM images of Cu coating from 100 mM $\text{CuCl}_2 \cdot 2\text{H}_2\text{O}$ in Ethaline on nickel substrate at 80°C obtained in (a) absence of surfactants, (b) with 25 mM SDS and (c) 25 mM with AOT at two magnifications right scale bar = 20 μm and left 5 μm ..

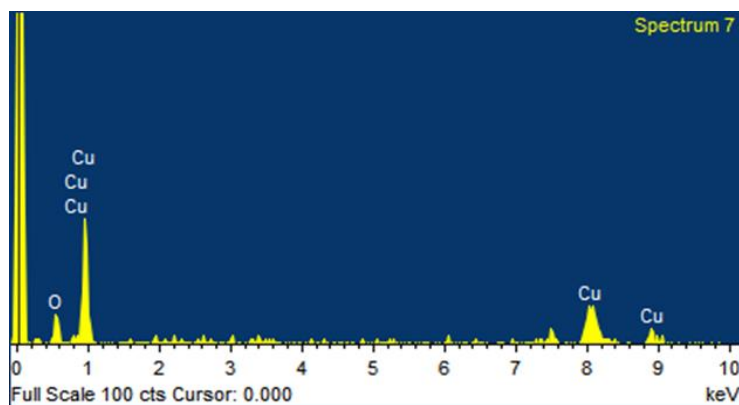


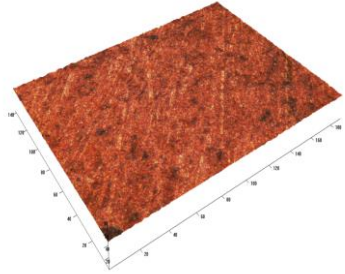
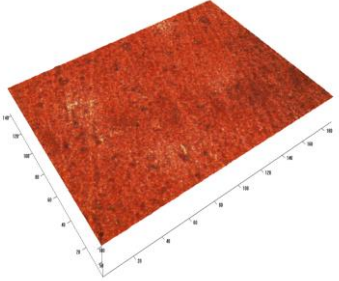
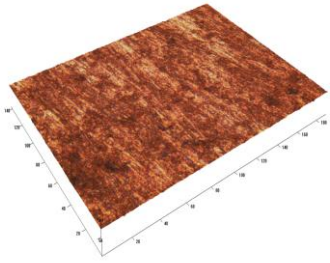
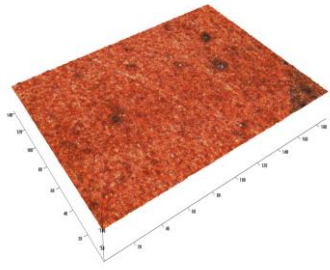
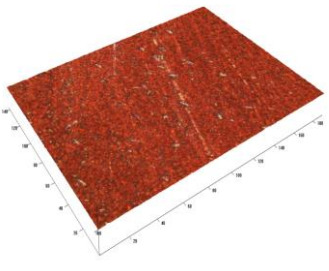
Figure 5-13: EDX for the part imaged by SEM of Cu coating in Ethaline in present of AOT.

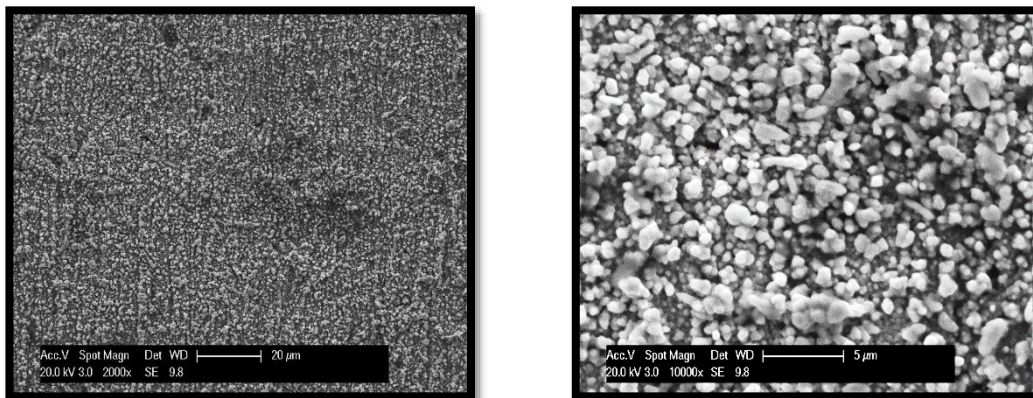
In the case of Cu deposited from Glyceline, increasing the temperature from 50 and 80°C has only a small effect on deposit appearance as shown in Tables 5-7 and 5-8. All samples are orange red in colour and become slightly darker when surfactants are added but the significant changes observed with Ethaline are not observed. This can be confirm by the using SEM of Cu coating from Glyceline in absence and presence of surfactants as shown in Figure 5-14. Also the surface roughness, see Table 5-6, does increase slightly when surfactants are added but not as much as that observed with Ethaline.

Table 5-7: Images for Cu coated in Ethaline in pure and with presence of surfactants at temperature 50 and 80°C.

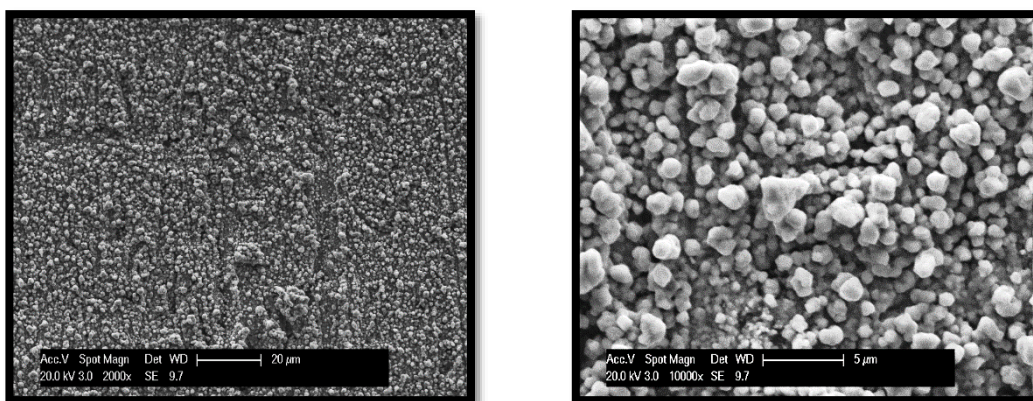
T (°C)	Glyceline	Glyceline with SDS	Glyceline with AOT
50			
80			

Table 5-8: 3D topographical images of copper deposited film from Glyceline in absent and presence of surfactants at temperature 50 and 80°C.

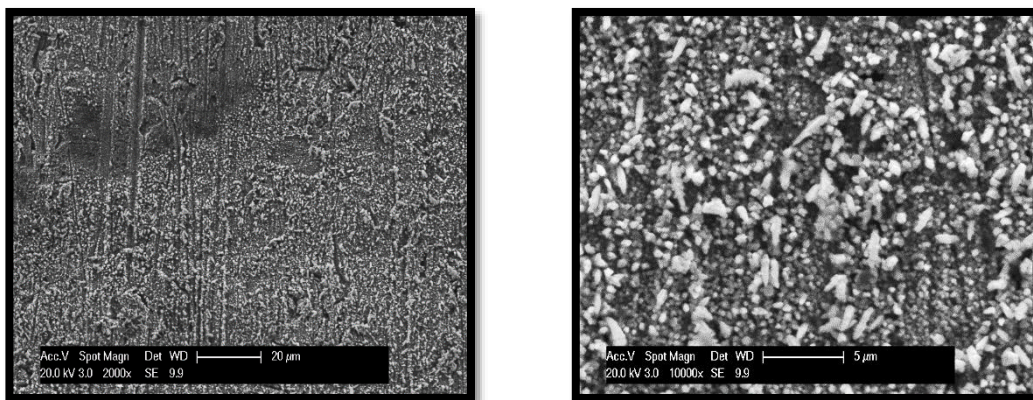
Surfactant	Cu coating at 50 (°C)	Cu coating at 80 (°C)
None		
SDS		
AOT		



(a)



(b)



(c)

Figure 5-14: SEM images of Cu coating from 100 mM $\text{CuCl}_2 \cdot 2\text{H}_2\text{O}$ in Glyceline on nickel substrate at 80°C obtained in (a) absence of surfactants, (b) with 25 mM SDS and (c) 25 mM with AOT at two magnifications right scale bar = 20 μm and left 5 μm.

5.3 Conclusion

The electrochemical reduction of Cu^{+2} to Cu^0 has been studied for Ethaline and Glyceline containing anionic surfactants, SDS and AOT as surface active agents. The effect of these surfactants as brightener on the copper deposit is probed using electrochemical techniques based on the analysis of cyclic voltammetry and chronoamperometry. The deposit morphology of Cu on a nickel substrate are characterized using scanning electron microscopy, X-ray diffraction and 3D optical microscopy.

Both surfactants SDS and AOT did not significantly affect the peak potentials for the oxidation and reduction of copper however AOT did significantly decreased in the charge for copper deposition compared with SDS. This suggests that AOT in Ethaline does have some blacking effect that does not affect the thermodynamics of reduction but does affect the mass transport of copper complex to the electrode surface for deposition and ligand (Cl^-) to the electrode for dissolution.

Chronoamperometry shows that nucleation and growth appear different in Ethaline and Glyceline. Scharifker-Hills analysis shows that while the nucleation of copper is more instantaneous in Ethaline and progressive in Glyceline the mechanism is not significantly affected by the presence of surfactants. This shows that they are not specifically adsorbed on the electrode surface. This is different to the findings of recent studies of brighteners with copper and nickel in the same DESs.

Bulk electrodeposition of copper resulted in different morphologies and different coloured deposits when surfactants were added to the DESs. The crystallographic phases of copper were also largely unaffected by the presence of surfactants again showing that the surfactants are not specifically adsorbed on the electrode surface. Analysis of the SEM images show that the nanostructures of copper are similar with and without surfactants, but the microstructures show evidence of deep grooves. These cannot originate from templating as has been observed previously with aqueous solutions as these tend to form regular structures on the nm scale. It is also unlikely that they form around micellar structures as these are of a different length-scale.

This chapter has shown that surfactants do not act as levellers or brighteners in DESs and by inference it shows that electrostatic interactions are insufficient to interact strongly enough with the electrode during deposition. It suggests that brighteners need to be based on specific metal-additive interactions which are either physisorbed or more likely chemisorbed on the metal surface.

5.4 References

1. S. Manne, J. Cleveland, H. Gaub, G. Stucky and P. Hansma, *Langmuir*, 1994, **10**, 4409-4413.
2. L. Zhong-Chun, L. Tian-Qing and G. Rong, *Chinese Journal of Chemistry*, 2005, **23**, 404-408.
3. J. F. Rusling, *Accounts of chemical research*, 1991, **24**, 75-81.
4. J. Kostela, M. Elmgren, P. Hansson and M. Almgren, *Journal of Electroanalytical Chemistry*, 2002, **536**, 97-107.
5. D. Gugala-Fekner, J. Nieszporek and D. Sieńko, *Monatshefte für Chemie-Chemical Monthly*, 2015, **146**, 541-545.
6. J. F. Rusling, *Colloids and Surfaces A: Physicochemical and Engineering Aspects*, 1997, **123**, 81-88.
7. C. Low and F. Walsh, *Journal of Electroanalytical Chemistry*, 2008, **615**, 91-102.
8. R. Vittal, H. Gomathi and K.-J. Kim, *Advances in Colloid and Interface Science*, 2006, **119**, 55-68.
9. L. Bonou, M. Eyraud, R. Denoyel and Y. Massiani, *Electrochimica Acta*, 2002, **47**, 4139-4148.
10. L. Oniciu and L. Mureşan, *Journal of Applied Electrochemistry*, 1991, **21**, 565-574.
11. T. C. Franklin, *Surface and Coatings Technology*, 1987, **30**, 415-428.
12. A. P. Abbott, J. C. Barron, G. Frisch, K. S. Ryder and A. F. Silva, *Electrochimica Acta*, 2011, **56**, 5272-5279.
13. O. Kardos, *Plating*, 1974, **61**, 129.
14. L. Vieira, R. Schennach and B. Gollas, *Physical Chemistry Chemical Physics*, 2015, **17**, 12870-12880.
15. A. P. Abbott, G. Capper, D. L. Davies and R. K. Rasheed, *Chemistry-A European Journal*, 2004, **10**, 3769-3774.
16. A. P. Abbott, K. El Ttaib, G. Frisch, K. J. McKenzie and K. S. Ryder, *Physical Chemistry Chemical Physics*, 2009, **11**, 4269-4277.
17. P. De Vreese, N. R. Brooks, K. Van Hecke, L. Van Meervelt, E. Matthijs, K. Binnemans and R. Van Deun, *Inorganic Chemistry*, 2012, **51**, 4972-4981.

18. A. P. Abbott, A. Ballantyne, R. C. Harris, J. A. Juma, K. S. Ryder and G. Forrest, *Electrochimica Acta*, 2015, **176**, 718-726.
19. M. R. Ali, M. Z. Rahman and S. S. Saha, *Indian Journal of Chemical Technology*, 2014, **21**, 127-133.
20. A. P. Abbott, G. Capper, K. J. McKenzie and K. S. Ryder, *Journal of Electroanalytical Chemistry*, 2007, **599**, 288-294.
21. A. Abbott, J. Barron and K. Ryder, *Transactions of the IMF*, 2009, **87**, 201-207.
22. S. Fashu, C.-d. Gu, J.-l. Zhang, M.-l. Huang, X.-l. Wang and J.-p. Tu, *Transactions of Nonferrous Metals Society of China*, 2015, **25**, 2054-2064.
23. J. C. Barron, PhD Thesis, University of Leicester, 2010.
24. M. Azam, PhD Thesis, University of Leicester, 2012.
25. A. Gomes and M. da Silva Pereira, *Electrochimica Acta*, 2006, **52**, 863-871.
26. A. Gomes and M. da Silva Pereira, *Electrochimica Acta*, 2006, **51**, 1342-1350.
27. A. Gomes, A. Viana and M. da Silva Pereira, *Journal of the Electrochemical Society*, 2007, **154**, D452-D461.
28. J. A. Juma, PhD Thesis, University of Leicester, 2016.
29. H. F. N. Al-Esary, PhD Thesis, University of Leicester, 2017.
30. D. Lloyd, T. Vainikka, L. Murtomäki, K. Kontturi and E. Ahlberg, *Electrochimica Acta*, 2011, **56**, 4942-4948.
31. B. G. Pollet, J.-Y. Hihn and T. J. Mason, *Electrochimica Acta*, 2008, **53**, 4248-4256.
32. C. Gu, Y. You, X. Wang and J. Tu, *Surface and Coatings Technology*, 2012, **209**, 117-123.
33. I. Lehr and S. Saidman, *Applied Surface Science*, 2012, **258**, 4417-4423.
34. R. Stefanovic, M. Ludwig, G. B. Webber, R. Atkin and A. J. Page, *Physical Chemistry Chemical Physics*, 2017, **19**, 3297-3306.
35. M. H. Chakrabarti, N. P. Brandon, M. A. Hashim, F. S. Mjalli, I. M. AlNashef, L. Bahadori, N. Abdul Manan, M. Hussain and V. Yufit, *International Journal of Electrochemical Science*, 2013, **8**, 9652-9676.
36. N. G. Tsierkezos, *Journal of Solution Chemistry*, 2007, **36**, 289-302.
37. B. Scharifker and G. Hills, *Electrochimica Acta*, 1983, **28**, 879-889.
38. D. Grujcic and B. Pesic, *Electrochimica Acta*, 2002, **47**, 2901-2912.

39. G. Gunawardena, G. Hills, I. Montenegro and B. Scharifker, *Journal of Electroanalytical Chemistry and Interfacial Electrochemistry*, 1982, **138**, 225-239.
40. A. Rouhollahi, O. Fazlollahzadeh, A. Dolati and F. Ghahramanifard, *Journal of Nanostructure in Chemistry*, 2018, 1-14.
41. L. Huang, H. Wang, Z. Wang, A. Mitra, K. N. Bozhilov and Y. Yan, *Advanced Materials*, 2002, **14**, 61-64.
42. C. Gu, Y. You, Y. Yu, S. Qu and J. Tu, *Surface and Coatings Technology*, 2011, **205**, 4928-4933.
43. S. Cihangir, PhD Thesis, University of Leicester, 2018.

6 Summary and Future Work

6	Summary and Future Work	180
6.1	Conclusions	181
6.2	Suggestions for Further Work	184

6.1 Conclusions

This project has investigated the behaviour of surfactants in deep eutectic solvents focussing on their aggregation in the bulk and at interfaces. The first issue addressed in this study is the reason why surfactants aggregate at all in media of high ionic strength. It is known that for aqueous solutions simple inorganic salts destabilise surfactant aggregation due to their neutralisation of the zeta potential enabling micelles to overcome the Coulombic repulsion of neighbouring micelles causing coagulation and precipitation. The unusual stability of surfactants dispersed in DESs appears to be due to the size of the choline cation. Given that the diameter of the choline cation is approximately 6.6 Å the distance of closest approach would be 1.3 nm at which point the micelles would be too distant to overcome the repulsive maximum which maintains stability. The large size of the cations also stops the Stern layer neutralising the charge on the micelle effectively so the zeta potential stays negative and neighbouring micelles can repel each other.

Chapter three investigated the physical properties of surfactant aggregates in DESs. It was found that non-ionic surfactants were insoluble and cationic surfactants showed poor solubility. This was thought to be due to high concentrations of chloride in the Stern layer reducing the zeta potential which encouraged precipitation. The CMC values were determined using 3 techniques; surface tension, fluorescence and UV-visible spectra. All three techniques gave comparable results. It was shown that the CMC of anionic surfactants was similar to their value in aqueous solutions despite the high ionic strength. The CMC was higher in Ethaline than in Glyceline and Reline because the former is less polar and so the monomer is more stable in solution. This means that a higher concentration is required before aggregation occurs. This indicated that the aggregation was favoured in media with a higher surface energy as this disfavoured the solubilisation of monomers in bulk solution.

The size of the aggregates in Ethaline was found to increase with increasing SDS concentration. DLS and viscosity results showed that the supramolecular aggregates of SDS in Ethaline change from cylindrical to liquid crystalline at about $3 \times \text{CMC}$.

The aggregation behaviour of SDS and its interaction with Ethaline at different temperatures have been investigated by conductivity measurements in order to calculate the thermodynamics of micellization. The Gibbs energy of micellization was found to

be negative showing that micelle formation was spontaneous. The enthalpy of micellization was also positive which is contrary to the value in aqueous solutions. The main driving force for micellization was a much larger positive entropy change than that in water. This occurs because the DES is more ordered than water and replacing a given volume with micelles will cause a bigger change in the disorder of the system.

Chapter four focuses on the interfacial properties of surfactants air, solid, charged electrode and liquid interfaces with DESs. Surface tension experiments were used to investigate the surfactant (air-DES) interface and these showed that the area occupied per surfactant molecule at the air-DES interface was considerably larger for Ethaline than for Glyceline. This could either be because the SDS molecule lies inclined to the interface, or more likely that an incomplete monolayer is formed due to the high solubility of SDS monomers in Ethaline.

For the solid-DES interface contact angle measurements was used and these showed that SDS was better at causing Glyceline to wet a stainless steel surface than Ethaline, presumably because it was more active at the interface. Above the CMC, both liquids wet the surface equally well but it was clear from the contact angle that neither formed a complete layer on the metal surface as the contact angle was still too high (c.a. 40°).

Electrochemical measurements indicated that far from blocking the electrode, as would be expected in an aqueous solution, SDS appeared to promote electron transfer for the oxidation of FeCl₂. It is proposed that this is due to a partial monolayer adsorption of SDS below the CMC breaking up the highly organised chloride layer at the electrode-DES interface and promoting electron transfer. Above the CMC micelles form and there appears to be some evidence that hydrophobic probes such as TTF partition into the micelles. Electron transfer is slowed which appears to be due to slower diffusion of the micelle containing the probe to the electrode surface.

In a study of the liquid-DES interface, it was found that O-DES emulsions are more stable in Glyceline than in Ethaline as it is more viscous and the high surface tension of the pure liquid pushes the surfactant to aggregate. It was noted that DES-O emulsions form and are stable with Glyceline. In Ethaline the oil phase separates as the surfactant is less likely to aggregate and stabilise the O-DES phase.

Chapter five examined the use of surfactants as brightener in Cu electrodeposition from DESs. Both SDS and AOT were used in Ethaline and Glyceline. Cyclic voltammetry results shows negligible shift in the redox potentials when surfactants are added suggesting that the surfactants are not strongly interacting with the electrode. The nucleation and growth mechanism of Cu electrodeposition however showed differing nucleation mechanisms in Ethaline and Glyceline presumably because of the different activity of Cl^- in both solvents. The addition of surfactants did not significantly change the nucleation mechanism and did not change the type or proportion of the crystal phases obtained. This reinforces the idea that the surfactant is not strongly adsorbed at the electrode-DES interface. Bulk electrodeposition of copper was affected by the presence of surfactants, particularly AOT which resulted in macroscopic grooves in the deposit. These are hard to explain other than some form of macroscopic aggregate close to the electrode surface resulted in uneven transport of copper.

In general, this thesis has shown that anionic surfactants can aggregate in media of high ionic strength and the stability of the aggregate is due to the size of the cation of the DES (or IL). The aggregation of the anionic surfactants at interfaces, particularly charged interfaces, depends on the relative anionic strength. Small, high charge density anions will destabilise the partitioning of anions to the interface and will destabilise emulsions. Emulsions will benefit from media of higher viscosity as these will slow down the mobility of charged aggregates.

6.2 Suggestions for Further Work

This work is not exhaustive in its study of surfactants in DESs. The conclusions it draws are strong in terms of understanding the conditions required to stabilise a colloidal dispersion and to make the surfactant more active at interfaces. Subsequently more work is required to characterise the behaviour of surfactants in DESs and the following areas of studies are suggested:

- 1- The current study was carried out with one type of surfactants (anionic) and a limited range of components. It would be interesting to expand this range of components to reinforce the conclusions of this study. Acidic DESs were not studied in detail due to their high viscosity. It could be envisioned that protons would destabilise the micelle by decreasing the zeta potential. Recent work in the group has quantified pH in DESs and it would be interesting to study the stability of DESs as a function of pH. Other less viscous DESs containing HBDs such as aromatic alcohols could be tested. It would also be important to look at the stability of different types of cations for the salt in the DES other than Ch^+ . Benzyl-alkylammonium salts have been studied for DESs. Cations such as hexyltrimethyl ammonium would be on the cusp of having surfactant like properties and it would be useful to understand the trade-off between hydrophobic and coulombic effects at stabilising colloidal dispersions. Increasing the carbon chain length will also decrease the surface tension of the liquid which should make it easier to stabilise monomers in solution which should increase the CMC.
- 2- There are numerous methods of studying interfacial structures that form at the electrode-DES interface. It would be important to use AFM approach force curves to probe for structures close to the electrode as has already been carried out by Atkin *et al.* for DESs without surfactants. It should also be possible to use neutron reflectivity studies to probe structures at the electrode-DES interface and this could be done for polarised and non-polarised electrode surfaces.
- 3- DESs have been studied as alternative lubricants. As part of this, initial investigations were made adding surfactants to decrease the wear volume. These were not as successful as had been anticipated but they were limited to SDS in Ethaline. It is clear from the above study that double chain surfactants would be more surface active, particularly in Glyceline and this would be important to test

as a performance enhancer. An area where viscous fluids are currently being used is in high performance greases. Lithium greases are salts of fatty acids and are used due to their high viscosity and high temperature stability. It would be useful to see if surfactants in high concentration can gel the properties of DESs sufficiently to match the performance requirements of modern greases

- 4- DES-surfactant systems are able to control microenvironments and in this study appear to be able to stabilise rod-like structures. DESs have been used to construct porous materials with novel porous nanostructures such as zeolites. It would be interesting to see whether novel pore geometries could be constructed by the inclusion of surfactants into the structures.
- 5- The Leicester Ionic Liquids group has pioneered miner processing using DESs. The observation that DES-surfactant solutions can form stable foams would be useful for froth floatation experiments. This would be particularly interesting as the density, surface tension and hydrophobicity/hydrophilicity of the DES can be tailored significantly. It would be interesting to measure the surface wetting of different minerals with DESs and see the effect of surfactants on the wettability.

These ideas show that the areas of surfactant aggregation in DESs is an interesting one with a variety of useful applications.

7 Appendix

7	Appendix	186
7.1	Surface Tension Raw Data.....	187
7.2	Conductivity Raw Data.....	192

7.1 Surface Tension Raw Data

Table 7-1: Raw data for surface tension measurements of SDS in Ethaline.

[SDS]	Surface tension	Surface tension	Surface tension	Average of surface tension (mN m ⁻¹)	SD
0.0	54.60	55.30	55.70	55.20	0.56
0.5	50.80	49.60	48.90	49.77	0.96
2.0	46.80	46.30	45.80	46.30	0.50
4.0	42.80	42.80	42.00	42.53	0.46
6.0	40.30	39.80	39.80	39.97	0.29
8.0	38.20	37.80	37.80	37.93	0.23
10.0	35.70	35.70	35.30	35.57	0.23
20.0	34.10	34.00	34.10	34.07	0.06
30.0	34.60	34.60	34.60	34.60	0.00

Table 7-2: Raw data for surface tension of SDS in Glyceline.

[SDS]	Three measurements of surface tension (mN m ⁻¹)			Average of surface tension (mN m ⁻¹)	SD
0.0	64.70	63.10	64.30	64.03	0.83
0.5	52.90	52.60	52.30	52.60	0.30
2.0	42.00	42.10	41.50	41.87	0.32
4.0	34.60	34.60	34.50	34.57	0.06
6.0	33.40	33.40	33.50	33.43	0.06
8.0	33.50	33.50	33.50	33.50	0.00
10.0	33.20	33.50	33.50	33.40	0.17
20.0	33.40	33.20	33.20	33.27	0.12
30.0	33.40	33.20	33.20	33.27	0.12

Table 7-3: Raw data for surface tension of SDS in Reline.

[SDS]	Three measurements of surface tension (mN m ⁻¹)			Average (mN m ⁻¹)	SD
0.0	73.40	71.70	72.60	72.57	0.85
0.5	44.50	45.20	46.00	45.23	0.75
2.0	33.90	33.90	33.70	33.83	0.12
4.0	32.50	32.30	32.50	32.43	0.12
6.0	32.50	32.40	32.30	32.40	0.10
8.0	32.10	32.30	32.30	32.23	0.12
10.0	32.30	32.10	32.30	32.23	0.12
20.0	33.30	32.10	32.30	32.57	0.64
30.0	32.10	31.90	32.10	32.03	0.12

Table 7-4: Raw data for surface tension of AOT in Ethaline.

[AOT]	Three measurements of surface tension (mN m ⁻¹)			Average (mN m ⁻¹)	SD
0.0	55.30	55.60	55.20	55.37	0.21
0.5	40.80	40.60	40.40	40.60	0.20
1.0	37.30	37.40	37.30	37.33	0.06
2.0	33.90	34.10	33.50	33.83	0.31
4.0	30.80	30.60	30.80	30.73	0.12
6.0	29.10	28.90	29.00	29.00	0.10
10.0	27.40	27.50	27.30	27.40	0.10
15.0	27.10	26.70	27.00	26.93	0.21
25.0	26.30	27.00	27.00	26.77	0.40
40.0	26.90	27.00	27.10	27.00	0.10

Table 7-5: Raw data for surface tension of AOT in Glyceline.

[AOT]	Three measurements of surface tension (mN m ⁻¹)			Average of surface tension (mN m ⁻¹)	SD
0.0	68.50	68.40	69.00	68.63	0.32
0.5	30.10	30.20	30.30	30.20	0.10
1.0	27.00	27.10	27.00	27.03	0.06
2.0	26.00	26.30	26.20	26.17	0.15
4.0	25.60	25.80	25.90	25.77	0.15
6.0	25.90	25.90	26.40	26.07	0.29
10.0	25.40	25.40	25.70	25.50	0.17
15.0	25.40	25.60	26.00	25.67	0.31
25.0	25.20	25.30	26.30	25.60	0.61
40.0	25.20	25.30	26.50	25.67	0.72

Table 7-6: Raw data for surface tension of AOT in Reline.

[AOT]	Three measurements of surface tension (mN m ⁻¹)			Average of surface tension (mN m ⁻¹)	SD
0.0	76.70	70.70	77.50	74.97	3.72
0.5	26.90	26.70	26.40	26.67	0.25
1.0	26.80	26.40	26.50	26.57	0.21
2.0	26.30	26.30	26.20	26.27	0.06
4.0	26.00	26.20	26.00	26.07	0.12
6.0	26.20	26.00	26.00	26.07	0.12
10.0	26.10	26.00	26.00	26.03	0.06
25.0	26.20	25.90	25.80	25.97	0.21
40.0	25.80	25.90	26.00	25.90	0.10

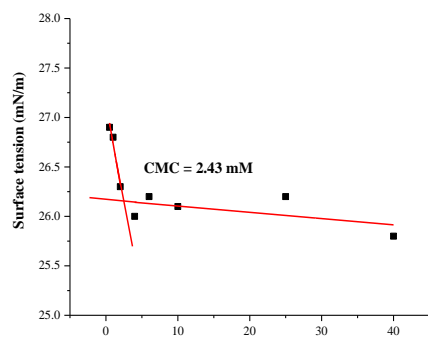
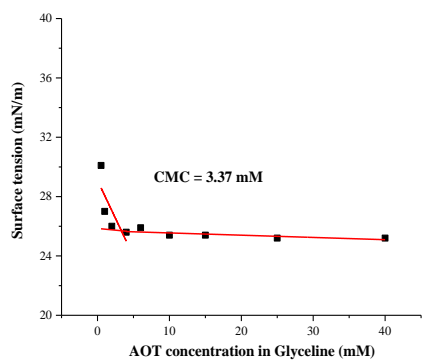
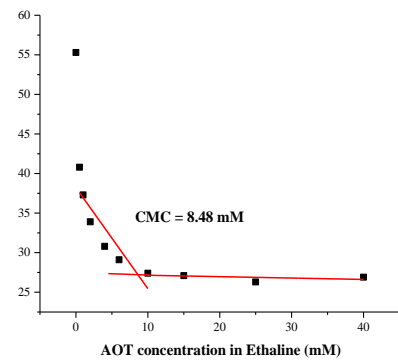
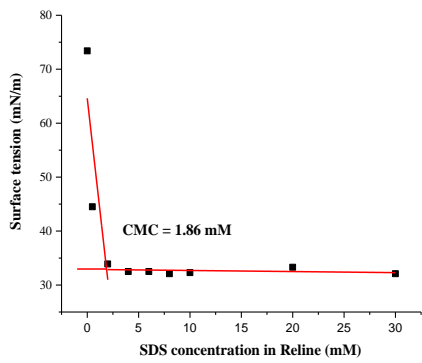
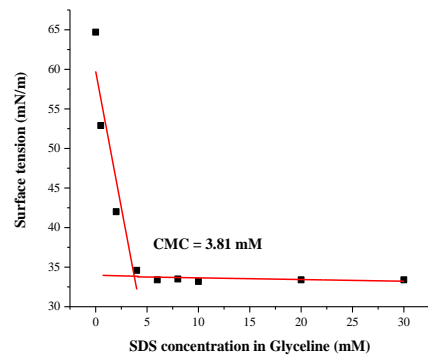
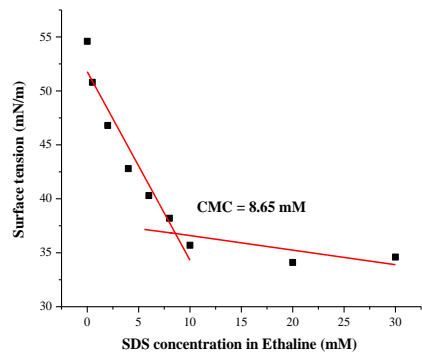


Figure 7-1: CMC determination as the intersection between the linear decline and the baseline of minimal surface tension.

Table 7-7: Values of CMC of SDS and AOT in DESs.

Surfactant	DESs	Three measurements of CMC (mM)			Average of CMC	SD
SDS	Ethaline	8.65	9.22	9.13	9.00	0.31
	Glyceline	3.81	3.81	3.67	3.76	0.08
	Reline	1.86	1.91	1.95	1.91	0.04
AOT	Ethaline	8.48	8.60	8.60	8.56	0.07
	Glyceline	3.37	3.50	3.32	3.40	0.09
	Reline	2.43	2.50	2.81	2.58	0.21

7.2 Conductivity Raw Data

Table 7-8: Raw data for conductivity of SDS in Ethaline at 30°C.

[SDS]	Three measurements of conductivity (mS cm ⁻¹)			Average of conductivity (mS cm ⁻¹)	SD
0.08	9.21	9.28	9.28	9.26	0.04
1.16	8.78	8.88	8.93	8.86	0.08
2.00	8.76	8.96	8.94	8.89	0.11
4.01	8.84	9.02	9.11	8.99	0.14
8.07	9.07	9.10	9.19	9.12	0.06
12.18	8.91	8.82	8.84	8.86	0.05
20.50	8.67	8.70	8.87	8.75	0.11
24.74	8.65	8.79	8.78	8.74	0.08
28.99	8.34	8.48	8.50	8.44	0.09

Table 7-9: Raw data for conductivity of SDS in Ethaline at 40°C.

[SDS]	Three measurements of conductivity (mS cm ⁻¹)			Average of conductivity (mS cm ⁻¹)	SD
0.08	11.19	11.30	11.34	11.28	0.08
1.16	11.33	11.19	11.34	11.29	0.08
2.00	11.35	11.45	11.24	11.35	0.11
4.01	11.37	11.43	11.46	11.42	0.05
8.07	11.38	11.40	11.67	11.48	0.16
12.18	11.19	11.24	11.39	11.27	0.10
20.50	11.17	11.28	11.25	11.23	0.06
24.74	11.10	11.15	11.22	11.16	0.06
28.99	11.02	10.93	11.07	11.01	0.07

Table 7-10: Raw data for conductivity of SDS in Ethaline at 50°C.

[SDS]	Three measurements of conductivity (mS cm ⁻¹)			Average of conductivity (mS cm ⁻¹)	SD
0.08	12.61	12.60	12.60	12.60	0.01
1.16	12.71	12.92	13.07	12.90	0.18
2.00	12.89	13.03	13.09	13.00	0.10
4.01	12.95	13.14	13.20	13.10	0.13
8.07	13.20	13.06	13.15	13.14	0.07
12.18	13.01	13.03	13.00	13.01	0.02
20.50	12.86	12.97	12.86	12.90	0.06
24.74	12.80	12.81	12.80	12.80	0.01
28.99	12.75	12.75	12.77	12.76	0.01

Table 7-11: Raw data for conductivity of SDS in Ethaline at 60°C.

[SDS]	Three measurements of conductivity (mS cm ⁻¹)			Average of conductivity (mS cm ⁻¹)	SD
0.08	15.14	15.21	15.36	15.24	0.11
1.16	15.18	15.35	15.38	15.30	0.11
2.00	15.17	15.54	15.47	15.39	0.20
4.01	15.66	15.32	15.41	15.46	0.18
8.07	15.47	15.47	15.48	15.47	0.01
12.18	15.32	15.25	15.21	15.26	0.06
20.50	15.21	14.94	15.18	15.11	0.15
24.74	14.99	14.99	15.16	15.05	0.10
28.99	14.79	14.90	14.79	14.83	0.06